Phosphoproteomic Analysis of *Craterostigma plantagineum* upon Abscisic Acid and Desiccation Stress

Dissertation

zur
Erlangung des Doktorgrades (Dr. rer. nat.)
der
Mathematisch-Naturwissenschaftlichen Fakultät
der
Rheinischen Friedrich-Wilhelms-Universität Bonn

vorgelegt von
Fabio Facchinelli
aus Bozen, Italien

Bonn 2009

Angefertigt mit Genehmigung der Mathematisch-Naturwissenschaftlichen Fakultät der
Rheinischen Friedrich-Wilhelms-Universität Bonn

1. Gutachter: Prof. Dr. Dorothea Bartels
2. Gutachter: Prof. Dr. Peter Dörmann

Tag der Promotion: 15. März 2010
Erscheinungsjahr: 2010

Contents

Abbreviations

% (w/v)	Weight percentage
% (v/v)	Volume percentage
2,4-D	2,4-Dichlorophenoxyacetic acid
2iP	2-isopentenyladenine
A	Adenin
ABA	Abscisic acid
ABRE	ABA responsive element
Amp	Ampicillin
APS	Amonium persulfate
bp	Base pair
bZIP	Basic leucine zipper
BSA	Bovine serum albumin
β-ME	β-mercaptoethanol
C	Cytosine
cDNA	Complementary DNA
Da	Dalton
DEPC	Diethylpyrocarbonate
DMSO	Dimethyl sulfoxide
DNA	Deoxyribonucleic acid
DNase	Deoxyribonuclease
dNTP	Deoxyribonucleotide triphosphate
DTT	Dithiothreitol
DRE	Dehydration responsive element
EDTA	Ethylenediaminetetraacetic acid
EST	Expressed sequence tag
g	Gram

g	Acceleration
G	Guanine
h	Hour
Hepes	4-(2-hydroxyethyl)-1-piperazineethanesulfonic acid
His	Histidine
IgG	Class G immunoglobulin
pI	Isoelectric point
IPTG	Isopropyl β-D-1-thiogalactopyranoside
Kan	Kanamycin sulfate
kb	Kilobase
kDa	Kilodalton
λ	Wavelenght
LB	Luria and Bertani medium
LEA	Late Embryogenesis Abundant
M	Molar, moles per liter
mA	Milliamperes
MCS	Multiple cloning site
MES	2-(N-morpholino)ethanesulfonic acid
min	Minute
ml	Milliliter
MOAC	Metal oxide affinity chromatography
MOC	Metal oxide chromatography
MOPS	3-(N-morpholino)propanesulfonic acid
MPa	Megapascal
MW	Molecular weight
mRNA	Messenger RNA
MS	Murashige and Skoog medium
nm	Nanometers
OD	Optical density
oligo (dT)	Oligodeoxythymidylic acid
ORF	Open reading frame
PCI	Phenol-chloroform-isoamyl alcohol
PCR	Polymerase chain reaction

PEG	Poly(ethylene glycol)
PMSF	Phenylmethanesulphonylfluoride
PVPP	Polyvinylpolypyrrolidone
RNA	Ribonucleic acid
rpm	Revolutions per minute
RT	Room temperature
SDS	Sodium dodecyl sulfate
T	Thymine
$\mathbf{T}_a$	Annealing temperature
TAE	Tris-acetate-EDTA
TE	Tris-EDTA
TEMED	Tetramethylethylenediamine
Tris	Tris(hydroxymethyl)aminomethane
Triton X-100	Polyoxyethylene octyl phenyl ether
UV	Ultraviolet
V	Volts

List of Figures

List of Tables

1. Introduction

1.1. The Importance of Water for Plant Survival

All physiological processes in plants depend on water, and water accounts for 80–95 % of the biomass of leaves and roots in non-woody plants (Hirt and Shinozaki, 2004). At the cellular level, water is the major medium for transporting metabolites and nutrients. Plants build a continuous column of water that flows from the roots to the leaves where water is lost by transpiration through the stomata. As the column of water moves through the roots, stem and leaves, nutritional elements are carried with it to the leaves. Water flow is driven by the water potential (Ψ) flowing from a higher to a lower water potential. In a plant the water potential (-1 to -4 MPa) is less than in the soil (-0.01 to -0.1 MPa) but is more than in the air (-100 MPa at 22 °C, even with 100 % relative humidity). This ensures that the water is continuously transported through the plant and lost at the leaf surface. If there is a break in the water column, since it is under tension, the broken end collapses into the xylem and continuity is lost. Water is important also because it maintains the structure of intracellular macromolecules and membranes; in absence of protective mechanisms, removing water from the cells irreversibly aggregates essential macromolecules and disintegrates organelles. A constant water availability is therefore of crucial importance for plant survival.

1.2. The Importance of Water in Agriculture

Adverse environmental conditions and particularly drought is one of the major factors restricting plant productivity and distribution.

The world population is now approaching 6 billion and is expected to reach 8 billion by year 2025. Statistics estimate that, to meet future food demand, at least another 2,000

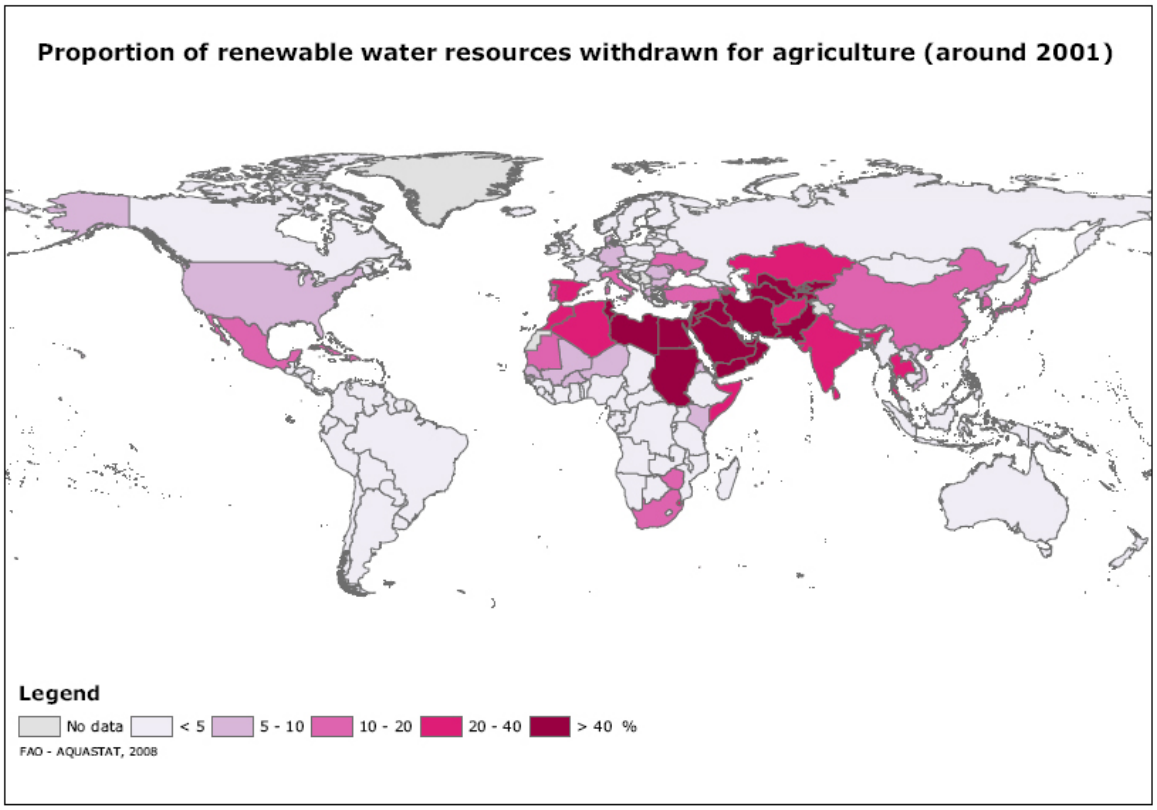

Figure 1.1: Surface water and groundwater withdrawal for agricultural purposes as percentage of total actual renewable water resources. From www.fao.org

cubic kilometers of water, corresponding to the mean annual flow of 24 additional Nile rivers, will be needed (Postel, 1999).

Irrigated land is of utmost importance to world food production. About 40 % of the global harvest comes from the 17 % of cropland that is irrigated. Irrigation accounts for 2–4 % of diverted water in Canada, Germany and Poland but is an impressive 90–95 % in Iraq, Pakistan, Bangladesh and Sudan (Figure 1.1). Given that nearly 80 % of all freshwater used by humans is for irrigation, the importance of irrigated areas cannot be underestimated. Therefore, it has become imperative for plant biologists to understand the mechanisms by which plants can adapt to suboptimal watering conditions while retaining their productivity.

1.3. Mechanisms of Adaptation to Water Deficit

Plants have adopted several strategies to cope with water scarcity. These forms of adaptation are termed 'avoidance', 'resistance' or 'tolerance' to desiccation according to the level of tolerance the plants display (Le and McQueen-Mason, 2006). Desiccation avoidance is performed by *e.g.* the annual plants which complete their life cycle in the period of the year where the growth conditions are most favorable and thus never face water deficiency. Desiccation resistance is accomplished by some plants that have developed morphological structures that allow them to retain the cellular water. These plants are able to overcome dry periods either by reducing water flux through the plant or by increasing their water uptake. While water uptake can only be increased by the development of specialized root structures, water loss can be avoided by various mechanisms such as stomatal closure, reduction of leaf growth or production of specialized leaf surfaces to avoid transpiration (*e.g.* waxes, hairs or embedded stomata). More complex mechanisms involve in the CAM (Crassulacean Acid Metabolism) plants the temporal separation of the CO_2 uptake from its assimilation in the Calvin cycle. The CO_2 is accumulated during the night when the stomata are opened and stored as malate in the vacuole, whereas during the day the CO_2 is released and supplies the Calvin cycle when the stomata are closed thus avoiding excessive water loss (Buchanan *et al.*, 2000).

Desiccation tolerance is defined as the ability of an organism to equilibrate its internal water potential with that of the air and then regain normal function after rehydration. Plants tolerant to desiccation can survive almost complete cellular dehydration, losing more than 90 % of their relative water content (RWC), and then resume normal physiological functions after rehydration (Rascio and La Rocca, 2005).

A quantitative definition of complete desiccation is drying to 0.1 g H_2O g^{-1} dry mass (10 % [v/v] water content [WC]) or less. This is roughly equivalent to air dryness at 50 % relative humidity and 20 °C and corresponds to a water potential of about -100 MPa (Alpert, 2005). The threshold of 10 % WC seems to have biological meaning, since it may correspond to the point at which there is no longer enough water to form a water film around macromolecules, stopping enzymatic reactions and thus metabolism (Billi and Potts, 2002).

The study of desiccation tolerant organism is of crucial importance for understanding the mechanism behind the response of plants to sub-optimal water availability and can in the

last instance be transferred to agronomical important crops in order to ensure the yield stability under mild water deficit.

1.4. Origins and Evolution of Desiccation Tolerance

Desiccation tolerance is an ancient trait in living organisms. Phylogenetic analyses and comparative surveys indicate that tolerance is an ancestral character in land plants or their spores (Oliver *et al.*, 2005) and that the character must have evolved very early during the evolution, since some features, like the occurrence of late embryogenesis abundant (LEA) proteins, are shared throughout kingdoms (Wise and Tunnacliffe, 2004).
Initial evolution of vegetative desiccation tolerance was a crucial step required for the colonization of the mainland by primitive plants. There are several lines of evidence supporting the assumption that desiccation tolerance is lost when organisms are no longer subject to desiccation, even when the genes for tolerance are still present (Alpert, 2006). With the evolution of the tracheophytes, vegetative desiccation tolerance was lost and its occurrence in a few clades of tracheophytes represents independent evolutions (or re-evolutions, at least 12 times), presumably in response to selection pressures associated with arid niches (Oliver *et al.*, 2005).
Tolerance in vegetative tissues of land plants may have been lost when the evolution of vascular water transport permitted adults the uptake and redistribution of water thus enabling them to cope with drought (Oliver *et al.*, 2005). Tolerance was conserved in seeds and spores, which were still subject to desiccation, and the genes needed for desiccation tolerance may be present in most desiccation-sensitive adult plants but not expressed or its function has diverged from the original one (Bartels and Salamini, 2001).
Porembski and Barthlott (2000) reported that rock outcrops (inselbergs) form a centre of diversity for desiccation-tolerant vascular plants. Inselbergs are monolithic rock outcrops which are sparsely covered with soil where water is seldom present and only for short periods in form of ephemeral pools. Of the 330 species of desiccation-tolerant vascular plants known, more than 90 % were found to occur on inselbergs (Porembski and Barthlott, 2000). The relative scarcity of desiccation-tolerant organisms in locations where water availability is high could depend on competition with desiccation-sensitive organisms, if there is a trade-off between tolerance and fitness. A plausible reason for competitive

inferiority of desiccation-tolerant organisms could be a trade-off between tolerance and growth or reproduction. Maximum growth or reproduction performance is often negatively associated with tolerance or resistance (Silvertown, 2004).
Selection for re-evolution of the desiccation tolerance may have occurred as various lineages spread into extremely dry habitats where they could not resist desiccation, such as onto rock outcrops in the tropics (Porembski and Barthlott, 2000). Re-evolution of tolerance in vegetative tissues may be mainly due to changes in regulatory genes and thus an example of evolution of development by re-programming the expression pattern of genes already present in the plant (Bartels and Salamini, 2001).

1.5. Desiccation Tolerance in Flowering Plants

Most flowering plants cannot survive exposure to a water content less than 85 % to 98 % (v/v) relative humidity during their vegetative growth period (Bartels and Salamini, 2001). Nevertheless, desiccation tolerance occurs in the developmental program of most higher plants during seed maturation. In fact, among the angiosperms, 95 % of the species have desiccation tolerant seeds.
The ability to tolerate complete desiccation in the vegetative tissues is found only in few plants; these include a small group of angiosperms, termed *resurrection plants* (Gaff, 1971), some ferns, algae, lichens, and bryophytes. Vegetative desiccation tolerance is common bryophytes (Oliver *et al.*, 2005) and rare in adult pteridophytes and angiosperms (Porembski and Barthlott, 2000).
Desiccation-tolerant vascular plants occur in 13 families and are most found within the monocotyledons and ferns. Of the 250,000 species of vascular plants, approximately 330 species have been documented as being able to survive desiccation in the vegetative growth phase (Porembski and Barthlott, 2000). Within the vascular plants, desiccation tolerance is found mainly in the monocotyledons. Only a few desiccation-tolerant dicots exist, in the families of the Gesneriaceae, Myrothamnaceae and Linderniaceae (Porembski and Barthlott, 2000).

1.5.1. *Craterostigma plantagineum* as Experimental System to Study the Desiccation Tolerance

C. plantagineum has been extensively used as a model organism to study the mechanisms involved in the desiccation tolerance. This plant is original from South Africa and its distribution correlates with dry habitats, mainly rock outcrops sporadically filled with water (Fischer, 2004). The interest in *C. plantagineum* derives from the fact that the desiccation tolerance is expressed both in the vegetative tissues and in the undifferentiated callus tissues (Bartels *et al.*, 1990). *C. plantagineum* calli are not intrinsically desiccation tolerant, but they acquire the ability to tolerate desiccation upon treatment with the plant hormone ABA (Bartels *et al.*, 1990). The ABA treatment induces in the callus a set of genes comparable to that induced by dehydration in the whole plant. This allows to study the mechanisms at the basis of desiccation tolerance in undifferentiated cells and to discriminate between the different contributions of the ABA and desiccation response.

1.5.2. The Linderniaceae Family

The Lamiales are one of the most diverse order of angiosperms, comprising more than 22,000 species. They are of particular importance because desiccation-tolerant plants like *Craterostigma plantagineum* Hochst. occur within this lineage (Takhtajan, 1997). Traditionally, *Craterostigma* and *Lindernia* species have been classified in the Scrophulariaceae family in the order Lamiales. Recently, the Scrophulariaceae have been reclassified by use of molecular markers and phylogenetic analyses demonstrated that this family is polyphyletic. As a consequence many *geni* belonging to the Scrophularieceae were reclassified and assigned to diverse families (Rahmanzadeh *et al.*, 2005). According to Rahmanzadeh *et al.* (2005), the analyses provide evidence for the monophyly of the *Craterostigma* and *Lindernia* lineages, which were included in the Linderniaceae family.
Besides all species of *Craterostigma*, several *Lindernia* species have been shown to be desiccation tolerant. However, the majority of *Lindernia* species such as *Lindernia rotundata* are desiccation sensitive (Fischer, 1992, 1995).
Recently it was reported that *Lindernia brevidens* Skan is desiccation tolerant (Phillips *et al.*, 2008). This is surprising since the plant is endemic to the montane rainforests of coastal Africa, a niche that does not experience drought. *Lindernia subracemosa* is a

close relative of *L. brevidens* and *C. plantagineum* and represents an example within the *Lindernia* genus of a species that is not able to survive desiccation.

1.6. The Role of Abscisic Acid in the Response to Water Stress

Abscisic acid (ABA) was discovered in the 1960s in studies aimed at discovering substances that regulate bud dormancy and leaf abscission. Later it turned out that ABA is a vital hormone that plants produce under adverse conditions. ABA is considered to be the 'stress hormone' integrating environmental limitations linked to changes in water activity with metabolic and developmental programs in plants (Zeevaart and Creelman, 1988).
Plants respond to environmental stimuli like drought and salt stress by changes in ABA level. This is exerted either by a re-distribution of the hormone (Slovik *et al.*, 1995) or by increased biosynthesis (Zeevaart and Creelman, 1988). However, ABA is not only a stress hormone but it has also been reported to control certain developmental or physiological functions in normal situations. Under non-stressed conditions, a basal ABA level fine-tunes optimal growth of plants by limiting ethylene production (Sharp, 2002). After exceeding certain threshold levels, ABA induces the effects linked to the stress response such as stomata closure and massive alteration of gene expression (Rock, 2000; Seki *et al.*, 2002).
The ABA biosynthetic pathway is a side-branch of the carotenoid pathway: ABA formation is the result of C_{40} carotenoid cleavage in plastids by a specific dioxygenase generating a C_{25} reaction product and the C_{15} compound xanthoxin, which is subsequently converted in the cytosol to abscisic aldehyde and ultimately to ABA (Hirt and Shinozaki, 2004). Many enzymes of the ABA biosynthetic pathway are upregulated by dehydration (Seo and Koshiba, 2002) and most genes involved in responses to dehydration are also induced by ABA.
Biochemical evidence supports the presence of both cell-surface and intracellular receptors for ABA (Assmann, 1994). Pandey *et al.* (2009) provided convincing evidences that the newly discovered GTG proteins with GPCR-like topology and GTPase activity are ABA receptors, thus throwing some new light in deciphering the first events in the ABA signalling relay.
Recently two groups ended up to the same ABA receptor complex using different ap-

proaches (Ma *et al.*, 2009; Park *et al.*, 2009). Ma and co-workers were searching for proteins that bind to ABI1 or ABI2. These are type 2C protein phosphatases (PP2C), the major group of protein phosphatases that have been identified in ABA signaling. Mutations in the genes for these proteins produce plants that are impaired in the normal ABA response. The researchers reported a new class of proteins that they called 'regulatory component of ABA receptor' (RCAR). Their experiments showed that although either ABI1 or ABI2 alone bind weakly to ABA, complexes of one of these enzymes and an RCAR bind quickly and strongly to the hormone. They concluded that the hormone starts its signaling cascade by binding to the RCAR-enzyme complexes and shutting down the enzymes activity.

1.6.1. Reversible Protein Phosphorylation in ABA Signalling

Phosphorylation is an effective and rapid mechanism of post-translational modification, which alters the activities of DNA binding factors and a plethora of intermediate molecules. Reversible protein phosphorylation is an early and central event in ABA signal transduction, at least in the guard cell (Leung *et al.*, 1997; Schmidt *et al.*, 1995; Sokolovski *et al.*, 2005). The major group of protein phosphatases involved in ABA signaling are the PP2Cs and at least four of them (ABI1, ABI2, AtPP2CA, HAB1; Schweighofer *et al.*, 2004) are genetically defined as negative regulators of ABA.

The mutant *abi1* and *abi2* proteins confer a genetically dominant ABA-insensitivity. Ectopic overexpression of abi1 and ABI1 in transient system were responsible for ABA-insensitivity indicating a negative regulatory role of the PP2C on ABA signalling (Sheen, 1998).

Tomato hypocotyls cells show an ABA-insensitive phenotype after injection with abi1 protein, while coinjection of ABI1 at a two- to threefold excess over the mutated protein rescued ABA-inducible transcription. Thus, ABI1 and abi1 compete for common binding sites and the wild-type protein is capable to restore proper ABA signal relay in agreement with a positive regulatory function of the specific PP2C (Wu *et al.*, 2003). The mechanism of ABI1 action was recently elucidated. The dominant phenotype is caused by a G to D mutation in the activation loop of the PP2C phosphatase. So far the dominant mutation was difficult to reconcile with the deleterious effect on its phosphatase activity. However, it has been shown that the *abi1* mutation causes a preferential accumulation of the protein

in the nucleus, where it acts as a negative ABA regulator (Moes *et al.*, 2008). The mutation also disrupts the interaction with the RCAR receptor, indicating that the mutant phosphatase escapes the negative regulation by ABA (Ma *et al.*, 2009).

The action of protein phosphatases such as ABI1 is counterbalanced by protein kinases. Several protein kinases have been implicated in ABA responses including Ca^{2+}-calmodulin regulated protein kinases (Sheen, 1996) and SNF1-like protein kinases such as PKABA1 (Anderberg and Walker-Simmons, 1992). One kinase crucial for the ABA signal transduction is AAKP (ABA Activated Protein Kinase) from *Vicia faba* (Li and Assmann, 1996). AAPK can directly phosphorylate in vitro the RNA-binding protein AKIP (AAPK Interacting Protein), which in turn binds to a mRNA encoding a dehydrin. AKIP is constitutively nuclear-localized, but becomes reorganized in 'nuclear speckles' subsequent to ABA activation (Li *et al.*, 2002). In *Arabidopsis thaliana* the orthologue kinase is OPEN STOMATA (OST)1/Srk2e/SnRK2.6. AAPK and OST1 belong to the protein family of SNF1-like protein kinases. Both kinases contain an N-terminal domain similar to SNF1/AMP-regulated protein kinase of yeast and a C-terminal domain with putative regulatory functions. Like the AAPK in *Vicia faba*, OST1 is also activated by ABA, and by hyperosmotic stress independently of ABA (Yoshida *et al.*, 2002; Boudsocq *et al.*, 2004). OST1 is one of the ten members belonging to the Sucrose Non-Fermenting Related Kinase 2 (SnRK2) family. These kinases are known as plant-specific, but they are named after their homology to the Sucrose Non-Fermenting kinase1 (SNF1) of yeast and the mammalian counterparts, the AMP-activated kinases. SNF1 and AMP-activated kinases have been primarily studied as metabolic regulators that are activated in response to energy deprivation. The ABA inducible kinases OST1, SnRK2.2 and SnRK2.3 all phosphorylate in vitro a motif in the Constant (C) subdomains found among basic-leucine zipper (b-ZIP) transcription factors, including ABA Responsive Element Binding protein (AREB)1, AREB2, and ABI5 (Furihata *et al.*, 2006).

Some b-ZIP transcription factors may also be the targets of calcium-dependent protein kinases (CPKs). Diverse CPKs were found to interact with and phosphorylate the ABA-Responsive Element Binding Factor (ABF)4 (Choi *et al.*, 2005).

In guard cells, ABA regulates repetitive cytosolic free Ca^{2+} ($[Ca^{2+}]_{cyt}$) oscillations. These repetitive Ca^{2+} transients play a role in both stomata opening and closure by regulating the ion channels responsible for the ion efflux (Israelsson *et al.*, 2006). In guard cells reversible protein phosphorylation depending on $[Ca^{2+}]_{cyt}$ activate anion channels, implying that

Ca^{2+}-regulated kinases may be involved in decoding the Ca^{2+} signal (Schmidt *et al.*, 1995). Reversible protein phosphorylation is also involved in stomata movement by H^+-ATPases. The calcium-dependent kinase PSK5 has been implicated as the negative regulating kinase, responsible for the phosphorylation on a specific Ser residue of the H^+-ATPase AHA2 (Fuglsang *et al.*, 2007).

ABA signaling events at the membrane level, involving many channels and transporters, have been elucidated using the guard cell system because of the clear role of ABA in stomatal closing to limit water loss through transpiration. Light induces stomatal opening, while ABA promotes closing. Light activates H^+-ATPases to hyperpolarize the plasma membrane, which drives potassium uptake and the increase in turgor of the guard cells to open the stomatal pore. ABA activates rapid and slow ion channels for $[Cl^-]$ efflux. In parallel, the hormone stimulates $[K^+]$ outward- and inhibits $[K^+]$ inward-rectifying channels to promote stomatal closure (Wasilewska *et al.*, 2008).

1.7. Synthesis of Protective Molecules

The final instance in the dehydration signalling cascade is the activation of genes responsible for the synthesis of compounds that protect cellular structures against the harmful effects of dehydration. Both desiccation-tolerant and -sensitive plants have been studied using different experimental system leading to the conclusion that the activation of protective mechanisms is a common theme in response to drought conditions. Trascriptome analysis in the sensitive plant *A. thaliana* could identify many genes that are cold- and drought-inducible and that share homologies to proteins involved in the seed development (Seki *et al.*, 2001). One question has therefore arisen: what makes a plant desiccation tolerant?

Desiccation tolerance is a complex trait and plants have obviously adopted a variety of different strategies. Studies conducted on desiccation tolerant seeds and the vegetative tissues of desiccation tolerant plants have identified some components of this complex protective mechanism (Bartels and Sunkar, 2005).

A prime secret of desiccation tolerance seems to be sugars. One function appears to be to protect the cell via glass formation. During desiccation, through the presence of sugars, a supersaturated liquid with the mechanical properties of a solid is produced, in a process

termed 'glass phase formation'. An important consequence of the formation of the glassy state is the absence of crystallization. It is proposed that loss of viability could rely on crystallization leading to the loss of membrane structure and cellular integrity (Sun and Leopold, 1993). One of the most addressed functions of the glasses is the maintenance of the structural and functional integrity of macromolecules. Sugars may maintain hydrogen bonds within and between macromolecules and preserve their structure (Hirt and Shinozaki, 2004; Buitink and Leprince, 2004).
Furthermore, it has been shown that glasses are able to prevent the fusion of membranes as a result of the loss of the hydration shell, by replacing the water molecules and interacting with the polar heads of the phospholipids. This propriety is of crucial importance in the rehydration process where otherwise membrane fusion would be responsible for the leakage of solutes and macromolecules from the lipid bilayer (Crowe *et al.*, 1996).
In *C. plantagineum*, the unusual sugar 2-octulose is present in leaves under normal growth conditions and is converted into sucrose upon water loss, comprising up to 40 % of dry weight in desiccated leaves. This conversion is reversible and 2-octulose accumulates again upon rehydration (Bianchi *et al.*, 1991). The close relative *L. brevidens* is also desiccation tolerant and sugar measurements showed similar values as *C. plantagineum* regarding the interconversion of 2-octulose and sucrose. Conversely, the desiccation-sensitive *L. subracemosa* does not accumulate sucrose upon dehydration, thus strengthening the hypothesis of a correlation in the Linderniaceae between sugar accumulation and osmotic stress tolerance (Phillips *et al.*, 2008).

1.7.1. Accumulation of Protective Proteins

Desiccation tolerant organisms, like the resurrection plant *C. plantagineum* and seeds of various plants have delivered a plethora of genes that are expressed upon dehydration and are likely to be involved in the acquisition of desiccation tolerance (Bartels *et al.*, 1990). Despite the large number of the up-regulated genes, our knowledge of the biochemical functions of their products is remarkably limited. A number of the genes isolated from resurrection plants share sequence homologies with genes that are expressed in maturing seeds, indicating a shared mechanism that operates in the seed development as well as in the acquisition of vegetative desiccation tolerance. The late embryogenesis abundant (LEA) proteins are the most evident and therefore studied class of proteins linked with the

response to severe water stress. The corresponding transcripts accumulate to high levels both in developing seeds and in vegetative tissues of desiccation-tolerant and -sensitive plants upon dehydration. Their occurrence in both tolerant and sensitive plants poses the challenge to identify the features defining their role in the desiccation tolerance.

Late Embryogenesis Abundant (LEA) Proteins

Late embryogenesis abundant proteins were first identified 20 years ago in developing cotton seeds (Dure *et al.*, 1981). Their name indicates the original discovery that they are expressed at high levels during the later stages of embryo development in plant seeds comprising up to 4 % of cellular proteins (Roberts *et al.*, 1993). Since the orthodox seeds acquire the ability to withstand extreme dehydration at this developmental stage, LEA proteins have been associated with desiccation tolerance (Cuming, 1999).

Expression profile The strongest support for a role of the LEA proteins during water stress comes from the observation that the accumulation of the proteins coincides with the acquisition of desiccation tolerance. Beside ABA and desiccation they have been found to respond to salt stress and cold stress.
The *Arabidopsis* genome contains 51 LEA proteins (Hundertmark and Hincha, 2008). The expression analysis of the whole set was performed in different tissues and developmental stages of *Arabidopsis* under a variety of conditions. The LEA protein gene set divides roughly into those with seed-specific expression and those expressed in vegetative tissues with surprisingly little overlap (Hundertmark and Hincha, 2008). This confirms that LEA proteins also have a role in vegetative tissues of non-desiccation tolerant plants like *e.g. Arabidopsis*.

Sequence Motifs and Classification LEA proteins were first classified in three groups by Dure *et al.* (1981), based on their sequence motifs. A more curated classification has been developed assigning Pfam motifs for the respective LEA protein groups, each defined by a Hidden Markov Model based in the first instance on a curated multiple sequence alignment (Bateman *et al.*, 2004).
The most widely used classification nomenclature is yet the one proposed by Bray (1993) based on predicted biochemical properties and sequence similarities. Group 1 LEA pro-

teins are characterized by a high proportion of glycine, glutamate and glutamine and an hydrophilic 20-amino-acid motif. This motif was first identified in the wheat Em protein, the first LEA protein identified (Cuming and Lane, 1979). Group 2 LEA proteins, also referred to as dehydrins, are the most widely studied LEA proteins (Close, 1997). Dehydrins are characterized by a 15 amino acid long lysine-rich motif (the K-segment), which is predicted to form an amphipathic α-helix, a tract of contiguous serine residues that can be phosphorylated and a conserved motif containing the consensus sequence DEYGNP (the Y segment), which is found close to the N-terminus of the protein. Group 3 LEA proteins share a characteristic repeat motif of 11 amino acids, predicted to form an amphipathic α-helix with possibilities for intra- and inter-molecular interactions. Group 4 LEA proteins are characterized by a conserved N-terminus predicted to form α-helices and a diverse C-terminal part with a random coil structure. Group 5 LEA proteins contain more hydrophobic residues than groups 1 to 4 and consequently are not soluble after boiling, leading to the suggestion that they probably adopt a globular conformation.
Wise (2003) has refined the group nomenclature based on newly-developed bioinformatics tools, the POPP (Protein or Oligonucleotide Probability Profile, Wise, 2001). The POPP analysis allows proteins to be compared based on similarities in their peptide compositions rather than similarities in their amino acid sequences. LEA proteins contain regions of low sequence complexity and these protein domains are routinely masked during sequence similarity searches because their inclusion can influence search statistics adapted to globular proteins. The POPP is designed to detect any over- or under-representation of particular amino acids or short peptides in a protein sequence. This has led to the definition of superfamilies (SFs) of LEA proteins, with one or more SFs comprising each of the main groups. In addition, the POPP approach was used to predict the function of the SFs, by querying proteins of unknown function against a database of POPPs for proteins of known function (Wise and Tunnacliffe, 2004).

Secondary modifications Phosphorylation has came out as an important secondary modification in LEA proteins. The serine stretch of the dehydrins can undergo phosphorylation and in the case of the maize DHN1/Rab17, distribution between nucleus and cytoplasm is controlled by phosphorylation of its serine stutter: removal of this sequence results in lack of phosphorylation and retention in the cytoplasm (Jensen *et al.*, 1998). Furthermore, the wheat dehydrin DHN–5, closely related to the maize RAB17, accumu-

lated differentially in two Tunisian durum wheat varieties with marked differences in salt and drought tolerance. The resistant variety accumulates the phosphorylated form of the protein whereas the susceptible variety accumulates only the unphosphorylated form (Brini *et al.*, 2007).

Irar *et al.* (2006) took advantage of the heat-stability of the LEA proteins to analyse the late-embryogenic-abundant phosphoproteome of *Arabidopsis* seeds. They found that several LEA-type and storage-like proteins were identified as components of the phosphoproteome of the *Arabidopsis* seed (Irar *et al.*, 2006).

Röhrig *et al.* (2006) investigated the phosphoproteome changes during dehydration in *C. plantagineum*, reporting that the major differences regarded the dehydration-dependent accumulation of two phosphoproteins, the dehydrin CDeT6–19 and the LEA-like protein CDeT11–24. Taken together, these observation strongly suggest that protein phosphorylation is pivotal for the ability of LEA proteins to exert an effect in the response of plants to dehydration stress.

Structure The first structural studies on LEA proteins arise from the wheat group 1 Em protein (McCubbin *et al.*, 1985). A variety of biophysical techniques indicated a lack of compactness, an asymmetrical or flexible conformation and little secondary structure, with as much as 70 % of the protein behaving as random coil. These early findings turn out to be largely typical for all groups of LEA proteins. In *C. plantagineum* attempts were made to resolve the structure of the CDeT6–19 protein, but it could not be crystallized due to the lack of a well-defined three-dimensional structure (Lisse *et al.*, 1996). Lack of conventional secondary structure means that members of the major LEA protein groups are included in the large class of proteins variously called 'natively unfolded', 'intrinsically disordered' or 'intrinsically unstructured' (Uversky *et al.*, 2000; Dunker *et al.*, 2001; Tompa, 2002).

Intrinsically disordered regions are highly abundant in nature. By estimations based on their sequence signature, about 10–20 % of full-length proteins belong to this class and 25–40 % of all residues fall into such regions.

One feature that distinguishes intrinsically unstructured proteins (IUPs) from globular proteins *in vivo* relates to the predictability of structural disorder from sequence. It is evident that IUPs identified *in vitro* have a distinct amino acid composition, in that they are enriched in disorder-promoting amino acids (A, R, G, Q, S, P, E and K) and depleted

in order-promoting amino acids (W, C, F, I, Y, V, L and N) (Tompa, 2005). Other manifestations of this distinct character is that they are usually characterized by a high net charge and low mean hydrophobicity.

IUPs are also characterized by a pronounced heat-stability. Having no hydrophobic core, they do not lose solubility at elevated temperatures; in fact, they are often purified via an intermittent heat-treatment step. A further indication is given by SDS polyacrylamide gel electrophoresis (SDS–PAGE), used to assess the molecular weight of proteins. Because of their unusual amino acid composition, IUPs bind less SDS than average proteins and their apparent mass is often 1.2–1.8 times higher than the real one calculated from sequence data.

Based on these sequence attributes, a range of bioinformatic predictors have been developed. Using the FoldIndex unfolded-protein prediction tool (Prilusky *et al.*, 2005) on a pool of LEA proteins it comes out that LEA proteins from groups 1, 2, 3 and the former group 4 are at least 50 % unfolded (Tunnacliffe and Wise, 2007). Such unfolded structure has implications on their functions: if they are almost entirely unstructured, it is unlikely that they have catalytic function unless, for example, they are induced to fold by co-factor or substrate binding.

The major functional benefit of IUPs is in fact the ability to adopt a structured conformation upon a disorder-order transition (i.e. induced local folding upon binding to their target). This transition is accompanied by a large decrease in conformational entropy, which uncouples binding strength from specificity and renders highly specific interactions reversible (Tompa, 2002; Dyson and Wright, 2005). An example is provided by the CREB transcription factor, which is intrinsically disordered in its isolated form, but it folds to form a pair of orthogonal helices upon binding to its target domain CBP, in a process modulated by phosphorylation (Radhakrishnan *et al.*, 1997).

IUPs fulfill functions often associated with signal transduction, gene expression and chaperone action (Tompa *et al.*, 2005). To perform these functions, structural disorder confers special advantages, such as the binding promiscuity, whereby an IUP binds distinct partners in a template-induced folding process. Accordingly, IUPs have the potential to modulate the action of different partner molecules, a propriety called *moonlighting* (Tompa *et al.*, 2005).

The template-induced folding and binding of IUPs could be the mode of action of the LEA proteins. Environmental conditions can also affect folding, and several LEA proteins

become more structured when dried (Goyal *et al.*, 2003; Tolleter *et al.*, 2007).
The group 3a LEA protein from the nematode *Aphelenchus avenae*, AavLEA1, show a conformational shift on dehydration (Goyal *et al.*, 2003). Although AavLEA1 is unstructured in solution, Fourier transform infrared (FT–IR) spectroscopic analysis shows that the protein becomes more folded upon drying, developing a significant α-helical component. Furthermore, spectral components were present that were consistent with the formation of superhelical structures, presumably coiled-coil like. This is an extremely unusual observation because protein dehydration is more often associated with a loss of structure and aggregation.
LEAM, a LEA protein expressed in mitochondria of pea seeds, also gain structure on drying (Tolleter *et al.*, 2007). LEAM is a natively unfolded protein, which reversibly folds into α-helices upon desiccation. Structural modeling revealed an analogy with class A amphipathic helices and liposome-drying assay demonstrated that LEAM interacts with membranes in the dry state and protects liposomes from drying.
In a recent work, Koag *et al.* (2009) showed that the K-segment of the maize dehydrin DHN1 is required for binding to anionic phospholipid vesicles, and adoption of α-helical structure of the K-segment accounts for most of the conformational change of DHN1 upon binding to anionic phospholipid vesicles or SDS.
Nevertheless, the picture coming out is that drying increases folding of at least some LEA proteins, supposing that such desiccation-induced conformational changes are related to their function.
Another recent observation on disordered regions indicates that phosphorylation commonly occurs within intrinsically disordered protein regions (Iakoucheva *et al.*, 2004). Relatively few regions of disorder have been structurally characterized, yet a significant fraction of them contain phosphorylation sites (Dunker *et al.*, 2002). Overall, disordered regions have a much higher frequency of known phosphorylation sites than ordered regions, suggesting a strong preference for locating phosphorylation sites in the regions of intrinsic disorder. Disordered regions also have significantly larger fractions of predicted phosphorylation sites than do ordered regions. Iakoucheva *et al.* (2004) exploited the similarity in sequence complexity, amino acid composition, flexibility parameters, and other properties between phosphorylation sites and disordered protein regions to develop a new predictor for phosphorylation sites. These common properties suggests in fact that intrinsic disorder in and around the potential phosphorylation target site is an essential common feature for

eukaryotic phosphorylation sites.
With regard to the structural consequences of phosphorylation, both disorder to order and order to disorder transitions have been observed to follow the phosphorylation event (Johnson and Lewis, 2001). In this way protein phosphorylation can trigger conformational changes affecting protein function.

Function Studies with plants transformed with LEA proteins could demonstrate a correlation between the over-expression of certain LEA proteins with the ability of the plant to perform better under diverse stress conditions (Xu *et al.*, 1996; Figueras *et al.*, 2004; Park *et al.*, 2005). Nevertheless, direct evidence of their mechanism of action comes predominantly by *in vitro* studies. Besides the functions proposed based on the conformational changes described in the previous paragraph, a number of recent studies could demonstrate that LEA proteins can protect enzymes like lactate dehydrogenase and citrate synthase against freezing and desiccation (Sanchez-Ballesta *et al.*, 2004; Goyal *et al.*, 2005). Goyal *et al.* (2005) could provide direct evidence that the protective function of the LEA proteins is due to their ability to prevent aggregation of desiccation-sensitive proteins. Moreover, they observed a synergistic effect of LEA and the sugar trehalose.
For some LEA proteins, an ion-binding activity has been observed. This activity seem to be due to the high content of histidine residues. The group 2 LEA proteins VCaB45 of celery and ERD10, ERD14 and COR47 of *Arabidopsis* can bind Ca^{2+} when phosphorylated (Heyen *et al.*, 2002; Alsheikh *et al.*, 2003, 2005). Some LEA proteins could also act as calcium buffers or be involved in the detoxification of metals.

Heat Shock Proteins (HSPs)

Another class of proteins that have recently been associated with desiccation tolerance are the HSPs (Alamillo *et al.*, 1995). The five major families of Hsps/chaperones are: the Hsp70 (DnaK) family; the chaperonins (GroEL and Hsp60); the Hsp90 family; the Hsp100 (Clp) family; and the small Hsp (sHsp) family.
In contrast to those of other eukaryotes, the most prominent HSPs of plants are small heat-shock proteins (sHSPs). They have monomeric molecular masses of 15–42 kDa, but assemble into oligomers of nine to over 20 subunits, depending on the protein (Waters *et al.*, 1996).

In vegetative tissues of *C. plantagineum*, constitutive expression of sHSPs has been detected (Alamillo *et al.*, 1995). Furthermore, in desiccation-sensitive callus tissue of *C. plantagineum* there was no accumulation of sHSPs protein, but sHSP expression and the subsequent acquisition of desiccation tolerance in the callus were induced by exogenous ABA treatment (Alamillo *et al.*, 1995).

Hsp70 chaperones, together with their co-chaperones, constitute a set of major cellular machineries that assist in almost all cellular compartments with a wide range of protein folding processes. Hsp70 has essential functions in preventing aggregation and in assisting refolding of non-native proteins under both normal and stress conditions (Hartl, 1996). Some family members of Hsp70 are constitutively expressed and are often referred to as Hsc70 (70-kDa heat-shock cognate). Other family members are expressed only when the organism is challenged by environmental constraints. Therefore, they are more involved in facilitating refolding and proteolytic degradation of non-native proteins (Hartl, 1996; Miemyk, 1997).

The major role of Hsp90 is to control protein folding (Frydman, 2001) but it also plays a key role in other contexts like signal-transduction networks, cell-cycle control, protein degradation and protein trafficking (Young *et al.*, 2001; Richter and Buchner, 2001). Although Hsp90 chaperones are constitutively expressed in most organisms, their expression increases in response to stress in both prokaryotes and eukaryotes. Expression of Hsp90 in *Arabidopsis* is developmentally regulated and responds to heat, cold, salt stress, heavy metals, phytohormones and light and dark transitions (Krishna and Gloor, 2001; Wang *et al.*, 2004).

1.8. The Importance of Protein Phosphorylation in Desiccation Stress Response

The proteome of an organism is a dynamic pool of proteins occurring in numerous isoforms each of them carrying different post-translational modifications (PTMs). PTMs of proteins are considered one of the major determinants responsible for the complexity of higher organisms, ensuring an appropriate response to diverse stimuli (Venter *et al.*, 2001).

There are at least 200 different types of PTMs known, but only few of them are reversible and crucial for the regulation of biological processes (Krishna and Wold, 1998). Among

all PTMs, the phosphorylation of proteins has attracted most interest. At least 30 % of all proteins are thought to contain covalently bound phosphate, often at multiple sites. Phosphorylation at multiple sites can have major effects on protein structure that can exert in changes in enzymatic activity, substrate specificity, complex formation, subcellular localization and stability. The most common type of phosphorylation, the O-phosphorylation, occurs on serine, threonine and tyrosine amino acids with a ratio of about 1000:100:1, respectively.

The importance and key role of reversible protein phosphorylation is supported by the high number of protein kinases and phosphatases contained in the genomes, constituting about 2 % of all genes in the humans (Manning *et al.*, 2002). In the plant kingdom this is even more evident, considering that plants devote to the phosphorylation of proteins more than 1000 kinases, approximately twice the number found in mammals (Arabidopsis-Genome-Initiative, 2000; Manning *et al.*, 2002). It is therefore of crucial importance to gather data on phosphorylated residues in order to help understanding the intricate regulation of proteins by phosphorylation.

Evidence is accumulating indicating that protein phosphorylation plays an important role in plant responses to water stress (Bartels and Sunkar, 2005; Röhrig *et al.*, 2006, 2008). Protein kinases and phosphatases are regulated by water stress (Bartels and Sunkar, 2005) and several LEA proteins have been documented to undergo phosphorylation (Irar *et al.*, 2006; Jensen *et al.*, 1998; Plana *et al.*, 1991; Jiang and Wang, 2004). Röhrig *et al.* (2006) reported the dehydration-induced protein phosphorylation in the resurrection plant *C. plantagineum*. Two major proteins undergo phosphorylation in response to desiccation, the LEA-like CDeT11–24 and the dehydrin CDeT6–19.

1.8.1. Methods for the Identification of Phosphoproteins

Standard procedures to identify phosphorylated proteins include isotopic labeling with ^{32}P followed by SDS–PAGE, Western blotting employing phosphospecific antibodies, direct staining of phosphoproteins by a fluorescent dye specific for phosphorylated proteins (ProQ Diamond) or phosphatase treatment coupled to 2D electrophoresis to exploit the charge variation occurring after phosphatase treatment to discriminate between phosphorylated and unphosphorylated proteins (Raggiaschi *et al.*, 2005).

However, the traditional methods are inadequate to identify the low abundant phospho-

proteins because of the low stoichiometry of the secondary modification. Moreover, mass spectrometry based approaches are biased by the presence of non-phosphorylated peptides which suppress the signal from their phosphorylated counterpart. This imposes the choice of a purification step to enrich phosphorylated proteins from non-phosphorylated proteins to provide better identification.

One such methods exploits the capacity of trivalent cations like Fe^{3+} and Al^{3+} to bind to phosphoaminoacids in order to enrich phosphopeptides (Immobilized Metal Affinity Chromatography, IMAC) or phosphoproteins (Metal Oxide Affinity Cromatography, MOAC). The major limitation of this approach is the aspecific binding of non-phosphorylated proteins to the matrix due to proteins or peptides containing a high number of acidic residues like glutamic and aspartic acid (Raggiaschi *et al.*, 2005). This drawback can be overcome either by the derivatization of the carboxylate groups to the corresponding methyl esters (Ficarro *et al.*, 2002) or by adding an excess of free acidic residues to compete for the binding to the matrix (Wolschin and Weckwerth, 2005).

An approach recently developed based on the MOAC procedure (Wolschin and Weckwerth, 2005; Wolschin *et al.*, 2005) has already been applied to phosphoproteins enriched from *C. plantagineum* leaves. The combination of phosphoprotein enrichment by aluminum hydroxide and phosphoprotein-specific staining of 2D PAGE separated samples by ProQ Diamond led to the identification by MS analysis of 22 phosphoproteins (Röhrig *et al.*, 2008).

1.9. Aims of this Study

In order to unravel the mechanisms at the basis of desiccation tolerance, a comparative approach was performed.

An objective of this study was to investigate the ability of *Lindernia brevidens* and *Lindernia subracemosa* to survive desiccation by means of phenotypic observation at the macroscopic level as well as at the cellular level.

Since the plants *L. brevidens* and *L. subracemosa* display different phenotypes regarding the desiccation tolerance trait, their comparison provides a testable system to gain more insights into the complex mechanism of water stress response.

In order to perform this, a candidate protein was chosen which has been shown to undergo phosphorylation during the onset of dehydration in the close relative *Craterostigma plantagineum*. The aim was to isolate the homologues of the candidate LEA-like protein CDeT11–24 from the *Lindernia* species for comparing their amino acidic sequences and secondary structure features.

Covalently bound phosphate has been suggested as a mechanism for regulating CDeT11–24. Therefore, the phosphorylation status of the 11–24 proteins was dissected in response to the tissue priming by the plant hormone ABA and by desiccation treatment to elucidate the regulation of the phosphorylation event. Moreover, the analysis on the phosphorylation status of the homologue proteins from *Lindernia* was crucial for revealing the correlation between their secondary modification status and the ability of the plant to withstand desiccation. The position of the phosphorylated residues was then analyzed to map their occurrence with respect to predicted secondary structures.

The *in silico* prediction and phosphorylation sites identification suggested a relationship between the secondary modification and the structure of the CDeT11–24 protein. To test this hypothesis, potential interaction partners were investigated. The goal of the affinity chromatography was to identify proteins differentially binding to the bait protein CDeT11–24 in its phosphorylated and unphosphorylated form to verify the potential role the phosphorylation event could have in determining the binding partners of CDeT11–24.

In order to identify other proteins which undergo phosphorylation during desiccation a phosphoproteomic approach was applied on *C. plantagineum* callus tissue to explore changes in the phosphoproteins upon ABA and desiccation treatment. Previous data indicated that reversible protein phosphorylation occurs in the dehydration/rehydration cycle of *C. plan-*

tagineum leaf tissues, leading to the identification of many proteins, mostly associated with the photosynthesis, in particular the high abundant protein RuBisCO. The callus system combines the advantage of lacking the abundant phosphoprotein RuBisCO, which would mask other low-abundant proteins, with the possibility to dissect the ABA induction from the dehydration treatment. An enrichment approach based on the affinity of phosphate groups for titanium dioxide coupled to a phosphoprotein-specific stain was applied to track the changes of the phosphoproteome of *C. plantagineum* callus. This enabled the comparison of the protein pattern in order to identify candidates regulated by the ABA and desiccation treatment.

2. Materials and Methods

2.1. Plant Material

The subject of this study were *Craterostigma plantagineum*, *Lindernia brevidens* and *Lindernia subracemosa*. The plants were cultivated in the botanical garden of the University of Bonn and in the case of *Lindernia brevidens* and *Lindernia subracemosa* they were originally collected from the Taita Hills, Kenya, by Prof. E. Fischer (University of Koblenz). *Craterostigma plantagineum* plants were collected as described in Bartels *et al.* (1990).

2.1.1. Growth Conditions

Craterostigma plantagineum plants were grown under sterile conditions in MS agar pots under a light intensity of 80 μE m^{-2} sec^{-1} at 22 °C with a day/night cycle of 13/11 hours and subcultivated every six weeks.
Craterostigma plantagineum calli were induced from leaf pieces on MS–IK22 medium under the same conditions and subcultivated every three weeks.
Non sterile plants were cultivated in pots with granulate, watered with a 0.1 % solution of Wuxal (Manna, Ammerbuch–Pfäffingen, GER) at 18 °C with a day/night cycle of 13/11 hours.
Lindernia brevidens and *Lindernia subracemosa* were grown on soil under a light intensity of 80 μE m^{-2} sec^{-1} at 22 °C with a day/night cycle of 13/11 hours.

2.1.2. Plant Stress Treatments

Dehydration stress was imposed to adult plants by withholding watering for different periods of time.

ABA treatment was imposed on *C. plantagineum* calli by incubating them for six days on MS–IK22 agar plates supplemented with 20 μM ABA. Detached leaves were incubated for 24 hours in an 100 μM ABA solution.
The water content of the plants subjected to the dehydration treatment was calculated as relative water content (RWC) according to the equation RWC $= \left[\frac{(FW-DW)}{(TW-DW)}\right] \times 100$, or only on dry weight basis expressing the water content as $\frac{(FW-DW)}{DW}$, where FW is the fresh weight, TW is the weight after incubating the plant tissue for 24 h in pure water, DW is the weight of the tissue after 24 h treatment at 80 °C.

2.2. Bacterial Strains

Escherichia coli DH10B (Lorow and Jessee, 1990)

Genotype: F^- mcrA Δ(mrr-hsdRMS-mcrBC) Φ80d lacZΔM15 ΔlacX74 endA1 recA1 deoR Δ(ara, leu)7697 araD139 galU galK nupG rpsL λ^-.
This *E. coli* strain was used for cloning purposes.

Escherichia coli XL1–Blue MRF´ (Stratagene, Amsterdam, NL)

Genotype: Δ(mcrA)183 Δ(mcrCB-hsdSMR-mrr)173 endA1 supE44 thi-1 recA1 gyrA96 relA1 lac [F´ proAB $lacI^qZ\Delta M15$ Tn10 (Tet^r)].
This *E. coli* was used as host strain for the UniZAP XR phage library.

Escherichia coli SOLR™ (Stratagene, Amsterdam, NL)

Genotype: e14$^-$(McrA$^-$) Δ(mcrCB-hsdSMR-mrr)171 sbcC recB recJ uvrC umuC::Tn5 (Kan^r) lac gyrA96 relA1 thi-1 endA1 λ^R [F´ proAB $lacI^qZ\Delta M15$] Su$^-$ (nonsuppressing).
This *E. coli* strain was used for the excision of the phagemid from the UniZAP XR vector.

Escherichia coli BL21(DE3) (Pharmacia, Freiburg, GER)

Genotype: F^-, ompT, hsdS(r^-_B, m^-_B), gal, dcm, λDE3 (lacI, lacUV5-T7 gene 1, ind1, sam7, nin5).
This *E. coli* strain was used for the overexpression of the His-tagged CDeT11–24 protein.

2.2.1. Growth of Microorganisms

E. coli strains were incubated and cultured either in liquid LB medium at shaking with 200 rpm or in solid LB–agar medium at 37 °C with the corresponding antibiotic for selection.

2.2.2. Glycerol Stocks

To store the bacteria bearing a construct of interest, glycerol stab cultures were produced by adding to 0.85 ml of an overnight culture 0.15 ml of sterile glycerol in a 2 ml screw cap tube. The tube was vortexed, frozen in liquid nitrogen and stored at −70 °C.

2.3. Phages and Vectors

The plasmid vectors used in this work are listed below. Details and sequence features of the vectors are provided in the appendix (see Appendix A.1 on page 154).

pBluescript® II SK(−)	Cloning vector for cloning the *C. plantagineum* cDNA library into the SOLR™ bacterial strain (Stratagene, Amsterdam, NL)
pJET	Cloning vector for PCR products (Fermentas, Burlington, CDA)
pET28a	Expression vector for His-tagged protein overexpression (Novagen, Darmstadt, GER)

2.4. Chemicals

The chemicals used in this work were purchased from: Amersham Biosciences (Little Chalfont, UK), Applichem (Darmstadt, GER), Biorad (Hercules, CA), GE Healthcare (Piscataway, NJ), Grüssing (Filsum, GER), Invitrogen (Carlsbad, CA), Macherey–Nagel (Düren, GER), Manna (Ammerbuch–Pfäffingen, GER), Merck (Darmstadt, GER), Millipore (Billerica, MA), Pharmacia (Uppsala, SW), Qiagen (Hilden, GER), Roche (Mannheim, GER),

Roth (Karlsruhe, GER), Serva (Heidelberg, GER), Sigma–Aldrich/Fluka (St. Louis, MO), Stratagene (La Jolla, CA), Whatman (Maidstone, UK).

2.5. Enzymes and Markers

Enzymes and the corresponding buffers were purchased from Fermentas (Burlington, CDA), Invitrogen (Carlsbad, CA), Stratagene (La Jolla, CA), Sigma–Aldrich (St. Louis, MO), Promega (Madison, WI), New England Biolabs (Ipswich, MA).

2.6. Membranes

Protein transfer was performed on Protran BA 85 (0.45 μm) membranes (Whatman, Maidstone, UK).

2.7. Kits

DNA fragments were isolated with the help of the QIAEX II Gel Extraction Kit (Qiagen, Hilden, GER) and NucleoSpin® Extract II Kit (Macherey–Nagel, Düren, GER). The RT–PCR was performed using the totalscript–OLS® Kit (OLS, Hamburg, GER).

2.8. Equipment

Device	Name	Company
PCR machine	T3 Thermocycler	Biometra, Göttingen, GER
Horizontal gel electrophoresis	Compact S/M	
SDS–PAGE	Minigel	Biometra, Göttingen, GER
	Ettan Daltsix	Amersham Biosciences, Piscataway, NJ

Device	Name	Company
Imaging system	Typhoon 9200 Variable Mode imager	Amersham Biosciences, Piscataway, NJ
Scanner	Imagescanner II	
Protein blotting cell	Criterion blotter	Biorad, Hercules, CA
Spectrophotometer	SmartSpec 3000	
Chemiluminescence detector	Intelligent Dark Box II	FUJIFILM Corporation, Tokyo, JP
Heating block	QBT digital block heater	Grant Instruments ltd, Shepreth, UK
Rotation shaker	Innova 4000 Incubator shaker	New Brunswick Scientific, Edison, NJ
	Incubator Shaker G25	
	Chromate® U	B. Braun Biotech Inc., Allentown, PA
Power supply	Electrophoresis power supply	Gibco BRL, Carlsbad, CA
UV illuminator	Intas UV systems series CONCEPT	Intas Pharmaceutical ltd., Gujarat, IN
Vortex	VTX–3000L	LMS, Tokyo, JPN
Centrifuge	Microcentrifuge 5415 D	Eppendorf, Hamburg, GER
	Microcentrifuge 5417 R	
	Centrifuge 5810 R	
	Sorvall RC 5C Plus	Du Pont, Bad Homburg, GER
	L8–70M Ultracentrifuge	Beckman Coulter, Fullerton, CA

Device	Name	Company
Balance	BL 1500 S	Sartorius, Göttingen, GER
	BP 61 S	
Electroporator	Gene Pulser II with Pulse Controller II and Capacitance Extender II	Biorad, Hercules, CA
Spot picker	Proteineer spII	Bruker Daltonics, Bremen, GER
Spot digester	Proteineer dp	
Mass spectrometer	Ultraflex III	

2.9. Databases and Softwares

Typhoon Scanner Control software 3.0 was used for detection of proteins stained with fluorescent dyes and images were edited with ImageQuant 5.2. Images were further rendered with Adobe Photoshop CS3. 2D gels were compared with the help of Proteomweaver (BioRad).

Sequence analysis, translation of sequences, cloning strategies and rendering of vector charts were performed with Vector NTI Advance™ 10 (Invitrogen, Carlsbad, CA). Furthermore open source programs and databases were used for DNA and protein analysis (ExPASy), for sequence alignment (ClustalW) and for databanks consultation (National Center of Biotechnological Information). Phosphoproteins search was done with the tools provided in the P^3DB database (http://digbio.missouri.edu/p3db/). For MS spectra analysis, database search was performed using Mascot 2.2 (Matrix Science).

The Ka/Ks ratio calculation was done with the MEGA4 package described in Tamura *et al.* (2007).

2.10. Media

MS–IK22 Medium	4.3 g/l MS Medium, 20 g/l sucrose, 250 mg/l antioxidant mix, adjust to pH 5.8 with NaOH, 8 g/l agar, 0.2 % (v/v) vitamin solution, 0.1 % (v/v) IAA solution, 0.02 % (v/v) Kinetin solution, 0.05 % (v/v) 2,4-D solution, 0.02 % (v/v) 2iP solution.
LB Medium	10 g/l peptone, 10 g/l NaCl, 5 g/l yeast extract, adjust pH to 7.5, and 15 g/l agar (optional) for agar plate cultures.
SOC Medium	20 g/l tryptone, 5 g/l yeast extract, 10 mM NaCl, 2.5 mM KCl, 10 mM $MgCl_2$, 10 mM $MgSO_4$, 20 mM glucose.
NZY Medium	5 g/l NaCl, 2 g/l $MgSO_4$, 5 g/l yeast extract, 10 g/l casein hydrolysate, 15 g/l agar.
NZY Top Agar	NZY Medium with an agarose concentration of 0.7 %.
HMFN buffer (10×)	**Part 1 (for 800 ml)** 760 mg $MgSO_4$, 4.5 g tri-sodium citrate, 9 g $(NH_4)_2SO_4$, 440 g glycerin. **Part 2 (for 200 ml)** 18 g KH_2PO_4, 47 g K_2HPO_4 Both solutions are separately autoclaved and put together.

2.10.1. Supplements for Media

Ampicillin	Stock solution: 100 mg/ml in water; Working solution: 1:1000 diluted.
Kanamycin	Stock solution: 50 mg/ml in water; Working solution: 1:1000 diluted.
Vitamin solution	Stock solution: 50 mg/ml myo-inositol, 0.5 g/ml ascorbic acid, 2.5 mg/ml pyridoxin-HCl, 0.5 g/ml nicotinic acid.
IAA	Stock solution: 2 mg/ml in EtOH

Kinetin	Stock solution: 1 mg/ml in EtOH
2,4-D	Stock solution: 1 mg/ml in EtOH
2iP	Stock solution: 1 mg/ml in NaOH
ABA	Stock solution: 100 mM in EtOH; Working solution: 1:5000 diluted in MS–IK22 Medium
IPTG	Stock solution: 100 mM in water; Working solution: 1:100 diluted in LB Medium
Supplements for LB	10 ml/l of 1 M $MgSO_4$, 3 ml/l of 2 M maltose

All the supplements were filter sterilized and added to the medium after the autoclaving.

2.11. Primers

Table 2.1: List of the primers used in this work. The nucleotides underlined represent the restriction sites introduced by mutagenesis PCR.

Primer	Sequence (5'→3')	Restriction site
11–24_fwd_Eco	AAGGTGTTAAAGAATTCGACG	*Eco*RI
11–24_rev_Xho	CGATCACTGCTCGAGCTTAGC	*Xho*I
11–24_full_Nde	ATAACATATGGAATCGCAATTGCACCGC	*Nde*I
11–24_full_Xho	ATATTCTCGAGCTGAAGATGATCACTGC	*Xho*I
cratero_fwd	TCCTTTCTCAGACAGTTCGAATAAG	–
cratero_rev	GATCACTGCTCAACCTTAGCAGCT	–
brev_fwd_up	TCTACATCGTCATTCGAGGAA	–
brev_fwd_down	AGAAAATGGAGTCGCAAATGC	–
brev_rev	TCCGATCACTCTACTGCTCC	–
subra_fwd	AGAATAGAAGATGGAATCGCAA	–
subra_middle	CCTCAAGATATGGAAACAGAGTTC	–
subra_rev	TCCTCCGATCACTGCTCCA	–

2.12. Scanning Electron Microscopy

The Scanning Electron Microscopy (SEM) images were taken as described by Phillips *et al.* (2008). Hydrated and rehydrated leaf samples were fixed in 2 % (v/v) glutaraldehyde in phosphate-buffered saline (PBS, pH 7.2; Maniatis *et al.* 1986), and were dehydrated through a graded ethanol series (from 10 % to 100 % in 10 % steps). The dehydrated samples were then diluted in PBS buffer prior to critical-point drying with a critical-point device (CPD 020, Balzers) according to the method of Svitkina *et al.* (1984). Desiccated leaf samples were observed directly without treatment. All leaf specimens were gold coated with a sputter-coater (SCD 040, Balzers) and viewed using an LEO 1450 scanning electron microscope (Carl Zeiss Jena).

2.13. Extraction of Nucleic Acids

2.13.1. Extraction of RNA from Plant Tissue

RNA extraction was performed according to Valenzuela-Avendaño *et al.* (2005). Plant material was frozen in liquid nitrogen and ground to a fine powder. Subsequently the material was resuspended in 1.5 ml of extraction buffer, homogenized and incubated at room temperature (RT) for 10 min. The samples were centrifuged at 10,000 *g* at (RT) for 10 min to separate the cell debris.

The supernatants were transferred to new tubes, 300 μl of chloroform:isoamylalcohol (24:1; v/v) were added and then vortexed for 10 s. The tubes were centrifuged at 10,000 *g* at 4 °C for 10 min. The clear aqueous phase was transferred to new tubes and 375 μl of isopropanol and 375 μl of 0.8 M sodium citrate/1 M sodium chloride mixture were added. The samples were mixed thoroughly and incubated at room temperature for 10 min, followed by a centrifugation at 12,000 *g* at 4 °C for 10 min. The supernatant was discarded and the pellet washed with 1 ml of 70 % ethanol at −20 °C, followed by a subsequent centrifugation at 10,000 *g* at 4 °C for 10 min. The pellet was dried and dissolved in DEPC-treated H_2O. 167 μl of 4 M LiCl (2.5 M final concentration) were added and the samples incubated on ice for 2 hours. The tubes were then centrifuged at 14,000 *g* at 4 °C for 20 min. The resulting pellet was washed twice with 1 ml of 70 %

ethanol at −20 °C, air-dried, resuspended in DEPC-treated H_2O and stored at −70 °C.

Extraction buffer	38 % (v/v) buffer-saturated phenol, 0.8 M guanidine thiocyanate, 0.4 M ammonium thiocyanate, 0.1 M sodium acetate pH 5.0, 5 % (v/v) glycerol, 0.1 % phenol red

2.13.2. Extraction of Plasmid DNA from *Escherichia coli*

Two ml of an overnight bacterial culture were spun down for 30 sec at maximal speed and the supernatant was removed. The resulting pellet was resuspended in 200 μl of TELT buffer and 20 μl lysozyme (10 mg/ml stock solution), incubated for 3 minutes at 95 °C and cooled on ice. The lysate was centrifuged at maximal speed at 4 °C for 15 min and the supernatant was transferred to a new tube with 100 μl isopropanol, mixed by inversion and spun again for 15 min. The resulting DNA pellet was washed with 70 % ethanol and resuspended in TE or TE/R buffer.

TELT buffer	50 mM Tris-Hcl pH 8.0, 62.5 mM EDTA, 2.5 M LiCl, 0.4 % Triton X100.
TE buffer	10 mM Tris-HCl pH 7.5, 1 mM EDTA.
TE/R buffer	RNase stock solution (100 μg/ml) diluted to a concentration of 10 μg/ml in TE.

2.13.3. Purification of DNA Fragments from Agarose Gels

After PCR amplification the DNA bands were isolated from agarose gels using the NucleoSpin® Extract II Kit (Macherey–Nagel). The extraction and purification were done after excising the bands from the agarose gel followed by the purification according to the instructions of the manufacturer.

2.13.4. Precipitation of DNA with Phenol-Chloroform-Isoamylalcohol (PCI)

To remove the enzymes after a digestion or to concentrate it, the DNA was precipitated by the PCI method. The sample was brought to a volume of 50–100 μl with water and diluted 1:1 with PCI (25:24:1). The tubes were thoroughly mixed and centrifuged for 5 min at 14,000 g at RT. The upper aqueous phase was mixed with 0.1 volumes of 3 M sodium acetate pH 5.2 and 2.5 volumes of 100 % ethanol and precipitated for 1 h at $-20\,^{\circ}$C. After a centrifugation for 20 min at 14,000 g at 4 °C, the pellet was washed with 70 % ethanol and air-dried.

2.13.5. Estimation of Nucleic Acids Concentration

Isolated nucleic acids (DNA and RNA) were qualitatively checked by agarose gel electrophoresis. The concentration of the nucleic acids was spectrophotometrically determined by measuring the absorbance at 260 nm. A solution of pure double-stranded DNA with a concentration of 50 μg/ml has an A_{260} of 1.0, this value for an RNA solution corresponds to a concentration of 40 μg/ml. To assess the purity of a nucleic acids preparation, the ratio A_{260}/A_{280} was measured. For DNA the ratio should lie between 1.8 and 2, a lower value indicates contamination by proteins or phenolic compounds; for RNA the ratio should be at least 2.

2.14. Electrophoresis of Nucleic Acids

In order to ascertain the quality of nucleic acids and the specificity of the restriction reactions, the DNA and RNA molecules were separated by electrophoresis on agarose gels with a concentration ranging from 1 % to 2 % depending on the size of the molecules to be separated. The gels were prepared in 1× TAE buffer containing 1:1,000 (v/v) ethidium bromide solution (10 mg/ml) and the samples were loaded in 1× gel loading buffer. The electrophoresis was performed in 1× TAE buffer at 5 V/cm and gels were observed under UV light.

TAE buffer (50×)	for 1 liter: 242 g Tris, 57.1 ml glacial acetic acid, 100 ml EDTA 0.5 M (pH 8.0).
Gel loading buffer (10×)	0.25 % bromophenol blue, 30 % glycerol, in 1× TAE.

2.15. Cloning Methods

2.15.1. Primer Design

For PCR amplification and DNA sequencing specific primers were designed according to the following criteria: The GC content of a primer should be close to 50 %. The melting temperature (TM) was calculated according to the equation $TM = 4 \times (G + C) + 2 \times (A + T)$. Ideally the TM lies aproximately between 60 and 65 °C. The primers were designed to avoid self-complementation using Vector NTI Advance™ 10 (Invitrogen). Forward and reverse primers of each PCR reaction were designed to have approximately the same TM. In the case of mutagenesis PCR mismatches were allowed to introduce novel restriction sites according to the cloning strategy.

2.15.2. Synthesis of cDNA

In order to be able to amplify by PCR the full length transcripts encoding the protein of interest, retrotranscription of the mRNA into cDNA was performed.

DNase Treatment

8 μg of total RNA
2 μl of RNase free DNase (10 U/μl, Boehringer/Roche)
x μl 100 mM sodium acetate pH 5.2, $MgCl_2$ 5 mM

---

up to 100 μl

The reaction was incubated at 37 °C for 1 h, extracted with PCI (described in section 2.13.4) and precipitated with 0.5 volumes 7.5 M ammonium acetate and 2 volumes 100 % ethanol for 1 h at −20 °C. After 20 min centrifugation at 14,000 *g* at 4 °C, the resulting

pellet was washed with 70 % (v/v) ethanol, air-dried and resuspended in 10 μl DEPC water. The RNA was then used as template for the retrotranscription.

cDNA Synthesis

5 μl DNase-treated RNA
2 μl Oligo(dT)$_{10}$-Primer (25 pmol/μl, Boehringer/Roche)
1 μl 10 mM dNTPs
4 μl DEPC water

To denature the RNA and to allow the primers to anneal the reaction was incubated at 65 °C for 5 minutes and immediately cooled on ice. Then the following components were added:

4 μl of the First-Strand 5$\times$ buffer (250 mM Tris-HCl pH 8.3,
375 mM KCl, 15 mM $MgCl_2$, Invitrogen)
2 μl of 0.1 M DTT
1 μl of RNaseOUT™(40 U/ μl, Invitrogen)

The samples were incubated at 42 °C for 2 min to reach the optimal temperature for the retrotranscription. To each tube 1 μl of SuperScript II Reverse Transcriptase (200 U/μl, Invitrogen) was added and the reaction mixture was incubated at 42 °C for 1h. To inactivate the enzyme the tubes were heated at 70 °C for 5 min. The cDNA obtained was further used as template for PCR reactions.

2.15.3. Polymerase Chain Reaction (PCR)

DNA fragments were amplified from plasmid DNA or cDNA by PCR. The mixture was prepared as follows:

Reagents (stock conc.)	**Final conc.**
$MgCl_2$ (25 mM)	1.25 mM
dNTPs (10mM)	200 μM
forward-primer (100 μM)	0.5 μM
reverse-primer (100 μM)	0.5 μM
template DNA	$\sim$2 ng
taq buffer (10$\times$)	1$\times$
taq DNA polymerase (2.5 U/μl)	1 U
H_2O	up to final volume

A standard PCR program follows:

First denaturation step	94 °C	5 min	
Denaturation step	94 °C	30 sec	} 35 cycles
Annealing step	T_a	30 sec	
Elongation step	72 °C	1–2 min	
Final elongation step	72 °C	5 min	
End	4 °C	∞	

The annealing temperature (T_a) was set 5 °C below the melting temperature of the primers.

2.15.4. PEG Precipitation and Cloning into pJET1.2

30 % (v/v) PEG 8000/30 mM $MgCl_2$ were used to purify PCR products from other DNA fragments smaller than 300 bp, including primer dimers. The PCR reaction was diluted 4-fold with TE buffer and $\frac{1}{2}$ volume of PEG solution was added (final concentration 10 % PEG, 10 mM $MgCl_2$). The mixture was shaked vigorously by vortexing and centrifuged at full speed for 15 min. The resulting pellet was resuspended in TE at a concentration greater than 10 μg/μl and used for cloning in pJET1.2 (see Appendix, A.1) according to the manufacturer's instructions (Fermentas).

2.15.5. Restriction Digestion

DNA digestion was carried out by restriction endonucleases as follows: $\sim 1 \mu g$ of DNA was digested with 5 U of each enzyme and 5× buffer for 1–2 hours at 37 °C. The reaction volume must be at least 10 times the volume of enzyme used to dilute the glycerol of the storage buffer.

2.15.6. Ligation

For cloning of DNA amplicons into plasmids, a ligation reaction was set up including the suitable controls without ligase (in the case of single enzyme restriction to check the amount of undigested plasmid) and without insert (in the case of double digestion to check the amount of single-site digested plasmid). The ligation reaction was performed in an 10 μl final volume comprising 1 μl ligase buffer (10×), x μl digested plasmid DNA vector, 1 μl T4-ligase (Roche), and y μl DNA insert. The reaction mix was brought to the final volume with sterile H_2O and incubated at 16 °C for 20 h. For an efficient ligation reaction the amount of plasmid vector must be one third of the insert. The ratio is referred to the number of molecules. The amount of insert to use, having a certain amount of vector, is given by the formula: $\mu g_{ins} = \frac{\mu g_{vec} \times Kb_{vec}}{Kb_{ins}} \times$ molar ratio $\frac{vector}{insert}$. The ligation reaction was then used for bacterial transformation.

2.15.7. Transformation

Preparation of Electrocompetent *Escherichia coli* cells

A single colony of either *E. coli* DH10B or BL21 was inoculated into 5 ml LB medium and cells were grown overnight at 37 °C with moderate shaking. 2 ml of the culture were used to inoculate 200 ml LB medium in a sterile 1 l flask. The flask was incubated at 37 °C with shaking at 300 rpm until an OD_{600} of ∼0.5–0.7 was reached. Cells were then chilled on ice and subsequently transferred in 4 tubes of 50 ml. Cells were kept on ice during all following steps. The tubes were centrifuged for 15 minutes at 4,000 *g* at 4 °C and the supernatant was poured off. Cells were then resuspended in ice cold water and the volume adjusted to 50 ml with water. The tubes were centrifuged as above, the resulting

pellets were resuspended in 25 ml ice cold water and the suspension brought together in two 50 ml tubes. After centrifugation the pellets were resuspended again in 25 ml water and transferred in one tube. The cells were spun down, resuspended in 25 ml of 10 % (v/v) glycerol and centrifuged again. The remaining pellet was resuspended in 2 ml 10 % (v/v) glycerol, divided in 50 μl aliquots and stored at $-80\,^{\circ}$C.

Transformation by Electroporation

Aliquots of electrocompetent cells were thawed on ice before transformation. About 5 pg to 0.5 μg DNA of a ligated vector or purified plasmid DNA was added to the competent cells and carefully mixed in a precooled electroporation cuvette. The electroporation apparatus (GenePulser II, BioRad) was set to 1.6 kV, 2.5 μF and the pulse controller set to 200 Ω. The electroporation was performed and 1 ml of SOC medium was immediately added to the transformed cells. The cells were transferred in a 5 ml tube and incubated for 1 h at 37 °C shaking at 250 rpm. Aliquots of the transformed cells were then plated on LB medium with the appropriate antibiotic and incubated overnight at 37 °C.

2.16. *In Vivo* Mass Excision of the pBluescript® Phagemid from the Uni–ZAP® XR Vector

To get more sequence information on *Craterostigma plantagineum* transcripts, an already available cDNA library constructed from RNA from dried leaves was used for sequencing purposes.
The vector (see Appendix, A.1) was digested with *Eco*RI and *Xho*I to accommodate DNA inserts up to 10 kb in length. The Uni–ZAP® XR vector allows the *in vivo* excision of the pBluescript® phagemid (see Appendix, A.1), enabling the insert to be characterized in a plasmid system.

2.16.1. Titration of the Phage Library

XL1–Blue MRF' cells were grown overnight at 37 °C on LB-tetracycline agar plates. The XL1–Blue MRF' cells were inoculated in 50 ml cultures of LB-broth with supplements and

grown at 37 °C for 4–6 hours not exceeding an OD_{600} of 1.0. The bacteria were then spun down at 1,000 *g* for 10 minutes and each pellet was gently resuspended in 25 ml sterile 10 mM $MgSO_4$. The XL1–Blue MRF' cells were diluted to an OD_{600} of 0.5 with 10 mM $MgSO_4$. To determine the titer of the packaged ligation product, the following components were mixed together:

1 μl of the final packaged reaction
200 μl of XL1–Blue MRF' cells at an OD_{600} of 0.5

and

1 μl of a 1:10 dilution of the final packaged reaction
200 μl of XL1–Blue MRF' cells at an OD_{600} of 0.5

The phage and the bacteria were then incubated at 37 °C for 15 min to allow the phage to attach to the cells. 3 ml of NZY top agar were melted, cooled down to 48 °C and added to the bacteria-phage solution. The mixture was then plated onto dry, prewarmed NZY agar plates and incubated at 37 °C. The plaques (visible after 6–8 hours) were counted and the titer in plaque-forming units per milliliter (pfu/ml) was determined.

2.16.2. *In Vivo* Mass Excision of the pBluescript® Phagemid

The Uni–ZAP® XR vector is designed to allow simple, efficient *in vivo* excision and recircularization of any cloned insert contained within the lambda vector to form a phagemid containing the cloned insert. The single-stranded DNA molecule is circularized by the gene II product from the f1 phage, forming a circular DNA molecule containing the DNA between the initiator and terminator. In the case of the Uni–ZAP® XR vector, this includes all sequences of the pBluescript® SK(−) phagemid and the insert, if one is present. The ExAssist helper phage with SOLR™ *E. coli* strain is designed to allow efficient excision of the pBluescript® phagemid from the Uni–ZAP® XR vector.
50-ml cultures of XL1–Blue MRF' and SOLR™ cells in LB-broth with supplements are grown overnight at 30 °C. The XL1–Blue MRF' and SOLR™ cells were gently spun down at 1,000 *g*. Each of the cell pellets was resuspended in 25 ml of 10 mM $MgSO_4$. The OD_{600} of the cell suspensions was measured and the concentration of the cells adjusted to an OD_{600} of 1.0 (8×10^8 cells/ml) in 10 mM $MgSO_4$. In a 50 ml conical tube a portion of the amplified lambda bacteriophage library was combined with XL1–Blue MRF' cells

at a multiplicity of infection (MOI) of 1:10 lambda phage-to-cell ratio. 10- to 100-fold more lambda phage than the size of the primary library was excised to ensure statistical representation of the excised clones. ExAssist helper phage was added at a 10:1 helper phage-to-cells ratio to ensure that every cell was co-infected with lambda phage and helper phage. The tube was incubated at 37 °C for 15 minutes to allow the phage to attach to the cells. 20 ml of LB-broth with supplements were added and the tube was incubated for 2.5–3 hours at 37 °C with shaking. The tube was heated at $65 - 70$ °C for 20 minutes to lyse the lambda phage particles and the cells. The mixture was centrifuged at 1,000 *g* for 10 minutes to pellet the cell debris and the supernatant recovered into a sterile conical tube.

To plate the excised phagemids, 1 μl of this supernatant was combined with 200 μl of SOLR™ cells previously prepared in a 1.5 ml microcentrifuge tube and incubated at 37 °C for 15 minutes. 100 μl of the cell mixture was finally plated onto LB-ampicillin agar plates and incubated overnight at 37 °C. Single colonies were picked and inoculated in microtiter plates containing 1× HMFN medium in LB with ampicillin. The overnight cultures were then frozen and stored at −80 °C.

2.17. Extraction of Proteins

2.17.1. Extraction of Total Proteins

Dense–SDS Protein Extraction Method

Total proteins were extracted essentially as described by Röhrig *et al.* (2006), with minor modifications. Polyvinylpolypyrrolidone (PVPP) was added to the leaves (10 % v/v for fresh plant material, 100 % v/v for dried plant material) and the samples were ground to a fine powder in liquid nitrogen. The powder was transferred to 15 ml tubes (a volume corresponding to 3.5 ml for fresh material; a volume of 1 ml for dehydrated material) and resuspended in 10 ml ice cold acetone. All the following steps were performed at 4 °C. The suspension was vortexed vigorously and centrifuged for 10 min at 4,000 *g*. After an additional washing step with acetone the pellet was resuspended in 10 % (w/v) TCA in acetone and sonified in a sonication water bath for 10 min. The samples were centrifuged

as above and the resulting pellets were washed three times with 10 % (w/v) TCA in acetone and then resupended in 20 % (w/v) TCA. The pellets were further washed three times with 80 % (v/v) acetone and air-dried. Dried pellets were resuspended in 5 ml dense SDS buffer. After addition of 5 ml Tris-buffered phenol, the mixtures were vortexed. The phenol phase was separated by centrifugation (10 min, 6,000 *g* at RT).
Proteins were recovered from the phenol phase by precipitation with five volumes of 0.1 M ammonium acetate in methanol and incubation for 60 min at −20 °C. After 10 min centrifugation at 6,000 *g* at 4 °C the pellet was washed twice with 0.1 M ammonium acetate in methanol and twice with 80 % (v/v) acetone. The protein pellet was air-dried and stored at −80 °C.
A separately precipitated aliquot of the phenol phase was dissolved in 8 M urea solution and used for the protein quantification using the Bradford assay (Bio–Rad) with BSA as standard (described in section 2.17.4).

Dense SDS buffer	30 % (w/v) sucrose, 2 % (w/v) SDS, 0.1 M Tris-HCl pH 8.0, 5 % (v/v) β-mercaptoethanol

Laemmli Extraction Method

Frozen and homogenized plant material (100 mg) or the pellet from a 2 ml overnight bacterial culture were resuspended in 200 μl of 1× Laemmli buffer (Laemmli, 1970). The samples were briefly vortexed and incubated at 95 °C for 5 min. Samples were then spun down at 14,000 *g* for 5 min at RT. Supernatants containing the crude protein extracts were transferred into new tubes and stored at −20 °C. For protein analysis, samples were incubated at 95 °C for 2 min before loading on an SDS–PAGE gel.

2× Laemmli buffer	4 % (w/v) SDS, 20 % (v/v) glycerol, 120 mM Tris-HCl pH 6.8, 0.2 M DTT, 0.01 % (w/v) bromophenol blue.

2.17.2. Enrichment of Phosphoproteins from Denatured Proteins

Phosphoproteins were enriched essentially as described (Röhrig *et al.*, 2008) with some modifications. 3 mg of total proteins (isolated as described in section 2.17.1) were dissolved in 2 ml IB/A buffer with a pipette. The suspension was sonicated for 10 minutes in a sonication water bath and the proteins were allowed to dissolve at RT for at least one hour. 2 volumes of IB/B buffer were then added to the solution and mixed.
4 $\times$ 120 mg of $Al(OH)_3$ were washed twice in 2 ml tubes with 1.5 ml of IB150 buffer as follows: the $Al(OH)_3$ was resuspended in IB150 buffer, centrifuged at 12,000 g for 1 min and the supernatant was discarded. For binding of the phosphoproteins, 1.5 ml of total protein suspension were added to the washed $Al(OH)_3$ pellet and the tubes were incubated on a rotator for 1 h at 10 °C. The aluminum bound phosphoproteins were washed six times with 1.5 ml of IB200, where washing means to centrifuge the tubes at 10,000 g for 1 min and discard the supernatant. The elution was performed with EB buffer for 30 minutes on a rotator at RT. After centrifugation for 5 minutes at 14,000 g, 900 μl of the clear supernatant were recovered and the eluted proteins were concentrated in an Amicon Ultra–4 centrifugal filter device (Ultracel–4K, Millipore) at 4,000 g to a final volume of 100 μl.
The retentate was transferred to an 1.5 ml tube and diluted with 400 μl of water to lower the concentration of the urea. 5 μl of a 2 % (w/v) solution of sodium deoxycholate were added and the samples were incubated for 5 minutes at RT, followed by the addition of 50 μl of 100 % (w/v) TCA. After 2 h of precipitation at 4 °C the proteins were recovered by centrifugation at 14,000 g for 10 min at 4 °C. The pellet was subsequently washed with 25 % (w/v) TCA, with 80 % acetone/20 % Tris-HCl (50 mM pH7.5) and with pure acetone. The proteins were air-dried and stored at −20 °C.

IB/A	30 mM MES-HCl pH 6.1, 0.25 % CHAPS, 7 M urea, 2 M Thiourea.
IB/B	30 mM MES-HCl pH 6.1, 0.25 % CHAPS, 8 M urea, 0.2 M Na-glutamate, 0.2 M K-aspartate, 30 mM imidazole.

IB150	30 mM MES-HCl pH 6.1, 0.25 % CHAPS, 8 M urea, 0.15 M Na-glutamate, 0.15 M K-aspartate, 20 mM imidazole.
IB200	30 mM MES-HCl pH 6.1, 0.25 % CHAPS, 8 M urea, 0.2 M Na-glutamate, 0.2 M K-aspartate, 20 mM imidazole.
EB	200 mM K-pyrophosphate pH 9.0, 8 M urea.

2.17.3. Enrichment of Phosphopeptides from Isolated Proteins

Protein Isolation and Digestion

CDeT11–24 protein from *C. plantagineum* and its homologues from *Lindernia* were isolated from dried leaves using an HiTrap NHS affinity column (GE Healthcare) cross-linked with the 11–24 monospecific IgGs (described in section 2.23).
After washing the homogenized plant material with acetone, 10 % TCA/acetone, 10 % TCA and 80 % acetone as described in 2.17.1, total denatured proteins were resuspended in PBS (Maniatis *et al.*, 1986), sonicated in a sonication water bath for 10 min, vortexed and subsequently pelleted by centrifugation. The resulting supernatant contained the water soluble protein fraction, including the 11–24 protein. The protein suspension was precipitated adding 100 % TCA in order to obtain a final concentration of 15 % TCA. After an incubation for 1 hour at 4 °C, the proteins were collected by centrifugation and the TCA was washed out with acetone. The pellet was air dried, resuspended in PBS and loaded on the IgG linked HiTrap NHS column in order to purify the CDeT11–24 protein. The column was washed with 10 column volumes of PBS and the bound proteins were eluted with 100 mM glycine, 150 mM NaCl, pH 2.5. The proteins were reduced with 2 % (w/v) DTT, alkylated with 2.5 % (w/v) iodoacetamide and digested in the presece of ProteaseMAX Sufactant (Promega) with 1.8 % trypsin at 37 °C o/n in 100 μl final volume. The detergent was eliminated by adsorption on Stage Tips (Millipore) with C18 disk membranes and the flow through containing the peptides was collected. The flow through and the fraction eluted with 20 μl 30 % (v/v) acetonitrile, 0.1 % (v/v) TFA were combined for subsequent enrichment.

Metal Oxide Chromatography (MOC)

Home-made MOC columns were prepared using C8 Stage Tips (Millipore) and TiO_2 beads (1 mg beads/200μl pipette tip). TiO_2 beads were resuspended in water and loaded on the Stage Tip followed by equilibration of the tip with 100 % (v/v) acetonitrile. The digested phosphoproteins (see 2.17.3) were diluted 1:5 with solution A and loaded on the previously prepared MOC tip. After washing the column with 30 μl of buffer A followed by 150 μl of solution B, phosphopeptides were eluted with 100 μl of 0.5 % (v/v) ammonium hydroxide. The eluate was acidified with 1 μl TFA. A second fraction was eluted with 20 μl 30 % (v/v) acetonitrile.

Solution A	80 % (v/v) acetonitrile, 0.1 % (v/v) TFA, 300 mg/ml lactic acid
Solution B	80 % (v/v) acetonitrile, 0.1 % (v/v) TFA

2.17.4. Estimation of Proteins Concentration

The estimation of protein concentration was carried out using a BioRad protein assay kit according to Bradford (1976). Protein aliquots were mixed with 200 μl BioRad protein assay kit and brought to 1000 μl with ultrapure water. The samples were incubated at room temperature for 5 min and the absorbance at 595 nm was measured. The concentration was calculated comparing the absorbance of the samples with that of a standard protein (BSA) of known concentration plotted on a calibration curve.

2.18. Electrophoresis of Proteins

2.18.1. Isoelectrofocusing (First Dimension)

Rehydration and Sample Application. For the isoelectrofocusing (IEF) the protein pellet was resuspended in an appropriate volume of rehydration buffer depending on the length of the strips (125 μl for the 7 cm strips and 315 μl for the 18 cm strips). The proteins were resuspended by pipetting and dissolved at room temperature for 1 h. The samples

were centrifuged to remove the insoluble particles and the supernatant was pipetted in the middle of the focusing tray. The IPG strip was gently placed, gel side down, onto the sample with the positive end on the anode side. To prevent evaporation during the rehydration process, each IPG strip was overlayed with mineral oil. The rehydration took place in the focusing tray for 12–16 hours at 20 °C.

IEF Rehydration buffer 7 M urea, 2 M thiourea, 2 % (w/v) CHAPS, 0.002 % (w/v) bromphenol blue (add freshly 0.5 % IPG-buffer and 20 mM DTT).

Focusing Conditions. The focusing conditions vary with sample composition, IPG pH range and stripes length. Table 2.2 describes the parameters used for the IEF. The current is set to 50 μA/IPG strip. The total time required for ramping will depend on the sample and buffer composition.

Table 2.2: Focusing conditions of the first dimension used in this work.

Ramp	Voltage [V]	Time [hours]	Ramp	Voltage [V]	Time [hours]
7 cm strips			18 cm strips		
Rapid	500	0:30	Linear	250	0:15
Rapid	1,000	0:30	Rapid	2,000	1:45
Rapid	5,000	1:40	Rapid	10,000	3:00
			Rapid	10,000	30,000 Vh

Equilibration. Prior to separating the proteins in the second dimension it is necessary to equilibrate the IPG strips in SDS-containing buffers. The 2-step equilibration also ensures that cysteine residues are reduced and alkylated, which minimizes vertical streaking that may be visible after staining of the 2D gels. Equilibration buffer I contains DTT which reduces sulfhydryl groups, while equilibration buffer II contains iodoacetamide which alkylates the reduced sulfhydryl groups.

The mineral oil was removed from the strips by placing them onto a piece of dry filter paper. The strips were then transferred to an equilibration tray and incubated for 15 min with equilibration buffer I and subsequently for 15 min with equilibration buffer II.

Equilibration buffer I	6 M urea, 50 mM Tris-HCl pH 6.8, 30 % (v/v) glycerol, 2 % (w/v) SDS, 2 % (w/v) DTT, 0,002 % bromphenol blue
Equilibration buffer II	6 M urea, 50 mM Tris-HCl pH 6.8, 30 % (v/v) glycerol, 2 % (w/v) SDS, 2.5 % (w/v) iodacetamide, 0,002 % bromphenol blue

The strips were removed and dip briefly into a graduated cylinder containing 1× SDS running buffer to drain any excess of equilibration buffer. The strips were then put on the surface of the SDS–PAGE gel and sealed with IEF-agarose melted at 65 °C (0.5 % [w/v] agarose, 0.002 % [w/v] bromphenol blue in SDS running buffer).

2.18.2. SDS–PAGE (Second Dimension)

The SDS–PAGE was performed according to Laemmli (1970). The gel was made of 4 % (w/v) acrylamide stacking gel and 12 % (w/v) acrylamide separating gel as described below. In the case of the one dimensional SDS–PAGE, the protein samples were boiled for 5 min and centrifuged briefly before loading onto the gel. The run was performed in 1× SDS running buffer at 20 mA for 2h.

Stock solution	**4 % stacking gel**	**12 % separating gel**
	final concentration	
30 % (w/v) acrylamide	4 %	12 %
1.5 M Tris-HCl pH 6.8	0.133 M	–
1 M Tris-HCl pH 8.8	–	0.375 M
10 % (w/v) SDS	0.1 %	0.1 %
10 % (w/v) APS	0.1 %	0.1 %
Temed	0.1 %	0.04 %
H_2O	up to final volume	up to final volume

SDS running buffer	25 mM Tris, 192 mM glycin, 0.1 % (w/v) SDS.

2.18.3. Staining of Polyacrylamide Gels

Coomassie Staining

The SDS–PAGE was stained with Coomassie according to Zehr *et al.* (1989). The gel was fixed for at least one hour and after 3 washes for 10 min with water to remove the alcohol and the acid, it was incubated in the staining solution on a shaker overnight. For destaining the gel was washed several times with water.

Fixing solution	50 % (v/v) methanol, 10 % (v/v) acetic acid
Staining stock solution	100 g/l ammonium sulfate, 1 % (v/v) phosphoric acid, 0.1 % (w/v) Coomassie G250
Staining solution	4 part Staining stock solution + 1 part methanol

Silver Staining

The gel was fixed for at least one hour and subsequently incubated in the incubation solution for 2 h. The gel was then washed 3 times for 20 min in water and stained with silver solution for 30 min. The proteins were finally visualized with the developing solution and the reaction was blocked with the stopping solution.

Fixing solution	50 % (v/v) ethanol, 10 % (v/v) acetic acid
Incubation solution	6.8 g sodium acetate, 0.2 g sodium thiosulfate, 30 ml ethanol, 1 ml 50 % (v/v) glutaraldehyde, water (up to 100 ml)
Silver solution	0.05 g silver nitrate, 15 μl 37 % (v/v) formaldehyde, water (up to 50 ml)
Developer	2.5 g sodium carbonate, 29 μl 37 % (v/v) formaldehyde, water (up to 100 ml)
Stopping solution	0.8 g glycine, water (up to 200 ml)

Pro–Q® Diamond Phosphoprotein Staining

To stain the phosphoproteins Pro–Q® Diamond Phosphoprotein Gel Stain (Invitrogen) was used. The gel was fixed overnight in fixing solution. After 3 washing steps for 10 min with water it was incubated in a minimal volume of phosphostain in the dark for 90 min under continuous shaking. To lower the background signal the gel was washed 3 times for 30 min with the destaining solution in the dark. Finally the gel was rinsed with water and the signal detected with the Typhoon scanner (excitation wavelength 532 nm, emission filter 610 nm).

Fixing solution	50 % (v/v) methanol, 10 % (v/v) acetic acid
Destaining solution	20 % (v/v) acetonitrile, 50 mM sodium acetate pH 4.0

2.19. Immunological Methods

2.19.1. Western Blot

To immunologically detect specific proteins, they were separated by SDS–PAGE and subsequently electrophoretically transferred from the gel onto a Protran nitrocellulose BA 85 membrane (Whatman) using a protein blot transfer buffer (PBTB) as described by Towbin *et al.* (1979). The transfer took place at 100 V for 1 h.

PBTB	25 mM Tris, 192 mM glycine, 20 % (v/v) methanol.

In order to confirm the transfer of the proteins on the membrane, this was stained for 10 min with Ponceau stain (Maniatis *et al.*, 1986). To visualize the proteins, the membrane was briefly washed with water and to remove the dye the filter was incubated in TBST.

Ponceau stain	0.2 % Ponceau S in 3 % TCA
10x TBS	200 mM Tris-HCl pH 7.5, 1.5 M NaCl
TBST	1x TBS; 0.1 % (v/v) Tween-20.

Blocking of the Membrane. To minimize any unspecific interaction of the antibody with the membrane, it was incubated overnight in blocking solution (4 % [w/v] non-fat milk powder in TBST) at 4 °C.

Incubation with Antibodies. Incubation with primary antibody was performed for 1 h at RT in blocking solution. The concentration of the primary antibodies ranged from 1:1,000 to 1:5,000 (v/v) depending on the antibody used. After incubation the membrane was washed with TBST as follows: once briefly, once for 15 min and three times for 5 min. Subsequently the membrane was incubated for 45 min at RT with the secondary antibody at a 1:5,000 dilution in the blocking solution. The membrane was again washed as described above.

Detection. Antibodies bound to the target protein were detected by means of the ECL Plus Western Blotting detection kit (Amersham Biosciences). The secondary antibody is an anti-rabbit IgG directly coupled to horseradish peroxidase. This antibody permits direct detection of antigen-antibody complexes on the membrane by chemiluminescence under a CCD camera (Intelligent Dark Box II, FUJIFILM Corporation).

2.19.2. Immunoprecipitation

Immunoprecipitations were performed essentially as as described by Röhrig *et al.* (2006). Plant material was frozen in liquid nitrogen, ground to a fine powder and transferred to a pre-chilled 2 ml tube. The amount of material taken was dependent on the water content of the plant, ranging from 20 μl for dried material to 50 μl for fresh material. 200 μl of lysis buffer were added to the frozen material and the tubes were incubated for 5 min at 100 °C.

To reduce the concentration of SDS that would compromise the structure of the antibody, 1.8 ml of washing buffer 1 were added to the tubes. The samples were then centrifuged for 10 min at 20,000 g at 4 °C. The clear supernatants were transferred to new tubes and 10 μl of serum containing the antibody of interest were added. The resulting solutions were incubated on a rotator for 1 h at 4 °C to allow the binding of the antibodies to the target proteins. 40 μl of protein A-agarose were then added to the tubes and the resulting mixtures were further incubated on the rotator for 3 h. The antigen-antibody-protein A

complexes were pulled down by centrifugation at 12,000 *g* for 1 min and the supernatant was discarded. To reduce unspecific binding, the agarose beads were washed twice with 1 ml of washing buffer 1, twice with washing buffer 2 and once with washing buffer 3. In each washing step the samples were incubated for 20 min on the rotator, centrifuged, and the supernatants discarded. After the last washing step, the pellets were resuspended in 50 μl of 1$\times$ Laemmli buffer and heated at 95 °C for 10 min. The proteins were rescued by centrifugation. The supernatants containing the released proteins were put into new tubes and separated by electrophoresis.

Lysis buffer	50 mM Tris-HCl pH 8.0, 1 % SDS, 1 mM EDTA
Washing buffer 1	50 mM Tris-HCl pH 7.5, 1 mM EDTA, 150 mM NaCl, 0.1 % Nonidet P40
Washing buffer 2	50 mM Tris-HCl pH 7.5, 1 mM EDTA, 500 mM NaCl, 0.1 % Nonidet P40
Washing buffer 3	10 mM Tris-HCl pH 7.5, 0.1 % Nonidet P40

2.20. Phosphatase Shift Assay

Total protein extraction from desiccated plants was performed by the Dense SDS extraction method (described in 2.17.1). Pellet was resolubilized in 50 mM NH_4HCO_3 (1.5 mg total proteins in 1.5 ml), and the hydrophilic proteins were brought in solution again whereas the globular proteins remain insoluble forming aggregates. Resolubilization was performed in a sonication water bath for 10 minutes. Insoluble proteins were collected by centrifugation (20,000 *g*, 5 min).

1 ml of the supernatant was split in 2 tubes: one tube was treated with 36U calf intestine phosphatase (CIP) for 60 min at 30 °C. Both samples were then precipitated with the TCA-Doc method (described in 2.17.2). Protein pellets were resuspended in 250 μl rehydration solution for 2D SDS–PAGE. 125 μl of the sample were taken, 3 μl Magic Marker added and IEF was performed as described in section 2.18.

On the next day second dimension was performed, the gels were blotted onto nitrocellulose membranes, blocked and finally immunologically detected with the *L. subracemosa* 11–24 antibody as described in section 2.19.1.

2.21. Overexpression and Isolation of a Recombinant Protein

Recombinant Protein Overexpression. Recombinant proteins were overexpressed using the BL21 *E. coli* strain bearing the pET–28 expression vector carrying the gene of interest fused with histidine tag. 2 ml of an overnight bacterial culture were used to inoculate 200 ml of LB with kanamycin in an 2 l flask. The cells were grown at 4 °C with shaking at 200 rpm till an OD_{600} of 0.5–0.6 was reached. The culture was pre-incubated in the dark at 26 °C for 15 min. 1 ml of the non-induced sample was collected (T_0), centrifuged and the resulting pellet resuspended in 100 μl of Laemmli buffer (described in section 2.17.1). The protein expression was induced with 1 mM Isopropyl β-D-1-thiogalactopyranoside (IPTG) and the bacteria incubated with shaking for 2 h in the dark at 26 °C. 1 ml of bacteria was collected (T_2). The cells were harvested by centrifugation at 3,000 *g*, 4 °C for 20 min. The bacterial pellets were stored at −20 °C.

Recombinant Protein Purification. The bacterial pellet was thawed on ice for 15 min and then resuspended in 5 ml of 50 mM NaH_2PO_4. The cells were treated with lysozyme (1mg/ml) and incubated on ice for 15 min.
The bacterial suspension was sonified (Branson sonifier, 6 × 20 s, output setting 3) until it was clear avoiding warming of the solution. The suspension was centrifuged at 12,000 *g* for 30 min at 4 °C to remove the cell debris and the clear supernatant was filtered through a 0.45 μm filter.
The filtrate was then heated at 95 °C for 10 min. This step keeps in solution all the hydrophilic/unstructured proteins, like 11–24 and all the dehydrins, whereas the bulk of the proteins are denaturated and coagulate enabling their removal by centrifugation. 10 μl of the supernatant were recovered and 90 μl of Laemmli buffer were added. Part of the denaturated protein pellet was collected with a spoon and the proteins resuspended in 100 μl Laemmli buffer and heated 10 min 95 °C. The other components of buffer A were then added to the supernatant by mixing the filtrate with an equal volume of 2× buffer A containing 50 mM NaH_2PO_4.
The Ni-NTA column with 1 ml bed volume was washed with 3 bed volumes of water, 5 bed volumes of loading buffer and 3 bed volumes of buffer A. The protein solution was then

loaded on the column and when about 2 ml were passed through the column, 10 μl were collected and 90 μl of Laemmli buffer was added. After all the protein solution passed the column, it was washed with 10 volumes of buffer A and 8 volumes of buffer B. The His-tagged proteins were eluted with 3 ml of buffer C. The eluted fractions were collected in 6 tubes, 500 μl eluate in each tube (E_1–E_6). 10 μl of each fraction were added to 90 μl of Laemmli buffer as described above. The column was regenerated by washing with 3 volumes of regeneration buffer and 3 volumes of 20 % ethanol. The regenerated column can be stored in 20 % ethanol at 4 °C. The samples in Laemmli buffer were used to check the induction and the purification of the overexpressed protein by separating them by SDS–PAGE and staining the gel with coomassie.

Loading buffer	50 mM $NiSO_4$
Buffer A	50 mM NaH_2PO_4, 300 mM NaCl, 5 mM imidazole, 10 % (v/v) glycerin, 0.1 % Triton X-100, 1.5 mM β-mercaptoethanol, pH 8.0 with NaOH.
Buffer B	50 mM NaH_2PO_4, 300 mM NaCl, 20 mM imidazole, 10 % (v/v) glycerin, 0.1 % Triton X-100, 1.5 mM β-mercaptoethanol, pH 8.0 with NaOH.
Buffer C	50 mM NaH_2PO_4, 300 mM NaCl, 250 mM imidazole, 10 % (v/v) glycerin, 0.1 % Triton X-100, 1.5 mM β-mercaptoethanol, pH 8.0 with NaOH.
Regeneration Buffer	100 mM EDTA, 500 mM NaCl, 20 mM Tris-HCl, pH 7.9

Desalting and Buffer Exchange of the Purified Protein. To remove salts and to exchange the buffer to one suitable for the lyophilization, the eluted proteins were loaded onto a PD-10 desalting column (GE Healthcare). The column performs a size exclusion chromatography with a Sephadex resin that permits the separation of high molecular weight substances like proteins from the low molecular weight substances like salts.
The chromatography was performed according to the manufacturer instructions and the buffer was exchanged to 50 mM NH_4HCO_3.

Lyophilization. Ammonium bicarbonate is a buffer suitable for the lyophilization of proteins that have to be used as antigens, as it has a pH of 7.8 and undergoes decomposition

by liberating carbon dioxide and ammonia. The proteins were lyophilized over three days in a lyophilizer and stored at $-20\,^{\circ}\mathrm{C}$.

2.22. Antibody Production

The antibody against the recombinant protein was raised in rabbit by Seqlab (Sequence Laboratories Göttingen GmbH) injecting three charges of purified protein according to the following immunization scheme:

Day	
0	**First injection** (200–400 μg protein). Before the injection, 5 ml of serum were taken to check the background signal of the rabbit antibodies (pre-immune serum)
21	**Second injection** (200 μg protein)
35	**First bleeding** (10–20 ml)
49	**Third injection** (200 μg protein)
53	**Second bleeding** (10–20 ml)
60	**Final bleeding** (>50 ml)

2.23. Production of a HiTrap NHS Column Coupled with a Protein

HiTrap NHS-activated HP columns (GE Healthcare) were used for preparative affinity chromatography. The column matrix is composed of sepharose and the activated group is comprised of an N-hydroxysuccinimide (NHS) ester attached by epichloro-hydrine to the 34 μm spherical sepharose matrix via a 6-atom spacer arm. This esterification leads to the formation of activated esters which react rapidly and efficiently with ligands containing amino groups resulting in a stable amide linkage.

2.23.1. Coupling the Protein to the Column

Ligand Coupling. The ligand was dissolved to a concentration of 0.5–10 mg/ml in 1 ml of coupling buffer. The top-cap of the column was removed and a drop of ice cold 1 mM HCl applied on the top of the column to avoid air bubbles. The HiTrap luer adaptor was connected to the top of the column and the snap-off end at the column outlet was removed.
The coupling and washing steps were performed with a 10 ml syringe connected to the luer adaptor. The isopropanol in the column was washed out with 6 ml 1 mM HCl and immediately the ligand solution was injected onto the column. The column was sealed and incubated for 15–30 minutes at 25 °C (or 4 hours at 4 °C) for the coupling reaction to occur.

Washing and Deactivation. Any excess of active groups that have not been coupled to the ligand were deactivated and the non-specifically bound ligands were washed out following the procedure below:

a. 3 × 2 ml of Buffer A

b. 3 × 2 ml of Buffer B

c. 3 × 2 ml of Buffer A

d. The column was incubated for 15–30 minutes at 25 °C (or 4 hours at 4 °C)

e. 3 × 2 ml of Buffer B

f. 3 × 2 ml of Buffer A

g. 3 × 2 ml of Buffer B

h. Finally, 2 ml of PBS buffer pH 8.0 (Maniatis *et al.*, 1986) were injected onto the column.

The column can be stored in a buffer with neutral pH supplemented with 0.1 % NaN_3 at 4 °C.

Coupling buffer	0.2 M $NaHCO_3$, 0.5 M NaCl, pH 8.0.
Buffer A	0.5 M ethanolamine, 0.5 M NaCl, pH 8.3
Buffer B	0.1 M sodium acetate, 0.5 M NaCl, pH 4.0

2.23.2. Measuring the Coupling Efficiency

After coupling, the coupling solution was washed out from the column with 3 column volumes of the coupling buffer.
A PD-10 column (GE Healthcare) was equilibrated with 50 mM phosphate buffer and 0.5 ml of the eluted coupling solution were loaded on the desalting column. The eluate was discarded and 2 ml of of buffer were loaded and discarded from the column. 1.5 ml of buffer were finally loaded to elute the high molecular weight components (e.g. the protein). The eluate was collected and the absorbance at 280 nm was measured.

Calculation of the Coupling Yield

Loaded coupling solution, $A_{280} \times$ ml:

$$A = A_{280,\ \text{coupling solution}} \times V_{\text{loaded volume of coupling solution}}$$

Amount not coupled, A_{280} x ml:

$$B = \frac{A_{280,\ \text{coupling solution after PD-10 run}} \times 1.5_{\text{volume collected from PD-10}} \times V_{\text{volume post coupling wash}}}{0.5_{\text{volume loaded on PD-10}}}$$

Coupling yield, %: $(A - B)/A \times 100$

2.24. Isolation of IgGs from Serum

The protein-coupled columns were used for the affinity purification of monospecific IgGs from serum which were used for immunoprecipitation, western blotting or for the subsequent coupling to a HiTrap NHS column. The serum was diluted 1:10 with 10 mM

Na-Hepes pH 8.0 and centrifuged for 30 min at 20,000 g at 4 °C to remove the insoluble material. The serum was then loaded on the 11–24 protein-coupled column with a peristaltic pump at 4 °C at a flow rate of 1 ml/min. The column was washed with 10 column volumes of 10 mM Na-Hepes pH 8.0 and the bound antibodies eluted with 100 mM glycine pH 2.5. The eluted fraction was immediately neutralized with $\frac{1}{10}$ vol of 1 M Tris pH 8.0 and the column neutralized with Na-Hepes pH 8.0. The isolated IgGs were then desalted with a PD-10 column (described in section 2.21), the buffer was exchanged to PBS (Maniatis *et al.*, 1986) and the sample concentrated with an Amicon Ultra Centrifugal Filter Device (Millipore) to reach a concentration of 1 mg/ml. The isolated IgGs were then tested by western blot analysis.

2.25. Identification of CDeT11–24 Interaction Partners

2.25.1. Coimmunoaffinity Chromatography

Craterostigma plantagineum leaf material from control (3 ml), ABA treated (3 ml) and dried plants (0.5 ml) was ground in liquid nitrogen to a fine powder and resuspended in 20 ml of either RIPA buffer or EBC buffer supplemented with phosphatase and protease inhibitor cocktail (Sigma). The resuspended material was incubated on ice for a few minutes and subsequently centrifuged at 12,000 g at 4 °C for 10 min to remove the cell debris. The supernatant was filtered through a 0.45 μm membrane and applied onto the IgG coupled column with a peristaltic pump at a flow rate of 1 ml/min, after the column was pre-equilibrated with 10 ml of the corresponding buffer. The solution was recirculated on the column for 1 h at 4 °C and subsequently the column was washed with 10 column volumes of buffer to remove the non-interacting proteins. To elute the bound proteins the column was washed with 100 mM glycine, 150 mM NaCl pH 2.5 and the eluted fraction was neutralized with 1 M Tris pH 8.0. The column was neutralized with PBS (Maniatis *et al.*, 1986) and stored in PBS supplemented with 0.1 % (w/v) NaN_3 at 4 °C. After the coimmunoaffinity chromatography the proteins were fractionated by SDS–PAGE and detected by gel staining with ProQ Diamond phosphoprotein gel stain (Invitrogen) and subsequently by Coomassie staining (as described in section 2.18.3).

RIPA buffer	50 mM Tris-HCl pH 8.0, 150 mM NaCl, 1 % (v/v) NP-40, 0.5 % (w/v) DOC, 0.1 % (w/v) SDS
EBC buffer	50 mM Tris-HCl pH 8.0, 120 mM NaCl, 0.5 % (v/v) NP-40

2.25.2. Weak Affinity Chromatography

The weak affinity chromatography was used to isolate the potential interaction partners of CDeT11–24 in the unphosphorylated and phosphorylated state.
Recombinant histidine-tagged unphosphorylated protein (isolated as described in section 2.21) and native phosphorylated protein isolated with the IgG coupled affinity column were separately coupled to two HiTrap NHS columns (see 2.23). These two columns were then used to perform the weak affinity chromatography on *Craterostigma plantagineum* extracts essentially according to Testerink *et al.* (2004).
For isolating the native phosphorylated protein, dried *C. plantagineum* leaves were resuspended in acetone and the leaf material was subsequently washed with acetone, 10 % (w/v) TCA/acetone, 10 % (w/v) TCA and 80 % (v/v) acetone as described in 2.17.1. The soluble protein fraction was brought into solution with PBS buffer (Maniatis *et al.*, 1986) and subsequently precipitated in a new reaction tube with 20 % (w/v) TCA for 1h at 4 °C. The proteins were collected by centrifugation at 10,000 *g* for 10 min and the pellet was washed twice with 80 % (v/v) acetone. The proteins were finally resuspended in PBS buffer and affinity purification on the IgG coupled column was performed.
For the weak affinity chromatography, *C. plantagineum* leaf material from ABA treated (3 ml) and dried plants (0.5 ml) was ground in liquid nitrogen and resuspended in 15 ml of protein isolation buffer. The extract was first centrifuged for 10 min at 10,000 *g* at 4 °C to remove the cell debris. The resulting supernatant was centrifuged again at 10,000 *g* and finally at 50,000 *g* for 30 min. The last supernatant contains the soluble protein fraction that was used for the binding assay.
For the binding assay the soluble protein was mixed with an equal volume of binding buffer and loaded onto the HiTrap NHS columns coupled with either the recombinant his-tagged CDeT11–24 protein or the native phosphorylated CDeT11–24 protein. In the case of the competition experiments, the binding buffer was supplemented with 100 μg recombinant CDeT11–24 protein. The loading was performed at 4 °C with a peristaltic pump at a flow

rate of 1 ml/min. The column was washed with 10 column volumes of washing buffer and the proteins were subsequently eluted with 2 ml of elution buffer (100 mM glycine, 150 mM NaCl, pH 2.5). The eluted fractions were precipitated with the TCA-Doc method and resuspended in Laemmli buffer (see 2.17).

Protein isolation buffer	50 mM Tris-HCl pH 7.5, 80 mM NaCl, 2 mM EGTA, 1 mM EDTA, 2 mM DTT, 300 mM sucrose, 1 % (w/v) PVPP, protease and phosphatase inhibitors
Binding buffer	50 mM Tris-HCl pH 8.0, 50 mM KCl, 10 mM EDTA, 1 % (v/v) NP-40 alternative, 0.5 % (v/v) protease and phosphatase inhibitors
Wash buffer	50 mM Tris pH 7.5, 150 mM NaCl, 5 mM EDTA, 0.1 % (v/v) Tween-20

2.26. Mass Spectrometry Analysis

The protein spots picking, digestion and mass spectrometric analysis was performed at the Max Planck Institute for Plant Breeding, Cologne, Germany as described in Röhrig *et al.* (2008).

Protein spots were picked from gels stained with Pro Q Diamond phosphoprotein stain by a Proteineer spII spot picker and transferred to a Proteineer dp robot (Bruker Daltonics) for automated tryptic digestion and target preparation. Samples were spotted onto Anchorchip targets (Bruker Daltonics) using a thin-layer protocol with HCCA matrix (Gobom *et al.*, 2001). MALDI PMF (peptide mass fingerprint) and MS/MS analyses were performed on an Ultraflex III system (Bruker Daltonics) as described below.

PMF's were collected on the thin-layer samples and post-calibrated using tryptic autodigestion masses, when present. These spectra were used for database searches using Mascot 2.2 (Matrix Science) against the database of cDNA sequences from *C. plantagineum* (described in section 2.16) and against the NCBInr database without taxonomic restrictions and with a 20 ppm mass tolerance.

Non-post-calibrated spectra which lead to no identifications in this round of searches were used to search with a 100 ppm mass tolerance. For each sample spot, precursor ions of sufficient intensity and quality were flagged automatically for fragmentation according

to the following strategy: when a PMF-based identification was successful, two assigned precursors were selected (if present) for validation by MS/MS. Then up to five further unassigned precursors were flagged for fragmentation. In cases where PMF-based identification failed, five precursors were selected on the basis of signal quality. All samples on the target were re-crystallized in preparation for MS/MS collection. The MS/MS spectra were also used to perform Mascot MS/MS searches against the same databases. Search results were evaluated on the basis of the following criteria: Mascot scores above corresponding significance thresholds (for the cDNA database PMF's: 50, PFF's: 21; for the NCBInr database PFF's: 51), a low mass error and continuous open reading frame (in the case of the cDNA database). Marginal hits were accepted if both MS and MS/MS searches returned sub-threshold scores for the same protein. The agreement between the observed and predicted MW and pI of the complete homologous sequence was used as a validation criterion.

3. Results

3.1. Desiccation Tolerance within the Linderniaceae

In this section it was determined the physiological response to water stress by phenotypic analysis and leaf ultrastructure observation.
Craterostigma plantagineum, *Lindernia brevidens* and *Lindernia subracemosa* belong to the Linderniaceae family, order of Lamiales (Rahmanzadeh *et al.*, 2005). All the *Craterostigma* species are desiccation tolerant, whereas the *Lindernia* genus shows more variability regarding the capability of withstanding severe water stress.
Most of the *Lindernia* species are desiccation sensitive, however recently it was shown that *Lindernia brevidens* is desiccation tolerant (Phillips *et al.*, 2008). Phylogenetic studies revealed that *Craterostigma* species are localized in one branch also containing *Lindernia brevidens*, *Lindernia subracemosa* and *Torenia vagans* (Rahmanzadeh *et al.*, 2005). *L. subracemosa* and *T. vagans* are not desiccation tolerant, whereas *L. brevidens* can withstand severe water stress. The capacity of *L. brevidens* to survive desiccation, defined as water content below 0.1 g H_2O g^{-1} dry weight (dw) (Alpert, 2005), was tested.

3.1.1. *Lindernia brevidens* Is Desiccation Tolerant

L. brevidens was subjected to dehydration by withholding watering over a period of 12 days. Hydrated plants with a water content of approximately 4 g H_2O g^{-1} dw were desiccated until reaching a value of 0.09 g H_2O g^{-1} dw ($\pm$ 0.02) and subsequently rehydrated for 48 hours by submerging them in water. Figure 3.1 shows a drying curve, illustrating the rate of water loss during drying and the recovering upon rehydration, demonstrating the capacity of *L. brevidens* to fully recover after desiccation.
The ability to be desiccation tolerant was further investigated at the structural level.

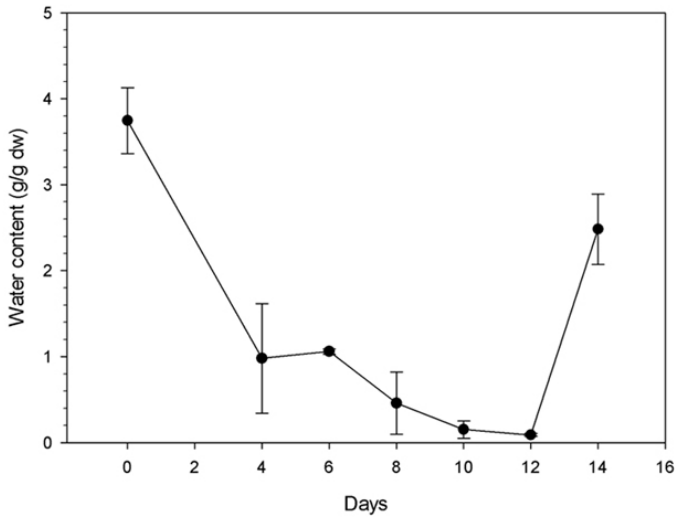

Figure 3.1: Graph showing the kinetic of water loss and rehydration of *Lindernia brevidens*. Water content is expressed on a dry weight basis. After 12 days of dehydration, plants were rehydrated for 24 hours and water content was measured. The values are shown as mean values with standard deviation for n = 3 replications. From Phillips *et al.* (2008).

Figure 3.2 illustrates a *L. brevidens* plant specimen undergoing dehydration followed by rehydration. Figure 3.2 (a) shows that the hydrated leaves are of a uniform green color. Upon desiccation the leaves became folded but retained the green coloration (b), indicating that the plant belongs to the so-called homoiochlorophyllous species, which include the majority of desiccation-tolerant plants. These species maintain the integrity of most chlorophylls and chloroplast membranes in the dried state. They activate mechanisms for actively protecting chloroplasts and cells from reactive oxygen species (ROS) damage, like reducing the light-chlorophyll interaction by leaf folding, which is also a characteristic of *L. brevidens*. Rehydrated leaves were almost indistinguishable from hydrated leaves, apart from the leaf tips which were necrotic in the rehydrated tissues (c).

Scanning electron microscope (SEM) pictures of the leaf surface (Figure 3.2 d–f) revealed that *L. brevidens* does not present any xerophytic structures like trichomes or embedded stomata.

Desiccation causes a significant shrinkage of leaf cells, a phenomenon that is more evident by observing the transverse sections (Figure 3.2 h). The cellular shrinkage was accompanied by extensive cell wall folding, an event that was reversed by rehydration, where the leaves returned to normal cellular morphology. The SEM pictures of hydrated and

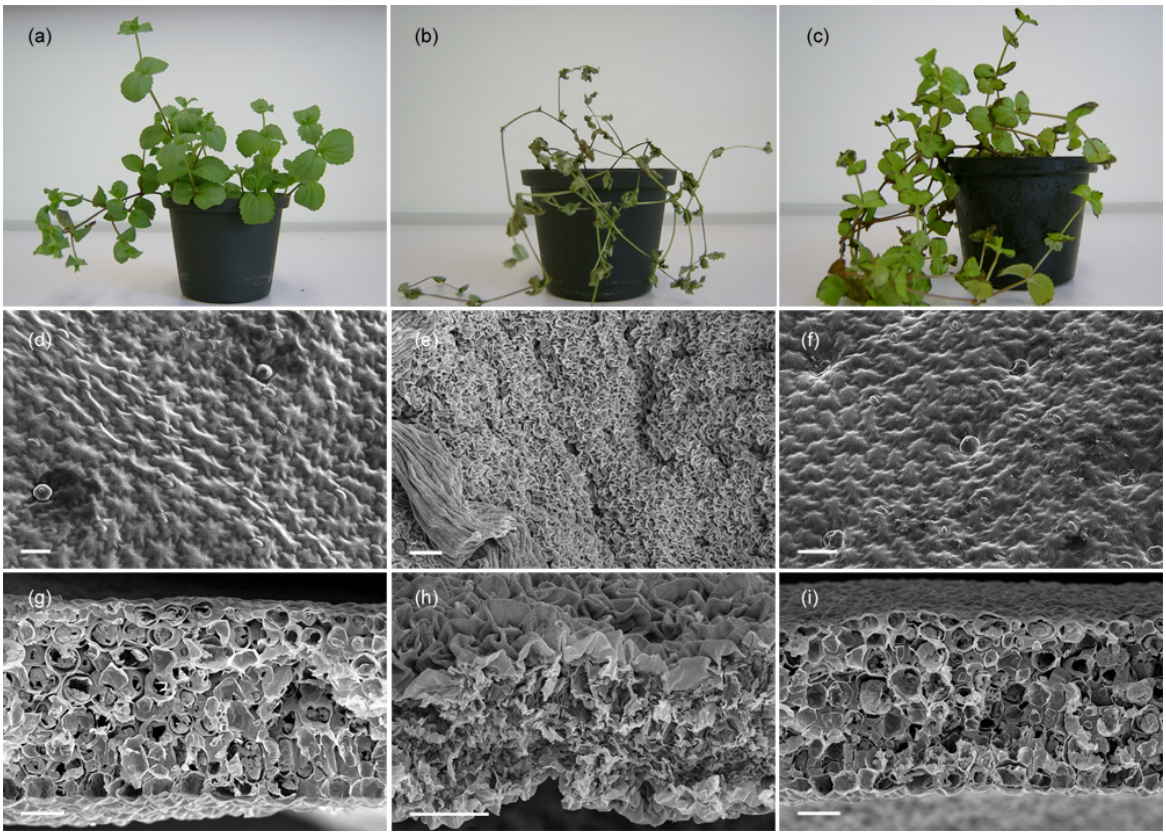

Figure 3.2: Plant and leaf morphology of *Lindernia brevidens*. *L. brevidens* (a) was dehydrated for 12 days (b) and subsequently rehydrated for 24 h (c) . Upon rehydration, the plants recovered and resumed normal physiological activity. (d–i) Scanning electron microscope pictures of hydrated, desiccated and rehydrated *L. brevidens* leaves. Surface view of the epidermis of hydrated (d), desiccated (e) and rehydrated (f) leaves. Transverse sections of hydrated (g), desiccated (h) and rehydrated (i) leaves. Scale bar: 40 μm. From Phillips *et al.* (2008).

rehydrated leaf tissues reveal that the desiccation-induced cellular damage is negligible and that there is broadly no difference in the cellular structure of the leaf specimens from hydrated and rehydrated leaves, indicating that the vegetative tissues of *L. brevidens* can completely recover from desiccation.

Lindernia subracemosa, a desiccation sensitive *Lindernia* species, was chosen to be compared with the desiccation tolerant *L. brevidens* and dehydrated under the same conditions (Figure 3.3). Hydrated leaves, like for *L. brevidens*, were of a uniform green color, but unlike the desiccation tolerant plant, *L. subracemosa* leaves became brown and necrotic upon dehydration. After rehydrating the plant, the tissues remained brown and failed to recover.

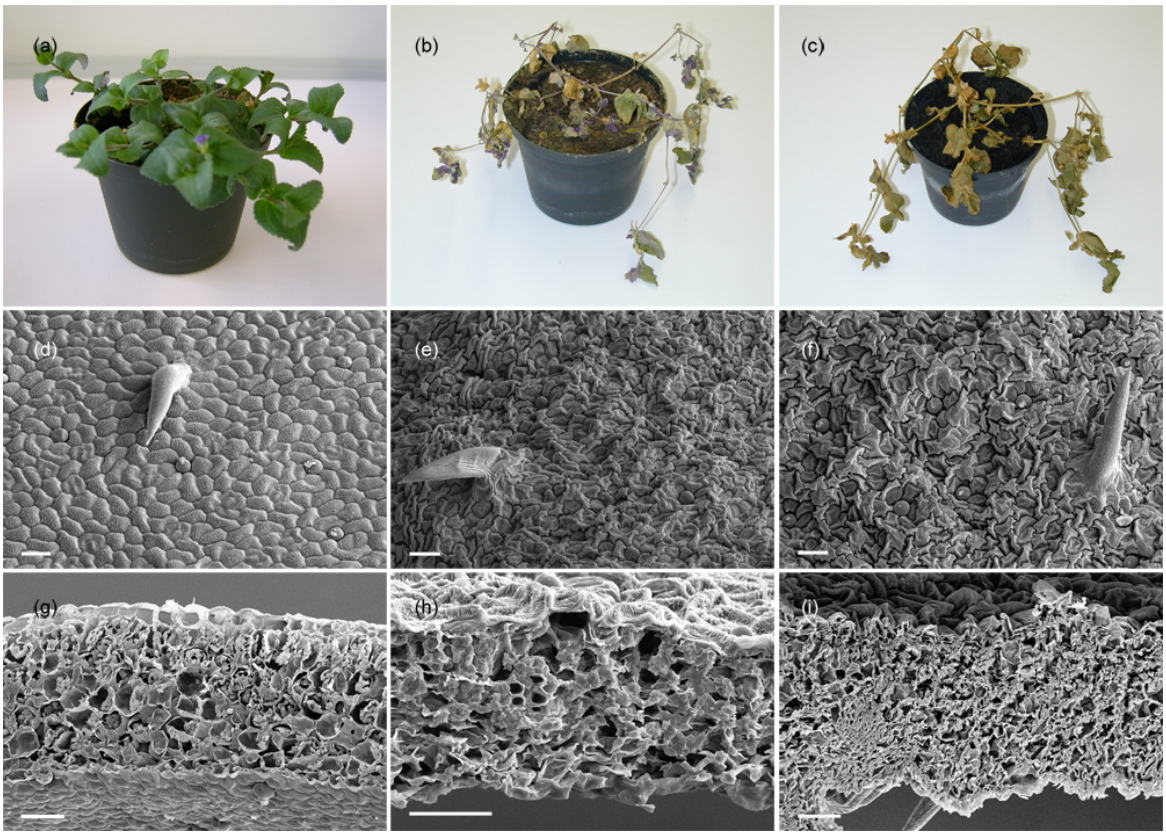

Figure 3.3: Plant and leaf morphology of *Lindernia subracemosa*. *L. subracemosa* (a) was dehydrated for 12 days (b) and subsequently rehydrated for 24 h (c). Upon rehydration, the leaves remained brown and did not recover. (d–i) Scanning electron microscope pictures of hydrated, desiccated and rehydrated *L. subracemosa* leaves. Surface view of the epidermis of hydrated (d), desiccated (e) and rehydrated (f) leaves. Transverse sections of hydrated (g), desiccated (h) and rehydrated (i) leaves. Scale bar: 40 μm. From Phillips *et al.* (2008).

As for *L. brevidens*, the leaf structure was characterized by an extensive folding of the cell walls upon dehydration (Figure 3.3 d-f). SEM pictures revealed that the leaf structure of *L. subracemosa* was broadly similar to that of of *L. brevidens*. However, the compact structure of the cells illustrated in Figure 3.3 (f) and 3.3 (i) revealed that *L. subracemosa* leaf tissues were not able to recover normal cellular morphology upon rehydration.
These results have been published in Phillips *et al.* (2008).

3.2. Analysis of the CDeT11–24 Protein and its Homologues from *Lindernia* Species

The *CDeT11–24* gene (*Craterostigma Desiccation Tolerant 11–24*) from *Craterostigma plantagineum* was reported as one of the transcripts most abundantly expressed in vegetative tissues upon desiccation (Bartels *et al.*, 1990). Velasco *et al.* (1998) showed that the CDeT11–24 protein has a similar accumulation pattern, thus strengthening the hypothesis for its potential role in the response to dehydration. The amino acid composition of the CDeT11–24 protein suggests a similarity with the late embryogenesis abundant (LEA) proteins. Partial sequencing data from cDNA libraries of desiccated leaves of *Lindernia brevidens* and *Lindernia subracemosa* indicated that homologues of the CDeT11–24 protein are also present in these species. The results presented in section 3.1 showed that the *Lindernia* genus displays a phenotypic variability regarding the ability of the vegetative tissues to withstand desiccation. The full length sequences of the CDeT11–24 homologues were therefore isolated and analyzed with respect to their sequence features.

3.2.1. Isolation of CDeT11–24 Homologues from *Lindernia* Species

The full length *L. brevidens* and *L. subracemosa* homologues of the CDeT11–24 protein were cloned by RT-PCR. RNA was isolated according to the method described by Valenzuela-Avendaño *et al.* (2005) and reverse transcription was performed as described in section 2.15. Gene-specific primers were designed based on previous sequence data from partial ESTs sequences. The *Lindernia* CDeT11–24 homologues were amplified using the oligo primers brev_fwd_up, brev_fwd_down, brev_rev and subra_fwd, subra_rev for *L. brevidens* and *L. subracemosa*, respectively (listed in section 2.11).
The DNA sequences cloned from *L. brevidens* and *L. subracemosa* were assembled and aligned with help of Vector NTI Advance™ 10 (Invitrogen) and the translation start codon was deduced based on the homology to the CDeT11–24 sequence of *C. plantagineum*. The coding sequence is 1350 bp long for the *L. brevidens* homologue (Lb11–24) and 1332 bp for the *L. subracemosa* homologue (Ls11–24), displaying a 55 % identity to each other and 58.8 % and 61.6 % to *C. plantagineum*, respectively (Figure 3.4).

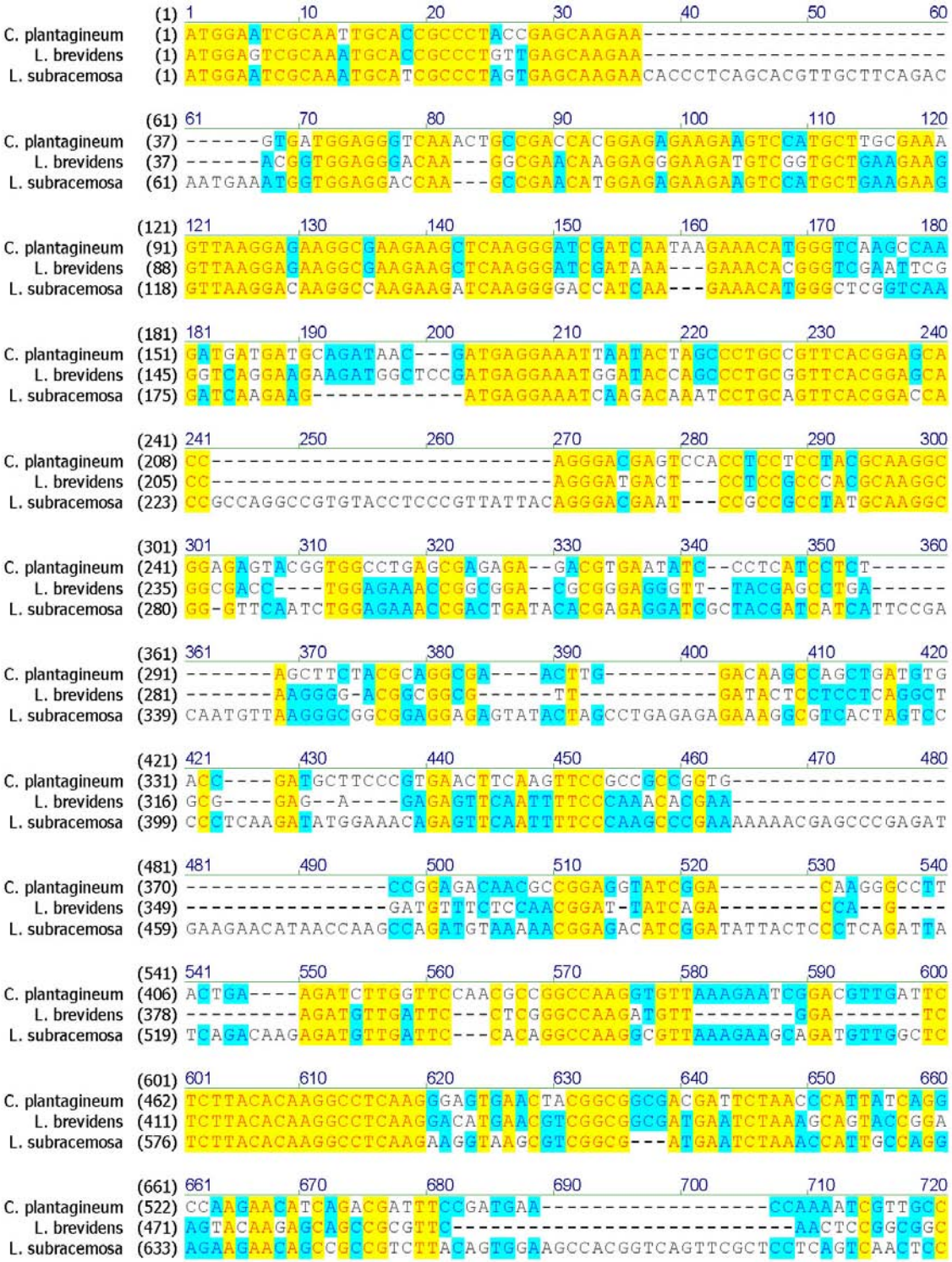
C. plantagineum
L. brevidens
L. subracemosa

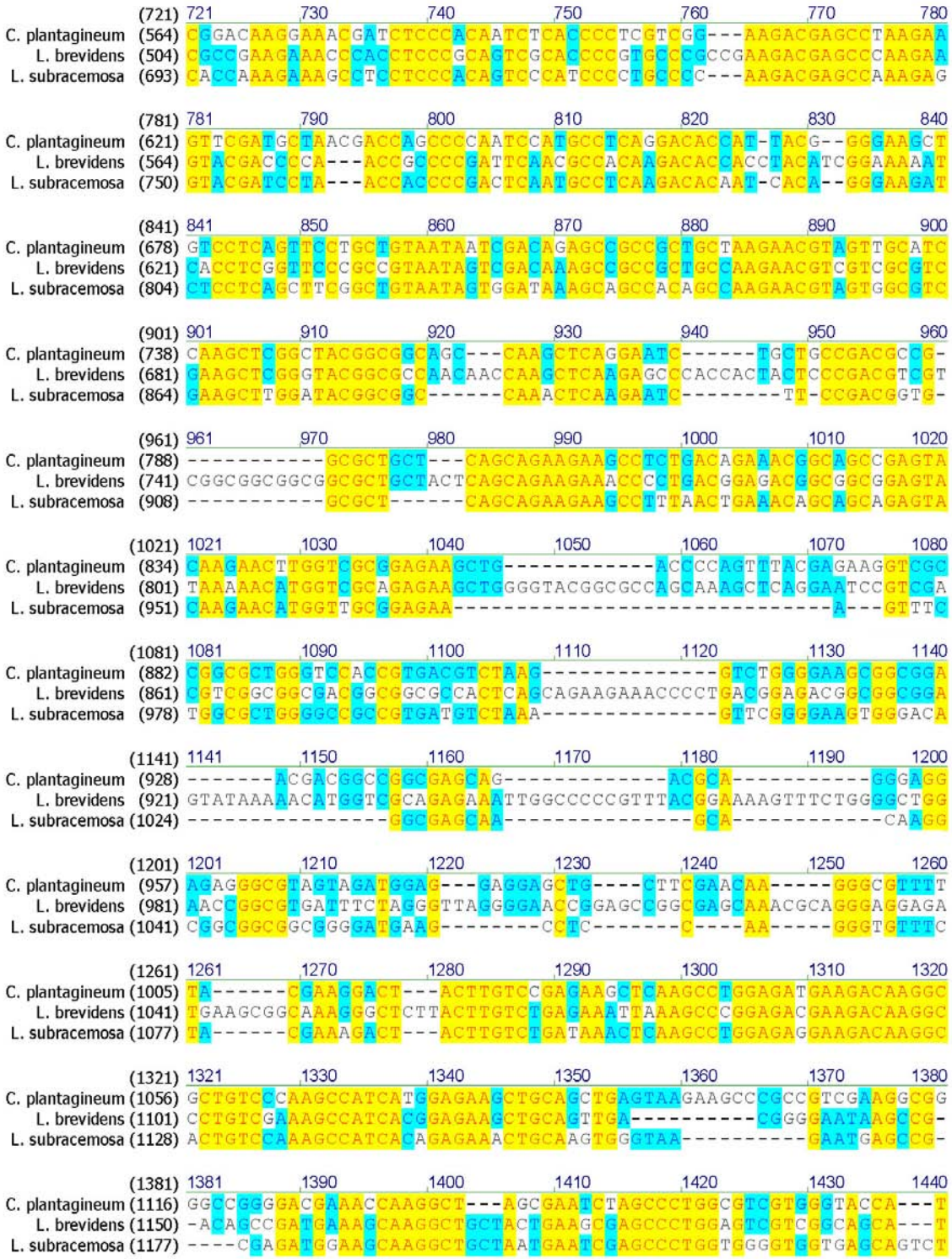
(721) 721 730 740 750 760 770 780
C. plantagineum (564) CGGACAAGGAAACGATCTCCCACAATCTCACCCCTCGTCGG---AAGACGAGCCTAAGAA
L. brevidens (504) CGCCGAAGAAACCCACCTCCCGCAGTCGCACCCCGTGCCCGCCGAAGACGAGCCCAAGAA
L. subracemosa (693) CACCAAAGAAAGCCTCCTCCCACAGTCCCATCCCCTGCCCC---AAGACGAGCCAAAGAG
(781) 781 790 800 810 820 830 840
C. plantagineum (621) GTTCGATGCTAACGACCAGCCCCAATCCATGCCTCAGGACACCAT-TACG--GGGAAGCT
L. brevidens (564) GTACGACCCCA---ACCGCCCCGATTCAACGCCACAAGACACCACCTACATCGGAAAAAT
L. subracemosa (750) GTACGATCCTA---ACCACCCCGACTCAATGCCTCAAGACACAAT-CACA--GGGAAGAT
(841) 841 850 860 870 880 890 900
C. plantagineum (678) GTCCTCAGTTCCTGCTGTAATAATCGACAGAGCCGCCGCTGCTAAGAACGTAGTTGCATC
L. brevidens (621) CACCTCGGTTCCCGCCGTAATAGTCGACAAAGCCGCCGCTGCCAAGAACGTCGTCGCGTC
L. subracemosa (804) CTCCTCAGCTTCGGCTGTAATAGTGGATAAAGCAGCCACAGCCAAGAACGTAGTGGCGTC
(901) 901 910 920 930 940 950 960
C. plantagineum (738) CAAGCTCGGCTACGGCGGCAGC---CAAGCTCAGGAATC------TGCTGCCGACGCCG-
L. brevidens (681) GAAGCTCGGGTACGGCGCCAACAACCAAGCTCAAGAGCCCACCACTACTCCCGACGTCGT
L. subracemosa (864) GAAGCTTGGATACGGCGGC------CAAACTCAAGAATC--------TT-CCGACGGTG-
(961) 961 970 980 990 1000 1010 1020
C. plantagineum (788) -----------GCGCTGCT---CAGCAGAAGAAGCCTCTGACAGAAACGGCAGCCGAGTA
L. brevidens (741) CGGCGGCGGCGGCGCTGCTACTCAGCAGAAGAAACCCCTGACGGAGACGGCGGCGGAGTA
L. subracemosa (908) -----------GCGCT------CAGCAGAAGAAGCCTTTAACTGAAACAGCAGCAGAGTA
(1021) 1021 1030 1040 1050 1060 1070 1080
C. plantagineum (834) CAAGAACTTGGTCGCGGAGAAGCTG------------ACCCCAGTTTACGAGAAGGTCGC
L. brevidens (801) TAAAAACATGGTCGCAGAGAAGCTGGGGTACGGCGCCAGCAAAGCTCAGGAATCCGTCGA
L. subracemosa (951) CAAGAACATGGTTGCGGAGAA------------------------------A---GTTTC
(1081) 1081 1090 1100 1110 1120 1130 1140
C. plantagineum (882) CGGCGCTGGGTCCACCGTGACGTCTAAG--------------GTCTGGGGAAGCGGCGGA
L. brevidens (861) CGTCGGCGGCGACGGCGGCGCCACTCAGCAGAAGAAACCCCTGACGGAGACGGCGGCGGA
L. subracemosa (978) TGGCGCTGGGGCCGCCGTGATGTCTAAA--------------GTTCGGGGAAGTGGGACA
(1141) 1141 1150 1160 1170 1180 1190 1200
C. plantagineum (928) -------ACGACGGCCGGCGAGCAG--------------ACGCA-----------GGGAGG
L. brevidens (921) GTATAAAAACATGGTCGCAGAGAAATTGGCCCCCGTTTACGGAAAAGTTTCTGGGGCTGG
L. subracemosa (1024) ----------------GGCGAGCAA---------------GCA-----------CAAGG
(1201) 1201 1210 1220 1230 1240 1250 1260
C. plantagineum (957) AGAGGGCGTAGTAGATGGAG---GAGGAGCTG-----CTTCGAACAA-----GGGCGTTTT
L. brevidens (981) AACCGGCGTGATTTCTAGGGTTAGGGGAACCGGAGCCGGCGAGCAAACGCAGGGAGGAGA
L. subracemosa (1041) CGGCGGCGGCGGGGATGAAG--------CCTC-------C-----AA-----GGGTGTTTC
(1261) 1261 1270 1280 1290 1300 1310 1320
C. plantagineum (1005) TA------CGAAGGACT---ACTTGTCCGAGAAGCTCAAGCCTGGAGATGAAGACAAGGC
L. brevidens (1041) TGAAGCGGCAAAGGGCTCTTACTTGTCTGAGAAATTAAAGCCCGGAGACGAAGACAAGGC
L. subracemosa (1077) TA------CGAAAGACT---ACTTGTCTGATAAACTCAAGCCTGGAGAGGAAGACAAGGC
(1321) 1321 1330 1340 1350 1360 1370 1380
C. plantagineum (1056) GCTGTCCCAAGCCATCATGGAGAAGCTGCAGCTGAGTAAGAAGCCCGCCGTCGAAGGCGG
L. brevidens (1101) CCTGTCGAAAGCCATCACGGAGAAGCTGCAGTTGA----------CGGGGAATAAGCCG-
L. subracemosa (1128) ACTGTCCAAAGCCATCACAGAGAAACTGCAAGTGGGTAA----------GAATGAGCCG-
(1381) 1381 1390 1400 1410 1420 1430 1440
C. plantagineum (1116) GGCCGGGGACGAAACCAAGGCT---AGCGAATCTAGCCCTGGCGTCGTGGGTACCA---T
L. brevidens (1150) -ACAGCCGATGAAAGCAAGGCTGCTACTGAAGCGAGCCCTGGAGTCGTCGGCAGCA---T
L. subracemosa (1177) ----CGAGATGGAAGCAAGGCTGCTAATGAATCGAGCCCTGGTGGGGTGGTGAGCAGTCT

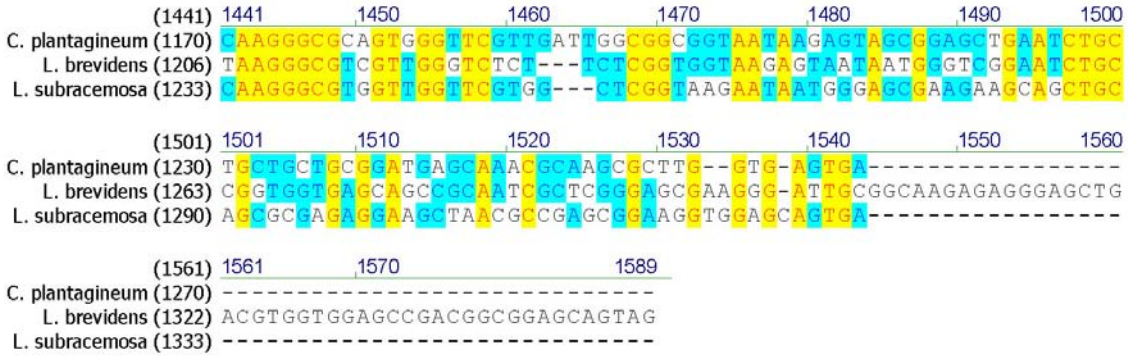

Figure 3.4: Comparison of the coding sequence of *L. brevidens* and *L. subracemosa* 11–24 homologues with CDeT11–24. Identical nucleotides are marked in yellow, nucleotides conserved between two sequences in blue. The nucleotide sequences were aligned with Vector NTI Advance™ 10 using the score matrix swgapdnamt.

The amino acid sequences of the *L. brevidens* and *L. subracemosa* 11–24 homologues compared with the CDeT11–24 reveal three proteins with similar properties (Table 3.1). The primary structure indicates that the *Lindernia* and *C. plantagineum* 11–24 homologues share similar molecular weights and an isoelectric point that ascribes them as acidic proteins.

The amino acid sequences of the three proteins contain a stretch of residues close to the N-terminal part that resembles the K-segment typical of the Group 2 LEA proteins, also called dehydrins (Close, 1996)(Figure 3.5).

Residues 207–233 of Lb11–24 and residues 268–294 of Ls11–24 match the CAP160 repeat pattern (Interpro entry IPR012418, red box in Figure 3.5). InterPro combines a number of databases that use different methodologies and a varying degree of biological information

Table 3.1: Physico-chemical parameters for the Lb11–24, Ls11–24 and CDeT11–24 proteins. The amino acid sequences were aligned with Vector NTI Advance™ 10 using the score matrix BLOSUM62.

	Length (aa)	MW	pI	similarity to CDeT11–24 (%)	similarity to Lb11–24 (%)	similarity to Ls11–24 (%)
C. plantagineum	428	44.0	4.77	–	57	55
L. brevidens	449	46.2	4.90	57	–	61
L. subracemosa	443	47.2	5.48	55	61	–

on well-characterized proteins to derive protein signatures (Hunter *et al.*, 2009). The CAP160 domain is also present in CDeT11–24 (residues 226–252) and was first described in the protein CAP160 of spinach where it appears three times (Kaye *et al.*, 1998). Besides the CAP160 protein from spinach and CDeT11–24 other seven proteins which contain the InterPro domain IPR012418 were found in the database (Table 3.2).

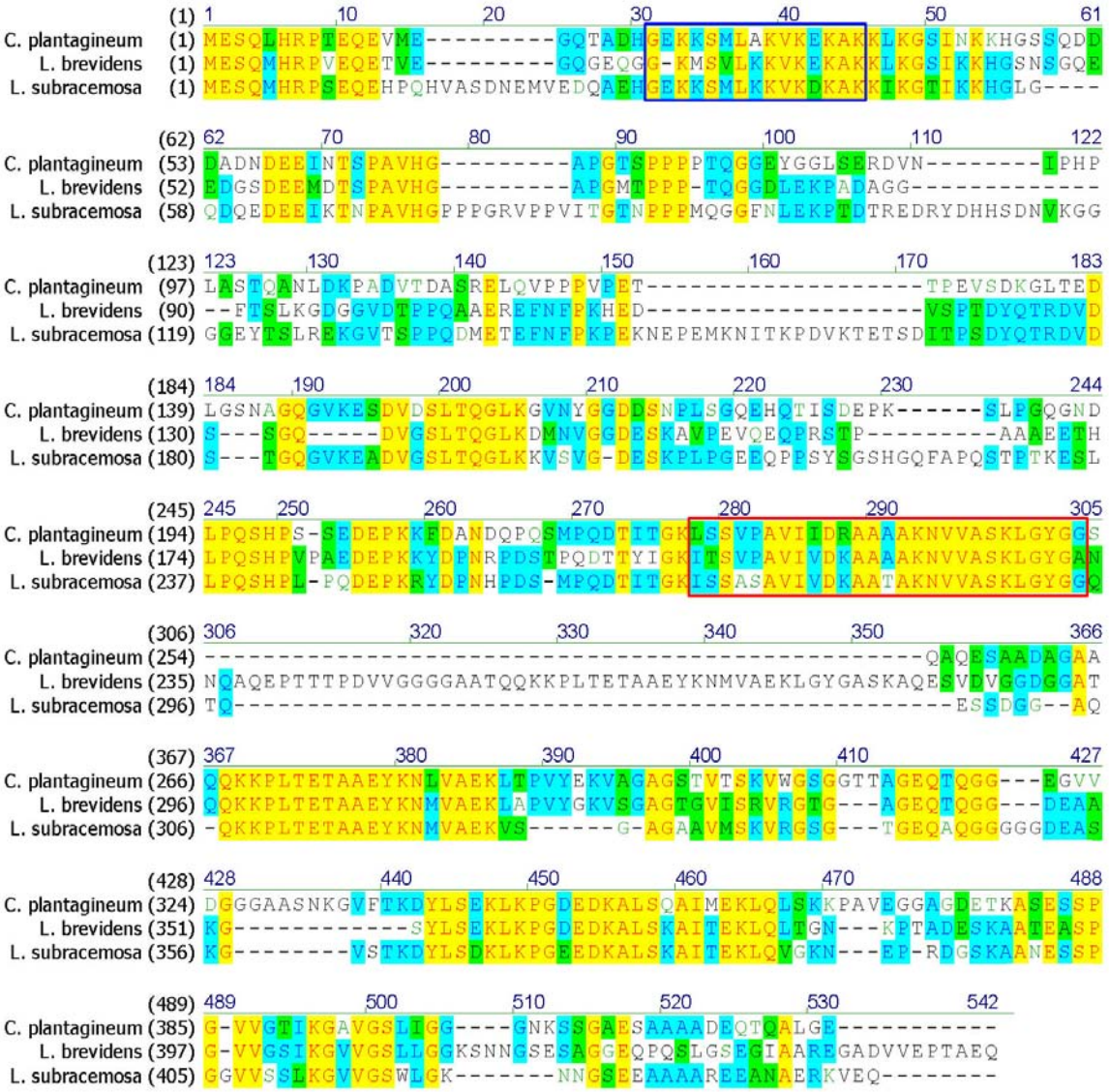

Figure 3.5: Comparison of the translated Lb11–24 and Ls11–24 with the *C.plantagineum* 11–24 protein. The blue box contains the putative K–segment like and the red box contains the CAP160 repeat (Interpro IPR012418).

Table 3.2: List of proteins containing the CAP160 domain (InterPro: IPR012418) sorted by name.

UniProtKB Accession	Protein Name	Organism	Match position
B9I491	Predicted protein	*Populus trichocarpa*	331–357
B9R9B7	Putative uncharacterized protein	*Ricinus communis*	325–351
O23764	CDeT11–24 protein	*Craterostigma plantagineum*	226–252
O50054	Cold acclimation protein	*Spinacia oleracea*	426–452, 491–517, 548–574
O65604	Putative uncharacterized protein M7J2.50	*Arabidopsis thaliana*	391–417
Q04980	LTI65/RD29B	*Arabidopsis thaliana*	486–412
Q2V2Z2	Putative uncharacterized protein At5g52300.2	*Arabidopsis thaliana*	385–411
Q8H0I1	Putative uncharacterized protein B57	*Nicotiana tabacum*	437–463
Q9SWB3	Seed maturation protein PM39	*Glycine max*	2–28, 52–78, 96–122, 144–170, 195–221
	Lb11–24	*Lindernia brevidens*	207–233
	Ls11–24	*Lindernia subracemosa*	268–294

The InterPro domain IPR012418 corresponds to the Pfam domain PF07918. The Pfam database is a large collection of protein families, each represented by multiple sequence alignments and hidden Markov models (HMMs). Figure 3.6 represents the HMM logo for the PF07918 domain. The logo provides a quick overview of the properties of an HMM in a graphical form (Schuster-Böckler *et al.*, 2004).

Figure 3.7 compares the CAP160 domain of CDeT11–24 with the predicted CAP160 domain of Lb11–24 and Ls11–24. The sequences of the *Lindernia* homologues are very closely related to the *Craterostigma* homologues, as highlighted in Figure 3.5, and fit to the HMM logo illustrated in Figure 3.6.

CDeT11–24 contains a conserved domain (ProDom entry PD010085) that spans residues 183 to 383. ProDom is a comprehensive set of protein domain families automatically generated from the UniProt Knowledge Database (Bru *et al.*, 2005). Lb11–24 and Ls11–24 also contain a stretch of amino acids with a high homology to the *C. plantagineum*

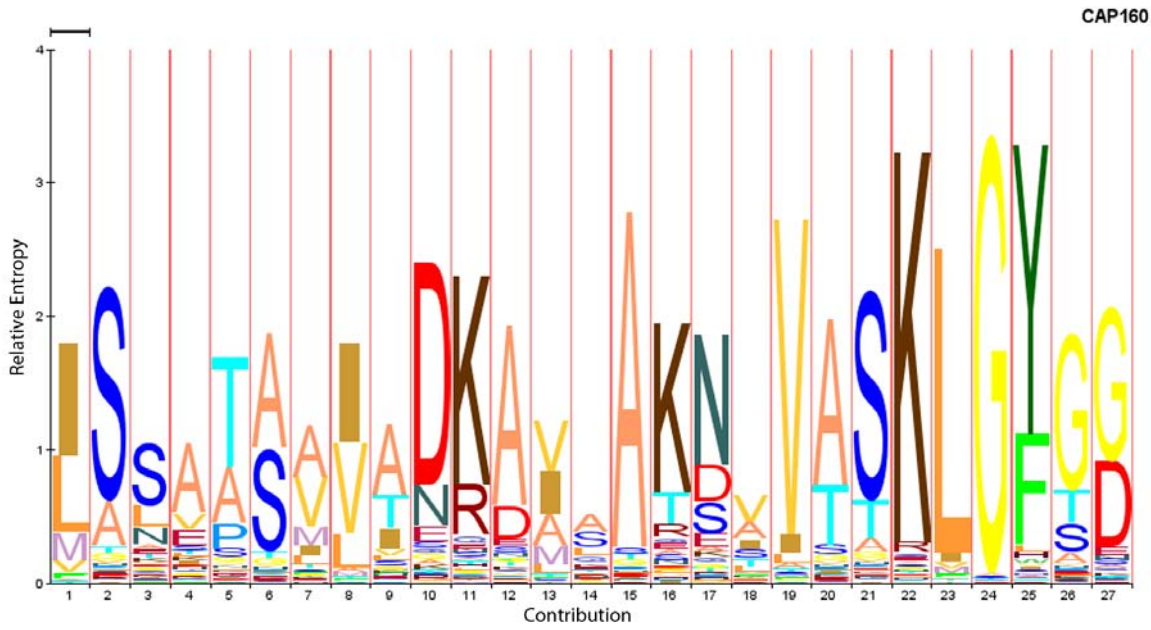

Figure 3.6: HMM logo of the PF07918 Pfam domain. Every position of the sequence family is represented by a different distribution over the alphabet. The height of the stack represents the relative entropy of the distribution of the probabilities.

C.plantagineum	LSSVPAVIIDRAAAAKNVVASKLGYGG
L.brevidens	ITSVPAVIVDKAAAAKNVVASKLGYGA
L.subracemosa	ISSASAVIVDKAATAKNVVASKLGYGG

Figure 3.7: Alignment of the Pfam domain PF07918 of the *C. plantagineum*, *Lindernia brevidens* and *Lindernia subracemosa* 11–24 homologues.

sequence that resembles the PD010085 domain. The domain is observed in ten other plant proteins from tobacco (B57, Q8H0I1), spinach (CAP160, O50054), *Brassica oleracea* (RS1, Q67BB3), rice (Q337E2; Q53RR4) and *Arabidopsis thaliana* (M7J2.50, O65604; RD29A/LTI78, Q06738; RD29B/LTI65, Q04980; Q9STE9 and Q5XVB0) (Figure 3.8).

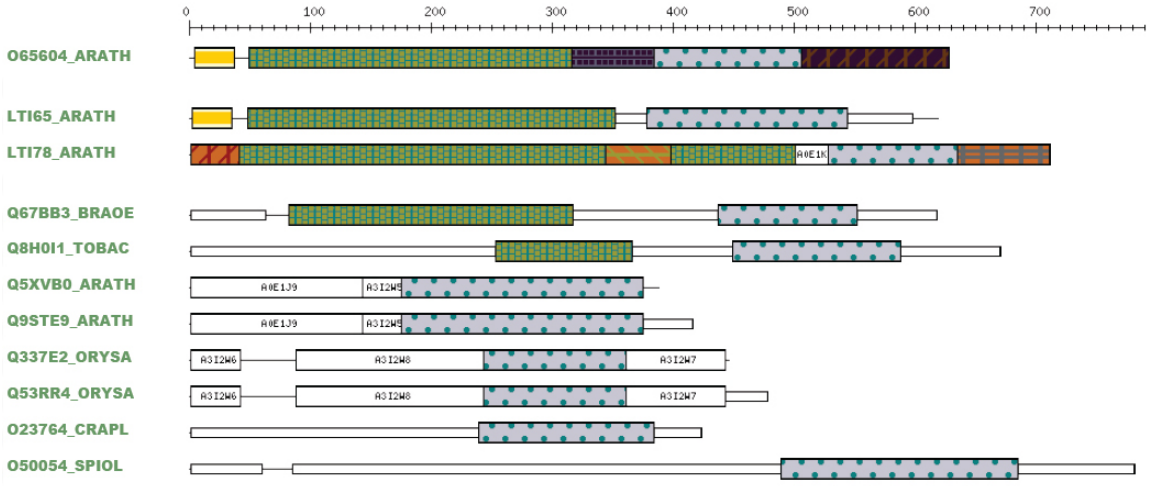

Figure 3.8: Graphical view of the proteins containing the ProDom domain PD010085. The domain containing sequence is indicated by the dotted blue boxes. The other patterned boxes correspond to additional ProDom domains present in the proteins. On the left the names of the proteins are indicated according to the UniProtKB/TrEMBL annotation.

3.2.2. Amino Acid Composition and Secondary Structure Features

Secondary structure predictions based on the Hierarchical Neural Network (HNN) method (Guermeur *et al.*, 1999) predict that 60 % of the CDeT11–24 sequence is random coil, implying an extended rather than a compact conformation (Röhrig *et al.*, 2006). This feature was exploited for the enrichment of this protein because having no hydrophobic core, it does not lose solubility at elevated temperatures and can be separated from the bulk of the protein fraction by its heat stability (described in section 3.3).

To further analyze the CDeT11–24 homologues from *Lindernia* species, the hypothesis of unfolded secondary structure was tested on their sequences. The HNN analysis predicted 71 % and 71.8 % random coil secondary structure for *L. brevidens* and *L. subracemosa*, respectively.

Due to their secondary structure, heat stability and atypical migration pattern on SDS–PAGE (shown in section 3.3), CDeT11–24 and its homologues can be defined as intrinsically unstructured proteins (IUPs)(Tompa, 2002).

A key feature of IUPs that discerns them from globular proteins is the predictability of

Table 3.3: Amino acid composition of CDeT11–24, Lb11–24 and Ls11–24. For every amino acid the absolute number and the frequency expressed as percentage are indicated.

Amino acid		*C. plantagineum*		*L. brevidens*		*L. subracemosa*		Globular[a]
		no.	(%)	no.	(%)	no.	(%)	(%)
Ala	(A)	44	10.4	47	10.5	31	7.0	8.15
Arg	(R)	4	0.9	8	1.8	11	2.5	4.61
Asn	(N)	14	3.3	12	2.7	16	3.6	4.66
Asp	(D)	30	7.1	27	6.0	28	6.3	5.78
Cys	(C)	0	0.0	0	0.0	0	0.0	1.64
Gln	(Q)	26	6.2	27	6.0	25	5.6	3.69
Glu	(E)	35	8.3	42	9.4	43	9.7	5.98
Gly	(G)	52	12.3	59	13.1	48	10.8	7.99
His	(H)	7	1.7	6	1.3	11	2.5	2.33
Ile	(I)	10	2.4	8	1.8	10	2.3	5.43
Leu	(L)	26	6.2	20	4.5	18	4.1	8.37
Lys	(K)	37	8.8	41	9.1	47	10.6	6.05
Met	(M)	5	1.2	8	1.8	10	2.3	2.03
Phe	(F)	2	0.5	3	0.7	4	0.9	3.95
Pro	(P)	29	6.9	32	7.1	36	8.1	4.61
Ser	(S)	41	9.7	34	7.6	40	9.0	6.31
Thr	(T)	26	6.2	32	7.1	27	6.1	6.15
Trp	(W)	1	0.2	0	0.0	1	0.2	1.55
Tyr	(Y)	6	1.4	9	2.0	8	1.8	3.64
Val	(V)	27	6.4	34	7.6	29	6.5	7.00

[a] Amino acid composition for globular proteins on average. Data from Tompa (2002).

structural disorder based on their sequences. A signature of presumably intrinsic disorder is on one hand the presence of low sequence complexity and biased amino acid composition, with a low percentage of hydrophobic, order-promoting amino acids (Trp, Met, Cys, Phe, Ile, Tyr, Val, Leu and Asn), which are normally found in the core of a folded globular protein. On the other hand, an indication of disorder is a high proportion of polar and charged amino acids (Gln, Ser, Pro, Glu, Lys and, Gly, Ala and Arg) which are over-

represented in the unstructured proteins (Dunker *et al.*, 2001; Dyson and Wright, 2005). Table 3.3 summarizes the amino acid composition of the 11–24 homologues from the three species and for globular proteins on average. According to the percentages the hydrophobic order-promoting amino acids account for 21.6 %, 21.1 % and 21.7 % of the total number of amino acids in *C. plantagineum*, *L. brevidens* and *L. subracemosa*, respectively. In contrast, the hydrophilic disorder-promoting amino acids account for 63.5 %, 64.6 % and 63.3 % of the sequences, respectively. The ratio between disorder-promoting and order-promoting amino acids is close to three, a value that is much greater than that for globular proteins. Here, in fact, the order-promoting amino acids account for 38.3 % of the sequence and the disorder-promoting amino acids for 47.4 %. These statistical comparisons of amino acid compositions indicate that ordered and disordered sequences differ to a significant extent. A range of bioinformatic predictors have been developed exploiting these sequence biases (Tompa, 2005). Most of them perform the prediction analysis to a degree comparable to the secondary structure prediction algorithms (e.g. Bracken *et al.*, 2004).

A different algorithm, IUPred (Dosztányi *et al.*, 2005b), estimates the total pairwise inter-residue interaction energy of sequences, which is significantly smaller for IUPs than for globular controls (Tompa, 2005). This predictor has not been trained to recognize disordered sequences and its correct recognition of IUPs reinforces the assumption that the lack of a stable structure is an intrinsic property. The IUPred algorithm was run on the CDeT11–24 sequence and on the *Lindernia* homologues.

Figure 3.9 shows the graphs of the pairwise interaction energies for the three proteins. The score can be between 0 and 1. Scores above 0.5 indicate disorder. All the three sequences have a similar pattern of disorder tendency. Notably is the fact that the N-terminal part of the sequences displays a greater score for unstructured conformation as compared to the C-terminal part. The latter has also stretches that span through the ordered region of the graph. Interestingly this part corresponds to the sequence containing the ProDom domain previously mentioned (PD010085, Figure 3.8).

An indirect observation that supports the unfolded structure *in vivo* is the high evolutionary rate of IUPs (Dunker *et al.*, 2002; Brown *et al.*, 2002). The evolutionary rate of a sequence is constrained by residues involved in functional and structural interactions, which keep the ratio of non-synonymous (K_A) versus synonymous (K_S) mutations low. Functionally essential side chain interactions within the regular cores of ordered proteins are thought to be subjected to slow rates of evolutionary changes. On the other hand, disordered regions

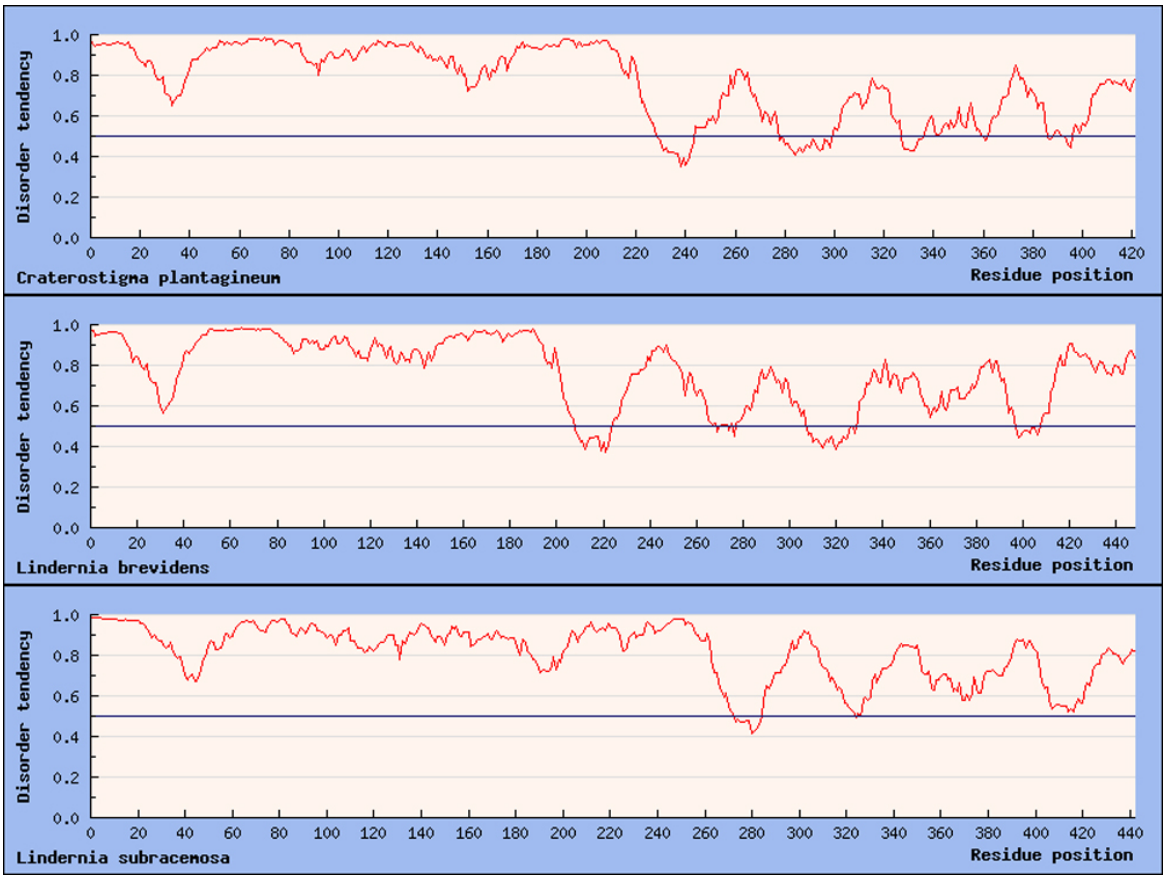

Figure 3.9: IUPred analysis of the amino acids sequences of CDeT11–24, Lb11–24 and Ls11–24. The score can be between 0 and 1. Scores above 0.5 (blue line) indicate a disordered structure.

are free to evolve at a faster rate because they lack crucial side chain interactions. From the K_A/K_S ratio one can therefore get informations about the tendency of evolution rate for a sequence.

The K_A/K_S ratio for all three proteins and for the two parts displaying such different pairwise interaction patterns were consequently calculated according to the Li-Wu-Luo method (Li *et al.*, 1985). Table 3.4 shows the K_A values, the K_S values, as well as their ratio. The values are given for the full length sequences and for both the N-terminal and C-terminal parts observed in the IUPred analysis. The N-terminal values are calculated based on the amino acids 1–229, 1–208, 1–273 of *C. plantagineum*, *L. brevidens* and *L. subracemosa*, respectively. The C-terminal values are calculated based on the amino acids 230–422, 209–449, 274–443 of *C. plantagineum*, *L. brevidens* and *L. subracemosa*, respectively.

Table 3.4: K_A values, K_S values (± std. error) and K_A/K_S ratio for the three 11–24 homologues. The N-terminal values are calculated based on the amino acids 1–229, 1–208, 1–273 of *C. plantagineum*, *L. brevidens* and *L. subracemosa*, respectively. The C-terminal values are calculated based on the amino acids 230–422, 209–449, 274–443 of *C. plantagineum*, *L. brevidens* and *L. subracemosa*, respectively. Calculations were made based on the Li-Wu-Luo method (Li *et al.*, 1985) using the MEGA4 package described in Tamura *et al.* (2007).

		11–24 full length	**11–24 N-terminus**	**11–24 C-terminus**
K_A	*C. plantagineum*/*L. brevidens*	0.312 ± 0.024	0.391 ± 0.038	0.234 ± 0.029
	C. plantagineum/*L. subracemosa*	0.275 ± 0.022	0.362 ± 0.035	0.214 ± 0.028
	L. brevidens/*L. subracemosa*	0.222 ± 0.019	0.198 ± 0.023	0.174 ± 0.024
K_S	*C. plantagineum*/*L. brevidens*	0.789 ± 0.092	0.766 ± 0.125	0.922 ± 0.163
	C. plantagineum/*L. subracemosa*	0.844 ± 0.098	0.812 ± 0.130	1.026 ± 0.189
	L. brevidens/*L. subracemosa*	0.752 ± 0.088	0.567 ± 0.091	0.972 ± 0.174
$\frac{K_A}{K_S}$	*C. plantagineum*/*L. brevidens*	0.39	0.51	0.25
	C. plantagineum/*L. subracemosa*	0.32	0.44	0.21
	L. brevidens/*L. subracemosa*	0.29	0.35	0.18

The K_A/K_S ratio values in Table 3.4 indicate that the N-terminal part of the sequences evolves at a rate that is twice as fast as the C-terminal part.

3.3. Production of an Antibody against CDeT11-24

In order to analyze CDeT11–24 more closely, an antibody against the protein was raised. An antibody recognising the 11–24 homologues of *Lindernia brevidens* and *Lindernia subracemosa* was already available. This antibody was raised against the Ls11–24 and was able to recognize also the Lb11–24 protein (Giarola, 2008).

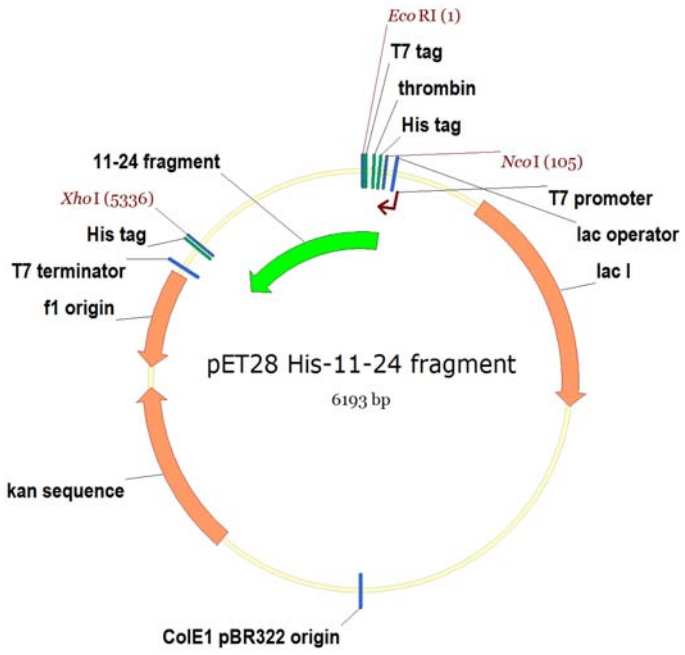

Figure 3.10: pET-28 expression vector containing the histidine-tagged fragment of CDeT11–24. The expressed fragment (green arrow) consists of the 858 bp amplified from the cDNA fused to the vector containing the sequences coding for the 6 histidines, both at the 3' and at the 5' end, resulting in a protein of 328 amino acids.

3.3.1. Amplification and Cloning of CDeT11–24 into pET28-a Expression Vector

To raise an antibody against CDeT11–24 of *C. plantagineum*, an 884 bp long N-terminal portion of the coding sequence was amplified by RT–PCR using the primers 11–24_fwd_Eco and 11–24_rev_Xho (listed in section 2.11). The primers contained *Eco*RI and *Xho*I restriction sites. The restriction sites were introduced by PCR to facilitate the in-frame cloning of the coding region into the pET28-a expression vector (see A.1 for the vector map). The resulting vector (pET 28 His–11–24 fragment) contained the 858 bp from the CDeT11–24 fragment cloned between the *Eco*RI and *Xho*I restriction sites under the control of the T7 promoter (Figure 3.10). The resulting 984 bp long transcript contains the sequences coding for the histidine tag both at the 3' and 5' end.

3.3.2. Protein Isolation

The induction by IPTG of the BL21 *E. coli* strain bearing this vector resulted in the production of a protein of 328 amino acids with a molecular weight of 33.2 kilodaltons (Figure 3.11). After 2 hours of induction the bacterial protein fraction shows a strong induction of the 11–24 fragment. The heat fractionation shows that the protein is retained in the heat-stable supernatant, thus enabling the separation of the 11–24 fragment from the bulk of the *E. coli* proteins. After the affinity chromatography on the Ni-NTA column a pure protein fraction was eluted, containing the histidine-tagged 11–24 fragment.

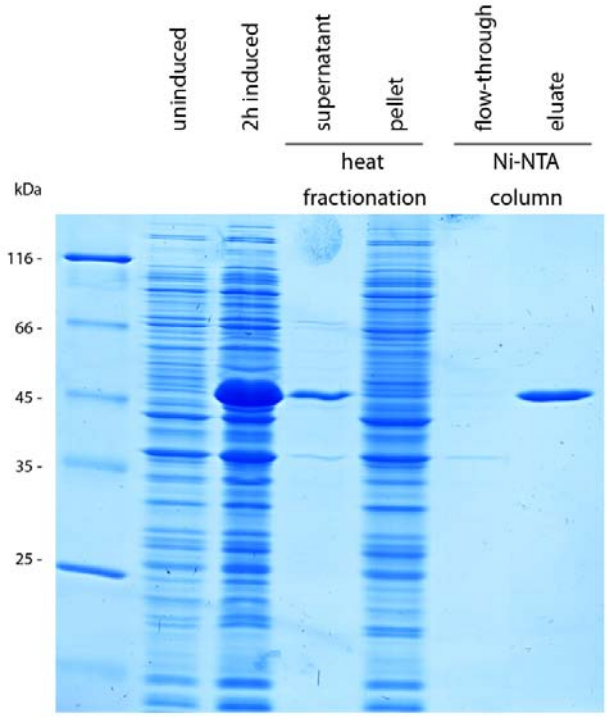

Figure 3.11: SDS–PAGE showing the induction and isolation of the histidine tagged CDeT11–24 protein fragment. Bacteria were induced for 2 hours with 1 mM IPTG and cells were harvested. The induced protein has an apparent mass of about 45 kilodaltons. The fragment was pre-fractionated based on its capacity to remain soluble after heat treatment (described in 2.21) and subsequently further purified by affinity chromatography on a Ni–NTA column suitable for the isolation of histidine-tagged recombinant proteins. This two-step purification strategy resulted in a highly pure protein fraction containing the 11–24 fragment (eluate).

In the SDS–PAGE showing the induction and isolation of the histidine tagged 11–24 protein fragment, 11–24 has an apparent molecular weight of 45 kilodaltons, more than 10 kDa higher than the expected calculated mass.

3.3.3. Antibody Production

The overexpressed and purified CDeT11–24 fragment was desalted and liophilized as described in section 2.21 and used for immunization (described in section 2.22). Figure 3.12 shows a test Western blot using the first bleeding on leaves and callus proteins of *C. plantagineum*. The signal shows a unique strong band in the ABA induced and dried samples, at a molecular weight of about 75 kDa.

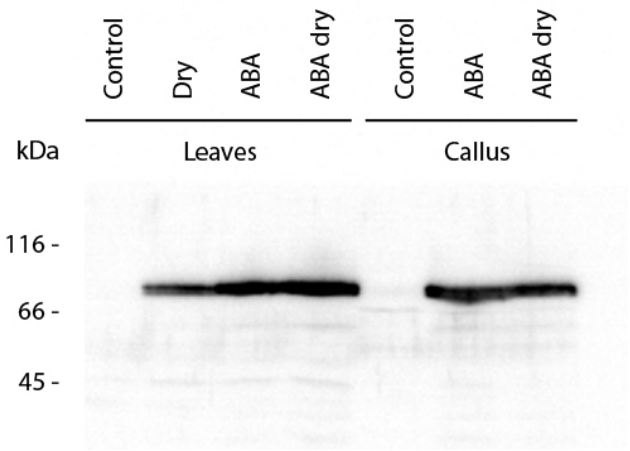

Figure 3.12: Western blot with the first bleed of the CDeT11–24 antiserum. *C. plantagineum* leaf and callus material were tested for the presence of CDeT11–24 upon ABA and dehydration induction. Uninduced material was taken as negative control. 10 μg of proteins per lane were separated by SDS–PAGE and electroblotted on a nitrocellulose membrane.

3.4. Analysis of the Phosphorylation Status of the 11–24 Proteins

In a recent work, Röhrig *et al.* (2006) reported that CDeT11–24 is one of the major phosphoproteins induced by desiccation in the vegetative tissues of *C. plantagineum*. Furthermore, the phosphorylation is an event that takes place in the late stage of dehydration. The hypothesis whether a correlation exists between the secondary modification state of the 11–24 protein and the ability of the plant to withstand desiccation was hence tested. Since the previous reports showed a variability regarding the desiccation tolerance trait within the *Lindernia* genus, the CDeT11–24 homologues from *L. brevidens* and *L. subracemosa* were analyzed with respect to their phosphorylation status during desiccation. Firstly, taking advantage of the availability of antibodies recognizing the 11–24 homologues, an immunoprecipitation was performed. The visualization of the separated samples by Western blotting gives information about the presence of the protein, whereas the staining of the gels containing the same samples by ProQ Diamond Phosphostain provides informations about the phosphorylation status of the proteins. Secondly, the presence of phosphate groups on the candidate proteins was further investigated by phosphatase treatment: the loss of a phosphate moiety causes changes in the isoelectric point of the protein which can be separated by isoelectrofocusing and detected by the specific antibodies. Finally, the phosphorylation sites of the 11–24 homologues were identified and compared. Phosphopeptides were enriched by affinity chromatography and identified by tandem mass spectrometry (MS/MS) on the basis of sequence information.

3.4.1. Immunoprecipitation of the 11–24 Proteins

The 11–24 protein was immunoprecipitated from plant and callus tissues subjected to different degrees of desiccation and to ABA treatment. The immunoprecipitated proteins were then separated by SDS–PAGE and visualized with the ProQ Diamond phosphoprotein gel stain. The same samples were also transferred to a nitrocellulose membrane in order to detect the presence of the protein by Western blotting. Comparing these two approaches of visualising the candidate protein one can draw conclusions about the phosphorylation status of the protein.

Immunoprecipitation of the the CDeT11–24 Protein

Röhrig *et al.* (2006) reported that CDeT11–24 is induced during the early stages of dehydration and phosphorylated at a very late stage. An immunoprecipitation with the CDeT11–24 antibody was therefore performed on *C. plantagineum* leaf material from fully hydrated plants, from plants with 50 % relative water content (RWC) and from desiccated plants (2 % RWC). In Figure 3.13 are illustrated the Western blot membrane probed with the CDeT11–24 antibody and the gel with the same samples stained with the phosphoprotein specific stain.

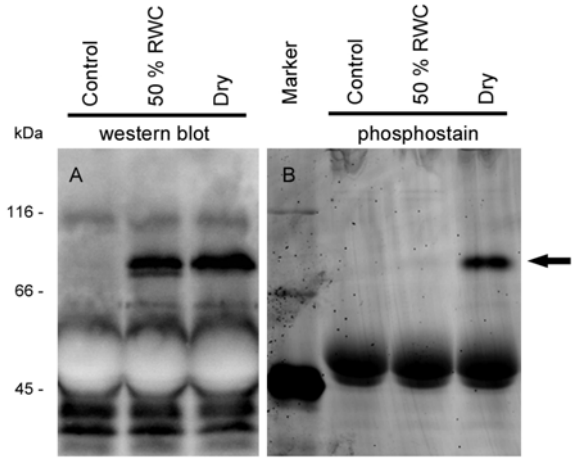

Figure 3.13: Immunoprecipitation with CDeT11–24 antibody on *C. plantagineum* leaf material from control (95 % RWC), partially dehydrated (50 % RWC) and desiccated plants (2 % RWC). The eluted proteins were separated by SDS-PAGE, blotted and the membrane probed with the 11–24 antibody (A) or the gel was stained with ProQ Diamond phosphostain (B). The arrow indicates the band corresponding to CDeT11–24 protein. The bands running at 50 kDa correspond to the heavy chain of the IgGs. The marker lane shows the staining of the phosphoprotein ovalbumin, running at a molecular size of 45 kDa.

The Western blot (Figure 3.13 A) shows that the CDeT11–24 protein is present when the plant is partially dried (50 % RWC) and completely dried (2 % RWC) but the phosphoprotein specific stain confirmed its phosphorylation only in the completely dried stage (Figure 3.13 B). Partial dehydration is therefore not sufficient to induce the phosphorylation of the CDeT11–24 protein.

In preliminary experiments, enriched phosphoproteins from ABA induced *C. plantagineum* leaves were separated by 2D–PAGE, leading to the observation that the spot corresponding

to CDeT11–24 was not present (data not shown). ABA is able to induce the expression of most dehydration responsive genes, among these also CDeT11–24. To gain more insight into the biphasic induction and phosphorylation of CDeT11–24, the same immunoprecipitation experiment was performed on *C. plantagineum* leaf and callus material, including ABA treated samples. In this way the hypothesis whether ABA induction and phosphorylation are decoupled was assayed.

Figure 3.14 shows the result of the immunoprecipitation experiment. The results indicate that CDeT11–24 is induced by ABA treatment (A and B) but the phosphorylation of the protein is an independent event (C and D). Only desiccation is able to induce CDeT11–24 phosphorylation in both callus and leaf tissues.

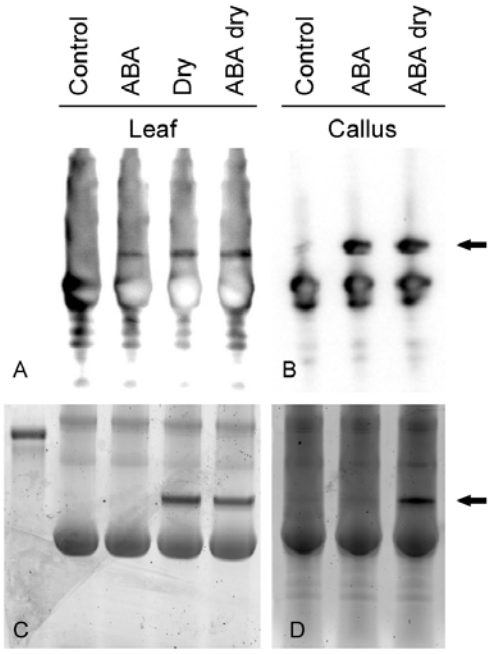

Figure 3.14: Immunoprecipitation with CDeT11–24 antibody on *C. plantagineum* leaf and callus material. Samples from callus material (A) and leaf material (B) were separated by SDS–PAGE, transferred on a nitrocellulose membrane and incubated with the same antibody used for the immunoprecipitation. Aliquots of the same samples were separated as above and the gels were stained with ProQ Diamond phosphostain (C and D). ABA treatment was imposed on leaves for 24 h with 100 μM ABA. Calli were incubated for 6 days on MS–IK22 agar plates supplemented with 20 μM ABA. The arrows indicate the bands corresponding to CDeT11–24. The band below the CDeT11–24 protein correspond to the heavy chain of the IgGs.

Immunoprecipitation of the 11–24 Homologues from *Lindernia*

The same immunoprecipitation experiment was performed on *L. brevidens* and *L. subracemosa* plant material. A dehydration kinetic along four stages from fully hydrated to dehydrated plants was set to test whether the induction and phosphorylation of the *Lindernia* 11–24 homologues display the same biphasic pattern.

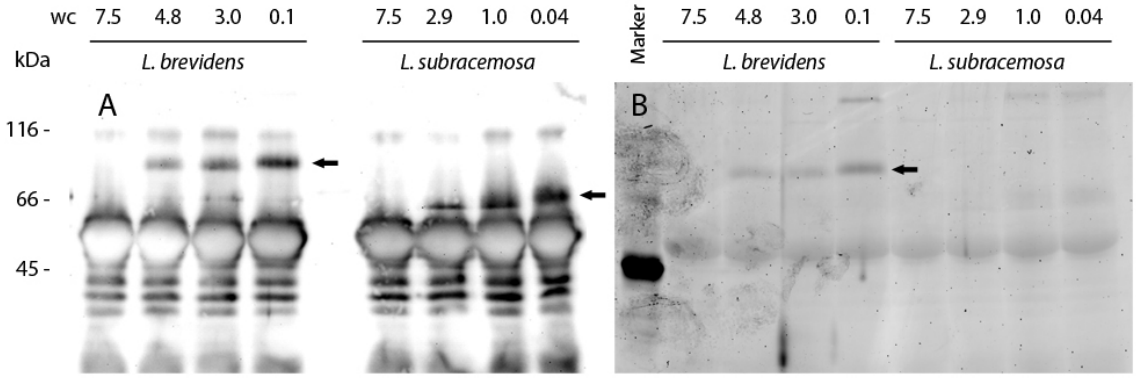

Figure 3.15: Immunoprecipitation with the Ls11–24 antibody on *L. brevidens* and *L. subracemosa* leaf material. Samples with different water contents (wc) were separated by SDS–PAGE, transferred on a nitrocellulose membrane and incubated with the same antibody used for the immunoprecipitation (A). Aliquots of the same samples were separated as above and stained with ProQ Diamond phosphostain (B). The arrows indicate the bands corresponding to Lb11–24 and Ls11–24. The bands below the 11–24 protein correspond to the heavy chain of the IgGs. The marker lane shows the staining of the phosphoprotein ovalbumin, running at a molecular size of 45 kDa.

Figure 3.15 presents the results of the immunoprecipitation with the Ls11–24 antibody on *L. brevidens* and *L. subracemosa* leaf material. The Western blot depicts the accumulation of the proteins along the dehydration process, indicating that the protein is induced upon dehydration in both plants (Figure 3.15 A, black arrows). The antibody precipitated about the same amount of 11–24 protein from both plants. In (B) the samples were separated by SDS–PAGE and the gel stained with ProQ Diamond phosphostain. The staining shows that only the samples of *L. brevidens* display a phosphorylation signal. This suggests that the Lb11–24 protein is phosphorylated, whereas the Ls11–24 may be not. Furthermore, the phosphostain reveals a weak signal also for the partially dehydrated *L. brevidens* samples. To obtain more information on the phosphorylation of the 11–24 homologues from *Linder-*

nia the immunoprecipitation experiment was also performed on plant material treated with ABA. Figure 3.16 shows the immunoprecipitation with the Ls11–24 antibody on *L. brevidens* and *L. subracemosa* detached leaves. For Lb11–24 the induction and phosphorylation pattern is similar to that of CDeT11–24, whereas for *L. subracemosa* ABA treatment is not as efficient in inducing Ls11–24 accumulation (Figure 3.16 A, black arrows). In (B) the gel was stained with ProQ Diamond phosphostain. A strong phosphorylation signal was detected only in the dried samples of *L. brevidens*. Furthermore, a weak signal was also present in the dried samples of *L. subracemosa* and in the ABA treated *L. brevidens* sample.

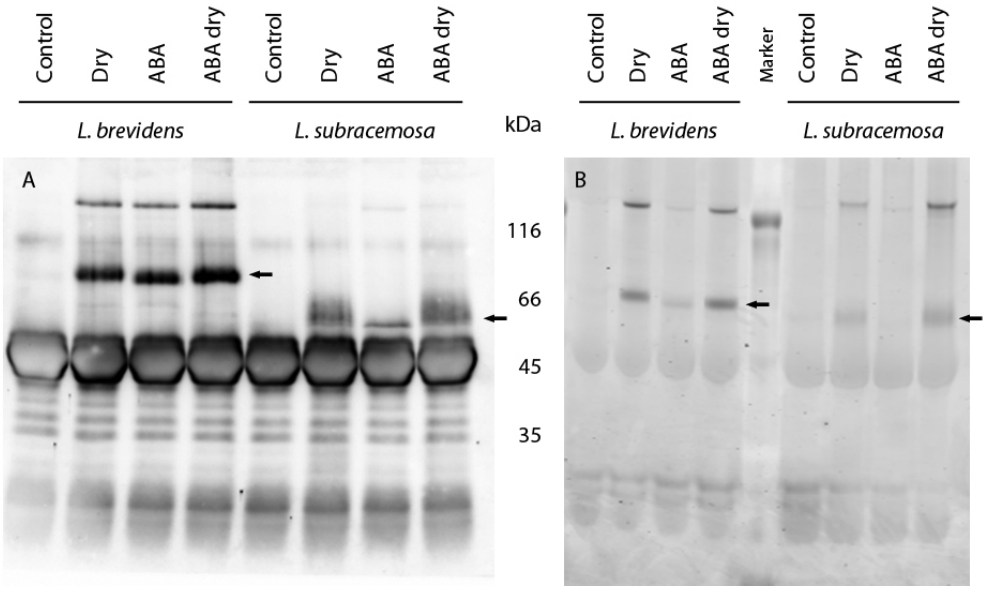

Figure 3.16: Immunoprecipitation with the Ls11–24 antibody on *L. brevidens* and *L. subracemosa* leaf material. ABA treatment was imposed on leaves for 24 h with 100 μM ABA. Samples were separated by SDS–PAGE, transferred on a nitrocellulose membrane and incubated with the same antibody used for the immunoprecipitation (A). Aliquots of the same samples were separated as above and stained with ProQ Diamond phosphostain (B). The arrows indicate the bands corresponding to Lb11–24 and Ls11–24. The bands below the 11–24 protein correspond to the heavy chain of the IgGs.

3.4.2. Phosphatase Shift Assay of *Lindernia* 11–24

To further confirm the differential secondary modification pattern of the *Lindernia* 11–24 homologues, a phosphatase shift assay was performed.

The phosphate group confers a more acidic isoelectric point (pI) to the protein. By treating the samples with a phosphatase and separating the proteins according to their pI, it is possible to compare their position before and after the phosphatase treatment. The loss of a phosphate group causes a shift of the protein towards the basic region of the gel. Heat stable total protein fractions from dehydrated leaves were treated with calf intestine phosphatase (CIP) and separated by 2D SDS–PAGE. Untreated sample was used as control to determine the eventual shift towards the basic region of the gel upon phosphatase treatment. The separated proteins were transferred onto nitrocellulose membranes and incubated with the Ls11–24 antibody. To be able to compare the protein spots and the shift upon CIP treatment, the MagicMark XP Western protein standard (Invitrogen) was loaded in combination with the protein sample. It contains standard proteins fused with an IgG binding site that can be recognized by the secondary antibody. In this way we were able to have a reference on the 2D membrane to compare with the spot specific for the 11–24 proteins. Figure 3.17 shows the MagicMark XP proteins precipitated and separated by 2D SDS–PAGE used as reference pattern.

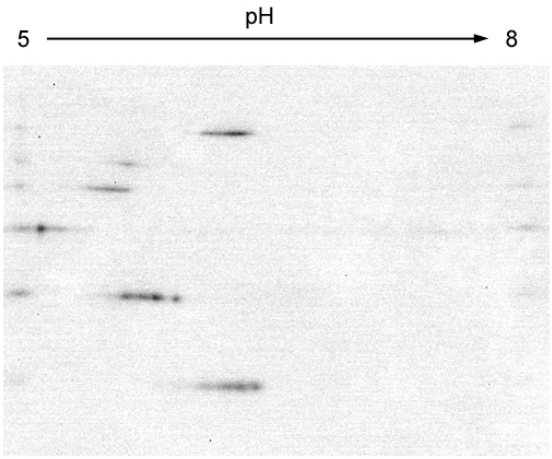

Figure 3.17: 2D SDS–PAGE of MagicMark XP Western protein standard. The proteins were precipitated with 20 % (w/v) TCA and resuspended in IEF rehydration buffer.

Figure 3.18 shows the phosphatase shift assay for *L. brevidens*. The superimposed images visualize the shift of the spot corresponding to Lb11–24 after CIP treatment indicating that the untreated sample has a more acidic isoelectric point due to the phosphate group(s).

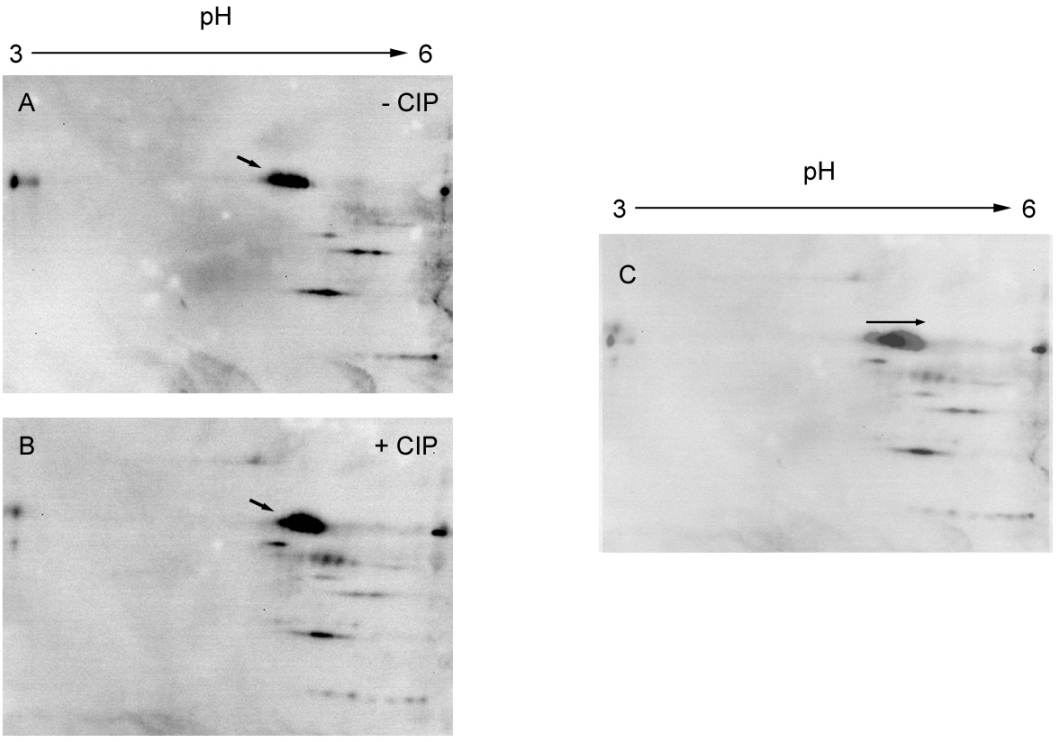

Figure 3.18: Phosphatase shift assay on Lb11–24. Heat stable total protein fraction was separated by 2D SDS–PAGE with (B) or without (A) prior CIP treatment. The gels were electrophoretically transferred on nitrocellulose membranes and incubated with the Ls11–24 antibody. The spot corresponding to Lb11–24 is indicated by an arrow. C shows an overlay of the two gel images to visualize the shift of the spot towards the basic region of the gel.

Figure 3.19 illustrates the phosphatase shift assay on *L. subracemosa*. In (C) no shift of Ls11–24 can be seen, thus strengthening the hypothesis that only the 11–24 homologue from the desiccation tolerant species (Lb11–24) undergoes phosphorylation upon desiccation.

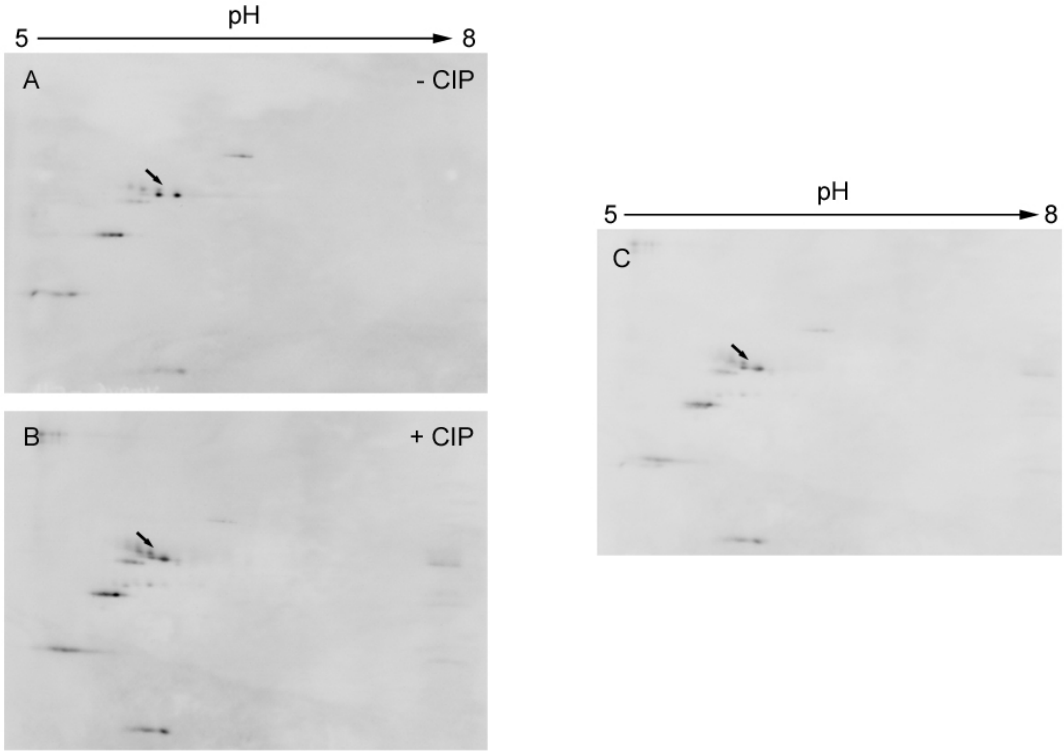

Figure 3.19: Phosphatase shift assay on Ls11–24. Heat stable total protein fraction was separated by 2D SDS–PAGE with (B) or without (A) prior CIP treatment. The gels were electrophoretically transferred on nitrocellulose membranes and incubated with the Ls11–24 antibody. The spot corresponding to Lb11–24 is indicated by an arrow. In C the two gel images are overlayed.

3.4.3. Phosphorylation Sites Identification

Röhrig *et al.* (2006) reported the phosphorylation sites of CDeT11–24. They used a Metal Oxide Affinity Chromatography (MOAC) approach to enrich phosphoproteins from *C. plantagineum* followed by 2D–PAGE and LC–MS/MS analysis to identify the phosphorylation sites of CDeT11–24.

Due to the sub-stoichiometry of phosphorylated proteins in complex mixtures and the suppression of non-phosphorylated peptides over phosphorylated peptides during MS analysis, often an enrichment step is required for the identification of phosphorylation sites. Sugiyama *et al.* (2007) reported an improvement of the phosphopeptide enrichment based

on TiO_2 Metal Oxide Chromatography (MOC) with aliphatic hydroxy acids as competitors for improving the specificity of the phosphopeptide isolation.
Here this approach was used for isolating the phosphopeptides of the CDeT11–24 protein to compare them with the ones reported by Röhrig *et al.* (2006). Additionally, the MOC enrichment was performed on the Lb11–24 and Ls11–24 homologue to confirm the results from the immunoprecipitation experiments (section 3.4.1) and the 2D shift assays (section 3.4.2).

Craterostigma plantagineum CDeT11–24 Phosphopeptide Enrichment and Phosphorylation Sites Identification

CDeT11–24 from *C. plantagineum* dried leaves was immunochromatographically purified using an IgG-coupled affinity column. Affinity-purified CDeT11–24 was digested with trypsin and subjected to phosphopeptide enrichment on TiO_2 columns. Nano–LC–MS/MS analysis of phosphopeptide-enriched tryptic digests yielded three phosphopeptides (Figure 3.20) with mass-to-charge ratios (m/z) of 686.36 (2+), 414.72 (2+) and 555.31 (2+), corresponding to the phosphorylated forms of tryptic peptides T15, T30 and T36 (Table 3.5). Alternative and equivocal phosphorylation sites are marked by letters.
Fragmentation spectra are illustrated in Figure 3.21 for peptide T15 and its three different alternative models, Figure 3.22 for peptide T30 and in Figure 3.23 for peptide T36. Alternative models represent MS/MS spectra that can support more than one unique phosphorylation pattern.

```
  1 MESQLHRPTE QEVMEGQTAD HGEKKSMLAK VKEKAKKLKG SINKKHGSSQ
 51 DDDADNDEEI NTSPAVHGAP GTSPPPPTQG GEYGGLSERD VNIPHPLAST
101 QANLDKPADV TDASRELQVP PPVPETTPEV SDKGLTEDLG SNAGQGVKES
151 DVDSLTQGLK GVNYGGDDSN PLSGQEHQTI SDEPKSLPGQ GNDLPQSHPS
201 SEDEPKKFDA NDQPQSMPQD TITGKLSSVP AVIIDRAAAA KNVVASKLGY
251 GGSQAQESAA DAGAAQQKKP LTETAAEYKN LVAEKLTPVY EKVAGAGSTV
301 TSKVWGSGGT TAGEQTQGGE GVVDGGGAAS NKGVFTKDYL SEKLKPGDED
351 KALSQAIMEK LQLSKKPAVE GGAGDETKAS ESSPGVVGTI KGAVGSLIGG
401 GNKSSGAESA AAADEQTQAL GE
```

Figure 3.20: Phosphopeptides identified for the CDeT11–24 protein of *C. plantagineum*. Phosphorylated peptides are indicated in red.

Table 3.5: Identification of phosphopeptides of CDeT11–24 by mass spectrometry (MS). Underlined sites represent models that best explain the majority of the tandem mass spectrometry (MS/MS) spectra collected for a given mass-to-charge ratio (m/z). Alternative and equivocal phosphorylation sites for a peptide are marked by letters.

Peptide (start – end)	Observed	Mr (exp)	Mr (calc)	Delta	Score	Sequence
T15A (149 - 160)	686.36	1370.71	1370.60	0.12	28	K.E<u>S</u>DVDSLTQGLK.G
T15B (149 - 160)	686.36	1370.71	1370.60	0.12	25	K.ESDVD<u>S</u>LTQGLK.G
T15C (149 - 160)	686.36	1370.71	1370.60	0.12	13	K.ESDVDSL<u>T</u>QGLK.G
T30 (338 - 343)	417.72	833.42	833.32	0.10	16	K.DYL<u>S</u>EK.L
T36 (392 - 403)	555.31	1108.60	1108.53	0.08	21	K.GAVG<u>S</u>LIGGGNK.S

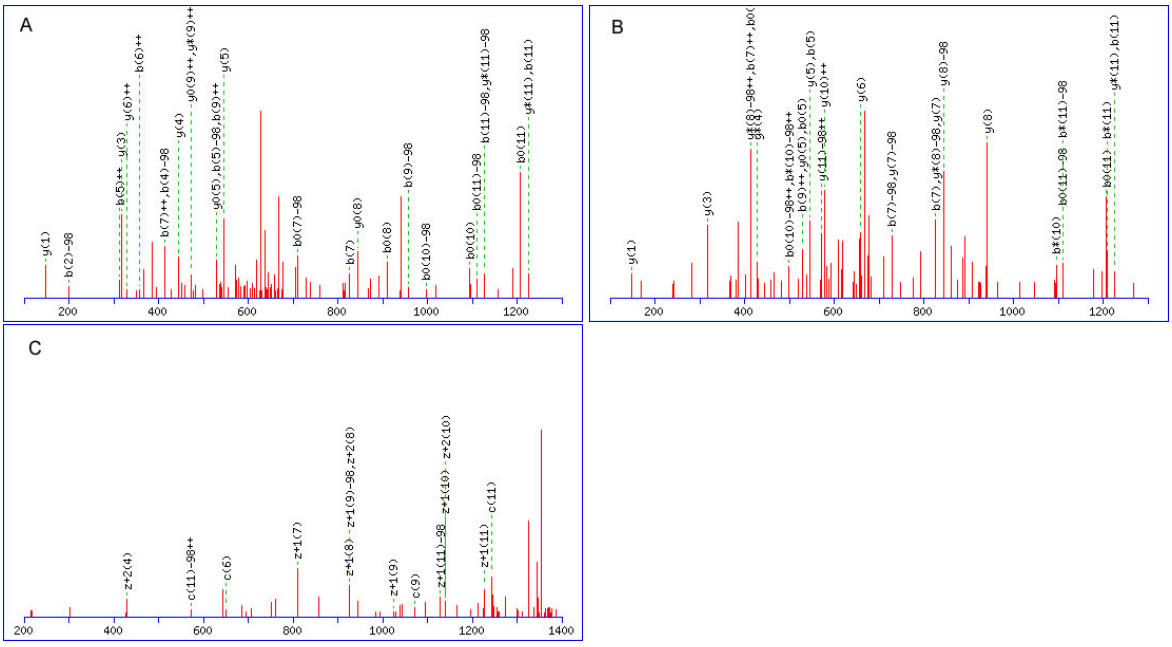

Figure 3.21: Fragmentation spectra of the peptide T15 with the three different alternative models.

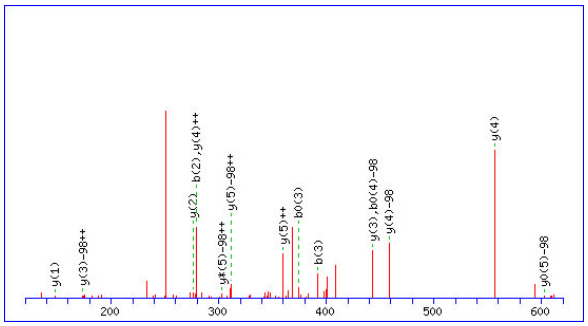

Figure 3.22: Fragmentation spectrum of the peptide T30.

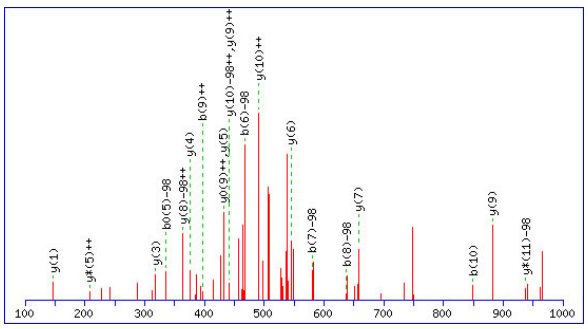

Figure 3.23: Fragmentation spectrum of the peptide T36.

Lindernia brevidens 11–24 Phosphopeptide Enrichment and Phosphorylation Sites Identification

Lb11–24 from *L. brevidens* dried leaves was immunochromatographically purified using an IgG-coupled affinity column. Affinity-purified Lb11–24 was digested with trypsin and subjected to phosphopeptide enrichment on TiO_2 columns. Nano–LC–MS/MS analysis of phosphopeptide-enriched tryptic digests yielded seven phosphopeptides (Figure 3.24) with mass-to-charge ratios (m/z) of 725.38 (2+), 764.68 (2+), 649.23 (3+), 946.82 (2+), 708.75 (3+), 683.92 (2+) and 795.04 (3+) corresponding to the phosphorylated forms of tryptic peptides T12, T14, T15, T33-34, T38-39, T40 and T42 (Table 3.6). Alternative and equivocal phosphorylation sites are marked by letters.
Fragmentation spectra are depicted in Figure 3.25 for peptide T12, Figure 3.26 for peptide T14, Figure 3.27 for peptide T15, Figure 3.28 for peptide T33-34, Figure 3.29 for peptide T38-39 and its two alternative models, Figure 3.30 for peptide T40 and its three alternative models and Figure 3.31 for peptide T42 and its five alternative models.

```
  1 MESQMHRPVE QETVEGQGEQ GGKMSVLKKV KEKAKKLKGS IKKHGSNSGQ
 51 EEDGSDEEMD TSPAVHGAPG MTPPPTQGGD LEKPADAGGF TSLKGDGGVD
101 TPPQAAEREF NFPKHEDVSP TDYQTRDVDS SGQDVGSLTQ GLKDMNVGGD
151 ESKAVPEVQE QPRSTPAAAE ETHLPQSHPV PAEDEPKKYD PNRPDSTPQD
201 TTYIGKITSV PAVIVDKAAA AKNVVASKLG YGANNQAQEP TTTPDVVGGG
251 GAATQQKKPL TETAAEYKNM VAEKLGYGAS KAQESVDVGG DGGATQQKKP
301 LTETAAEYKN MVAEKLAPVY GKVSGAGTGV ISRVRGTGAG EQTQGGDEAA
351 KGSYLSEKLK PGDEDKALSK AITEKLQLTG NKPTADESKA ATEASPGVVG
401 SIKGVVGSLL GGKSNNGSES AGGEQPQSLG SEGIAAREGA DVVEPTAEQ
```

Figure 3.24: Phosphopeptides identified for the Lb11–24 protein of *L. brevidens*. Phosphorylated peptides are indicated in red.

Table 3.6: Identification of phosphopeptides of Lb11–24 by mass spectrometry (MS). Underlined sites represent models that best explain the majority of the tandem mass spectrometry (MS/MS) spectra collected for a given mass-to-charge ratio (m/z). Alternative and equivocal phosphorylation sites for a peptide are marked by letters.

Peptide (start - end)	Observed	Mr (exp)	Mr (calc)	Delta	Score	Sequence
T12 (95 - 108)	725.38	1448.75	1448.59	0.16	12	K.GDGGVD<u>T</u>PPQAAER.E
T14 (115 - 126)	764.68	1527.35	1526.60	0.75	2	K.HEDVSP<u>T</u>DYQTR.D
T15A (127 - 143)	649.23	1944.67	1944.72	−0.04	3	R.DVDS<u>S</u>GQDVG<u>S</u>L<u>T</u>QG-LK.D
T15B (127 - 143)	649.23	1944.67	1944.72	−0.04	3	R.DVD<u>S</u>SGQDVG<u>S</u>L<u>T</u>QG-LK.D
T33-34 (334 - 351)	946.82	1891.82	1890.75	0.87	3	R.VRG<u>T</u>GAGEQ<u>T</u>QGGDE-AAK.G
T38-39A (371 - 389)	708.75	2123.23	2123.05	0.17	11	K.AI<u>T</u>EKLQLTGNKPT-ADESK.A
T38-39B (371 - 389)	708.75	2123.23	2123.05	0.17	10	K.AITEKLQL<u>T</u>GNKPT-ADESK.A
T40A (390 - 403)	683.92	1365.82	1365.65	0.17	28	K.AA<u>T</u>EASPGVVGSIK.G
T40B (390 - 403)	683.92	1365.82	1365.65	0.17	31	K.AATEA<u>S</u>PGVVGSIK.G
T40C (390 - 403)	683.92	1365.82	1365.65	0.17	23	K.AATEASPGVVG<u>S</u>IK.G
T42A (414 - 437)	795.04	2382.11	2382.01	0.10	16	K.<u>S</u>NNGSESAGGEQPQS-LGSEGIAAR.E
T42B (414 - 437)	795.04	2382.11	2382.01	0.10	20	K.SNNG<u>S</u>ESAGGEQPQS-LGSEGIAAR.E
T42C (414 - 437)	795.04	2382.11	2382.01	0.10	20	K.SNNGSE<u>S</u>AGGEQPQS-LGSEGIAAR.E
T42D (414 - 437)	795.04	2382.11	2382.01	0.10	18	K.SNNGSESAGGEQPQ<u>S</u>-LGSEGIAAR.E
T42E (414 - 437)	795.04	2382.11	2382.01	0.10	14	K.SNNGSESAGGEQPQS-LG<u>S</u>EGIAAR.E

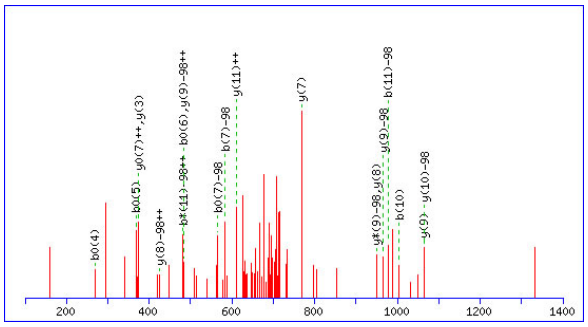

Figure 3.25: Fragmentation spectrum of the peptide T12.

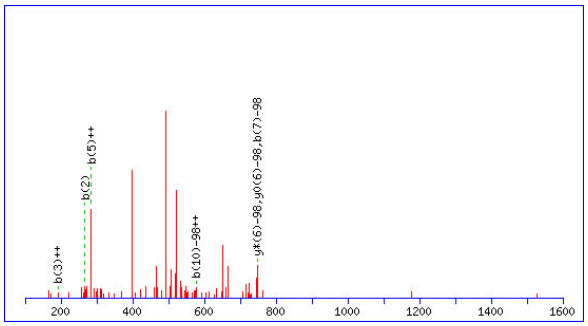

Figure 3.26: Fragmentation spectrum of the peptide T14.

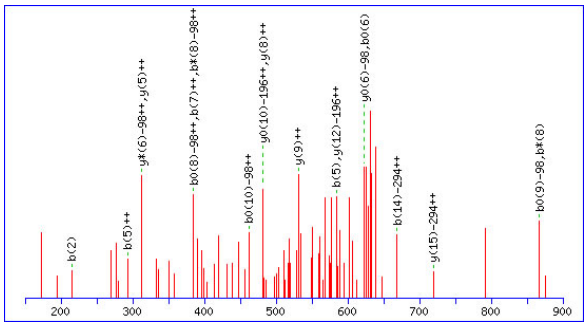

Figure 3.27: Fragmentation spectrum of the peptide T15.

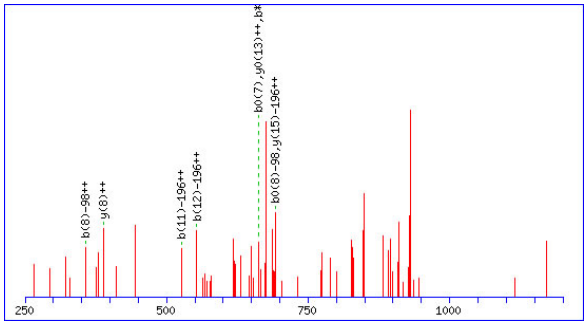

Figure 3.28: Fragmentation spectrum of the peptide T33-34.

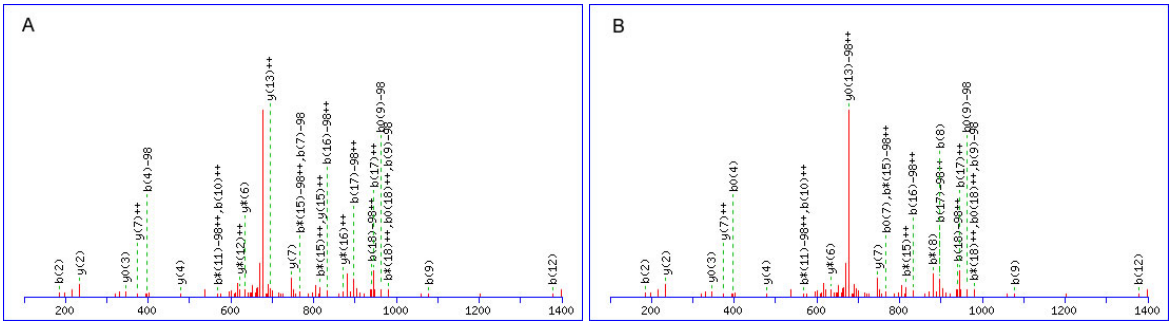

Figure 3.29: Fragmentation spectra of the peptide T38-39 with the two different alternative models.

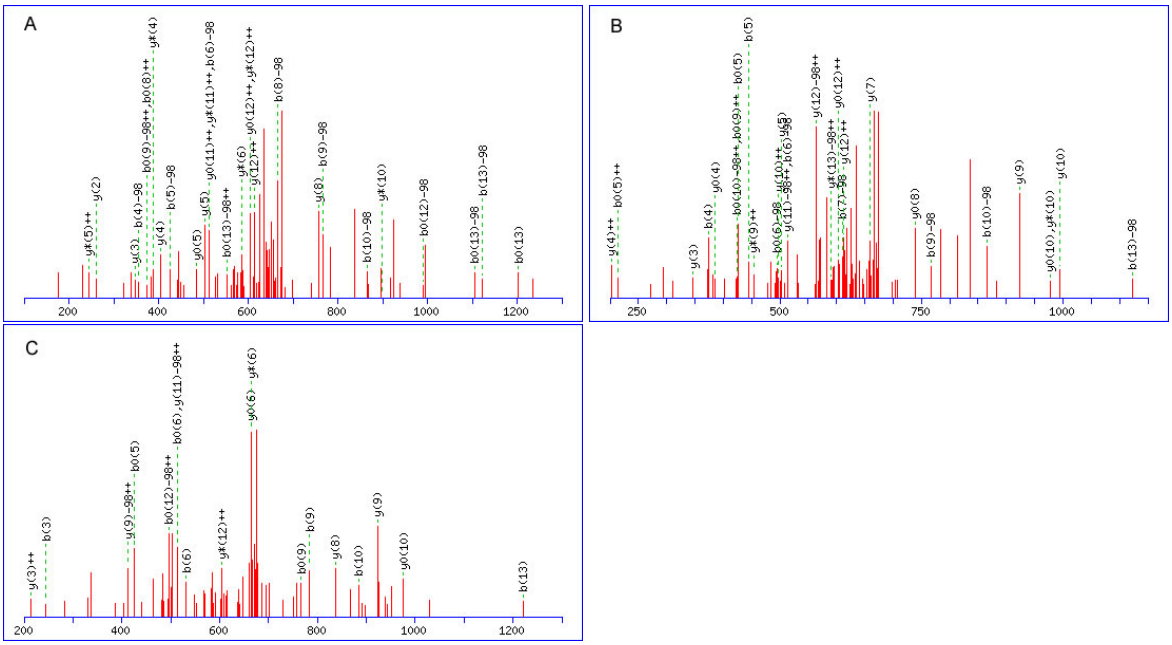

Figure 3.30: Fragmentation spectra of the peptide T40 with the three different alternative models.

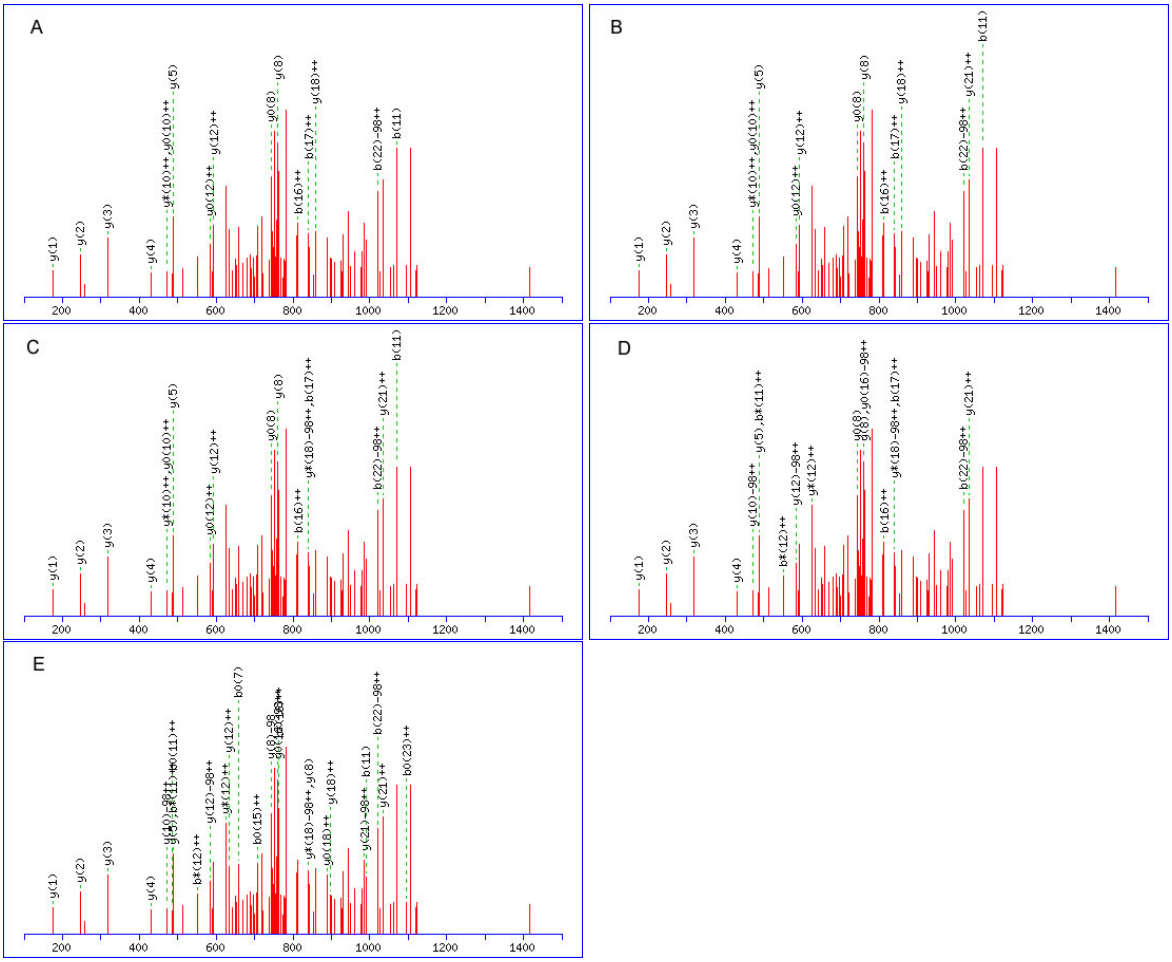

Figure 3.31: Fragmentation spectra of the peptide T42 with the five different alternative models.

Lindernia subracemosa 11–24 Phosphopeptide Enrichment and Phosphorylation Sites Identification

Ls11–24 from *L. subracemosa* dried leaves was immunochromatographically purified using an IgG-coupled affinity column. Affinity-purified Ls11–24 was digested with trypsin and subjected to phosphopeptide enrichment on TiO_2 columns. Nano–LC–MS/MS analysis of phosphopeptide-enriched tryptic digests yielded seven phosphopeptides (Figure 3.32) with mass-to-charge ratios (m/z) of 543.27 (2+), 632.35 (3+), 585.77 (2+), 873.84 (2+), 491.78 (3+), corresponding to the phosphorylated forms of tryptic peptides T23, T27, T30, T35-36, T48 (Table 3.7). Alternative and equivocal phosphorylation sites are marked by letters. Fragmentation spectra are depicted in Figure 3.33 for peptide T23 and its two different alternative models, Figure 3.34 for peptide T27, Figure 3.35 for peptide T30 and its two different alternative models, Figure 3.36 for peptide T35-36 and its two different alternative models and Figure 3.37 for peptide T48.

```
  1 MESQMHRPSE QEHPQHVASD NEMVEDQAEH GEKKSMLKKV KDKAKKIKGT
 51 IKKHGLGQDQ EDEEIKTNPA VHGPPPGRVP PVITGTNPPP MQGGFNLEKP
101 TDTREDRYDH HSDNVKGGGG EYTSLREKGV TSPPQDMETE FNFPKPEKNE
151 PEMKNITKPD VKTETSDITP SDYQTRDVDS TGQGVKEADV GSLTQGLKKV
201 SVGDESKPLP GEEQPPSYSG SHGQFAPQST PTKESLLPQS HPLPQDEPKR
251 YDPNHPDSMP QDTITGKISS ASAVIVDKAA TAKNVVASKL GYGGQTQESS
301 DGGAQQKKPL TETAAEYKNM VAEKVSGAGA AVMSKVRGSG TGEQAQGGGG
351 GDEASKGVST KDYLSDKLKP GEEDKALSKA ITEKLQVGKN EPRDGSKAAN
401 ESSPGGVVSS LKGVVGSWLG KNNGSEEAAA AREEANAERK VEQ
```

Figure 3.32: Phosphopeptides identified for the Ls11–24 protein of *L. subracemosa*. Phosphorylated peptides are indicated in red.

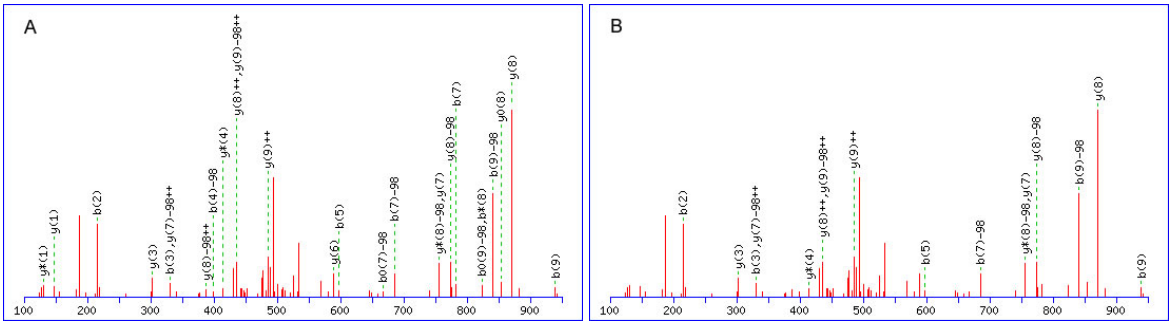

Figure 3.33: Fragmentation spectra of the peptide T23 with the two different alternative models.

Table 3.7: Identification of phosphopeptides of Ls11–24 by mass spectrometry (MS). Underlined sites represent models that best explain the majority of the tandem mass spectrometry (MS/MS) spectra collected for a given mass-to-charge ratio (m/z). Alternative and equivocal phosphorylation sites for a peptide are marked by letters.

Peptide (start - end)	Observed	Mr (exp)	Mr (calc)	Delta	Score	Sequence
T23A (177 - 186)	543.27	1084.52	1084.44	0.07	32	R.DVDSTGQGVK.E
T23B (177 - 186)	543.27	1084.52	1084.44	0.07	24	R.DVDSTGQGVK.E
T27 (234 - 249)	632.35	1894.01	1893.89	0.13	9	K.ESLLPQSHPLPQ-DEPK.R
T30A (268 - 278)	585.77	1169.53	1168.57	0.96	4	K.ISSASAVIVDK.A
T30B (268 - 278)	585.77	1169.53	1168.57	0.96	4	K.ISSASAVIVDK.A
T35-36A (319 - 335)	873.84	1745.66	1744.79	0.87	4	K.NMVAEKVSGAGAAV-MSK.V
T35-36B (319 - 335)	873.84	1745.66	1744.79	0.87	4	K.NMVAEKVSGAGAAV-MSK.V
T48 (413 - 421)	491.78	981.55	981.47	0.08	47	K.GVVGSWLGK.N

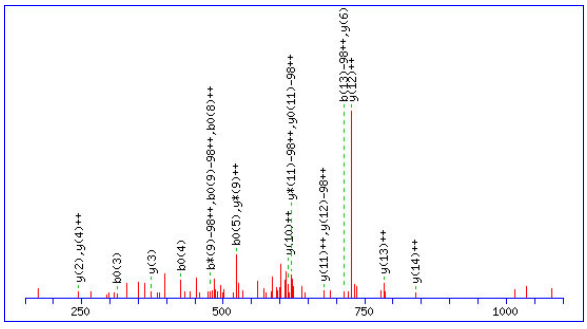

Figure 3.34: Fragmentation spectrum of the peptide T27.

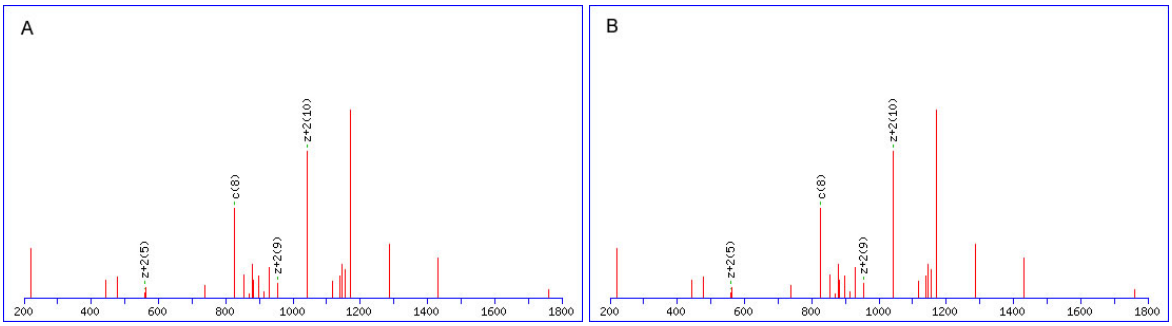

Figure 3.35: Fragmentation spectra of the peptide T30 with the two different alternative models.

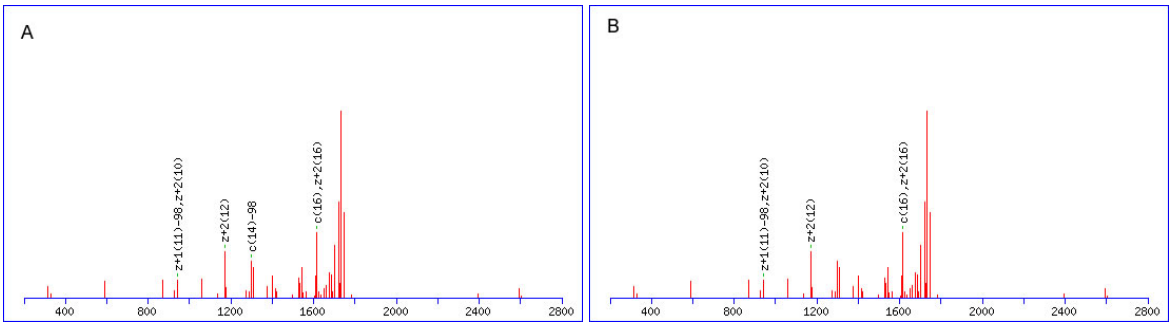

Figure 3.36: Fragmentation spectra of the peptide T35-36 with the two different alternative models.

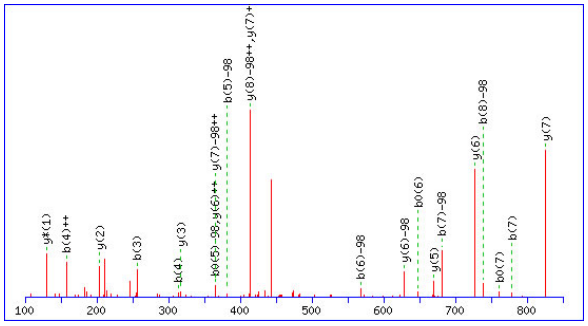

Figure 3.37: Fragmentation spectrum of the peptide T48.

Sequence Comparison among *C. plantagineum*, *L. brevidens* and *L. subracemosa* 11–24 Sequences and their Phosphorylation Sites.

```
C.plantagineum      MESQLHRPTEQEV---------MEGQTADHGEKKSMLAKVKEKAKKLKGSINKKHGSSQD 51
L.subracemosa       MESQMHRPSEQEHPQHVASDNEMVEDQAEHGEKKSMLKKVKDKAKKIKGTI-KKHGLGQD 59
L.brevidens         MESQMHRPVEQET----------VEGQGEQGGKMSVLKKVKEKAKKLKGSIKKHGSNSGQ 50
                    ****:*** ***              .::* * *:* ***:****:**:* *: . . :

C.plantagineum      DDADNDEEINTSPAVHG-APGTSP-------PPPTQG---------------------- 80
L.subracemosa       Q---EDEEIKTNPAVHGPPPGRVPPVITGTNPPPMQGGFNLEKPTDTREDRYDHHSDNVK 116
L.brevidens         EEDGSDEEMDTSPAVHG-APGMTP--------PPTQGG----------------DLEKP 84
                    :   .***:.*.***** .**  *        ** **

C.plantagineum      ---GEYGGLS-ERDVNIPHPLASTQANLDKPADVTDASRELQVPPPVPETTPEVSDKGLT 136
L.subracemosa       GGGGEYTSLR-EKGVTSPPQDMETEFNFPKPEKNEPEMKNITKPDVKTETSDITPSDYQT 175
L.brevidens         ADAGGFTSLKGDGGVDTPPQAAEREFNFPKHEDVS------------------PTDYQT 125
                       * : .*  : .*  *    . : *: *  .                    . .  *

C.plantagineum      EDLGSNAGQGVKESDVDSLTQGLKGVNYGGDDSNPLSGQEHQTISD------EPKSLPGQ 190
L.subracemosa       RDVDS-TGQGVKEADVGSLTQGLKKVSVG-DESKPLPGEEQPPSYSGSHGQFAPQSTPTK 233
L.brevidens         RDVDS-SGQ-----DVGSLTQGLKDMNVGGDESKAVPEVQEQPRST---------PAAAE 170
                    .*:.* :**     **.******* :. * *:*:.:.  :. .            . . :

C.plantagineum      GNDLPQSHPS-SEDEPKKFDANDQPQSMPQDT-ITGKLSSVPAVIIDRAAAAKNVVASKL 248
L.subracemosa       ESLLPQSHPL-PQDEPKRYDPN-HPDSMPQDT-ITGKISSASAVIVDKAATAKNVVASKL 290
L.brevidens         ETHLPQSHPVPAEDEPKKYDPN-RPDSTPQDTTYIGKITSVPAVIVDKAAAAKNVVASKL 229
                     . ******  .:****::*.* :*:* ****   **::*..***:*:**:*********

C.plantagineum      GYGGS-----------------------------------------------QAQESAADA 262
L.subracemosa       GYGG-------------------------------------------------QTQESSD-- 301
L.brevidens         GYGANNQAQEPTTTPDVVGGGGAATQQKKPLTETAAEYKNMVAEKLGYGASKAQESVDVG 289
                    ***.                                                ::***

C.plantagineum      ---GAAQQKKPLTETAAEYKNLVAEKLTPVYEKVAGAGSTVTSKVWGSGGTTAGEQTQGG 319
L.subracemosa       ---GGAQQKKPLTETAAEYKNMVAEKVS-------GAGAAVMSKVRGSG---TGEQAQGG 348
L.brevidens         GDGGATQQKKPLTETAAEYKNMVAEKLAPVYGKVSGAGTGVISRVRGTG---AGEQTQGG 346
                       *.:***************:****::       ***: * *:* *:*   :***:***

C.plantagineum      EGVVDGGGAASNKGVFTKDYLSEKLKPGDEDKALSQAIMEKLQLSKKPAVEGGAGDETKA 379
L.subracemosa       -----GGGDEASKGVSTKDYLSDKLKPGEEDKALSKAITEKLQVGKNEPRDG----SKAA 399
L.brevidens         --------DEAAKG----SYLSEKLKPGDEDKALSKAITEKLQLTGNKPTAD---ESKAA 391
                             : **    .***:*****:******:** ****:  : .  .    .. *

C.plantagineum      SESSPG-VVGTIKGAVGSLIGGGNKSSGAESAA------------AADEQTQALGE---- 422
L.subracemosa       NESSPGGVVSSLKGVVGSWLG---KNNGSEEAA------------AAREEANAERKV-EQ 443
L.brevidens         TEASPG-VVGSIKGVVGSLLGG-KSNNGSESAGGEQPQSLGSEGIAAREGADVVEPTAEQ 449
                    .*:*** **.::**.*** :*   ...*:*.*.           ** * ::.     **
```

The amino acid sequence alignment of the three sequences is shown: the identified phosphorylation sites are underlined. "*":identical. ":":conserved substitutions. ".":semi-conserved substitutions.

3.5. Identification of CDeT11–24 Interaction Partners

The results of section 3.4.1 indicate that the induction and the phosphorylation of CDeT11–24 from *Craterostigma plantagineum* are indipendent events. Therefore, it was tested whether the dehydration-dependent phosphorylation could have an effect on the ability of the protein to interact with other proteins.
Röhrig *et al.* (2006) reported that the sequence of CDeT11–24 presents streches of coiled-coil secondary structures. Some predicted phosphorylation sites fall within three stretches of lower probability coiled-coil sequences.
Coiled-coil structures are characterized by a sequence heptad (conventionally referred to as positions a to g, where a and d are generally apolar) involved in protein interactions, the most important represented by the leucine zipper transcription factors (Cohen and Parry, 1994; Mason and Arndt, 2004; O'Shea *et al.*, 1989). Since phosphorylation has been proposed as a mechanism for influencing the stability and interaction of coiled-coil structures (Steinmetz *et al.*, 2001), it was ascertained whether the two different isoforms of the protein, namely the phosphorylated and the unphosphorylated one, could interact with other proteins.
To perform this, two strategies based on an affinity chromatography were carried out: The immunoaffinity chromatography that enriches pre-formed complexes by adsorption on the antibody-coupled column, and the weak affinity chromatography that enriches the potential binding partners on the basis of their affinity for the bait-coupled column.

3.5.1. Coimmunoaffinity Chromatography

An approach based on the coimmunoaffinity chromatography was performed on *C. plantagineum* plant material from ABA treated leaves (as a source of unphosphorylated protein) and from ABA treated and dried leaves (as a source of phosphorylated protein).
The strategy used to isolate the potential interaction partners consisted of an immunoaffinity chromatography performed under native conditions using a column covalently coupled with the purified IgGs against CDeT11–24 (described in section 2.25.1). The purpose is to fish the pre-formed complexes from the total protein extract. Separation of the eluted

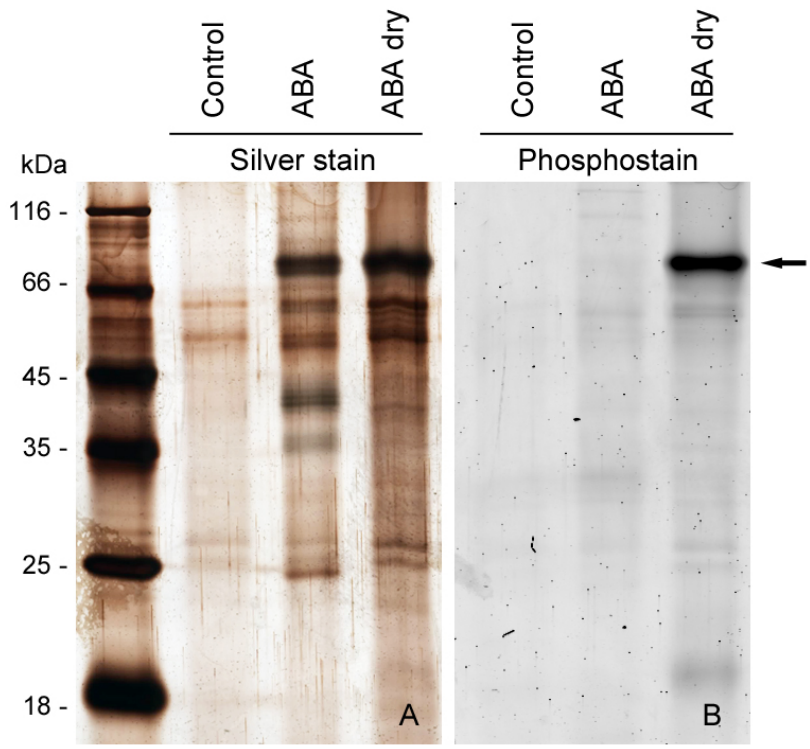

Figure 3.38: Coimmunoaffinity chromatography with RIPA buffer. The fractions eluted from the column were separated by SDS–PAGE and stained either by silver staining (A) or by ProQ Diamond phosphostain (B). The arrow indicates the CDeT11–24 protein.

fractions by SDS–PAGE resolves the single polypeptides that can be identified by mass spectrometry.

To minimize the risk of identifying unspecific interactors, a control based on the bait exclusion strategy was included. This consists on side-by-side coimmunoaffinity chromatographies from starting materials which differ only in the presence or absence of the bait protein (CDeT11–24). As all steps of the process employ the same reagents and procedures, differences in the final list of candidate protein interactors are derived from the presence/absence of the bait protein CDeT11–24.

Two different buffer conditions were tested for the resuspension of the plant material, which differ in the composition and concentration of the detergents (EBC buffer, containing 0.5 % (v/v) NP–40, and RIPA buffer, containing 1 % (v/v) NP–40, 0.5 % (w/v) DOC, 0.1 % (w/v) SDS).

Figure 3.38 illustrates the SDS–PAGE of the eluted proteins. In A the gel stained with silver reveals the presence of the protein in the ABA-treated and in the ABA-treated and dried samples. The phosphostained gel in B confirms the dehydration-dependent phosphorylation of CDeT11–24.
Besides these major bands, some other weak bands can be detected. The most intense bands can be considered as unspecific interactors since they are also present in the control lane, thus indicating that they are not retained by the bait protein. The other bands failed to be identified by MS analysis or matched to keratin contaminations.
The same experiment was therefore performed using other buffer conditions, resuspending the proteins in a buffer containing less detergents (EBC buffer, section 2.25.1) in order to eventually favor some weak interactions decreasing the concentration of the surfactants that could disrupt these interactions.
As in the previous experiment, additional bands other than the bait protein could not be identified by reducing the detergents, thus forcing to adopt another approach for identifying potential interaction partners of the CDeT11–24 protein.

3.5.2. Weak Affinity Chromatography

One reason for the failure of the coimmunoaffinity chromatography approach could rely on the displacement effect that the antibodies might have had on the potential interactors of the CDeT11–24 protein. Since the binding strength of the IgG is quite high, weak interactions could be unfavored and depleted by the IgG coupled column. To overcome this possible negative effect, the bait protein was directly coupled to the column (described in 2.23).
To be able to compare the effect of the phosphorylation on the CDeT11–24 interaction, two different columns were produced: one coupled to the recombinant overexpressed protein (unphosphorylated 11–24), and one coupled to the native proteins isolated from dehydrated leaves using the IgG coupled column (phosphorylated 11–24).

Isolation of the Recombinant Full Length CDeT11–24

The full length clone was isolated by RT–PCR using the primer pair cratero_fwd and cratero_rev. The sequence was then amplified with the primers 11–24_full_Nde and 11–

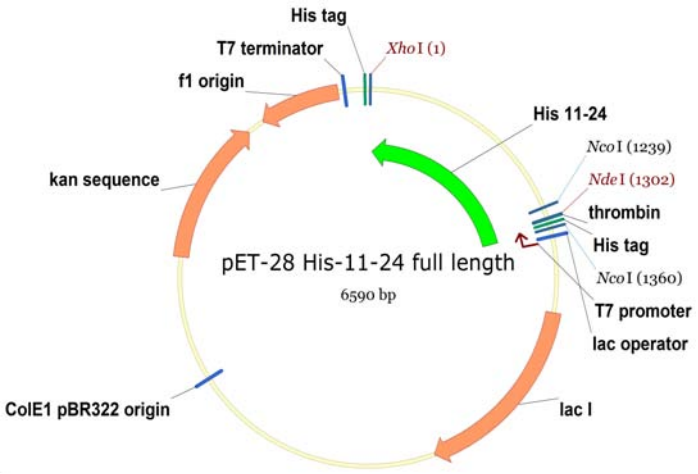

Figure 3.39: pET-28 expression vector containing the histidine-tagged full length CDeT11–24 clone. The expressed protein (green arrow) consists of the 1284 bp amplified from the cDNA fused to the vector containing the sequences coding for the 6 histidines at the N-terminal, resulting in a protein of 448 amino acids.

24_full_Xho (listed in section 2.11). The primers contained *Nde*I and *Xho*I restriction sites. The restriction sites were introduced to facilitate the in-frame cloning of the coding region into the pET28-a expression vector (see A.1). The recombinant vector contained the 1284 bp from the CDeT11–24 full length sequence cloned between the *Nde*I and *Xho*I restriction sites, under the control of the T7 promoter and comprised an histidine tag at its N-terminal (Figure 3.39). The resulting open reading frame was 1344 bp long and coded for a protein of 448 amino acids with a molecular weight of 46 kDa.
BL21 *E. coli* cells bearing the vector were induced with IPTG and recombinant protein was isolated as described in section 3.3. Figure 3.40 shows the induction and purification of the recombinant full length CDeT11–24. In A the Coomassie stained gel follows the protein enrichment across the induction and purification steps. The induction triggers the accumulation of a protein of about 60 kDa that localizes in the water soluble fraction (supernatant) after heat fractionation and centrifugation. This fraction is furthermore enriched in the recombinant protein by affinity chromatography on the Ni-NTA column via the histidine tag. In B the identity of the induced protein is confirmed by its reactivity with the CDeT11–24 antibody.

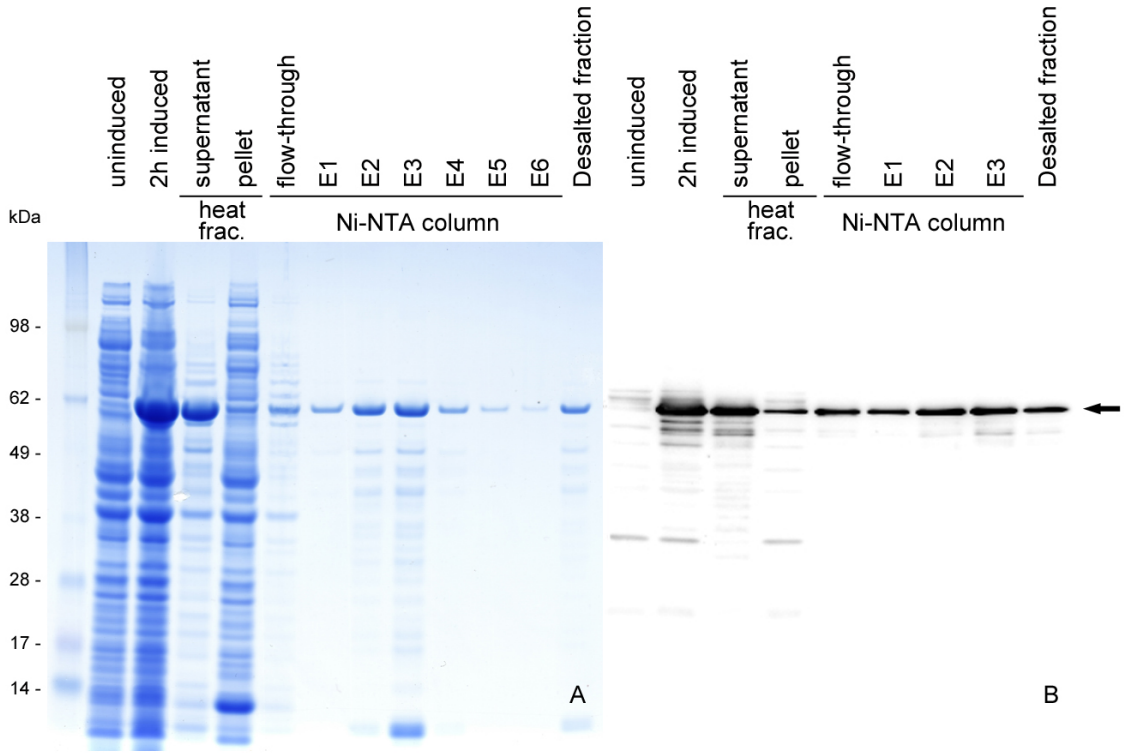

Figure 3.40: SDS–PAGE showing the induction and isolation of the histidine tagged 11–24 full length protein (A). Bacteria were induced for 2 hours with 1 mM IPTG and cells were harvested. The induced protein has an apparent mass of about 62 kilodaltons. The protein was pre-fractionated based on its capacity to remain soluble after heat treatment (see 2.21) and subsequently further purified by affinity chromatography on a Ni–NTA column suitable for the enrichment of histidine-tagged recombinant proteins. The eluate was finally desalted by gel filtration with a PD–10 column. The identity of the protein was further confirmed by immunoblotting (B). The arrow indicates the CDeT11–24 protein.

Isolation of the Native CDeT11–24 from Dried Leaves

In order to isolate the phosphorylated version of CDeT11–24, an affinity chromatography using the IgG coupled column was performed.

The soluble protein fraction was isolated as described in section 2.25.2 and loaded on the column. Figure 3.41 shows the purified native CDeT11–24 from dried leaves. Known amounts of recombinant protein (His-11-24) were loaded to estimate the concentration of the native protein, as revealed by the Coomassie-stained gel (A). In B the same gel was stained with ProQ Diamond phosphostain to ensure that the *in vivo* isolated protein was

phosphorylated. The immunoblot with the CDeT11–24 antibody (C) further confirms the identity of the purified protein.
Starting from 10 g of dried leaf material 750 μg of native phosphorylated protein could be isolated.

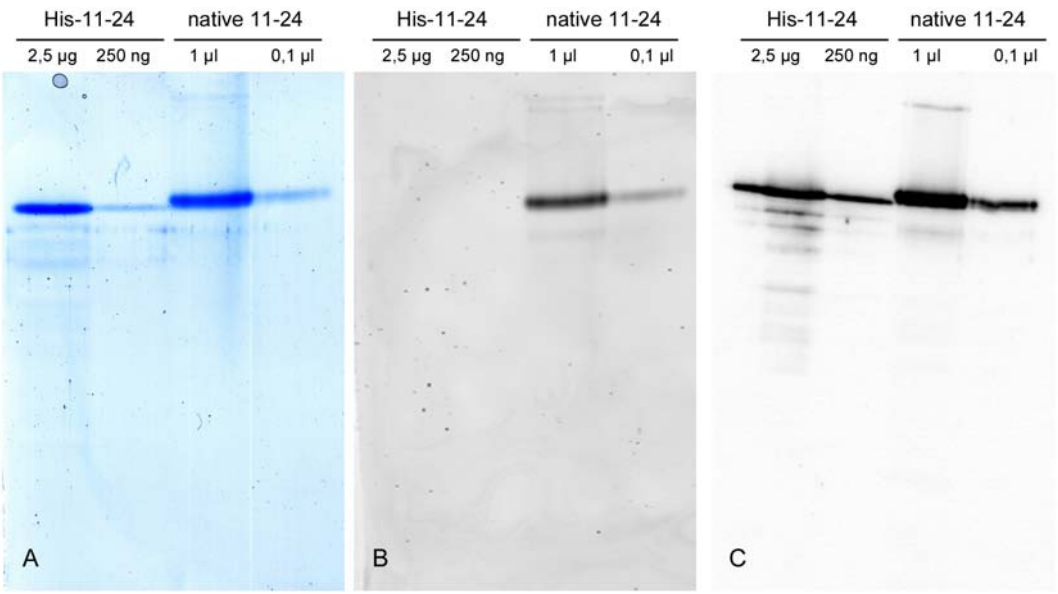

Figure 3.41: Isolation of the native phosphorylated CDeT11–24 protein from *C. plantagineum* dried leaves. The eluted fraction was separated by SDS–PAGE and visualized by Coomassie staining. To estimate the concentration of the purified protein, known amounts of recombinant protein were loaded together with a ten-fold dilution of the protein (A). The same gel was stained with ProQ Diamond phosphostain indicating that the native protein is strongly phosphorylated (B). Panel C shows the Western blot with the 11–24 antibody confirming the identity of the proteins.

Isolated proteins (7 mg of recombinant 11–24 protein and 750 μg of native phosphorylated protein) were then coupled to the HiTrap NHS columns (described in section 2.23). The coupling efficiency, calculated according to the method described in section 2.23.2, was in the range of 60–70 %.

Identification of the Interaction Partners

The two columns were then used to perform the weak affinity chromatography. The column coupled to the recombinant protein was loaded with leaf material from plants with about 50 % RWC, since this is the stage where the protein is induced but not phosphorylated (see 3.4.1). The column coupled with the native protein was instead loaded with leaf material from dried plants, where CDeT11–24 occurs in its phosphorylated state.

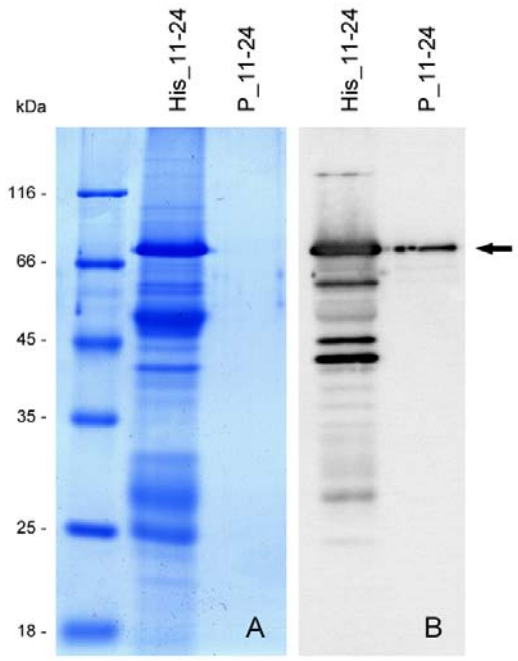

Figure 3.42: Weak affinity chromatography using the CDeT11–24 coupled columns. *C. plantagineum* leaves with 50 % RWC were loaded on the recombinant 11–24 coupled column (His_11–24) and dried leaves were loaded on the phosphorylated 11–24 coupled column (P_11–24). In A are shown the eluates separated on a gel and stained with Coomassie. Panel B shows the same samples blotted and incubated with the antibody against 11–24. The black arrow indicates the band corresponding to CDeT11–24.

Figure 3.42 shows the fractions eluted from the two columns separated by SDS–PAGE. In panel A the Coomassie stained gel indicates that the column coupled with the phosphorylated form of 11–24 did not retain any other protein, whereas the column coupled with the recombinant unphosphorylated protein shows some bands indicating candidate inter-

action partners. One of the major bands has a molecular size that resembles the size of CDeT11–24, therefore the same samples were transferred onto a nitrocellulose membrane and incubated with the 11–24 antibody. Panel B reveals that the antibody recognizes the 11–24 protein plus some other smaller bands. Traces of 11–24 protein are also present in the sample eluted from the phosphorylated 11–24 coupled column.

Since the sample from the 50 % RWC is the only one showing potential interaction candidates, this fraction was further analyzed. To test whether the bands on the gel were real potential interactors of CDeT11–24, 1 mg of recombinant 11–24 was added to the soluble protein extract from partially dehydrated *C. plantagineum* leaves to compete with the 11–24 coupled column for binding to the proteins. Adding an excess of recombinant 11–24 protein to the plant extract before the chromatography will adsorb the protein that is interacting with CDeT11–24, thus making the interactor no more available for the column-coupled CDeT11–24. Therefore it was looked for proteins that bound to the column in the absence of soluble 11–24, but not in its presence.

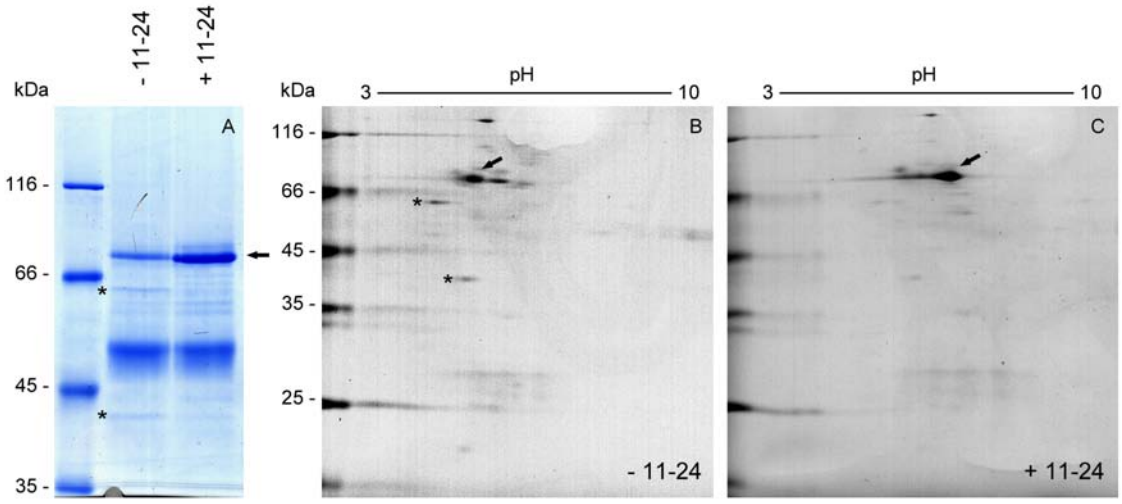

Figure 3.43: Weak affinity chromatography with competitor. In A *C. plantagineum* proteins from leaves with 50 % RWC were loaded on the recombinant 11–24 coupled column without (- 11–24) or with free recombinant protein (+ 11–24). Bands with reduced intensity in the presence of soluble 11–24 are marked with asterisks. In B and C the same samples were separated by 2D–PAGE. The arrows indicate the CDeT11–24 protein.

Figure 3.43 shows the result of the competition experiment. The bands showing a decrease in intensity in the presence of free 11–24 are marked by asterisks. In B and C the same samples were separated by 2D–PAGE and stained with Coomassie to obtain a better resolution of the proteins.
The spots corresponding to the proteins marked in A were excised from the 2D gels and subjected to MS/MS analysis. The spots were identified as CDeT11–24 protein, therefore it was concluded that they could be degradation products of the protein.
The spot corresponding to CDeT11–24 was also analyzed by mass spectrometry. In Figure 3.43 B and C the spot appears to have different isoelectric points.
In the presence of free 11–24 protein the spot has a more basic isoelectric point as compared to the spot without competitor. This is in accordance with the protein sequence of the histidine tagged 11–24 which has an isoelectric point of 5.57 whereas the native 11–24 protein has an isoelectric point of 4.73. This was also confirmed by MS analysis, in fact the most abundant spot in B contains the peptides with the six histidines. These results indicate that the CDeT11–24 protein of *C. plantagineum* may interact with itself. The binding is further confirmed by the competition experiment: pre-incubating the protein extract with the recombinant protein, present in excess, precludes the native protein for the binding.

3.6. Comparison of *Craterostigma plantagineum* Callus Phosphoproteins upon ABA and Dehydration Stress

3.6.1. Use of *Craterostigma plantagineum* Callus System to Identify Changes in the Phosphoproteome

For the analysis of the *Craterostigma plantagineum* phosphoproteome changes upon ABA and dehydration stress, callus tissue was chosen as experimental system. Phosphoprotein enrichment of *C. plantagineum* from leaf material was already performed and published by Röhrig *et al.* (2008). In this work it was shown how the enriched phosphoproteins change as a consequence of the dehydration of *C. plantagineum* leaves and how this changes are

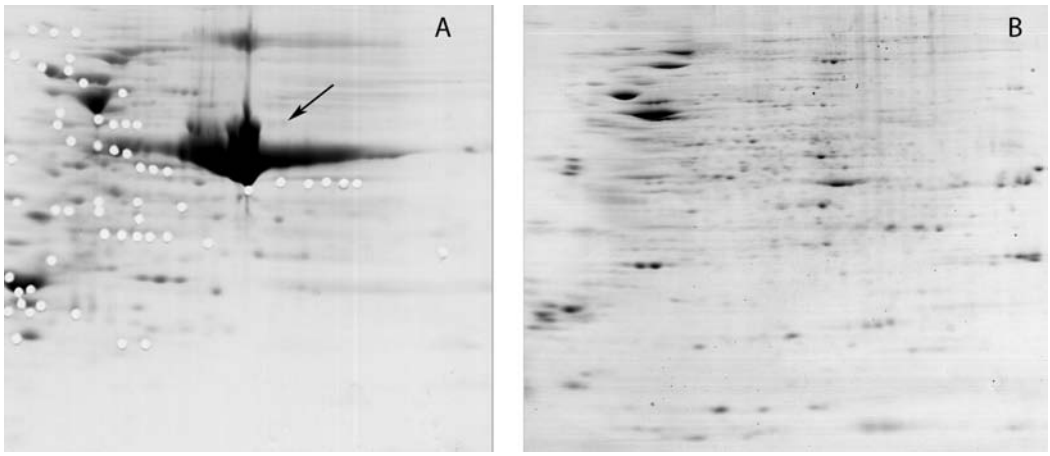

Figure 3.44: Comparison between phosphoproteins enriched from *C. plantagineum* leaf tissues (A) and callus tissue (B) separated by 2D gel electrophoresis. The RuBisCO phosphoprotein is indicated by the arrow. Gels were stained with Coomassie.

reversible upon rehydration.

One of the major drawbacks of the leaf system is the presence of the ribulose-1,5-bisphosphate carboxylase oxygenase (RuBisCO). The RuBisCO accounts for about 30 % of the total proteins in leaves tissues and it has been shown that it is a phosphoprotein (Foyer, 1985; Parry *et al.*, 2003). In the leaf system the less abundant phosphoproteins remain therefore under-represented (Fig. 3.44, arrow). Since the callus tissue contains a negligible amount of RuBisCO, the negative effect of this abundant protein is overcome.

The *C. plantagineum* callus is capable of surviving severe desiccation only upon ABA

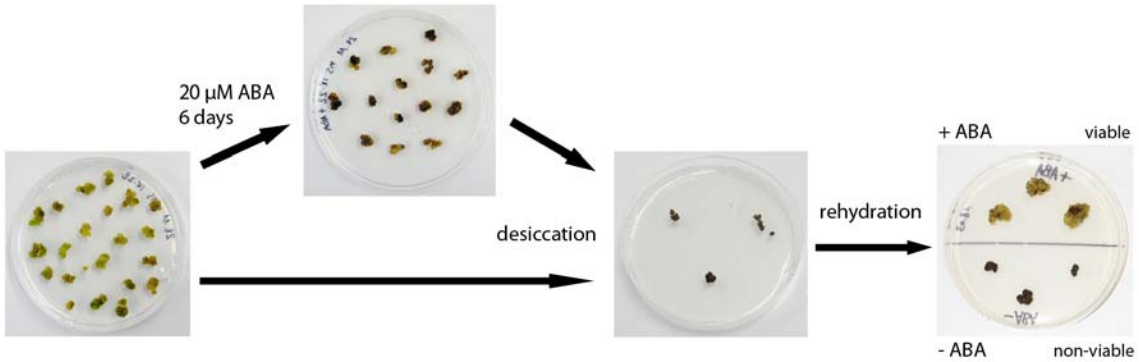

Figure 3.45: Dehydration/rehydration cycle of *C. plantagineum* calli.

treatment (Bartels *et al.*, 1990). The ability of the callus to withstand water stress was verified as described in 2.1.1.

Figure 3.45 shows the calli subjected to dehydration with or without prior ABA treatment. Only the calli pre-treated with ABA can rehydrate and grow on the medium after dehydration, whereas the calli dried without prior ABA treatment are unable to rehydrate and grow.

In the callus, ABA treatment and dehydration induce a set of genes comparable to that induced in the whole plant by dehydration. This fact was exploited to test the calli for stress induction. The candidate protein chosen for the induction test was the dehydrin-like CDeT11–24 for which an antibody was produced (described in section 3.3) and which is known to be expressed in ABA and dehydration stressed calli and leaf tissues (Bartels *et al.*, 1990).

The Western blot in Figure 3.46 shows the ABA dependent induction of CDeT11–24 and that the protein is accumulating in dried calli only upon prior ABA treatment, whereas drought stress alone is not sufficient for the induction of the protein. This points out another advantage of the callus system, where the priming effect of ABA and the desiccation treatment can be separated and independently analyzed.

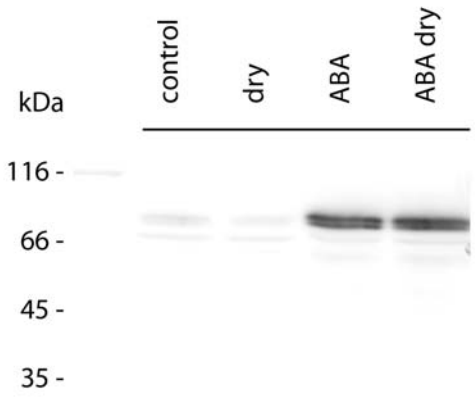

Figure 3.46: Western blot analysis on *C. plantagineum* total protein from control, dried, ABA treated and ABA dried calli. The membrane was incubated with the CDeT11–24 specific antibody.

3.6.2. Phosphoprotein Enrichment

Starting from total protein extracts of untreated (control), dried, ABA treated and ABA treated and dried *C. plantagineum* callus, a phosphoprotein enrichment was performed according to the method described by Röhrig *et al.* (2008) with some modifications (see 2.17.2). Figure 3.47 depicts an overview of the isolation method used to enrich phosphoproteins from total proteins of *C. plantagineum* calli. Total proteins were extracted from homogenized callus material by the dense–SDS method as described in 2.17.1. The protein pellets were then resuspended in a denaturing buffer containing competitors (i.e. Na-glutamate, K-aspartate, imidazole) to reduce the background of acidic and histidine-rich proteins that behave similar to phosphorylated proteins and bind to the aluminum matrix. The enrichment was performed by incubating the total proteins on a rotator with aluminum hydroxide, a trivalent cation which has an affinity for the phosphate groups and is poorly soluble in water. The matrix-bound phosphoproteins can therefore be washed by centrifugation to get rid of the aspecifically bound proteins. Tipically, from 3 mg of total proteins 250 μg of MOAC-enriched proteins could be eluted.

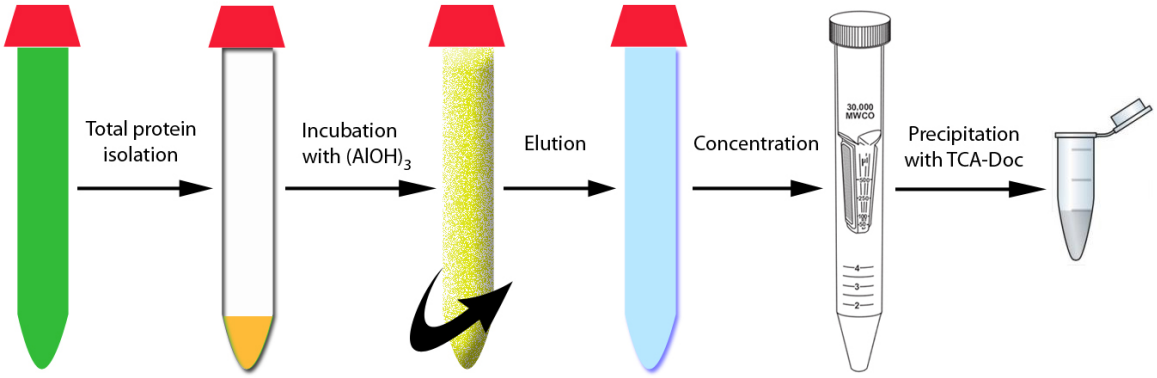

Figure 3.47: Overview of the phosphoprotein enrichment protocol.

To estimate the amount of phosphoproteins enriched using the MOAC protocol, 10 μg of enriched proteins and 10 μg of total proteins for each sample were separated by SDS–PAGE. The gel was stained with ProQ Diamond Phosphostain (Invitrogen) and the signal intensity

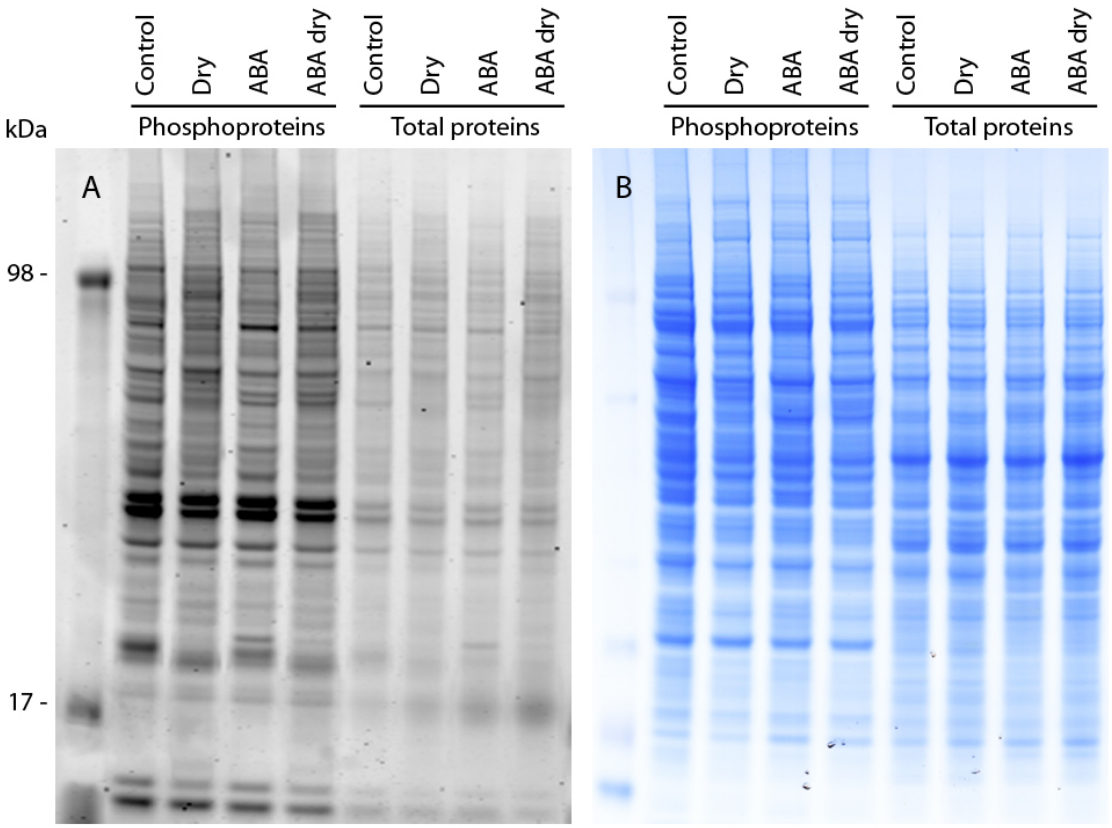

Figure 3.48: Comparison between enriched phosphoproteins and total proteins. 10 μg of each sample were separated by SDS–PAGE and stained with ProQ Diamond Phosphostain (A) and subsequently with Coomassie stain (B).

evaluated by ImageQuant (Figure 3.48 A). The evaluation revealed that phosphoproteins have been enriched by a factor 8–9 over total proteins. To ascertain the equal loading of enriched phosphoproteins and total proteins, the same gel was subsequently stained with Coomassie stain (Figure 3.48 B).

Section 3.4.1 reports the biphasic ABA-dependent induction and dehydration-dependent phosphorylation of the CDeT11–24 protein. This finding was exploited to validate the MOAC enrichment protocol for the *C. plantagineum* calli. In Figure 3.49 total proteins and MOAC enriched proteins are compared using the CDeT11–24 antibody to confirm the presence of the protein in the different treatments. In A the Western blot with the total proteins indicates the presence of the CDeT11–24 protein in the ABA-treated callus and in

the ABA-treated and dried callus as already shown in Figure 3.46. In B the MOAC isolated phosphoproteins tested with the same antibody confirm the specificity of the enrichment step since the signal for CDeT11–24 is only present in the ABA treated and dried callus sample whereas ABA treatment alone is not sufficient to induce the phosphorylation of the protein. This confirms the drought-dependent phosphorylation of CDeT11–24 as already shown trough the immunoprecipitation in Figure 3.14.

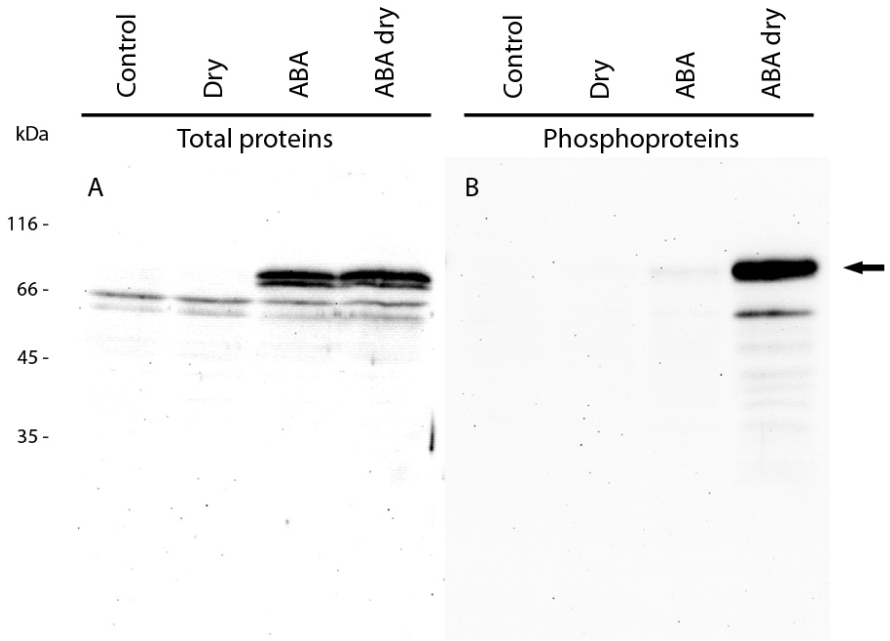

Figure 3.49: Immunoblot of *C. plantagineum* callus total proteins (A) and enriched phosphoproteins (B). Equal amounts (10 μg) of proteins were separated by SDS–PAGE, blotted on a nitrocellulose membrane and immunologically detected with the CDeT11–24 antibody. The 11–24 band is indicated by the arrow.

3.6.3. 2D SDS–PAGE Separation of the Enriched Phosphoproteins and Spot Analysis

About 100 μg of MOAC-enriched phosphoproteins were separated by 2D SDS–PAGE, using 17 cm long IPG strips (pH 3-10 NL) and separated in the second dimension on large 12 % acrylamide gels.

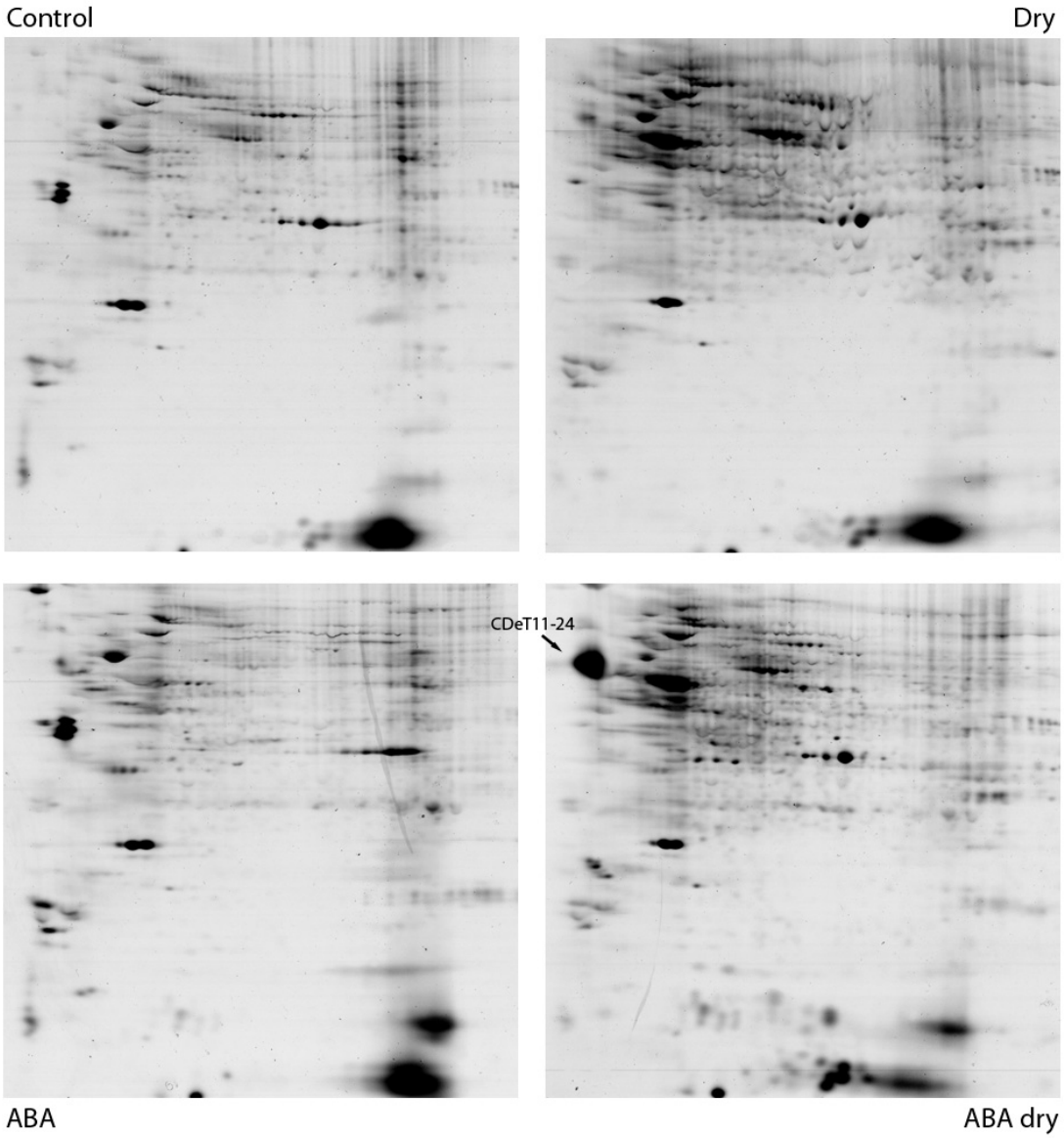

Figure 3.50: Phosphoproteins enriched from control, dried, ABA treated and ABA treated and dried *C. plantagineum* calli. Proteins were focussed on 17 cm IPG strips (pH 3-10 NL) and separated on 12 % SDS–PAGE gels. The gels were stained with ProQ Phosphoprotein gel stain.

Figure 3.50 shows four gels stained with ProQ Diamond Phosphostain of enriched phosphoproteins from calli. For the comparison of the protein patterns, the gels were superimposed by the help of the program Proteomweaver (BioRad). Figure 3.51 shows the pairwise comparison of selected gels, with each gel represented by false colours.

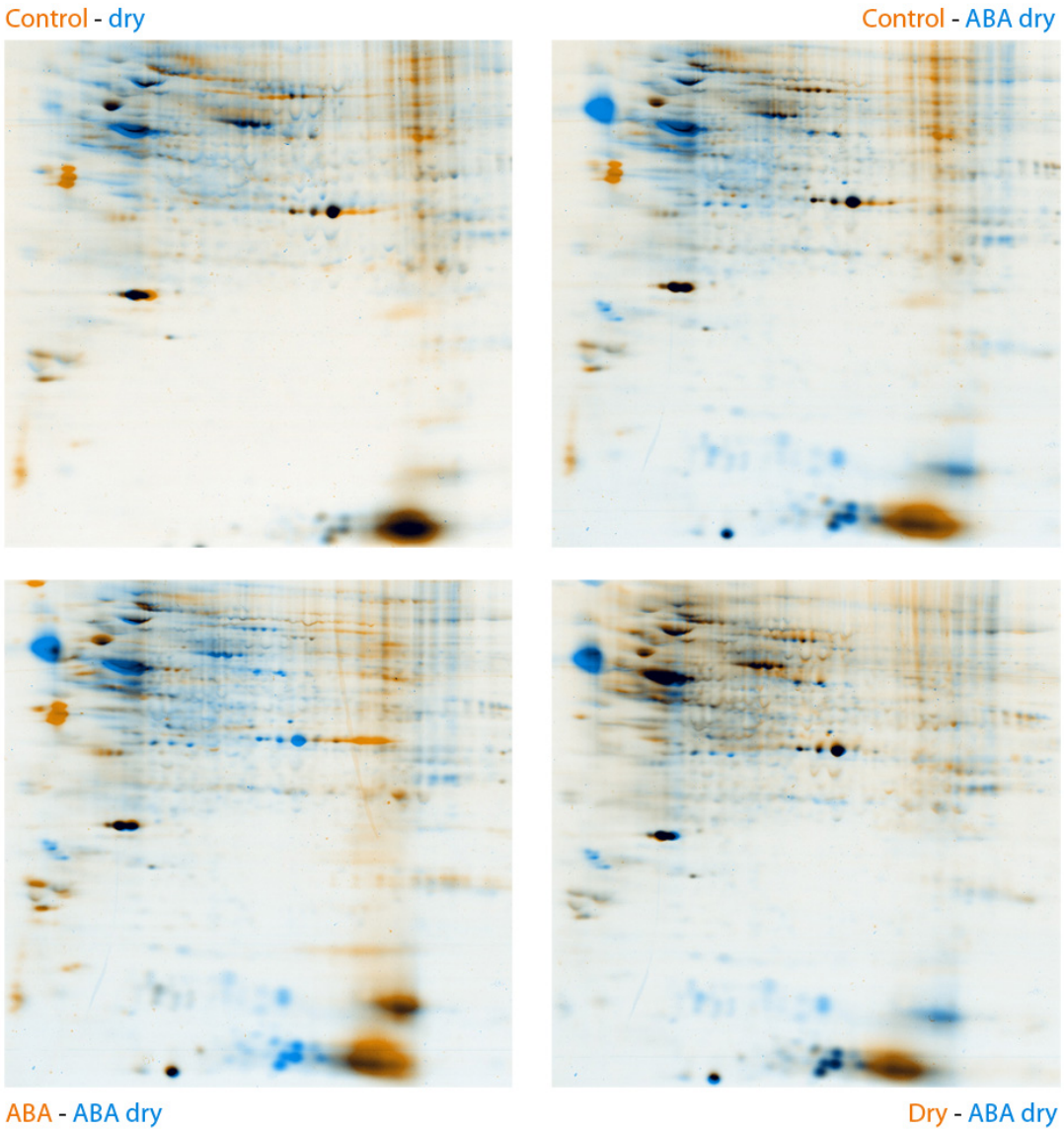

Figure 3.51: Pairwise comparison of the phosphostained gels by Proteomweaver. Gels are visualized in false colours. Protein spots that give a phosphorylation signal only in one gel are depicted with the corresponding colour, as indicated by the label. Overlapping spots indicating no change in intensity are coloured black. The samples matched are indicated by the name in the colour used for the pairwise comparison.

Figure 3.52 A shows a detail of the phosphoproteins separated by 2D SDS–PAGE. The most noticeable differences reside in the acidic, high molecular weight region of the gel. The identified proteins showing a change in the phosphorylation status are indicated by

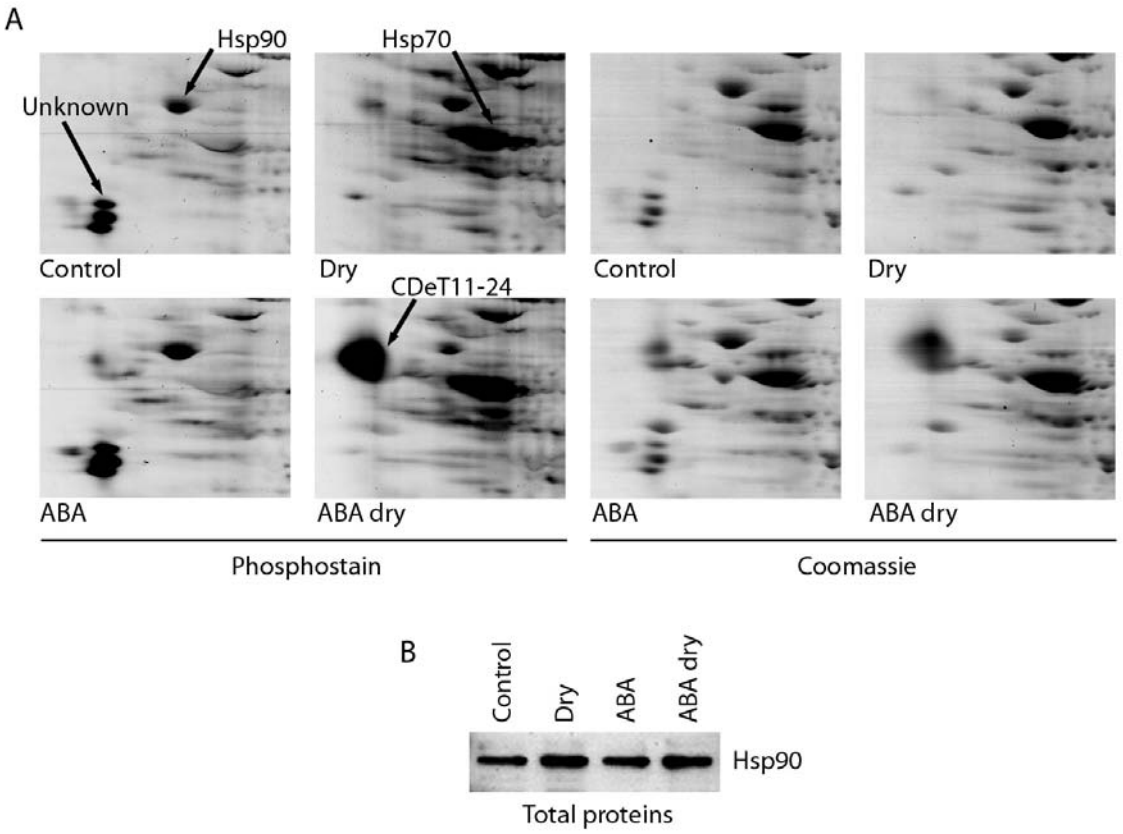

Figure 3.52: Detail of the gels in Figure 3.50 showing the Hsp70, Hsp90 and unknown proteins (A). On the left is depicted a set of gels stained with Coomassie showing the same area. B shows a Western blot of callus total proteins. Equal amounts (10 μg) of proteins were separated by SDS–PAGE, blotted on a nitrocellulose membrane and immunologically detected with the human Hsp90 antibody.

an arrow. The protein spot identified as homologue to the Heat shock protein 70 (Hsp70) is appearing only after dehydration treatment, regardless of the priming of the callus with ABA. The Coomassie stained gels show the spot corresponding to Hsp70 in all the samples, with no evident change in amount. This could be due to the acidic isoelectric point of the protein (ca. 5) which could be responsible for the enrichment of the unphosphorylated form as a result of its negative net charge. This also indicates that the protein is phosphorylated upon dehydration and not actively synthesized.

The spot identified as homologue to the Heat shock protein 90 (Hsp90) is downregulated upon dehydration treatment, but only in the callus sample which was pre-treated with ABA, indicating an effect that is dehydration-dependent, but also involving the ABA-

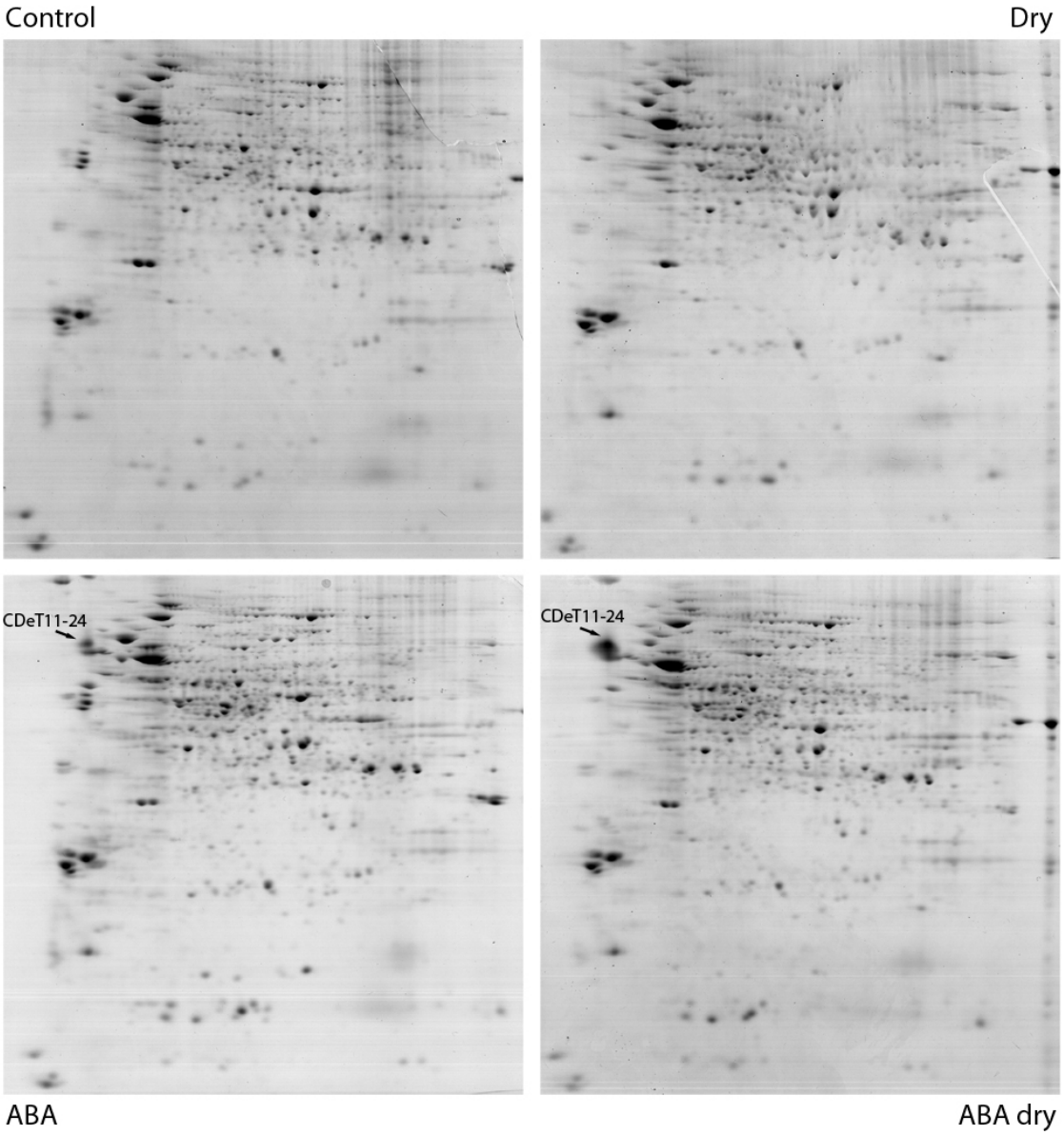

Figure 3.53: Enriched phosphoproteins from *C. plantagineum* callus. Proteins were focussed on 17 cm IPG strips (pH 3-10 NL) and separated on 12 % SDS–PAGE gels. The gels were stained with Coomassie.

dependent pathway. Looking at the Coomassie stained gels, it can be inferred that the phosphorylated Hsp90 is either dephosphorylated or actively degraded, as the stain for total proteins shows a very faint spot for this protein in the ABA-dried sample.

The human antibody for the Hsp90 protein was able to recognize a band of the expected size in *C. plantagineum*. The western blot shown in Figure 3.52 B indicates the amount

Figure 3.54: Example gel showing the enriched phosphoproteins from control callus separated by 2D SDS–PAGE and stained with Coomassie. The spots identified by MALDI–TOF are indicated by the arrows.

of the Hsp90 protein in the total protein of the four samples. No changes occur in the proteome of *C. plantagineum* regarding the amount of Hsp90 suggesting that dephosphorylation may be the mechanism of regulation.

The set of three spots corresponding to the hypotethical protein of *Vitis vinifera* show a phosphorylation pattern which is dehydration-dependent, irrespective of the ABA treatment. The proteins are phosphorylated in the control and ABA-treated samples, and are disappearing upon dehydration.

Figure 3.53 depicts the four 2D gels of the separated phosphoproteins stained with the Coomassie stain. The total protein stain reveals only minor differences in the pattern

of the enriched phosphoproteins. The Coomassie stained gels were used to identify the proteins by mass spectrometry.

Figure 3.54 summarizes all the spots identified. The spots are enumerated on the control sample gel. Table 3.8 lists the spots identified by PMF and MS/MS. The blast column represents the score and the E-value of a blastp search used to annotate the cDNA of *C. plantagineum* identified by PMF. The phagemids containing a cDNA library from *C. plantagineum* dried leaves were converted into plasmids, transformed into *E. coli* as described in section 2.16 and subsequently sequenced. The resulting database of 925 ESTs was used as auxiliary entry for the Mascot search.

Table 3.8: Identification of phosphoproteins from *C. plantagineum* calli upon ABA and dehydration treatment.

Spot[1]	Protein[2]	Organism[3]	Accession[4]	BLAST[5]		PMF[6]			MS/MS[7]			Predicted M_r/pI[8]	P[3]DB[9]
				Score	E-value	Score	Coverage (%)	NP	Score	Coverage (%)	NP		
1	hypotethical protein	*Vitis vinifera*	GI:147790496						52.4	6.6	1	12.1/4.1	-42
2	putative vesicle transport protein	*Oryza sativa*	GI:75119745	213	6.0E-54	48.2	5.2	8				27.1/9.5	-70
3,4	translation initiation factor eIF-1A-like	*Solanum tuberosum*	GI:122245496	274	3.0E-72	75.7	15.2	9	35.1	9	1	16.6/4.7	
5,6	eucaryotic initiation factor 5A	*Nicotiana plumbaginifolia*	GI:829282						356.1	29	5	15.7/6.3	*
7	tumor protein homolog	*Pseudotsuga menziesii*	GI:9979193						93.3	11.4	2	18.8/4.5	-57
8	20S proteasome alpha subunit B	*Arabidopsis thaliana*	GI:15219317						137.7	5.5	2	25.7/5.4	0
9	20S proteasome subunit G1	*Arabidopsis thaliana*	GI:15225839						219.6	12	2	27.4/5.9	-125
10,11, 12	GTP-binding protein RAN1	*Lycopersicum esculentum*	GI:585777	450	1.0E-125	193	50.4	21	176.3	14	2	25.2/6.3	-22
13	unknown protein	*Picea sitchensis*	GI:116785722						233.8	13.6	3	22.5/4.1	-80
14	elongation factor 1-beta	*Arabidopsis thaliana*	GI:30691619						68.3	4.3	1	25.1/4.3	*

Spot[1]	Protein[2]	Organism[3]	Accession[4]	BLAST[5]		PMF[6]			MS/MS[7]			Predicted M_r/pI[8]	P[3]DB[9]
				Score	E-value	Score	Coverage (%)	NP	Score	Coverage (%)	NP		
15	WRKY DNA-binding protein	*Nicotiana tabacum*	GI:75185587	159	2.0E-37	51.5	2.9	6				26.2/8.1	-25
16	unknown protein	*Vitis vinifera*	GI:157335851						107.5	13.1	2	29.3/4.5	-126
17	G protein beta subunit	*Solanum tuberosum*	GI:77745452						65.2	7.3	1	28.6/7.8	-112
18	40S ribosomal protein SA	*Glycine max*	GI:3334320						52.6	5.8	1	33.9/4.9	
19,20	60S acidic ribosomal protein P0	*Oryza sativa*	GI:115474653						134.2	7.8	2	34.4/5.2	-138*
21	malate dehydrogenase	*Oryza sativa*	GI:125532368	549	1.0E-155	123	23.9		224.6	17.8	3	34.3/5.8	-137
22	fructose bisphosphate aldolase	*Solanum tuberosum*	GI:122212992	530	1.0E-149	127	13.1	14				38.4/8.5	-173*
23,24	glyceraldehyde 3-phosphate dehydrogenase	*Solanum tuberosum*	GI:82400130	514	1.0E-144	67.3	19.9	8	210.3	12.4	3	36.7/6.4	-178
25	initiation factor 3g	*Arabidopsis thaliana*	GI:12407751						48.6	3.4	1	32.6/9.4	-170
26,27, 28	60S ribosomal protein L5-2	*Oryza sativa*	GI:55976534						238.2	16.1	3	34.6/9.4	
29,30	eucaryotic release factor (ERF1-1)	*Arabidopsis thaliana*	GI:15215863						132.3	7.3	3	48.7/5.0	0
31	actin	*Torenia fournieri*	GI:150375631	473	1.0E-140	164	34.1	18	333.7	18.6	3	32.4/5.5	-158

Spot[1]	Protein[2]	Organism[3]	Accession[4]	BLAST[5]		PMF[6]			MS/MS[7]			Predicted M_r/pI[8]	P[3]DB[9]
				Score	E-value	Score	Coverage (%)	NP	Score	Coverage (%)	NP		
32	S-adenosylmethionine synthetase	*Actinidia chinensis*	GI:1709006						162.1	8.6	3	39.5/6.2	0
33	malate dehydrogenase	*Beta vulgaris*	GI:11133601	549	1.0E-155	150	16.6	17	76.2	4.8	1	35.4/5.9	-167
34	phosphoglycerate kinase	*Nicotiana tabacum*	GI:2499498						51.5	2.2	1	42.3/5.6	0
35,36, 37	alcohol dehydrogenase	*Alnus glutinosa*	GI:71793966						255.3	8.4	2	41.0/6.3	0
38,39, 40	DEAD-box RNA helicase	*Vitis vinifera*	GI:157356562						469.6	11.3	5	48.8/5.5	-65*
41,42, 59	adenosylhomocysteinase	*Medicago sativa*	GI:1710838	89	3.0E-17	51.1	1.1	6	235.3	8.7	3	53.1/5.6	0
43	EBP1 aminopeptidase	*Vitis vinifera*	GI:157356189	467	1.0E-130	116	12.9	17	237.5	9.4	3	41.0/9.0	-175*
44	glyceraldehyde 3-phosphate dehydrogenase	*Solanum tuberosum*	GI:75315131	514	1.0E-144	54.9	8.4	7				36.7/7.7	-175
45,46, 47,48	salt tolerance protein 2	*Beta vulgaris*	GI:75137157	314	2.0E-84	70.7	42.0	8				38.4/5.4	-95
49	aspartate aminotransferase	*Populus trichocarpa*	GI:118488006						131.3	5.9	2	44.4/8.7	0
50,51	elongation factor (eEF-1a)	*Glycine max*	GI:1352345	572	1.0E-162	88.2	41.8	11	174.6	9.6	3	49.3/9.7	0

Spot[1]	Protein[2]	Organism[3]	Accession[4]	BLAST[5]		PMF[6]			MS/MS[7]			Predicted M_r/pI[8]	P[3]DB[9]
				Score	E-value	Score	Coverage (%)	NP	Score	Coverage (%)	NP		
52	Calreticulin	*Beta vulgaris*	GI:11131631	366	1.0E-99				101.3	2.4	1	48.1/4.3	-70
53,54, 55	hypotethical protein	*Vitis vinifera*	GI:225452887	222	8.0E-17				420	39	3	42.8/4.7	-35
56	alpha tubulin	*Populus tremuloides*	GI:29124983	549	1.0E-158	112	41.6	15	226.4	13.1	3	49.6/4.8	0
57	ATP synthase beta subunit	*Triticum aestivum*	GI:525291						278.9	11.8	4	59.2/5.5	0
58,60	enolase	*Gossypium hirsutum*	GI:158144895	375	1.0E-103	85.4	25.2	11	268.8	11.0	3	47.8/5.4	-136*
61	RuBisCO large subunit	*Jasminium suavissimus*	GI:131983						314.9	9.9	4	51.8/6.7	0*
62	DnaJ-like protein	*Solanum tuberosum*	GI:122212989	486	1.0E-136	61.4	3.4	11				46.7/6.0	-41
63,64	prolyl-tRNA synthetase	*Populus trichocarpa*	GI:118486938						130.5	5.6	3	56.8/5.9	-05
65	lipoamide dehydrogenase subunit E3	*Populus euphratica*	GI:68052018						55.4	100	1	1.2/11.5	
66	serine hydroxymethyltransferase	*Arabidopsis thaliana*	GI:15236375						106.6	5.7	2	51.7/7.0	0
67	peptidylprolyl isomerase	*Oryza sativa*	GI:75139222	315	1.0E-84				41	5	1	64.1/5.1	0

Spot[1]	Protein[2]	Organism[3]	Accession[4]	BLAST[5]		PMF[6]			MS/MS[7]			Predicted M_r/pI[8]	P[3]DB[9]
				Score	E-value	Score	Coverage (%)	NP	Score	Coverage (%)	NP		
68	GDP dissociation inhibitor 1	*Solanum tuberosum*	GI:82623395						106.9	5.0	2	49.7/5.5	
69	putative chaperonin 60	*Populus trichocarpa*	GI:118482230						104.7	4.2	2	58.7/5.2	-66*
70,74	aspartyl-tRNA synthetase	*Vitis vinifera*	GI:157339444						144.9	4.4	2	60.8/6.0	-23
71,72	pyruvate decarboxylase	*Lotus japonicus*	GI:51587336						220.9	6.6	2	62.6/5.7	0
73	ATP synthase alpha subunit	*Phaseolus vulgaris*	GI:114411						207.2	11.8	4	55.3/6.6	-23
75	enolase	*Hevea brasiliensis*	GI:14423688						261.3	7.9	2	47.8/5.5	-134
76	phosphoglyceromutase	*Mesembryanthemum crystallinum*	GI:3914394	468	1.0E-130	48.3	11.5	8	117	4.3	2	61.1/5.3	-95
77	chaperonin, t-complex alpha subunit	*Arabidopsis thaliana*	GI:9293959						59.5	2.0	1	59.9/6.4	-92
78	polyphenol oxidase	*Camellia nitidissima*	GI:222093457	182	4.0E-44	98.3	9.7	12				65.9/6.6	0
79	putative chaperonin	*Oryza sativa*	GI:115468394						66.8	2.2	1	60.9/6.2	-80
80	heat shock protein hsp70	*Pisum sativum*	GI:445605	456	1.0E-127	57.3	7.4	6	180.2	6.2	3	75.4/5.1	0*

Spot[1]	Protein[2]	Organism[3]	Accession[4]	BLAST[5]		PMF[6]			MS/MS[7]			Predicted M_r/pI[8]	P[3]DB[9]
				Score	E-value	Score	Coverage (%)	NP	Score	Coverage (%)	NP		
81	heat shock protein hsp90	*Arabidopsis thaliana*	GI:15228059						279.1	5.4	3	88.6/4.8	-176
82	heat shock protein hsp90	*Vitis pseudo-reticulata*	GI:159459822						450.1	9.0	4	80.2/4.8	0
83	heat shock protein hsp70	*Zea mays*	GI:123593	590	1.0E-174	175	27.6	17	466.6	11.3	5	70.6/5.1	0*
84	heat shock protein hsp90	*Arabidopsis thaliana*	GI:15228059						62.9	1.8	1	88.6/4.8	-176
85,86	heat shock protein hsp70	*Nicotiana tabacum*	GI:729623						202.8	4.6	2	73.7/4.9	0
87	translation initiation factor eIF-3	*Arabidopsis thaliana*	GI:15241470						41.2	2.2	1	66.2/5.3	
88,89, 90	methionine synthase	*Solenostemon scutellarioides*	GI:8134569						252.0	5.8	4	84.5/6.1	0
91	ubiquitin family protein	*Vitis vinifera*	GI:147836211						65.2	3.4	2	87.6/4.9	0
92	heat shock protein hsp70	*Arabidopsis thaliana*	GI:30699467						50.4	1.5	1	81.7/9.7	0*
93	CDC48	*Arabidopsis thaliana*	GI:15231775	498	1.0E-148	89.2	8.7	12	355.9	9.8	5	90.3/4.9	0
94	aconitate hydratase	*Arabidopsis thaliana*	GI:15233349						43.7	1.1	1	98.1/6.0	0

Spot[1]	Protein[2]	Organism[3]	Accession[4]	BLAST[5]		PMF[6]			MS/MS[7]			Predicted M_r/pI[8]	P^{3}DB[9]
				Score	E-value	Score	Coverage (%)	NP	Score	Coverage (%)	NP		
95,96	sucrose synthase	*Solanum lycopersicum*	GI:3758873						105.0	3.7	3	92.5/5.9	0
97,98, 99	translation elongation factor eEF-2	*Beta vulgaris*	GI:6015065	342	7.0E-93	80.8	13.2	9	202.0	4.7	3	93.7/5.9	0

[1]Spot number corresponding to spots in Figure 3.54.
[2]Protein name.
[3]Plant species from which the protein was identified.
[4]Accession number of the identified protein from NCBI database.
[5]Bit score and E-value of a blastp search used to annotate cDNA identified by PMF. When blank, then the given accession number was identified directly.
[6]Mascot score, sequence coverage (%), and number of matched peptide masses (NP) where PMF's contributed to the identification. The mascot score is presented as the ratio of the actual mascot score and the decoy score. See www.matrixscience.com for an explanation of score significance and decoy.
[7]Mascot score, sequence coverage and number of peptides used for identification of proteins by MALDI MS/MS in the NCBI database.
[8]Predicted molecular mass (kDa) and isoelectric point of the identified proteins.
[9]Proteins that show an evidence for phosphorylation from the P^{3}DB database (http://digbio.missouri.edu/p3db/). Numbers represent the E-value exponent of a BLAST search of the queried protein against the P^{3}DB phosphoprotein database (0 indicates identity). Proteins already identified in *C. plantagineum* leaves by Röhrig *et al.* (2008) are marked by an asterisk.

4. Discussion

The aim of this work is to contribute to the understanding of the mechanisms at the basis of the desiccation tolerance by comparing plants that are closely related but differ in their ability to survive desiccation. The data presented here indicate that the candidate protein 11–24 from *Craterostigma* and *Lindernia* is linked to the response of these plants to severe water stress and that its regulation by phosphorylation correlates with the ability of the plants to withstand desiccation. An extensive screening retrieved further candidate proteins that are regulated by phosphorylation in response to ABA and desiccation in *C. plantagineum* callus tissues.

4.1. Distribution of the Desiccation Tolerance within the Linderniaceae

Among the dicotyledonous resurrection plants, studies aimed at understanding the molecular basis of desiccation tolerance have focused on the South African plant *Craterostigma plantagineum* Hochst. (Bartels *et al.*, 1990). Traditionally, *Craterostigma* and its relatives have been treated as members of the family Scrophulariaceae in the order Lamiales. The Scrophulariaceae have recently been shown to be polyphyletic. As a consequence, the family was re-classified and several groups of former scrophulariaceous genera now belong to different families (Rahmanzadeh *et al.*, 2005). Rahmanzadeh *et al.* (2005) demonstrated the monophyly of the lineage that includes the genera *Craterostigma* and *Lindernia*. All the *Craterostigma* species are desiccation tolerant, however, the vast majority of the *Lindernia* species are desiccation sensitive (Fischer, 1992, 1995).

4.1.1. *L. brevidens* and *L. subracemosa* Display Different Phenotypes Regarding Desiccation Tolerance

L. brevidens Skan is a novel desiccation tolerant angiosperm. Figure 3.1 depicts the water status of *L. brevidens* during the dehydration and rehydration process. The desiccation process and the recovery after dehydration were followed on the basis of leaf ultrastructure. Figure 3.2 (a–c) shows that the desiccated plant is able to recover full turgor and viability after rehydration. SEM pictures of the leaf surface (Figure 3.2 d–f) and cross section (Figure 3.2 g–i), further confirm the ability of the plant to withstand the dehydration treatment: the plant cells are collapsing upon water loss, leading to a shrinkage of the cell walls and an extensive folding of the leaf tissues (Figure 3.2 e,h). Rehydration leads to a complete recovery of the cell structure (compare Figure 3.2 d,g with f,i).
On the contrary, *L. subracemosa* is not able to recover cell viability and turgor after severe water stress (Figure 3.3). The leaf cells undergo the same ultrastructural changes like in *L. brevidens* (Figure 3.3 e,h) but the tissues are not capable to revert the deleterious effects of dehydration to the initial state (compare Figure 3.3 d,g with f,i).
Desiccation tolerance in general correlates positively with dry habitats (Alpert, 2006). Engelbrecht *et al.* (2007) collected data about the regional distribution of plant species across the rainfall gradient in central Panama with respect to their water requirements. They reported that the species' density at the dry Pacific side correlated positively with the drought tolerance. On the contrary, species exhibiting high sensitivity to water deprivation occurred more often towards the wet Atlantic end of the climatic gradient of the Panamas isthmus. The results of Engelbrecht *et al.* (2007) suggest that drought sensitivity has a direct role in determining species distribution with respect to water availability.
The desiccation tolerance trait of *L. brevidens* assumes particular relevance together with its ecological distribution. Whereas *C. plantagineum* colonizes areas typical for resurrection plants like rocky outcrops and locations with restricted water availability in Niger, Ethiopia, Sudan, South Africa, Arabia and India (Fischer, 1992), *L. brevidens* was only reported in the Usambara mountains in Tanzania and in the Taita hills in Kenya, in habitats that never experience drought (Fischer, 1992). The occurrence of *L. brevidens* is indeed associated with the tropical rainforest. The area of the African rainforest has been reduced by the climatic changes that have occurred during the Pleistocene. This has caused a fragmentation of the rainforest in the Eastern Africa, which has survived as for-

est patches surrounded by arid woodland for about 30 million years (Phillips *et al.*, 2008). The age and the fragmentation have contributed to produce a high level of endemism and has favored speciation. *L. brevidens* has evolved in the rainforest area. It is proposed that *L. brevidens* is a neoendemic plant, a taxon rapidly evolving, that did not lose the ability to adapt to severe desiccation. One possible reason for the maintenance of this trait, normally associated with lower growth rate, is a lack of positive selection against it or the linkage of the desiccation tolerance to a yet unknown favorable trait (Phillips *et al.*, 2008).

However, the fact that a *genus* close to the model plant *C. plantagineum* displays such opposite phenotypes regarding the ability to survive desiccation provides a useful tool for deciphering the complex trait of the desiccation tolerance. In a system where genetic studies are precluded because of the poliploidy, genome size and lack of complete sequence, a comparative approach offers the possibility to conduct studies based on the direct comparison of close relatives by testable hypotheses including the analysis of candidate genes.

4.2. Analysis of the 11–24 Protein Sequences

The gene *CDeT11–24* was first isolated in a screen aimed to identify transcripts rapidly and abundantly induced by dehydration in *C. plantagineum* (Bartels *et al.*, 1990). The gene is induced in response to dehydration in leaves but the transcript is constitutively expressed in roots of soil grown-plants. Velasco *et al.* (1998) performed an analysis on the gene structure and expression of *CDeT11–24* and isolated two other cDNA clones. *CDeT11–24* belongs to a small gene family of which three members have been sequenced. Their coding sequence is almost identical and differ mainly in the presence of an insertion at the 3' end of two clones which shifts the TGA stop codon by 120 bp thus producing two transcripts of different sizes (Velasco *et al.*, 1998). The CDeT11–24 protein was proposed to be a novel late embryogenesis abundant (LEA) protein since it shares sequence features of this class of proteins, namely a stretch of amino acids rich in lysine that resembles the K-segment typical of the group 2 LEA proteins (dehydrins) and a discrepancy between the molecular weight predicted from the cloned transcripts and the molecular mass determined for the proteins by SDS–PAGE (Velasco *et al.*, 1998).

The conclusion that the CDeT11–24 protein could have a role in balancing the cellular

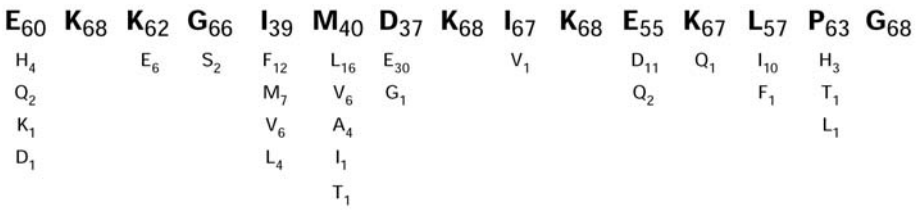

Figure 4.1: The consensus sequence of angiosperm dehydrin K-segment. Amino acids are listed as single letter abbreviations and the number of occurrences of each residue as a subscript. From Campbell and Close (1997).

water content during dehydration in the vegetative tissues of *C. plantagineum* justified the extension of the research to its close relatives belonging to the *Lindernia* genus, namely the desiccation tolerant *L. brevidens* and the desiccation sensitive *L. subracemosa*.

4.2.1. The 11–24 Homologues from *L. brevidens* and *L. subracemosa* Are LEA-like Proteins

The amino acid sequence of the isolated full length cDNAs of the CDeT11–24 homologues from *L. brevidens* and *L. subracemosa* (Figure 3.5) identifies two proteins of similar properties. The homologues from *Lindernia* display, as in CDeT11–24, an N-terminal stretch of sequence similar to the K-segment of the group 2 LEA proteins (Figure 4.1). This supports the assumption that the CDeT11–24 protein and its *Lindernia* homologues are dehydrin-like proteins.

4.2.2. The 11–24 Homologues from *L. brevidens* and *L. subracemosa* Share Sequence Features Common to Other Stress Responsive Proteins

Another feature of the primary structure of the 11–24 proteins is the presence of a conserved stretch of amino acids matching the CAP160 repeat pattern. The CAP160 repeat corresponds to the InterPro domain IPR012418 (www.ebi.ac.uk/interpro/).
InterPro is an integrated documentation resource for protein families, domains, regions and sites. InterPro combines a number of databases (referred to as member databases)

that use different methodologies and a varying degree of biological information on well-characterized proteins to derive protein signatures (Hunter *et al.*, 2009).
The CAP160 domain was first observed in the CAP160 protein of spinach (Kaye *et al.*, 1998). CAP160 is an acidic protein linked with cold acclimation. Expression of the CAP160 mRNA was increased by low temperature exposure and water stress indicating that its regulation is influenced by stresses that involve dehydration (Kaye *et al.*, 1998). The CAP160 protein provides therefore a link between cold and water stress response. Its precise function is unknown but the CAP160 protein has been implicated in the stabilization of membranes, cytoskeletal elements, and ribosomes (Kaye *et al.*, 1998).
Besides the CAP160 protein from spinach and CDeT11–24 other seven proteins contain the InterPro domain IPR012418 (Table 3.2). Interestingly, all the proteins but the ones from *Ricinus communis* and *Populus trichocarpa*, whose function is not yet annotated, are linked with the abiotic stress response. The LTI65/RD29A protein of *Arabidopsis thaliana* was discovered in a screening aimed at finding low-temperature-induced (LTI) transcripts (Nordin *et al.*, 1993). Furthermore it was shown that the protein is also responding to ABA and water deprivation (Yamaguchi-Shinozaki and Shinozaki, 1993). The protein At5g52300.2 from *A. thaliana* is belonging as well to the LTI65 protein family. The *Arabidopsis* protein M7J2.50 is classified in the superfamily of low-temperature-induced 78 kDa protein. The B57 protein from tobacco was identified in the cloning of cDNAs associated with embryogenic dedifferentiation of immature pollen grains (Kyo *et al.*, 2003), whereas the PM39 protein of soybean is involved in the seed maturation. Taken together, this list of proteins sharing common sequence features provide evidence for the involvement of these proteins in the response to suboptimal watering conditions consequently to environmental constrains as well during the normal plant development that involves desiccation, as in pollen and seeds.
Since the common features of these sequence is the CAP160 domain, it can be speculated that this stretch of amino acids is of crucial importance for the function of this protein.
The list of proteins that share sequence features common to 11–24 is expanded by searching in the ProDom database. Residues 183 to 383 of CDeT11–24 match the ProDom entry PD010085. In the *L. brevidens* and *L. subracemosa* protein sequences Lb11–24 and Ls11–24, this window corresponds to the most conserved region. The N-terminal end of the PD010085 domain overlaps with the CAP160 domain, although it does not contain it entirely. The list of proteins comprising this domain (Figure 3.8) contains some accessions

that were already present in the previous list of the CAP160-containing proteins (Table 3.2). These are the CDeT11–24 protein, CAP160 of spinach, the *Arabidopsis* protein M7J2.50 and LTI65, and the tobacco B57 protein. The novel proteins on the list are two putative rice proteins (Q337E2 and Q53RR4), three *Arabidopsis* proteins (Q9STE9, Q5XVB0 and LTI78/RD29B) and a protein from *Brassica oleracea*, RS1. The RS1 protein is up-regulated by cold, mannitol, NaCl and ABA (Tang *et al.*, 2004) whereas LTI78 is related to LTI65 (Nordin *et al.*, 1993).

The two databases make use of different approaches for clustering the protein sequences, by multiple sequence alignments and Hidden Markov Models in the Pfam database (Finn *et al.*, 2008), and by the MKDOM2 algorithm in the ProDom database (Gouzy *et al.*, 1999; Bru *et al.*, 2005). The consensus motifs of the two databases are only marginally coincident in their sequence, thus indicating that the different clustering approaches independently recognize a similar set of proteins.

Besides the accessions not yet classified, the information available for the known proteins identifies them as stress-related proteins. They are either directly involved in diverse abiotic stress responses or play a role in the embryo and pollen development, where the tissues face the same conditions occurring during the desiccation stress: CAP160, RS1, RD29A and RD29B are induced during abiotic stress (Nordin *et al.*, 1993; Yamaguchi-Shinozaki and Shinozaki, 1993; Kaye *et al.*, 1998; Tang *et al.*, 2004) whereas B57 of tobacco and PM39 of soybean are associated with the embryo and pollen development, respectively (Kyo *et al.*, 2003). Furthermore the M7J2.50 and At5g52300.2 proteins from *Arabidopsis* are classified in the superfamily of low-temperature-induced 78 and 65 kDa proteins, respectively.

The CDeT11–24 and its *Lindernia* homologues are thus related in their primary structure to a group of stress-related proteins. A BLAST search retrieves the same set of proteins, with the most similar being the B57 protein from tobacco with 39 % identity to CDeT11–24. The recognition in the BLAST search is always determined by the C-terminal region of the CDeT11–24 protein, corresponding to the sequence stretch annotated in the ProDom database. This could reflect not only a structural motif common to all the related proteins, but it could be also linked to a yet unknown function involved in the abiotic stress response.

4.2.3. The 11–24 Proteins Are Intrinsically Unstructured

The inclusion of the 11–24 proteins in the class of LEA-like proteins is supported by the occurrence of the K-segment. The LEA proteins are moreover characterized by the lack of a compact secondary structure. Lack of conventional compact structure means that members of the major LEA protein groups are included in the large class of the proteins so called 'natively unfolded', 'intrinsically disordered' or 'intrinsically unstructured' (Uversky *et al.*, 2000; Dunker *et al.*, 2001; Tompa, 2002).

The propensity for disordered structure was investigated by means of predictor programs based on the Hierarchical Neural Network (HNN). It was already mentioned by Röhrig *et al.* (2006) that the CDeT11–24 protein is 68 % random coil. Similar values were also found for the Lb11–24 and Ls11–24 proteins, which display 71 and 71.8 % of random coil sequence, respectively.

Since intrinsically unstructured proteins (IUPs) are to a large extent random coil, they do not have an hydrophobic core. This lack of compactness confers them the capability to remain soluble even at high temperatures. Any treatment that triggers the denaturation of the proteins causes the aggregation of the globular, ordered proteins, whereas the IUPs stay in solution. This property has been exploited to purify IUPs by heat fractionation (Irar *et al.*, 2006). The heat-stable phosphoproteome of *A. thaliana* was separated by 2D SDS–PAGE and revealed that the majority of the fraction contained LEA proteins (Irar *et al.*, 2006). The 11–24 protein has been fractionated by this method as well, to purify the recombinant protein (shown in Figure 3.11) and for the purification of the native protein used in the phosphatase shift assay (Figure 3.18 and 3.19). Conversely, this property can also be exploited to bring the denatured proteins into solution again since the globular proteins can not resolubilize. In this way the native protein was isolated and used to couple the affinity column (Figure 3.41).

Another feature that characterizes the IUPs is the anomalous migration on SDS–PAGE. In the SDS–PAGE showing the induction and isolation of the histidine tagged 11–24 proteins (Figures 3.11 and 3.40) and in the Western blots (Figures 3.13, 3.14, 3.15, 3.16), 11–24 has an apparent molecular weight that does not fit with the expected calculated mass. This is due to the particular feature of its amino acidic sequence. The electrophoretic mobility of proteins on denaturing SDS gels depends on their net charge, given by the number of SDS molecules binding to the protein. Since the SDS unfolds the proteins by the interaction

of its hydrophobic tail with the hydrophobic side chains of the normally masked amino acids, highly hydrophilic proteins like 11–24 are supposed to bind less SDS molecules. As a result the protein behaves unusually during SDS–PAGE, showing an apparent higher molecular weight, typically 1.2–1.8 times higher than the one calculated from sequence data (Tompa, 2002). This is also confirmed by the aliphatic index (the relative volume occupied by aliphatic side chains) of the CDeT11–24 protein, which is extremely low (60) as compared to globular proteins (80–90) (Ikai, 1980).

The heat stability derived from their sequence features is not unusual in the stress-responsive proteins. Besides the LEAs, other classes of proteins that correlate with the stress response present the ability to be heat stable. The protein SP1 from *Populus tremula* represents a novel class of proteins (Wang *et al.*, 2002). The *sp1* gene encodes a 12.4 kDa boiling-stable hydrophilic protein which is constitutively expressed in plants, but its accumulation is stimulated by stress conditions (Wang *et al.*, 2002). However, it is not included in the Class of LEA proteins since it forms a dodecamer composed of two stacking hexamers (Dgany *et al.*, 2004).

The amino acid composition is therefore a key feature in defining IUPs. They are depleted in the order-promoting hydrophobic amino acids which form the core of the folded globular proteins and are enriched in disorder-promoting residues with low mean hydrophobicity and high net charge (Dunker *et al.*, 2001; Tompa, 2005; Dyson and Wright, 2005). Table 3.3 depicts the relative contribution of the order-promoting and the disorder-promoting amino acids of the three 11–24 homologues. The sum of the order-promoting residues accounts for about 21 % of the total amino acids in the 11–24 proteins, a percentage much lower than for the globular proteins (38 %). On the other hand, the disorder-promoting residues are the 64 % of the total in the 11–24 sequences, whereas globular proteins have a frequency of only 47 %. This indicates that the lack of structure of the 11–24 proteins is an intrinsic property derived from their primary structure. The assumption is moreover reinforced by the IUPred analysis.

IUPred recognizes unstructured regions from the amino acid sequence based on estimating the capacity of polypeptides to form stabilizing contacts. Globular proteins are composed of amino acids which have the potential to form a large number of favorable interactions, whereas intrinsically unstructured proteins have sequences that do not have the capacity to form sufficient interresidue interactions (Dosztányi *et al.*, 2005a). Since the algorithm has not been trained on known sequences, the correct recognition of disordered struc-

tures substantiates the intrinsic property of sequence disorder. The output of the IUPred analysis presented in Figure 3.9 indicates that the 11–24 sequences possess pairwise interaction energies that are typical of unstructured proteins. The curve indicating the disorder tendency spans through the disordered region along the entire length of the sequences. Interestingly, for all three proteins a recurrent pattern can be recognized: the C-terminal part of the sequence is alternating disordered regions with short ordered stretches, whereas the N-terminal part is highly disordered. Remarkable is the fact that the C-terminal part of the proteins corresponds approximately in its length to the previously mentioned PD010085 ProDom domain (Figure 3.8). The less disordered part of the proteins corresponds thus to the most conserved region that is common to diverse stress responsive proteins.

4.2.4. The C-terminal of the 11–24 Proteins Shows a Higher Sequence Stability

An indirect confirmation of the unfolded structure of the IUPs *in vivo* is their high evolutionary rate. In the ordered cores of globular proteins the functionally crucial side chain interactions are thought to be responsible for slow rates of evolutionary changes. The faster rates of evolution imply that disordered regions have a lack of crucial side chain interactions, and thus provide additional support for the existence of disorder *in vivo* (Dunker *et al.*, 2002). A measure for this is the K_A/K_S ratio. Sequences containing residues involved in functional or structural interactions will have low levels of non-synonymous (K_A) vs. synonymous (K_S) mutations. On the contrary, disordered proteins which lack functional side chain interactions are more free to evolve.

Table 3.4 shows the K_A/K_S ratio not only for the full length 11–24 homologues, but also the value for the highly disordered N-terminal part and for the less disordered C-terminal part comprising the conserved ProDom domain. Interesting is the fact that according to the K_A/K_S ratio the N-terminal part is evolving at a rate that is twice as fast as the C-terminal part. This difference indicates that the 11–24 proteins are to some extent divided in two different part: the N-terminal half of the protein is highly disordered and this is reflected by the fast evolutionary rate, whereas the more conserved C-terminal half is subjected to more conservative sequence changes.

This inhomogeneous behavior of a protein sequence is not unfamiliar in the literature. There is evidence for other proteins with different K_A/K_S ratios. The sex-determining gene

SRY from mammals presents a similar architecture: alignment of SRY genes indicates that sequence conservation is largely confined to the HMG box, a DNA binding motif. The flanking regions are characterized on the contrary by a rapid divergence rate (Whitfield *et al.*, 1993). Tucker and Lundrigan (1993) performed the same analysis on the rat SRY gene and interestingly found a pattern similar to the 11–24 protein. The rat SRY protein consists on an N-terminal (HMG box) displaying a low K_A/K_S ratio, and on a C-terminal region rich in glutamine (Q), a disorder-promoting amino acid. The Q-rich region results from a frame-shift mutation in the ancestral sequence where a single-nucleotide insertion gives rise to a CAG repeat. This C-terminal region is moreover displaying a K_A/K_S ratio that is twice as high as the N-terminal DNA-binding domain, with values that are similar to those found in the 11–24 proteins (Tucker and Lundrigan, 1993).
The secondary structure revealed by the IUPred analysis, together with the sequence evolutionary rate, provide strong evidence for a dual nature of this protein where a disordered, rapid-evolving N-terminal region coexist with a more structured, conserved C-terminal region common to other stress-responsive proteins (Table 3.1). Taken together, these results suggest a not yet unveiled functional role for the C-terminal part of the 11–24 proteins.

4.3. Analysis of the Phosphorylation Status of the 11–24 Homologues

The lack of a defined structure has implications for the function of IUPs. Since they are almost entirely unfolded, it is improbable that they exert any catalytic function. Nevertheless, the data presented in section 3.2.2 show some putative secondary structure in the LEA-like protein 11–24. Many IUPs perform their function either fluctuating over different structural states, or via binding to one or several partner molecules in an adaptive manner. Generally their function involves binding to a partner ligand, such as other proteins, nucleic acids or membranes, and eventually such an interaction promotes the induction of local folding from the previously disordered structure. The intrinsic lack of structure can confer functional advantages on a protein, including the ability to bind to several different ligands, a feature called 'moonlighting' (Tompa *et al.*, 2005).
Disordered regions can confer several advantages to protein functions, since they permit efficient interaction with different regions of either a single partner or multiple targets and

provide a simple mechanism for the regulation of many cellular processes (Fink, 2005).
It has been reported that disorder correlates with the sites of post-translational modification, such phosphorylation (Iakoucheva *et al.*, 2004). Secondary modification of amino acids requires tight association between the target protein and the modifying enzyme. If the side chain is modified within a structured region, steric constraints could prevent or slow the association. On the contrary, a side chain within a disordered region facilitates substrate binding because the disordered region can adapt to the modifying enzyme (Dunker *et al.*, 2002). Iakoucheva *et al.* (2004) noted a correlation between phosphorylatable sequences and occurrence of local disorder. The similarity in sequence properties between phosphorylation sites and disordered regions supports the assumption that intrinsic disorder in and around the potential phosphorylation target site could be a common feature for protein phosphorylation.

4.3.1. Desiccation Tolerance Correlates with the Extent of Phosphorylation of the 11–24 Proteins

The CDeT11–24 protein was recently discovered as one of the major phosphoproteins induced in *C. plantagineum* upon desiccation together with the dehydrin CDeT6–19 (Röhrig *et al.*, 2006). Furthermore, it was observed that CDeT11–24 is induced during the early stages of dehydration and phosphorylated at a very late stage. Figure 3.13 confirms this dual behavior of the protein: whereas the Western blot reveals the presence of the protein in both the samples from 50 % RWC and dried leaves, the phosphostain indicates that CDeT11–24 is present in its phosphorylated form only in the dried sample.
In preliminary experiments, enriched phosphoproteins from ABA induced *C. plantagineum* leaves separated by 2D–PAGE led to the observation that the CDeT11–24 protein was not present, even if ABA is able to induce the accumulation of the protein. It was therefore speculated that ABA alone is not able to induce the phosphorylation of the protein.
The immunoprecipitation (Figure 3.14) demonstrates the ABA-dependent induction of the CDeT11–24 protein and its dehydration-induced phosphorylation. This confirms the hypothesis that the protein is early induced as a consequence of an ABA-mediated rapid response and phosphorylated during the late dehydration process as a consequence of delayed events linked to the extreme water loss.
Taking advantage of the occurrence of desiccation tolerant and non-tolerant plants within

the same *genus*, together with the availability of the sequences of the 11–24 homologues of *Lindernia* and an antibody reacting with both the *L. brevidens* and *L. subracemosa* proteins, it was tested whether the phosphorylation of the 11–24 protein correlated with desiccation tolerance.

For this, two approaches were taken into consideration: the first one was based on the same immunoprecipitation procedure performed to demonstrate the induction and phosphorylation of the CDeT11–24 protein. The second approach exploits the change of the isoelectric point of proteins as a result of the loss of one or more phosphate groups.

The immunoprecipitation experiment shown in Figure 3.15 indicates that in the presence of equal loading of precipitated proteins, the Lb11–24 homologue reveals a signal for phosphorylation, whereas the Ls11–24 homologue does not provide hints for phosphorylation, even though a weak band can be observed in the latest stages of dehydration. Furthermore the Lb11–24 homologue, unlike for the CDeT11–24 of *C. plantagineum*, shows some degree of phosphorylation already in the early stages of dehydration, when the water content is still at 4.8 g H_2O g^{-1} dry mass. The second approach based on the phosphatase shift assay reinforces the above mentioned results. The phosphatase-induced shift towards the more basic region of the 2D gel is seen in Figure 3.18 for the Lb11–24 protein from *L. brevidens*, whereas in Figure 3.19 the shift of the Ls11–24 homologue is not obvious.

The immunoprecipitation experiment was also conducted on detached leaves induced with ABA. Figure 3.16 surprisingly reveals a weak signal for phosphorylation even in the ABA-induced *L. brevidens* leaves. In addition, the dried samples of *L. subracemosa* also present a faint band corresponding to a phosphorylated Ls11–24. This is different to the previous results reported for the CDeT11–24 protein, where the ABA-treated leaves do not present a signal for the phosphorylated version of the protein. Nevertheless, the amount of phosphorylated protein is extremely low as compared to the dried samples, also taking into consideration that the amount of total protein revealed by the Western blot indicates an equal amount of Lb11–24. For the Ls11–24 the reduced presence of phosphorylated protein in the dried sample is intriguing. One explanation could be that the phosphorylation-dependent importance of this protein in the desiccation stress response does not rely on an on/off status which is mutually exclusive, but perhaps acts rather according to a quantitative effect depending on the amount of a more physiologically 'active' phosphorylated isoform over a less 'active' unphosphorylated one. The phosphorylation status of the 11–24 protein encounters a parallel in the LEA protein DHN-5 of wheat. The DHN-5

protein accumulates differentially in two Tunisian durum wheat (*Triticum durum* Desf.) varieties with marked differences in salt and drought tolerance. The variety more resistant to these stresses accumulates phosphorylated DHN-5, whereas in the susceptible variety the phosphorylated form is only weakly detectable (Brini *et al.*, 2007).
The differential phosphorylation status of the 11–24 homologues in response to severe water stress provides an important contribution to the assumption that this protein is an important player in the process of acquisition of desiccation tolerance, and that its role implies a phosphorylation step. In fact, the 11–24 isoforms of the desiccation tolerant plants *C. plantagineum* and *L. brevidens* undergo phosphorylation in response to dehydration, whereas in the 11–24 homologue from the desiccation-sensitive *L. subracemosa* the phosphorylation is much weaker.

4.3.2. Phosphorylation of the 11–24 Homologues Occurs within Predicted Coiled-Coil Domains

To further investigate the importance of the phosphorylation event in the 11–24 homologues, the sites of phosphorylation were identified. Röhrig *et al.* (2006) performed a phosphoprotein affinity chromatography to raise the sensitivity of the analysis. The proteins were then separated by 2D SDS–PAGE and the spot corresponding to CDeT11–24 analyzed by LC–MS/MS. The MS analysis yielded two phosphopeptides that were further confirmed on an HTCultra ion trap mass spectrometer, together with additional phosphorylation sites. The whole-protein MALDI–TOF analyses indicated that most CDeT11–24 proteins carry only one phosphate group, leading to the conclusion that the protein has multiple independent phosphorylation sites.
For the 11-24 homologues the affinity purified proteins were digested and the phosphoproteins enriched with TiO_2 columns. The CDeT11–24 sample was included as comparator to validate the enrichment procedure. The MS analysis on the enriched phosphopeptides confirmed five phosphorylation sites out of seven identified by Röhrig *et al.* (2006). Among these was Ser341, the strongest site observed.
The MS analysis on Lb11–24 retrieved 15 phosphorylation sites with different degrees of confidence according to the model supported. For Ls11–24 the phosphopeptide identification confirmed the observation already made by the immunoprecipitation experiments where there were hints for a weak phosphorylation of the 11–24 homologue from the

desiccation-sensitive plant. The MS analysis identified five phosphopeptides with eight possible phosphorylation sites. This is not surprising since the approach based on the selective enrichment of phosphopeptides coupled to LC–MS/MS has a much greater sensitivity compared to the immunodetection-based approach. However, the MS analysis is not quantitative, so the speculation that the amount of phosphorylated Ls11–24 is less than the phosphorylated Lb11–24 is still not disproved.

A closer look to the sequence comparison among the three 11–24 homologues with respect to their phosphorylated residues reveals that the strong phosphorylated Ser341 of CDeT11–24 is not phosphorylated in its *Lindernia* homologues, at least after the enrichment step chosen in this work. Intriguingly, certain phosphorylation sites identified in the *C. plantagineum* homologue protein by Röhrig *et al.* (2006) are also present in the *Lindernia* counterparts (underlined in the sequence comparison on page 98). Noteworthy is the presence of some phosphorylated residues in the desiccation-tolerant species *C. plantagineum* and *L. brevidens*, whereas these were not identified in the sensitive species *L. subracemosa*. These residues belonging to the tryptic peptide 15 occur in the more disordered N-terminal stretch.

The fact that the desiccation sensitive species *L. subracemosa* has a phosphorylation pattern that differs from that of the desiccation tolerant species *C. plantagineum* and *L. brevidens* provides evidence for the importance of the 11–24 protein phosphorylation in the desiccation response. The extent of phosphorylation correlates in fact with the ability of the plant to withstand desiccation. Moreover, a qualitatively effect cannot be excluded since sequence features revealed phosphopeptides exclusively occurring in the tolerant species.

Röhrig *et al.* (2006) noted that the CDeT11–24 is predicted to have two high-probability coiled-coil forming regions and three low-probability coiled-coils. They observed that the predicted phosphorylation sites fall within the lower coiled-coil probability and proposed that the phosphorylation of these residues could influence the stability and interactions of coiled-coil structures. Coiled-coil predictions (http://www.ch.embnet.org/software/COILS_form.html) performed on the *Lindernia* 11–24 sequences indicate a similar distribution of low- and high-probability coiled-coil structures.

Looking at the schematic representation of the three 11–24 protein homologues with the annotation of the identified phosphorylation sites, it is evident that their occurrence within the low probability coiled-coil regions is a common feature of all the 11–24 proteins (Figure 4.2). Moreover, the *Lindernia* sequences contain phosphorylated residues within or close

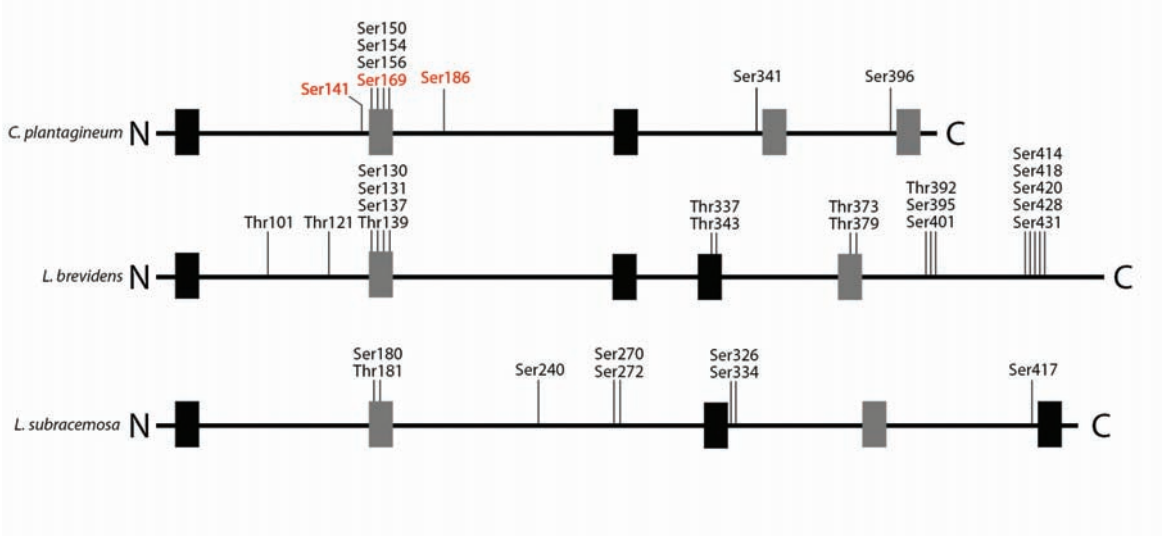

Figure 4.2: Schematic representation of the 11–24 protein homologues. The boxes show the position of the sequence stretches with high coiled-coil probability (black) and lower coiled-coil probability (grey). The scheme depicts the positions of the phosphorylation sites identified by LC–MS/MS. Besides the sites confirmed in this study, in red are labeled the phosphorylated amino acids found by Röhrig *et al.* (2006).

to the high probability coiled-coils.

Since it has been observed that phosphorylation can either disrupt (Steinmetz *et al.*, 2001) or favor (Liang *et al.*, 1999) coiled-coil structures, it is tempting to speculate such a mechanism for the 11–24 protein. In addition, phosphorylation could also influence the structure of the protein. With regard to the structural consequences of phosphorylation, both disorder to order and order to disorder transitions have been observed to follow the phosphorylation event (Johnson and Lewis, 2001).

Concerning this point, previous studies excluded such a mechanism for the class 2 LEA proteins. Mouillon *et al.* (2006) could demonstrate that dehydrins from *A. thaliana* and the isolated K-segment do not undergo increased folding upon treatment with stabilizing compounds or high temperatures. Moreover, the effect of phosphorylation was tested and resulted in the conclusion that such modification has no effect on the structure of the dehydrins in response to osmolytes and crowding agents (Mouillon *et al.*, 2008). It was hence speculated that the function of the dehydrins could rely in the interaction of their conserved segments with specific biological targets. In such a scenario, phosphorylation could still play a role as regulatory mechanism for the interaction with other cellular partners.

4.4. Identification of CDeT11–24 Interaction Partners

Conformational changes upon phosphorylation often affect protein function, hence the identification of the interaction partners of the proteins would result in an advance for understanding its function.

The presence of phosphorylatable residues near or within coiled-coil interaction domains provides a mechanism of probable protein oligomerization. Previous analyses showed that many natively unfolded proteins undergo increased folding upon dehydration. The LEAM protein from pea mitochondria gains structure upon dehydration adopting an α-helical conformation capable of interacting with membranes and protecting liposomes subjected to drying (Tolleter *et al.*, 2007). The AavLEA1 group 3 LEA-like protein from the nematode *Aphelencus avenae* is natively unfolded in solution, but its conformation changes upon dehydration. Fourier transform-infrared spectroscopy revealed a dramatic but reversible increase in α-helix and, possibly, coiled-coil structures upon dehydration (Goyal *et al.*, 2003).

Since phosphorylation has been shown to either disrupt or induce coiled-coil structures (Liang *et al.*, 1999; Steinmetz *et al.*, 2001), the delayed phosphorylation of the CDeT11–24 protein during the late stages of dehydration becomes intriguing. If phosphorylated amino acids can affect the stability of coiled-coil structures, this regulation could exert in different binding properties of the 11–24 protein, depending on its phosphorylation status. It was therefore tested whether the different forms of CDeT11–24, namely the phosphorylated and the unphosphorylated one, have different binding partners. As source for native unphosphorylated CDeT11–24 protein *C. plantagineum* leaf material treated with ABA was used, whereas the phosphorylated CDeT11–24 protein was enriched from leaves treated with ABA and subsequently dried.

4.4.1. The Coimmunoaffinity Chormatography Did not Retrieve Interaction Partners

The first strategy based on the coimmunoaffinity-based enrichment approach did not provide any candidate interactor in the eluted fractions (see Figure 3.38 on page 100). This

approach relies on the immunoadsorption of the pre-formed complexes on a column linked with the purified IgGs specific for the bait protein CDeT11–24. One reason for the failure of the coimmunoaffinity chromatography could be the binding strength of the purified IgGs bound to the column. The range of measured values of affinity constants for antibody–antigen binding spans from 10^5 M^{-1} to 10^{12} M^{-1}, whereas a typical enzyme–substrate interaction (e.g. trypsin) has an affinity constant of 10^4 M^{-1} (Harlow and Lane, 1988). In the case of a coiled-coil interaction, a typical binding constant for leucine zipper moieties that interact is in the range of 10^7 M^{-1} (Phizicky and Fields, 1995). This points out the far greater affinity the IgGs have over other protein-protein interactions. Since they can differ in their affinity constants for several orders of magnitude, it is not unlikely that the interacting proteins could be displaced by the antibody molecules.

4.4.2. The Weak Affinity Chromatography Suggests that CDeT11–24 Interacts With Itself

To overcome the plausible drawback of the coimmunoaffinity chromatography another approach was taken, where the column was directly coupled with the bait protein. To do this two columns were prepared, one coupled with the unphosphorylated form of CDeT11–24, and a second one coupled with the phosphorylated CDeT11–24. For this pourpose the unphosphorylated protein consisted in the recombinant full length histidine-tagged CDeT11–24. For the phosphorylated form, the native CDeT11–24 protein was isolated from dried *C. plantagineum* leaves. In this way two different columns covalently linked to the two isoforms of the bait protein were made available. The matrix of the two columns differed in the phosphorylation status of the bait protein, thus enabling an affinity chromatography to enrich the plant extracts in proteins that were differentially interacting with the solid phase, depending on the secondary modification status of CDeT11–24.
The eluted fractions separated by SDS–PAGE indicate that the column coupled with the recombinant protein is able to retain different polypeptides, whereas the phosphorylated version of CDeT11–24 does not. Interestingly, the major band in the Coomassie-stained gel in Figure 3.43 has a molecular size compatible with that of the CDeT11–24 protein. Its identity was confirmed by Western blot analysis, indicating that the band corresponds to CDeT11–24 and besides the full length protein, other smaller bands are recognized by the antibody. The meaning of this remains elusive, perhaps indicating degradation products

of the protein. The Western blot analysis also revealed that from the column coupled with the native phosphorylated protein it was eluted a band corresponding to the CDeT11–24 protein. Since the protein could not be observed in the Coomassie-stained gel, it is likely that this weak signal comes from protein bleeding from the column.

The only sample showing potential interaction candidates is the one from the partially dried leaves loaded on the column coupled with the recombinant protein. This finding is in line with previous experiments conducted on CDeT11–24 by 2D Blue Native SDS–PAGE (H. Röhrig, personal communication). It was observed that in native conditions the 11–24 protein from partially dehydrated plants localizes in a region of the gel between 100 and 200 kilodaltons, whereas the protein from fully dehydrated plants occurs at its predicted monomeric molecular size.

The competition experiment depicted in Figure 3.43 is aimed at confirming the specificity of the interaction between the bait protein and the potential interaction partners. An excess of the free CDeT11–24 protein added to the plant extract before the weak affinity chromatography would prevent the adsorption of the proteins on the column. The disappearance of bands in the lane treated with free bait protein would strengthen the assumption that they are specific interactors. The Coomassie-stained gel in Figure 3.43 reveals two bands showing the expected pattern. In order to identify them, the same samples were separated by 2D SDS–PAGE and the spots corresponding to the two candidates subjected to MS/MS analysis. The Mascot search revealed that they correspond to CDeT11–24 fragments, indicating that the outcompeted proteins belong to the protein itself.

Nevertheless, the 2D SDS–PAGE revealed another intriguing aspect of the competition experiment. The full-size CDeT11–24 protein appears to localize at two different isoelectric points along the pH gradient in the first dimension. The spot in the gel without the competitor has a more acidic pI as compared to the same spot belonging to the sample with competitor. The two spots were analyzed by MS/MS revealing that in the sample with the free 11–24 protein added as competitor, peptides corresponding to the recombinant histidine-tagged protein were present. This finding is in accordance with the protein sequence of the recombinant protein, which is predicted to have a pI of 5.57 due to the basic histidine tag, whereas the native CDeT11–24 has a more acidic pI (4.73). The occurrence of the histidine-tagged recombinant protein in the spot corresponding to the full length CDeT11–24 indicates that the protein is able to interact with itself in the unphos-

phorylated form, and this interaction can be depleted by adding an excess of recombinant 11–24, which outcompetes the binding of the native protein.

These results deliver additional informations about the features of the LEA-like protein CDeT11–24 of *C. plantagineum*, indicating that phosphorylation is able to regulate protein oligomerization. LEA proteins have the capability to form homo-oligomers (Ceccardi *et al.*, 1994; Kazuoka and Oeda, 1994). It might be speculated that CDeT11–24, similar to what Goyal *et al.* (2003) propose for the nematode protein AavLEA1, could form higher order coiled-coil interactions with itself. These interactions could form a network of protein filaments reminiscent of the cytoskeletal intermediate filaments, thus providing additional mechanical support to the cell.

Alternatively, the phosphorylation-dependent release of the monomer in the later stages of dehydration could represent a mechanism of regulation of the protein based on the early production of CDeT11–24 when the plant is sensing the stress, and the phosphorylation-driven activation and liberation of a putative active monomeric form in the later stages of desiccation. Supporting this model is the fact that the desiccation sensitive plant *L. subracemosa* presents a protein isoform with a reduced or completely absent phosphorylated isoform, as reported in section 3.4.

However, it has to be pointed out that this experiment was focused on the identification of potential proteinaceous interaction partners. It cannot be excluded that other compounds interact with CDeT11–24. CDeT11–24 contains a K-segment reminiscent of that occurring in the group 2 LEA proteins. For some proteins of this group, an ion-binding activity has been demonstrated (Battaglia *et al.*, 2008). The acidic dehydrin VCaB45 from celery and the *Arabidopsis* ERD14 possess calcium-binding properties, a feature that seems to be positively mediated by phosphorylation (Heyen *et al.*, 2002; Alsheikh *et al.*, 2003, 2005). Furthermore, recently it has been shown that the K-segment of the maize dehydrin DHN1 is able to bind to anionic phospholipids vesicles, and that the segment adapts an α-helical conformation upon binding (Koag *et al.*, 2009).

In conclusion the oligomerization of the LEA-like CDeT11–24 protein could represent a mechanism for its action, together with other not yet unveiled putative functions related to known properties typical of dehydrins, like binding to ions and phospholipidis. In the latter case different approaches have to be considered to test the hypothesis of non-proteinaceous binding partners.

4.5. Phosphoproteomic Analysis of the *C. plantagineum* Callus Tissue upon ABA and Dehydration Stress

4.5.1. The MOAC-based Enrichment Is Suitable for the Analysis of Changes Occuring in the *C. plantagineum* Callus Phosphoproteins

The metal oxide affinity chromatography (MOAC) enrichment protocol performed on the four samples revealed an homogeneous enrichment. The isolated phosphoproteins account for about 8 % of the starting total proteins, a value that is in accordance with the assumption that about 10 % of the proteins are phosphorylated at a certain time (Wolschin *et al.*, 2005). The separation of the samples by 1D SDS–PAGE gives further indication that the enriched proteins are phosphorylated. Staining of equal amounts of total proteins and MOAC-enriched proteins with the phosphoprotein-specific stain, reveals that the enriched fraction contains 8–9 times more phosphorylated proteins as compared to the total proteins.

Moreover, the enrichment of the CDeT11–24 protein was followed to test the specificity of the MOAC protocol. In section 3.4 it was demonstrated that the protein is induced by ABA but its phosphorylation is triggered only upon desiccation treatment. Hence, after the MOAC enrichment of phosphoproteins, a signal for the CDeT11–24 protein has to be detected only in the ABA-treated and dried sample. Indeed, Figure 3.49 shows that while in the total protein fraction CDeT11–24 occurs in equal amounts both in the ABA-treated and in the ABA-treated and dried samples, after the enrichment the protein is present only in the ABA-treated and dried sample, in the condition when CDeT11–24 undergoes phosphorylation. This internal control reinforces the usefulness and strength of the MOAC-based enrichment as a tool to analyze the phosphoproteome.

The separation of the samples by 2D SDS–PAGE followed by the phosphostain gives an overview of the changes occurring in the phosphoproteome of *C. plantagineum* calli in response to ABA and/or desiccation treatment. A direct observation of the set of four gels points out that changes occur upon the treatment imposed. These changes are

more evident after a pairwise comparison of the gels by superimposition (Figure 3.51). However, after the Coomassie staining of the same gels these differences are less evident, indicating that the phosphoprotein-specific stain is essential to highlight the presence of phosphorylated proteins, presumably due to the higher sensitivity of the phosphostain. The most noticeable differences reside in the acidic, high molecular weight region of the gel illustrated in detail in Figure 3.52.

4.5.2. The ABA and Desiccation Treatment Induces Changes in the Phosphoproteome of *C. plantagineum* Callus

GI:225452887

An interesting phosphoprotein identified in this study and regulated in response to desiccation is the set of three spots corresponding to the hypotethical protein GI:225452887 of *Vitis vinifera* (spots 53,54,55 in Figure 3.54). They show a phosphorylation pattern which is desiccation-dependent, irrespective of the ABA treatment. The proteins are phosphorylated in the control and ABA-treated samples, and are disappearing upon dehydration. A BLAST search does not retrieve any significant match to annotated proteins, however, when searching for conserved motifs in the ProDom database, two domains are recognized, PD339343 and PD888510, with an E-value of 4e-21 and 2e-07, respectively. Interestingly, the same architecture with the two ProDom domains is encountered in the uncharacterized *Arabidopsis* protein At5g39570. The At5g39570 protein was identified as a phosphoprotein in two independent screens (Laugesen *et al.*, 2006; de la Fuente van Bentem *et al.*, 2008). Moreover, searching for its expression profile by Genevestigator (www.genevestigator.ethz.ch) it turns out that its induction is maximal in the seed endosperm and upon external stimuli the transcription is mostly responsive to cold, drought and osmotic stress. These indications strongly support the involvement of the *Craterostigma* protein in the desiccation stress response, even if its precise function remains elusive. Moreover, the phosphoprotein At5g39570 correlates with the presence of the Phospholipase D (PLD) α1, suggesting that this protein is linked to the lipid signalling (Kuhn, 2009). The MOAC-enriched fraction from the *PLDα1* mutant of *A. thaliana* does not present the spot corresponding to the At5g39570 protein which is by contrast present in the wild type (Kuhn, 2009). PLD activity has been shown to be rapidly stimulated by

dehydration in *C. plantagineum* (Frank *et al.*, 2000). In *C. plantagineum* both constitutive (CpPLD–1) and desiccation- and ABA-inducible (CpPLD–2) PLD isoforms have been isolated (Frank *et al.*, 2000). The presence of the At5g39570 protein could therefore represent a link between the constitutive lipid signalling and the downstream desiccation-specific signalling.

Hsp70

Another protein showing a regulation in response to dehydration is the one identified as homologue to the Heat shock protein 70 (Hsp70, spot 83 in Figure 3.54). The spot is appearing only after desiccation treatment, regardless of the priming of the callus with ABA. The Coomassie stained gels show the spot corresponding to Hsp70 in all the samples, with no evident change in amount. This can be explained by the acidic isoelectric point of the protein which could be responsible for the enrichment of the unphosphorylated form as a result of its negative net charge. This also indicates that the protein is phosphorylated upon dehydration and not actively synthesized.
Both autophosphorylation and protein kinase-mediated phosphorylation appear to take place *in vivo* in the Hsp70 protein (Miernyk *et al.*, 1992a). More recently, phosphopeptides belonging to Hsp70 have been identified in a large-scale phosphoproteomic analysis in *Arabidopsis thaliana* (Sugiyama *et al.*, 2008). Phosphorylated Hsp70 has also been reported to accumulated in dehydrated leaves of *C. plantagineum* (Röhrig *et al.*, 2008).
Hsp70 functions as a molecular chaperone in a variety of cellular processes. It helps the cell to cope with a variety of adverse environmental conditions, such as heat, cold, drought, chemicals and other stresses. Hsp70 prevents protein aggregation, facilitates the translocation of nascent chains across membranes and mediates the assembly or disassembly of multimeric protein complexes and the targeting of proteins to lysosomes or proteasomes for degradation. Some members of the Hsp70 family are constitutively expressed and are often referred to as Hsc70 (70 kDa heat shock cognate). The Hsc70 are often involved in assisting the folding of *de novo* synthesized polypeptides and the translocation of precursor proteins. Other family members are expressed only when the organism is challenged by unfavorable conditions (Wang *et al.*, 2004). Hsp70 has two functional domains, the ATP-binding domain and the substrate-binding domain.
Phosphorylation regulates the activity of the Hsp70. Autophosphorylation, which occurs on a conserved threonine residue, inhibits the ATPase and chaperone activity by block-

ing the nucleotide binding (Miernyk *et al.*, 1992a). Miernyk *et al.* (1992b) proposed that Hsp70 could play multiple roles during membrane translocation of secretory precursors and that not all of these roles require ATP hydrolysis. Similarly, a phosphorylation-dependent redirection of the Hsp70 function could take place during the desiccation process in *C. plantagineum*. Interestingly, it has been reported that eukaryotic mitochondrial Hsp70 homologues could be phosphorylated *in vitro* in a calcium-stimulated reaction, a secondary messenger associated with the stress response (Leustek *et al.*, 1989).

Hsp90

Another member belonging to the Hsp family found in this study is the 90 kDa Heat Shock Protein Hsp90 (spot 82 in Figure 3.54). The protein is down-regulated upon desiccation treatment, but only in the callus sample pre-treated with ABA, indicating an effect that is desiccation-dependent, but also involving the ABA-dependent pathway. Looking at the Coomassie stained gels, it can be inferred that the phosphorylated Hsp90 is either dephosphorylated or actively degraded, in fact the stain for total proteins reveals a weak signal for this protein in the ABA-dried sample.

The main function of Hsp90 is to handle protein folding but it also plays a key role in signal-transduction networks, cell-cycle control, protein degradation and protein trafficking (Wang *et al.*, 2004). In addition, it is involved in the morphological evolution and stress adaptation of *Drosophila* and *Arabidopsis* (Rutherford and Lindquist, 1998; Queitsch *et al.*, 2002). Hsp90 acts as part of a multichaperone machinery together with Hsp70 and co-operates with a cluster of co-chaperones.

As for the Hsp70, it has been reported that Hsp90 is able to autophosphorylate *in vivo* (Park *et al.*, 1998). Bykova *et al.* (2003) reported that phosphorylated Hsp90 was accumulating in potato tuber mitochondria. In a study aimed at identifying the defence phosphoproteome of *A. thaliana* induced by the application of the pathogen *Pseudomonas syringae*, Hsp90 was one of the 14 phosphoproteins accumulating upon infection (Jones *et al.*, 2006). An increase of phosphorylated Hsp90 was reported following bacterial infection of leaves.

The function of its phosphorylation is still unknown, but the decrease of the phosphorylated form could play a role in the response to the stress stimulus. Western blot analysis using the antibody against the human Hsp90 isoform revealed that in total protein extracts the protein remains constant in the four samples, suggesting that a dephosphorylation event rather than an active degradation is taking place upon the treatments (Figure 3.52). No-

tably, as opposed to Hsp70, the effect is triggered by dehydration but only in the presence of the hormone ABA, indicating that the eventual phosphatase activity is regulated by both an ABA- and dehydration-dependent pathway.

4.5.3. Most Phosphoproteins Do not Show a Regulation Upon ABA and Desiccation Treatment

Besides these major phosphoproteins showing an ABA- and/or desiccation-dependent regulation, a list of other putative phosphoproteins was produced by analyzing the spots in the Coomassie stained gels. The MALDI–TOF MS/MS analysis of the other spots gives valuable informations about the phosphoproteins enriched by the MOAC approach. Figure 3.54 summarizes all the spots identified. The mass spectrometric analysis could identify 99 proteins, listed in Table 3.8. The discrepancy between the Coomassie and the phosphostain patterns could be explained by the sensitivity of the stain, which is one order of magnitude higher for the phosphostain. The signal intensity of the phosphostain is proportional to the number of phosphorylated residues in a protein, and does therefore not reflect the actual abundance of a protein. It can also not be excluded that some proteins revealed by the Coomassie staining are not truly phosphoproteins but reflect an unspecific enrichment. Nevertheless, a search for the identified phosphoproteins in the P^3DB database strengthens the hypothesis that the proteins identified are true phosphoproteins. The P^3DB database (http://digbio.missouri.edu/p3db/) collects 14,670 non-redundant phosphorylation sites from 8,894 phospho-peptides in 6,382 substrate proteins from *Glycine max* and 2,172 phosphorylation sites from *A. thaliana* (Sugiyama *et al.*, 2008). Table 3.8 shows the expectation values for the identified proteins queried against the P^3DB database, indicating that the majority of them have a strong homology to the annotated phosphoproteins and about one quarter of them display identity.

Further evidence indicating that the proteins enriched are phosphorylated is provided by the comparison with the list of phosphoproteins identified in *C. plantagineum* leaves by Röhrig *et al.* (2008). The majority of the phosphoproteins enriched from the leaves were also found in the callus. On the other hand, the phosphoproteins that were only found in the leaves are either involved in the phothosynthesis or found in chloroplasts, like the Ribonucleoprotein A, the Chlorophyll a/b binding protein, the Chloroplast drought-induced stress protein 34, the Hydroxymethylbilane synthase, the Fructose bisphosphatase and the

Phosphoribulokinase (Röhrig *et al.*, 2008). The lack of these proteins is not surprising since the calls tissue does not contain photosynthetic organelles. The analysis of the changes in the phosphoproteome of *C. plantagineum* leaves upon desiccation and rehydration could show that major changes occur during the onset of desiccation (Röhrig *et al.*, 2008). These changes are mainly represented by proteins involved in the photosynthesis. The fact that the callus phosphoproteome shows less dramatic changes in response to the ABA and desiccation stress suggests that regulation by phosphorylation is mostly acting on the photosynthetic apparatus and the related metabolism.

In conclusion, the data presented here provide evidence that the 2D SDS–PAGE separation of metal oxide affinity-enriched phosphoproteins, combined with a specific phosphostain, is a useful tool for the analysis of the phosphoproteome of the callus tissue of *C. plantagineum*, a species for which few sequencing information is available, thus precluding any high-throughput-based approach. This methodology, although not quantitative, permits the identification of major changes occurring in the phosphoproteome, delivering valuable informations about the regulation of protein phosphorylation in *C. plantagineum* in response to ABA and desiccation. In addition, the use of the callus tissue allows the identification of low-abundant phosphoproteins which would not be identifiable in the green tissues.

4.6. Conclusions and Outlook

The results presented here show that plant species belonging to the Linderniaceae family, a clade containing different desiccation tolerant angiosperms, display different phenotypes regarding the ability to tolerate desiccation. *Lindernia brevidens* is desiccation-tolerant whereas *Lindernia subracemosa* is desiccation-sensitive.

This intra-genus variability can be exploited as a tool for studying the complex trait of the acquisition of desiccation tolerance in plants. Focusing on other candidate proteins predicted to have a role in the desiccation response could reveal mechanisms that are exclusive to the desiccation tolerant species.

The sequences of the ABA- and desiccation-inducible proteins Lb11–24 and Ls11–24 homologue to the *Craterostigma plantagineum* CDeT11–24 protein were isolated. Secondary structure predictions revealed the the 11–24 proteins are natively unfolded and the disorder is mostly confined to the N-terminal part. Sequence analysis identified conserved motifs

common to other proteins known as stress responsive, even if the conservation among the sequences is poor. Interestingly the sequence recognized by the alignment search is confined in the more conserved C-terminal part, indicating that this domain is possibly relevant for the function of the protein.

The advantage of comparing close relatives by looking at candidate proteins is more evident when looking at the phosphorylation status of the 11–24 proteins. It was shown that the protein is induced as a consequence of an early signal involving the ABA response and phosphorylated upon desiccation. The picture coming out from this study reinforces the role of the 11–24 protein from *Craterostigma* and *Lindernia* that is linked to the response of these plants to severe water stress. The 11–24 protein is regulated by phosphorylation and its phosphorylation correlates with the ability of the plants to withstand desiccation, since *L. subracemosa* is not phosphorylated as strongly as the protein from desiccation-tolerant plants. The analysis of the phosphorylation status of the 11–24 proteins from the desiccation-tolerant tissues of the seeds would offer additional informations to verify this model.

The identification of the phosphorylation sites provided additional clues about the putative function of the phosphorylation event, since it occurs in proximity of predicted coiled-coil regions. Due to the ability of phosphorylation to influence coiled-coil interactions, the individuation of interaction partners modulated by phosphorylation would confer valuable informations in understanding the role of the CDeT11–24 protein. In this work could be demonstrated that CDeT11–24, in its unphosphorylated form, is able to oligomerize. Future studies should focus on the function this interaction can have and test the importance of the coiled-coil stretches. In addition, alternative approaches that do not restrict the search to proteinaceous interaction partners have to be adopted.

The MOAC-based phosphoprotein enrichment turned out to be a valuable tool for a low to middle throughput analysis of the phosphoproteome of *C. plantagineum*, delivering a list of candidate proteins that can be the starting point of future research. The use of the callus system provided an advantage over green tissues for the identification of less abundant proteins that would otherwise be masked by the abundant photosynthesis-related proteins. In order to validate the candidate proteins regulated by phosphorylation, antibodies should be produced to confirm the changes in their phosphorylation status by immunoprecipiation.

5. Summary

The ability of two *Lindernia* species to withstand severe water stress was investigated at the cellular level, leading to the conclusion that the close relatives *Lindernia brevidens* and *Lindernia subracemosa* display different phenotypes regarding the ability to survive desiccation: *L. brevidens* is desiccation tolerant, whereas *L. subracemosa* is not.

The fact that a *genus* close to the model plant *C. plantagineum* displays such opposite phenotypes regarding the ability to survive desiccation provides a useful tool for deciphering the complex trait of the desiccation tolerance. This variability was exploited to analyse a candidate protein whose homologue CDeT11–24 of *C. plantagineum* has been implicated in the desiccation response and is considered to be related to the late embryogenesis abundant (LEA) proteins.

The protein sequences of the *Lindernia brevidens* (Lb11–24) and *Lindernia subracemosa* (Ls11–24) counterparts were isolated. The primary structure of the candidate protein 11–24 from these *Lindernia* species was analysed in terms of amino acidic sequence properties. Sequence analysis identified conserved motifs common to other proteins known as stress responsive.

Secondary structure predictions revealed the the 11–24 proteins are natively unfolded and the disorder is mostly confined to the N-terminal part, whereas the C-terminal is more conserved among the homologues and contains the motif common to the stress-responsive proteins.

The LEA-like protein CDeT11–24 was reported as one of the major phosphoproteins accumulating upon desiccation in the vegetative tissues of *C. plantagineum*. The phosphorylation status of the 11–24 proteins was dissected in response to the tissue priming by the plant hormone ABA and by desiccation treatment, providing evidence of the advantage of comparing close relatives by looking at candidate proteins. It could be concluded that ABA is able to induce the protein synthesis and that desiccation is necessary and sufficient to trigger its phosphorylation. However, the 11–24 homologue of the desiccation sensitive

L. subracemosa is not phosphorylated as strongly as the desiccation-tolerant plants. The 11–24 protein is therefore regulated by phosphorylation and its phosphorylation correlates with the ability of the plants to withstand desiccation.

The identification of the phosphorylation sites of the three homologues could then provide additional information about the distribution and conservation of the phosphorylatable residues, since they occur in proximity of predicted coiled-coil regions.

The particular regulation and distribution of the phosphorylation led to the investigation of the potential interaction partners of the CDeT11–24 protein. To do this an antibody was raised against the candidate protein. A biochemical approach using the bait protein as interactor immobilised on an affinity column was performed. The affinity chromatography could reveal that the CDeT11–24 protein interacts with itself in its unphosphorylated form, providing evidence for a phosphorylation-driven regulation of its oligomerisation.

Finally, a more extensive screening was performed to identify protein whose phosphorylation is regulated in response to the ABA and desiccation treatment. In this study an approach based on phosphoprotein enrichment and 2D SDS–PAGE was applied on *C. plantagineum* callus tissue. Treatment of callus with ABA induces the expression of a set of genes comparable with that activated upon drying in the whole plant. The callus was dried with or without prior ABA treatment, in order to dissect the different contribution of ABA induction and drought stress on phosphoprotein changes. Moreover, the callus tissue presents the advantage of lacking in the photosynthesis-related proteins, which turned to be the main phosphoproteins identified in leaves, with the RuBisCO being the most abundant. This approach provided a list of candidate proteins whose phosphorylation is regulated during the treatments imposed and furnished novel elements involved in the mechanisms of the desiccation tolerance.

A. Appendix

A.1. Vectors

Uni-ZAP® XR

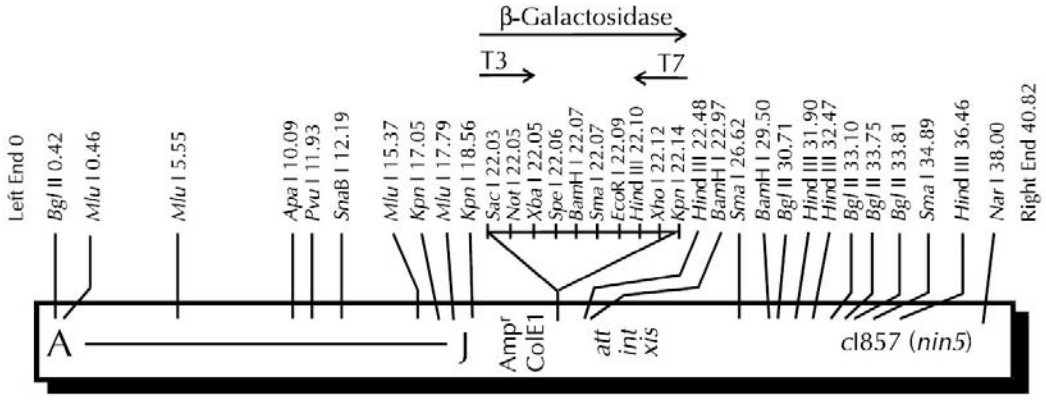

Figure A.1: Map of the Uni-ZAP XR insertion vector.

pBluescript® SK(-)

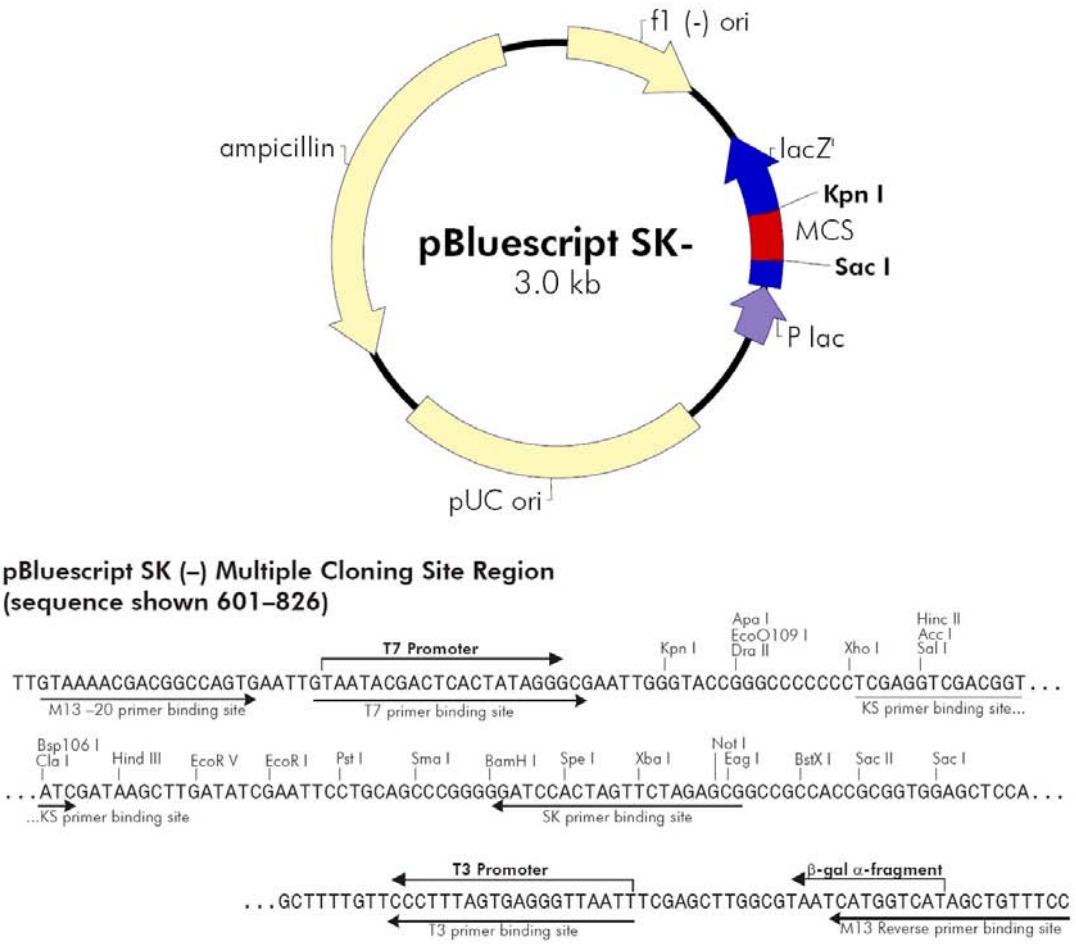

Feature	Nucleotide Position
f1 (–) origin of ss-DNA replication	24–330
β-galactosidase α-fragment coding sequence (lacZ')	463–816
T7 promoter transcription initiation site	643
multiple cloning site	653–760
T3 promoter transcription initiation site	774
lac promoter	817–938
pUC origin of replication	1158–1825
ampicillin resistance (*bla*) ORF	1976–2833

Figure A.2: Circular map and polylinker sequence of the pBluescript SK(-) phagemid.

pJET1.2/blunt

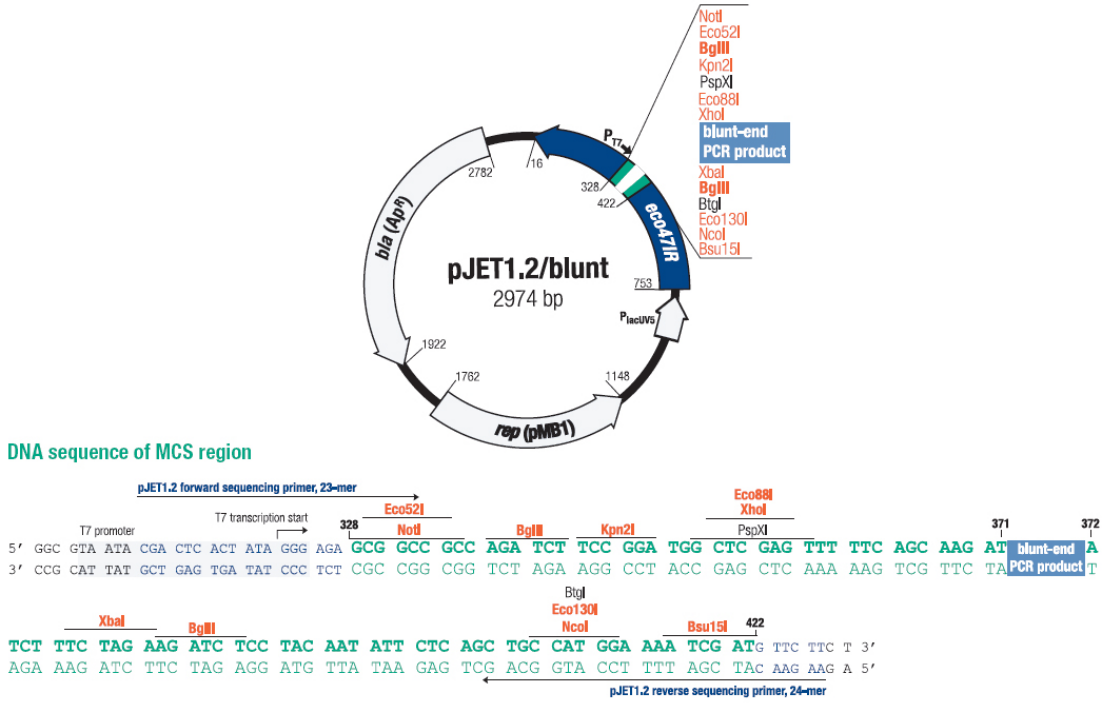

Figure A.3: Circular map and polylinker sequence of the pJET1.2/blunt plasmid.

pET-28a

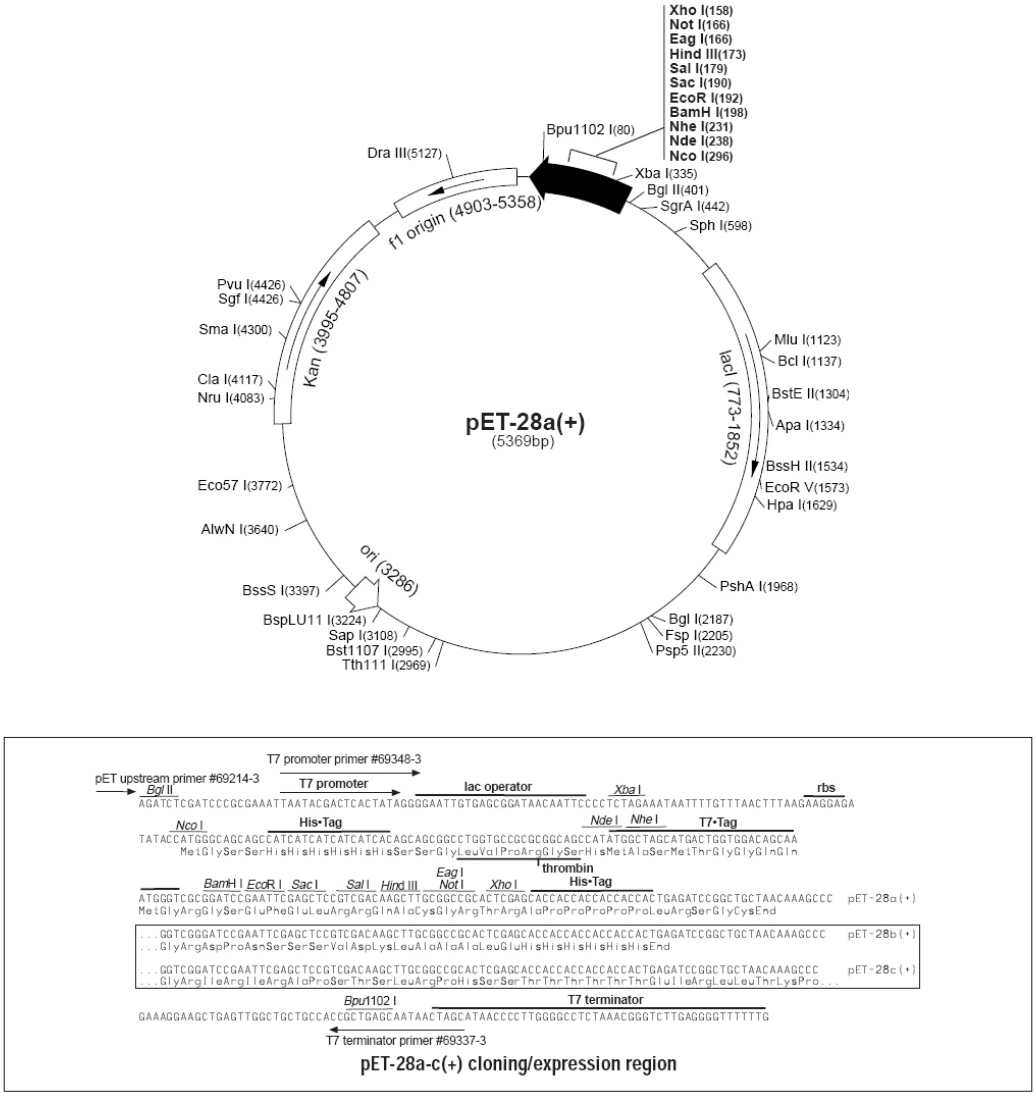

Figure A.4: Circular map and polylinker sequence of the pET-28a plasmid.

Bibliography

Alamillo, J., Almoguera, C., Bartels, D. and Jordano, J. (1995). Constitutive expression of small heat shock proteins in vegetative tissues of the resurrection plant *Craterostigma plantagineum*. *Plant Mol Biol* **29**, 1093–1099.

Alpert, P. (2005). The limits and frontiers of desiccation-tolerant life. *Integ Comp Biol* **45**, 685–695.

Alpert, P. (2006). Constraints of tolerance: why are desiccation-tolerant organisms so small or rare? *J Exp Biol* **209**, 1575–1584.

Alsheikh, M., Svensson, J. and Randall, S. (2005). Phosphorylation regulated ion-binding is a property shared by the acidic subclass dehydrins. *Plant Cell Environ* **28**, 1114.

Alsheikh, M. K., Heyen, B. J. and Randall, S. K. (2003). Ion binding properties of the dehydrin ERD14 are dependent upon phosphorylation. *J Biol Chem* **278**, 40882–40889.

Anderberg, R. J. and Walker-Simmons, M. K. (1992). Isolation of a wheat cDNA clone for an abscisic acid-inducible transcript with homology to protein kinases. *Proc Natl Acad Sci U S A* **89**, 10183–10187.

Arabidopsis-Genome-Initiative (2000). Analysis of the genome sequence of the flowering plant *Arabidopsis thaliana*. *Nature* **408**, 796–815.

Assmann, S. (1994). Ins and outs of guard cell ABA receptors. *Plant Cell* **6**, 1187–1190.

Bartels, D. and Salamini, F. (2001). Desiccation tolerance in the resurrection plant *Craterostigma plantagineum*. A contribution to the study of drought tolerance at the molecular level. *Plant Physiol* **127**, 1346–1353.

Bartels, D., Schneider, K., Terstappen, G., Piatkowski, D. and Salamini, F. (1990). Molecular cloning of abscisic acid-modulated genes which are induced during desiccation of the resurrection plant *Craterostigma plantagineum*. *Planta* **181**, 27–34.

Bartels, D. and Sunkar, R. (2005). Drought and salt tolerance in plants. *Crit Rev Plant Sci* **24**, 23–58.

Bateman, A., Coin, L., Durbin, R., Finn, R. D., Hollich, V., Griffiths-Jones, S., Khanna, A., Marshall, M., Moxon, S., Sonnhammer, E. L. L., Studholme, D. J., Yeats, C. and Eddy, S. R. (2004). The Pfam protein families database. *Nucl Acids Res* **32**, D138–D141.

Battaglia, M., Olvera-Carrillo, Y., Garciarrubio, A., Campos, F. and Covarrubias, A. A. (2008). The enigmatic lea proteins and other hydrophilins. *Plant Physiol* **148**, 6–24.

Bianchi, G., Gamba, A., Murelli, C., Salamini, F. and Bartels, D. (1991). Novel carbohydrate metabolism in the resurrection plant *Craterostigma plantagineum*. *Plant J* **1**, 355–359.

Billi, D. and Potts, M. (2002). Life and death of dried prokaryotes. *Res Microbiol* **153**, 7–12.

Boudsocq, M., Barbier-Brygoo, H. and Lauriere, C. (2004). Identification of nine sucrose nonfermenting 1-related protein kinases 2 activated by hyperosmotic and saline stresses in *Arabidopsis thaliana*. *J Biol Chem* **279**, 41758.

Bracken, C., Iakoucheva, L. M., Romero, P. R. and Dunker, A. K. (2004). Combining prediction, computation and experiment for the characterization of protein disorder. *Curr Opin Struct Biol* **14**, 570–576.

Bradford, M. M. (1976). A rapid and sensitive method for the quantitation of microgram quantities of protein utilizing the principle of protein-dye binding. *Anal Biochem* **72**, 248–254.

Bray, E. A. (1993). Molecular responses to water deficit. *Plant Physiol* **103**, 1035–1040.

Brini, F., Hanin, M., Lumbreras, V., Irar, S., Pages, M. and Masmoudi, K. (2007). Functional characterization of DHN-5, a dehydrin showing a differential phosphorylation pattern in two Tunisian durum wheat (*Triticum durum* desf.) varieties with marked differences in salt and drought tolerance. *Plant Sci* **172**, 20–28.

Brown, C. J., Takayama, S., Campen, A. M., Vise, P., Marshall, T. W., Oldfield, C. J., Williams, C. J. and Dunker, A. K. (2002). Evolutionary rate heterogeneity in proteins with long disordered regions. *J Mol Evol* **55**, 104–110.

Bru, C., Courcelle, E., Carrere, S., Beausse, Y., Dalmar, S. and Kahn, D. (2005). The ProDom database of protein domain families: more emphasis on 3D. *Nucl Acids Res* **33**, D212.

Buchanan, B., Gruissem, W. and Jones, R. (2000). *Biochemistry & molecular biology of plants*. American Society of Plant Physiologists, Rockville, MD.

Buitink, J. and Leprince, O. (2004). Glass formation in plant anhydrobiotes: survival in the dry state. *Cryobiol* **48**, 215–228.

Bykova, N. V., Egsgaard, H. and Moller, I. M. (2003). Identification of 14 new phosphoproteins involved in important plant mitochondrial processes. *FEBS Lett* **540**, 141–146.

Campbell, S. and Close, T. (1997). Dehydrins: genes, proteins, and associations with phenotypic traits. *New Phytol* , 61–74.

Ceccardi, T. L., Meyer, N. C. and Close, T. J. (1994). Purification of a maize dehydrin. *Protein Expr Purif* **5**, 266–269.

Choi, H.-I., Park, H.-J., Park, J. H., Kim, S., Im, M.-Y., Seo, H.-H., Kim, Y.-W., Hwang, I. and Kim, S. Y. (2005). *Arabidopsis* calcium-dependent protein kinase AtCPK32 interacts with ABF4, a transcriptional regulator of abscisic acid-responsive gene expression, and modulates its activity. *Plant Physiol* **139**, 1750–1761.

Close, T. (1996). Dehydrins: emergence of a biochemical role of a family of plant dehydration proteins. *Physiol Plant* **97**, 795–803.

Close, T. (1997). Dehydrins: a commonalty in the response of plants to dehydration and low temperature. *Physiol Plant* **100**, 291–296.

Cohen, C. and Parry, D. A. (1994). Alpha-helical coiled coils: more facts and better predictions. *Science* **263**, 488–489.

Crowe, J. H., Hoekstra, F. A., Nguyen, K. H. and Crowe, L. M. (1996). Is vitrification involved in depression of the phase transition temperature in dry phospholipids? *Biochim Biophys Acta* **1280**, 187–196.

Cuming, A. (1999). LEA proteins. *Seed Proteins. Kluwer Academic Publishers, Dordrecht, The Netherlands* , 753–780.

Cuming, A. C. and Lane, B. G. (1979). Protein synthesis in imbibing wheat embryos. *Eur J Biochem* **99**, 217–224.

de la Fuente van Bentem, S., Anrather, D., Dohnal, I., Roitinger, E., Csaszar, E., Joore, J., Buijnink, J., Carreri, A., Forzani, C., Lorkovic, Z. J., Barta, A., Lecourieux, D., Verhounig, A., Jonak, C. and Hirt, H. (2008). Site-specific phosphorylation profiling of *Arabidopsis* proteins by mass spectrometry and peptide chip analysis. *J Proteome Res* **7**, 2458–2470.

Dgany, O., Gonzalez, A., Sofer, O., Wang, W., Zolotnitsky, G., Wolf, A., Shoham, Y., Altman, A., Wolf, S. G., Shoseyov, O. and Almog, O. (2004). The structural basis of the thermostability of SP1, a novel plant (*Populus tremula*) boiling stable protein. *J Biol Chem* **279**, 51516–51523.

Dosztányi, Z., Csizmók, V., Tompa, P. and Simon, I. (2005a). The pairwise energy content estimated from amino acid composition discriminates between folded and intrinsically unstructured proteins. *J Mol Biol* **347**, 827–839.

Dosztányi, Z., Csizmók, V., Tompa, P. and Simon, I. (2005b). IUPred: web server for the prediction of intrinsically unstructured regions of proteins based on estimated energy content. *Bioinformatics* **21**, 3433–3434.

Dunker, A. K., Brown, C. J., Lawson, J. D., Iakoucheva, L. M. and Obradovic, Z. (2002). Intrinsic disorder and protein function. *Biochemistry* **41**, 6573–6582.

Dunker, A. K., Lawson, J. D., Brown, C. J., Williams, R. M., Romero, P., Oh, J. S., Oldfield, C. J., Campen, A. M., Ratliff, C. M., Hipps, K. W., Ausio, J., Nissen, M. S., Reeves, R., Kang, C., Kissinger, C. R., Bailey, R. W., Griswold, M. D., Chiu, W., Garner, E. C. and Obradovic, Z. (2001). Intrinsically disordered protein. *J Mol Graph Model* **19**, 26–59.

Dure, L., Greenway, S. C. and Galau, G. A. (1981). Developmental biochemistry of cottonseed embryogenesis and germination: changing messenger ribonucleic acid populations as shown by in vitro and in vivo protein synthesis. *Biochemistry* **20**, 4162–4168.

Dyson, H. J. and Wright, P. E. (2005). Intrinsically unstructured proteins and their functions. *Nat Rev Mol Cell Biol* **6**, 197–208.

Engelbrecht, B. M. J., Comita, L. S., Condit, R., Kursar, T. A., Tyree, M. T., Turner, B. L. and Hubbell, S. P. (2007). Drought sensitivity shapes species distribution patterns in tropical forests. *Nature* **447**, 80–82.

Ficarro, S. B., McCleland, M. L., Stukenberg, P. T., Burke, D. J., Ross, M. M., Shabanowitz, J., Hunt, D. F. and White, F. M. (2002). Phosphoproteome analysis by mass spectrometry and its application to saccharomyces cerevisiae. *Nat Biotechnol* **20**, 301–305.

Figueras, M., Pujal, J., Saleh, A., Savé, R. and Goday, A. (2004). Maize rab17 overexpression in *Arabidopsis* plants promotes osmotic stress tolerance. *Ann App Biol* **144**, 251–257.

Fink, A. L. (2005). Natively unfolded proteins. *Curr Opin Struct Biol* **15**, 35–41.

Finn, R. D., Tate, J., Mistry, J., Coggill, P. C., Sammut, S. J., Hotz, H.-R., Ceric, G., Forslund, K., Eddy, S. R., Sonnhammer, E. L. L. and Bateman, A. (2008). The Pfam protein families database. *Nucl Acids Res* **36**, D281–D288.

Fischer, E. (1992). Systematik der afrikanischen Lindernieae (*Scrophulariaceae*). *Trop. Subtrop. Pflanzenwelt* **81**, 1–365.

Fischer, E. (1995). Revision of the Lindernieae (Scrophulariaceae) in Madagascar. I: The genera *Lindernia* All. and *Crepidorhopalon*. *Bulletin du Muséum national d'histoire naturelle. Section B, Adansonia* **17**, 227–257.

Fischer, E. (2004). *Scrophulariaceae. in 'The families and genera of vascular plants'*. Springer Berlin.

Foyer, C. H. (1985). Stromal protein phosphorylation in spinach (*Spinacia oleracea*) chloroplasts. *Biochem J* **231**, 97–103.

Frank, W., Munnik, T., Kerkmann, K., Salamini, F. and Bartels, D. (2000). Water deficit triggers phospholipase d activity in the resurrection plant *Craterostigma plantagineum*. *Plant Cell* **12**, 111–124.

Frydman, J. (2001). Folding of newly translated proteins in vivo: the role of molecular chaperones. *Annu Rev Biochem* **70**, 603–647.

Fuglsang, A. T., Guo, Y., Cuin, T. A., Qiu, Q., Song, C., Kristiansen, K. A., Bych, K., Schulz, A., Shabala, S., Schumaker, K. S., Palmgren, M. G. and Zhu, J.-K. (2007). *Arabidopsis* protein kinase PKS5 inhibits the plasma membrane H^+ -ATPase by preventing interaction with 14-3-3 protein. *Plant Cell* **19**, 1617–1634.

Furihata, T., Maruyama, K., Fujita, Y., Umezawa, T., Yoshida, R., Shinozaki, K. and Yamaguchi-Shinozaki, K. (2006). Abscisic acid-dependent multisite phosphorylation regulates the activity of a transcription activator AREB1. *Proc Natl Acad Sci U S A* **103**, 1988–1993.

Gaff, D. F. (1971). Desiccation-tolerant flowering plants in southern Africa. *Science* **174**, 1033–1034.

Giarola, V. (2008). *Expression study of Ls11-24, a dehydration-induced gene in Lindernia subracemosa (Linderniaceae)*. Master's thesis, Universitá degli Studi di Verona.

Gobom, J., Schuerenberg, M., Mueller, M., Theiss, D., Lehrach, H. and Nordhoff, E. (2001). Alpha-cyano-4-hydroxycinnamic acid affinity sample preparation. a protocol for MALDI-MS peptide analysis in proteomics. *Anal Chem* **73**, 434–438.

Gouzy, J., Corpet, F. and Kahn, D. (1999). Whole genome protein domain analysis using a new method for domain clustering. *Comput Chem* **23**, 333–340.

Goyal, K., Tisi, L., Basran, A., Browne, J., Burnell, A., Zurdo, J. and Tunnacliffe, A. (2003). Transition from natively unfolded to folded state induced by desiccation in an anhydrobiotic nematode protein. *J Biol Chem* **278**, 12977–12984.

Goyal, K., Walton, L. J. and Tunnacliffe, A. (2005). Lea proteins prevent protein aggregation due to water stress. *Biochem J* **388**, 151–157.

Guermeur, Y., Geourjon, C., Gallinari, P. and Deleage, G. (1999). Improved performance in protein secondary structure prediction by inhomogeneous score combination. *Bioinformatics* **15**, 413–421.

Harlow, E. and Lane, D. (1988). Antibodies. A laboratory manual. Cold Spring Harbor Laboratory.

Hartl, F. U. (1996). Molecular chaperones in cellular protein folding. *Nature* **381**, 571–579.

Heyen, B. J., Alsheikh, M. K., Smith, E. A., Torvik, C. F., Seals, D. F. and Randall, S. K. (2002). The calcium-binding activity of a vacuole-associated, dehydrin-like protein is regulated by phosphorylation. *Plant Physiol* **130**, 675–687.

Hirt, H. and Shinozaki, K. (2004). *Plant responses to abiotic stress*. Springer Verlag Berlin.

Hundertmark, M. and Hincha, D. K. (2008). LEA (late embryogenesis abundant) proteins and their encoding genes in *Arabidopsis thaliana*. *BMC Genomics* **9**, 118.

Hunter, S., Apweiler, R., Attwood, T. K., Bairoch, A., Bateman, A., Binns, D., Bork, P., Das, U., Daugherty, L., Duquenne, L., Finn, R. D., Gough, J., Haft, D., Hulo, N., Kahn, D., Kelly, E., Laugraud, A., Letunic, I., Lonsdale, D., Lopez, R., Madera, M., Maslen, J., McAnulla, C., McDowall, J., Mistry, J., Mitchell, A., Mulder, N., Natale, D., Orengo, C., Quinn, A. F., Selengut, J. D., Sigrist, C. J. A., Thimma, M., Thomas, P. D., Valentin, F., Wilson, D., Wu, C. H. and Yeats, C. (2009). InterPro: the integrative protein signature database. *Nucl Acids Res* **37**, D211–D215.

Iakoucheva, L. M., Radivojac, P., Brown, C. J., O'Connor, T. R., Sikes, J. G., Obradovic, Z. and Dunker, A. K. (2004). The importance of intrinsic disorder for protein phosphorylation. *Nucl Acids Res* **32**, 1037–1049.

Ikai, A. (1980). Thermostability and aliphatic index of globular proteins. *J Biochem* **88**, 1895–1898.

Irar, S., Oliveira, E., Pages, M. and Goday, A. (2006). Towards the identification of late-embryogenic-abundant phosphoproteome in *Arabidopsis* by 2-DE and MS. *Proteomics* **6 Suppl 1**, S175–S185.

Israelsson, M., Siegel, R. S., Young, J., Hashimoto, M., Iba, K. and Schroeder, J. I. (2006). Guard cell ABA and CO_2 signaling network updates and Ca^{2+} sensor priming hypothesis. *Curr Opin Plant Biol* **9**, 654–663.

Jensen, A. B., Goday, A., Figueras, M., Jessop, A. C. and Pages, M. (1998). Phosphorylation mediates the nuclear targeting of the maize Rab17 protein. *Plant J* **13**, 691–697.

Jiang, X. and Wang, Y. (2004). Beta-elimination coupled with tandem mass spectrometry for the identification of in vivo and in vitro phosphorylation sites in maize dehydrin DHN1 protein. *Biochemistry* **43**, 15567–15576.

Johnson, L. N. and Lewis, R. J. (2001). Structural basis for control by phosphorylation. *Chem Rev* **101**, 2209–2242.

Jones, A. M. E., Bennett, M. H., Mansfield, J. W. and Grant, M. (2006). Analysis of the defence phosphoproteome of *Arabidopsis thaliana* using differential mass tagging. *Proteomics* **6**, 4155–4165.

Kaye, C., Neven, L., Hofig, A., Li, Q. B., Haskell, D. and Guy, C. (1998). Characterization of a gene for spinach CAP160 and expression of two spinach cold-acclimation proteins in tobacco. *Plant Physiol* **116**, 1367–1377.

Kazuoka, T. and Oeda, K. (1994). Purification and characterization of COR85-oligomeric complex from cold-acclimated spinach. *Plant Cell Physiol* **35**, 601.

Koag, M., Wilkens, S., Fenton, R., Resnik, J., Vo, E. and Close, T. (2009). The-K segment of maize DHN1 mediates binding to anionic phospholipid vesicles and concomitant structural changes. *Plant Physiol* **150**, 1503–1514.

Krishna, P. and Gloor, G. (2001). The Hsp90 family of proteins in *Arabidopsis thaliana*. *Cell Stress Chaperones* **6**, 238–246.

Krishna, R. G. and Wold, F. (1998). *Proteins - Analysis and Design*. Academic Press, San Diego.

Kuhn, A. (2009). *Molekulare analysen von Phospholipase D (PLD) mutanten*. Master's thesis, Universität Bonn.

Kyo, M., Hattori, S., Yamaji, N., Pechan, P. and Fukui, H. (2003). Cloning and characterization of cDNAs associated with the embryogenic dedifferentiation of tobacco immature pollen grains. *Plant Sci* **164**, 1057–1066.

Laemmli, U. K. (1970). Cleavage of structural proteins during the assembly of the head of bacteriophage T4. *Nature* **227**, 680–685.

Laugesen, S., Messinese, E., Hem, S., Pichereaux, C., Grat, S., Ranjeva, R., Rossignol, M. and Bono, J.-J. (2006). Phosphoproteins analysis in plants: a proteomic approach. *Phytochemistry* **67**, 2208–2214.

Le, T. and McQueen-Mason, S. (2006). Desiccation-tolerant plants in dry environments. *Rev Environ Sci Biotechnol* **5**, 269–279.

Leung, J., Merlot, S. and Giraudat, J. (1997). The *Arabidopsis* ABSCISIC ACID-INSENSITIVE2 (ABI2) and ABI1 genes encode homologous protein phosphatases 2C involved in abscisic acid signal transduction. *Plant Cell* **9**, 759–771.

Leustek, T., Dalie, B., Amir-Shapira, D., Brot, N. and Weissbach, H. (1989). A member of the Hsp70 family is localized in mitochondria and resembles *Escherichia coli* DnaK. *Proc Natl Acad Sci U S A* **86**, 7805–7808.

Li, J. and Assmann, S. M. (1996). An abscisic acid-activated and calcium-independent protein kinase from guard cells of fava bean. *Plant Cell* **8**, 2359–2368.

Li, J., Kinoshita, T., Pandey, S., Ng, C. K.-Y., Gygi, S. P., ichiro Shimazaki, K. and Assmann, S. M. (2002). Modulation of an RNA-binding protein by abscisic-acid-activated protein kinase. *Nature* **418**, 793–797.

Li, W. H., Wu, C. I. and Luo, C. C. (1985). A new method for estimating synonymous and nonsynonymous rates of nucleotide substitution considering the relative likelihood of nucleotide and codon changes. *Mol Biol Evol* **2**, 150–174.

Liang, W., Warrick, H. M. and Spudich, J. A. (1999). A structural model for phosphorylation control of dictyostelium myosin ii thick filament assembly. *J Cell Biol* **147**, 1039–1048.

Lisse, T., Bartels, D., Kalbitzer, H. R. and Jaenicke, R. (1996). The recombinant dehydrin-like desiccation stress protein from the resurrection plant *Craterostigma plantagineum* displays no defined three-dimensional structure in its native state. *Biol Chem* **377**, 555–561.

Lorow, D. and Jessee, J. (1990). Max efficiency DH10B: a host for cloning methylated DNA. *Focus* **12**, 19.

Ma, Y., Szostkiewicz, I., Korte, A., Moes, D., Yang, Y., Christmann, A. and Grill, E. (2009). Regulators of PP2C phosphatase activity function as abscisic acid sensors. *Science* **324**, 1064.

Maniatis, T., Fritsch, E. and Sambrook, J. (1986). *Molecular cloning*. Cold Spring Harbor Laboratory Cold Spring Harbor, NY.

Manning, G., Whyte, D. B., Martinez, R., Hunter, T. and Sudarsanam, S. (2002). The protein kinase complement of the human genome. *Science* **298**, 1912–1934.

Mason, J. and Arndt, K. (2004). Coiled coil domains: stability, specificity, and biological implications. *ChemBioChem* **5**.

McCubbin, W., Kay, C. and Lane, B. (1985). Hydrodynamic and optical properties of the wheat germ Em protein. *Biochem Cell Biol* **63**, 803–811.

Miemyk, J. (1997). The 70 kDa stress-related proteins as molecular chaperones. *Trends Plant Sci* **2**, 180–187.

Miernyk, J. A., Duck, N. B., David, N. R. and Randall, D. D. (1992a). Autophosphorylation of the pea mitochondrial heat-shock protein homolog. *Plant Physiol* **100**, 965–969.

Miernyk, J. A., Duck, N. B., Shatters, R. G. and Folk, W. R. (1992b). The 70-kilodalton heat shock cognate can act as a molecular chaperone during the membrane translocation of a plant secretory protein precursor. *Plant Cell* **4**, 821–829.

Moes, D., Himmelbach, A., Korte, A., Haberer, G. and Grill, E. (2008). Nuclear localization of the mutant protein phosphatase abi1 is required for insensitivity towards ABA responses in *Arabidopsis*. *Plant J* **54**, 806–819.

Mouillon, J.-M., Eriksson, S. K. and Harryson, P. (2008). Mimicking the plant cell interior under water stress by macromolecular crowding: disordered dehydrin proteins are highly resistant to structural collapse. *Plant Physiol* **148**, 1925–1937.

Mouillon, J.-M., Gustafsson, P. and Harryson, P. (2006). Structural investigation of disordered stress proteins. comparison of full-length dehydrins with isolated peptides of their conserved segments. *Plant Physiol* **141**, 638–650.

Nordin, K., Vahala, T. and Palva, E. T. (1993). Differential expression of two related, low-temperature-induced genes in *Arabidopsis thaliana* (L.) Heynh. *Plant Mol Biol* **21**, 641–653.

Oliver, M., Velten, J. and Mishler, B. (2005). Desiccation tolerance in bryophytes: A reflection of the primitive strategy for plant survival in dehydrating habitats? *Integ Comp Biol* **45**, 788–799.

O'Shea, E. K., Rutkowski, R. and Kim, P. S. (1989). Evidence that the leucine zipper is a coiled coil. *Science* **243**, 538–542.

Pandey, S., Nelson, D. C. and Assmann, S. M. (2009). Two novel GPCR-type G proteins are abscisic acid receptors in *Arabidopsis*. *Cell* **136**, 136–148.

Park, B., Liu, Z., Kanno, A. and Kameya, T. (2005). Genetic improvement of chinese cabbage for salt and drought tolerance by constitutive expression of a *B. napus* LEA gene. *Plant Sci* **169**, 553–558.

Park, M., Kang, C. Y. and Krishna, P. (1998). *Brassica napus* hsp90 can autophosphorylate and phosphorylate other protein substrates. *Mol Cell Biochem* **185**, 33–38.

Park, S.-Y., Fung, P., Nishimura, N., Jensen, D. R., Fujii, H., Zhao, Y., Lumba, S., Santiago, J., Rodrigues, A., Chow, T.-F. F., Alfred, S. E., Bonetta, D., Finkelstein, R., Provart, N. J., Desveaux, D., Rodriguez, P. L., McCourt, P., Zhu, J.-K., Schroeder, J. I., Volkman, B. F. and Cutler, S. R. (2009). Abscisic acid inhibits type 2C protein phosphatases via the PYR/PYL family of START proteins. *Science* **324**, 1068–1071.

Parry, M. A. J., Andralojc, P. J., Mitchell, R. A. C., Madgwick, P. J. and Keys, A. J. (2003). Manipulation of Rubisco: the amount, activity, function and regulation. *J Exp Bot* **54**, 1321–1333.

Phillips, J. R., Fischer, E., Baron, M., van den Dries, N., Facchinelli, F., Kutzer, M., Rahmanzadeh, R., Remus, D. and Bartels, D. (2008). *Lindernia brevidens*: a novel desiccation-tolerant vascular plant, endemic to ancient tropical rainforests. *Plant J* **54**, 938–948.

Phizicky, E. M. and Fields, S. (1995). Protein-protein interactions: methods for detection and analysis. *Microbiol Rev* **59**, 94–123.

Plana, M., Itarte, E., Eritja, R., Goday, A., Pagés, M. and Martínez, M. C. (1991). Phosphorylation of maize RAB-17 protein by casein kinase 2. *J Biol Chem* **266**, 22510–22514.

Porembski, S. and Barthlott, W. (2000). Granitic and gneissic outcrops (inselbergs) as centers of diversity for desiccation-tolerant vascular plants. *Plant Ecology* **151**, 19–28.

Postel, S. (1999). When the world's wells run dry. *World Watch* **12**, 30–38.

Prilusky, J., Felder, C. E., Zeev-Ben-Mordehai, T., Rydberg, E. H., Man, O., Beckmann, J. S., Silman, I. and Sussman, J. L. (2005). FoldIndex: a simple tool

to predict whether a given protein sequence is intrinsically unfolded. *Bioinformatics* **21**, 3435–3438.

Queitsch, C., Sangster, T. A. and Lindquist, S. (2002). Hsp90 as a capacitor of phenotypic variation. *Nature* **417**, 618–624.

Radhakrishnan, I., Perez-Alvarado, G. C., Parker, D., Dyson, H. J., Montminy, M. R. and Wright, P. E. (1997). Solution structure of the kix domain of cbp bound to the transactivation domain of creb: a model for activator:coactivator interactions. *Cell* **91**, 741–752.

Raggiaschi, R., Gotta, S. and Terstappen, G. C. (2005). Phosphoproteome analysis. *Biosci Rep* **25**, 33–44.

Rahmanzadeh, R., Müller, K., Fischer, E., Bartels, D. and Borsch, T. (2005). The Linderniaceae and Gratiolaceae are further lineages distinct from the Scrophulariaceae (Lamiales). *Plant Biol* **7**, 67–78.

Rascio, N. and La Rocca, N. (2005). Resurrection plants: the puzzle of surviving extreme vegetative desiccation. *Crit Rev Plant Sci* **24**, 209–225.

Richter, K. and Buchner, J. (2001). Hsp90: chaperoning signal transduction. *J Cell Physiol* **188**, 281–290.

Roberts, J. K., DeSimone, N. A., Lingle, W. L. and Dure, L. (1993). Cellular concentrations and uniformity of cell-type accumulation of two Lea proteins in cotton embryos. *Plant Cell* **5**, 769–780.

Rock, C. (2000). Pathways to abscisic acid-regulated gene expression. *New Phytol* **148**, 357–396.

Röhrig, H., Colby, T., Schmidt, J., Harzen, A., Facchinelli, F. and Bartels, D. (2008). Analysis of desiccation-induced candidate phosphoproteins from *Craterostigma plantagineum* isolated with a modified metal oxide affinity chromatography procedure. *Proteomics* **8**, 3548–3560.

Röhrig, H., Schmidt, J., Colby, T., Bräutigam, A., Hufnagel, P. and Bartels, D. (2006). Desiccation of the resurrection plant *Craterostigma plantagineum* induces dynamic changes in protein phosphorylation. *Plant Cell Environ* **29**, 1606–1617.

Rutherford, S. L. and Lindquist, S. (1998). Hsp90 as a capacitor for morphological evolution. *Nature* **396**, 336–342.

Sanchez-Ballesta, M., Rodrigo, M., Lafuente, M., Granell, A. and Zacarias, L. (2004). Dehydrin from citrus, which confers in vitro dehydration and freezing protection activity, is constitutive and highly expressed in the flavedo of fruit but responsive to cold and water stress in leaves. *J Agric Food Chem* **52**, 1950–1957.

Schmidt, C., Schelle, I., Liao, Y. J. and Schroeder, J. I. (1995). Strong regulation of slow anion channels and abscisic acid signaling in guard cells by phosphorylation and dephosphorylation events. *Proc Natl Acad Sci U S A* **92**, 9535–9539.

Schuster-Böckler, B., Schultz, J. and Rahmann, S. (2004). HMM logos for visualization of protein families. *BMC Bioinformatics* **5**, 7.

Schweighofer, A., Hirt, H. and Meskiene, I. (2004). Plant PP2C phosphatases: emerging functions in stress signaling. *Trends Plant Sci* **9**, 236–243.

Seki, M., Ishida, J., Narusaka, M., Fujita, M., Nanjo, T., Umezawa, T., Kamiya, A., Nakajima, M., Enju, A., Sakurai, T., Satou, M., Akiyama, K., Yamaguchi-Shinozaki, K., Carninci, P., Kawai, J., Hayashizaki, Y. and Shinozaki, K. (2002). Monitoring the expression pattern of around 7,000 *Arabidopsis* genes under ABA treatments using a full-length cDNA microarray. *Funct Integr Genomics* **2**, 282–291.

Seki, M., Narusaka, M., Abe, H., Kasuga, M., Yamaguchi-Shinozaki, K., Carninci, P., Hayashizaki, Y. and Shinozaki, K. (2001). Monitoring the expression pattern of 1300 *Arabidopsis* genes under drought and cold stresses by using a full-length cDNA microarray. *Plant Cell* **13**, 61–72.

Seo, M. and Koshiba, T. (2002). Complex regulation of ABA biosynthesis in plants. *Trends Plant Sci* **7**, 41–48.

Sharp, R. E. (2002). Interaction with ethylene: changing views on the role of abscisic acid in root and shoot growth responses to water stress. *Plant Cell Environ* **25**, 211–222.

Sheen, J. (1996). Ca^{2+}-dependent protein kinases and stress signal transduction in plants. *Science* **274**, 1900–1902.

Sheen, J. (1998). Mutational analysis of protein phosphatase 2C involved in abscisic acid signal transduction in higher plants. *Proc Natl Acad Sci U S A* **95**, 975–980.

Silvertown, J. (2004). Plant coexistence and the niche. *Trends Ecol Evol* **19**, 605–611.

Slovik, S., Daeter, W. and Hartung, W. (1995). Compartmental redistribution and long-distance transport of abscisic acid (ABA) in plants as influenced by environmental changes in the rhizosphere: a biomathematical model. *J Exp Bot* **46**, 881–894.

Sokolovski, S., Hills, A., Gay, R., Garcia-Mata, C., Lamattina, L. and Blatt, M. R. (2005). Protein phosphorylation is a prerequisite for intracellular Ca^{2+} release and ion channel control by nitric oxide and abscisic acid in guard cells. *Plant J* **43**, 520–529.

Steinmetz, M. O., Jahnke, W., Towbin, H., García-Echeverría, C., Voshol, H., Müller, D. and van Oostrum, J. (2001). Phosphorylation disrupts the central helix in Op18/stathmin and suppresses binding to tubulin. *EMBO Rep* **2**, 505–510.

Sugiyama, N., Masuda, T., Shinoda, K., Nakamura, A., Tomita, M. and Ishihama, Y. (2007). Phosphopeptide enrichment by aliphatic hydroxy acid-modified metal oxide chromatography for nano-LC-MS/MS in proteomics applications. *Mol Cell Proteomics* **6**, 1103–1109.

Sugiyama, N., Nakagami, H., Mochida, K., Daudi, A., Tomita, M., Shirasu, K. and Ishihama, Y. (2008). Large-scale phosphorylation mapping reveals the extent of tyrosine phosphorylation in *Arabidopsis*. *Mol Syst Biol* **4**, 193.

Sun, W. and Leopold, A. (1993). The glassy state and accelerated aging of soybeans. *Physiol Plant* **89**, 767–774.

Svitkina, T. M., Shevelev, A. A., Bershadsky, A. D. and Gelfand, V. I. (1984). Cytoskeleton of mouse embryo fibroblasts. Electron microscopy of platinum replicas. *Eur J Cell Biol* **34**, 64–74.

Takhtajan, A. (1997). *Diversity and classification of flowering plants*. Columbia Univ Press.

Tamura, K., Dudley, J., Nei, M. and Kumar, S. (2007). MEGA4: Molecular Evolutionary Genetics Analysis (MEGA) software version 4.0. *Mol Biol Evol* **24**, 1596–1599.

Tang, D., Qian, H., Yu, S., Cao, Y., Liao, Z., Zhao, L., Sun, X., Huang, D. and Tang, K. (2004). cDNA cloning and characterization of a new stress-responsive gene BoRS1 from *Brassica oleracea* var. acephala. *Physiol Plant* **121**, 578–585.

Testerink, C., Dekker, H. L., Lim, Z.-Y., Johns, M. K., Holmes, A. B., Koster, C. G., Ktistakis, N. T. and Munnik, T. (2004). Isolation and identification of phosphatidic acid targets from plants. *Plant J* **39**, 527–536.

Tolleter, D., Jaquinod, M., Mangavel, C., Passirani, C., Saulnier, P., Manon, S., Teyssier, E., Payet, N., Avelange-Macherel, M.-H. and Macherel, D. (2007). Structure and function of a mitochondrial late embryogenesis abundant protein are revealed by desiccation. *Plant Cell* **19**, 1580–1589.

Tompa, P. (2002). Intrinsically unstructured proteins. *Trends Biochem Sci* **27**, 527–533.

Tompa, P. (2005). The interplay between structure and function in intrinsically unstructured proteins. *FEBS Lett* **579**, 3346–3354.

Tompa, P., Szász, C. and Buday, L. (2005). Structural disorder throws new light on moonlighting. *Trends Biochem Sci* **30**, 484–489.

Towbin, H., Staehelin, T. and Gordon, J. (1979). Electrophoretic transfer of proteins from polyacrylamide gels to nitrocellulose sheets: procedure and some applications. *Proc Natl Acad Sci U S A* **76**, 4350–4354.

Tucker, P. K. and Lundrigan, B. L. (1993). Rapid evolution of the sex determining locus in old world mice and rats. *Nature* **364**, 715–717.

Tunnacliffe, A. and Wise, M. J. (2007). The continuing conundrum of the LEA proteins. *Naturwissenschaften* **94**, 791–812.

Uversky, V. N., Gillespie, J. R. and Fink, A. L. (2000). Why are natively 'unfolded' proteins unstructured under physiologic conditions? *Proteins* **41**, 415–427.

Valenzuela-Avendaño, J., Mota, I., Uc, G., Perera, R., Valenzuela-Soto, E. and Aguilar, J. (2005). Use of a simple method to isolate intact RNA from partially hydrated *Selaginella lepidophylla* plants. *Plant Mol Biol Rep* **23**, 199–200.

Velasco, R., Salamini, F. and Bartels, D. (1998). Gene structure and expression analysis of the drought- and abscisic acid-responsive CDeT11-24 gene family from the resurrection plant *Craterostigma plantagineum* Hochst. *Planta* **204**, 459–471.

Venter, J. C., Adams, M. D., Myers, E. W., Li, P. W., Mural, R. J., Sutton, G. G., Smith, H. O., Yandell, M., Evans, C. A., Holt, R. A., Gocayne, J. D., Amanatides, P., Ballew, R. M., Huson, D. H., Wortman, J. R., Zhang, Q., Kodira, C. D., Zheng, X. H., Chen, L., Skupski, M., Subramanian, G., Thomas, P. D., Zhang, J., Miklos, G. L. G., Nelson, C., Broder, S., Clark, A. G., Nadeau, J., McKusick, V. A., Zinder, N., Levine, A. J., Roberts, R. J., Simon, M., Slayman, C., Hunkapiller, M., Bolanos, R., Delcher, A., Dew, I., Fasulo, D., Flanigan, M., Florea, L., Halpern, A., Hannenhalli, S., Kravitz, S., Levy, S., Mobarry, C., Reinert, K., Remington, K., Abu-Threideh, J., Beasley, E., Biddick, K., Bonazzi, V., Brandon, R., Cargill, M., Chandramouliswaran, I., Charlab, R., Chaturvedi, K., Deng, Z., Francesco, V. D., Dunn, P., Eilbeck, K., Evangelista, C., Gabrielian, A. E., Gan, W., Ge, W., Gong, F., Gu, Z., Guan, P., Heiman, T. J., Higgins, M. E., Ji, R. R., Ke, Z., Ketchum, K. A., Lai, Z., Lei, Y., Li, Z., Li, J., Liang, Y., Lin, X., Lu, F., Merkulov, G. V., Milshina, N., Moore, H. M., Naik, A. K., Narayan, V. A., Neelam, B., Nusskern, D., Rusch, D. B., Salzberg, S., Shao, W., Shue, B., Sun, J., Wang, Z., Wang, A., Wang, X., Wang, J., Wei, M., Wides, R., Xiao, C., Yan, C., Yao, A., Ye, J., Zhan, M., Zhang, W., Zhang, H., Zhao, Q., Zheng, L., Zhong, F., Zhong, W., Zhu, S., Zhao, S., Gilbert, D., Baumhueter, S., Spier, G., Carter, C., Cravchik, A., Woodage, T., Ali, F., An, H., Awe, A., Baldwin, D., Baden, H., Barnstead, M., Barrow, I., Beeson, K., Busam, D., Carver, A., Center, A., Cheng, M. L., Curry, L., Danaher, S., Davenport, L., Desilets, R., Dietz, S., Dodson, K., Doup, L., Ferriera, S., Garg, N., Gluecksmann, A., Hart, B., Haynes, J., Haynes, C., Heiner, C., Hladun, S., Hostin, D., Houck, J., Howland, T., Ibegwam, C., Johnson, J., Kalush, F., Kline, L., Koduru, S., Love, A., Mann, F., May, D.,

McCawley, S., McIntosh, T., McMullen, I., Moy, M., Moy, L., Murphy, B., Nelson, K., Pfannkoch, C., Pratts, E., Puri, V., Qureshi, H., Reardon, M., Rodriguez, R., Rogers, Y. H., Romblad, D., Ruhfel, B., Scott, R., Sitter, C., Smallwood, M., Stewart, E., Strong, R., Suh, E., Thomas, R., Tint, N. N., Tse, S., Vech, C., Wang, G., Wetter, J., Williams, S., Williams, M., Windsor, S., Winn-Deen, E., Wolfe, K., Zaveri, J., Zaveri, K., Abril, J. F., Guigó, R., Campbell, M. J., Sjolander, K. V., Karlak, B., Kejariwal, A., Mi, H., Lazareva, B., Hatton, T., Narechania, A., Diemer, K., Muruganujan, A., Guo, N., Sato, S., Bafna, V., Istrail, S., Lippert, R., Schwartz, R., Walenz, B., Yooseph, S., Allen, D., Basu, A., Baxendale, J., Blick, L., Caminha, M., Carnes-Stine, J., Caulk, P., Chiang, Y. H., Coyne, M., Dahlke, C., Mays, A., Dombroski, M., Donnelly, M., Ely, D., Esparham, S., Fosler, C., Gire, H., Glanowski, S., Glasser, K., Glodek, A., Gorokhov, M., Graham, K., Gropman, B., Harris, M., Heil, J., Henderson, S., Hoover, J., Jennings, D., Jordan, C., Jordan, J., Kasha, J., Kagan, L., Kraft, C., Levitsky, A., Lewis, M., Liu, X., Lopez, J., Ma, D., Majoros, W., McDaniel, J., Murphy, S., Newman, M., Nguyen, T., Nguyen, N., Nodell, M., Pan, S., Peck, J., Peterson, M., Rowe, W., Sanders, R., Scott, J., Simpson, M., Smith, T., Sprague, A., Stockwell, T., Turner, R., Venter, E., Wang, M., Wen, M., Wu, D., Wu, M., Xia, A., Zandieh, A. and Zhu, X. (2001). The sequence of the human genome. *Science* **291**, 1304–1351.

Wang, W., Vinocur, B., Shoseyov, O. and Altman, A. (2004). Role of plant heat-shock proteins and molecular chaperones in the abiotic stress response. *Trends Plant Sci* **9**, 244–252.

Wang, W.-X., Pelah, D., Alergand, T., Shoseyov, O. and Altman, A. (2002). Characterization of SP1, a stress-responsive, boiling-soluble, homo-oligomeric protein from aspen. *Plant Physiol* **130**, 865–875.

Wasilewska, A., Vlad, F., Sirichandra, C., Redko, Y., Jammes, F., Valon, C., Frey, N. and Leung, J. (2008). An update on abscisic acid signaling in plants and more... *Mol Plant* **1**, 198.

Waters, E., Lee, G. and Vierling, E. (1996). Evolution, structure and function of the small heat shock proteins in plants. *J Exp Bot* **47**, 325–338.

Whitfield, L. S., Lovell-Badge, R. and Goodfellow, P. N. (1993). Rapid sequence evolution of the mammalian sex-determining gene SRY. *Nature* **364**, 713–715.

Wise, M. J. (2001). 0j.py: a software tool for low complexity proteins and protein domains. *Bioinformatics* **17 Suppl 1**, S288–S295.

Wise, M. J. (2003). LEAping to conclusions: a computational reanalysis of late embryogenesis abundant proteins and their possible roles. *BMC Bioinformatics* **4**, 52.

Wise, M. J. and Tunnacliffe, A. (2004). POPP the question: what do LEA proteins do? *Trends Plant Sci* **9**, 13–17.

Wolschin, F. and Weckwerth, W. (2005). Combining metal oxide affinity chromatography (moac) and selective mass spectrometry for robust identification of in vivo protein phosphorylation sites. *Plant Methods* **1**, 9.

Wolschin, F., Wienkoop, S. and Weckwerth, W. (2005). Enrichment of phosphorylated proteins and peptides from complex mixtures using metal oxide/hydroxide affinity chromatography (moac). *Proteomics* **5**, 4389–4397.

Wu, Y., Sanchez, J. P., Lopez-Molina, L., Himmelbach, A., Grill, E. and Chua, N.-H. (2003). The abi1-1 mutation blocks ABA signaling downstream of cADPR action. *Plant J* **34**, 307–315.

Xu, D., Duan, X., Wang, B., Hong, B., Ho, T. and Wu, R. (1996). Expression of a late embryogenesis abundant protein gene, HVA1, from barley confers tolerance to water deficit and salt stress in transgenic rice. *Plant Physiol* **110**, 249.

Yamaguchi-Shinozaki, K. and Shinozaki, K. (1993). Characterization of the expression of a desiccation-responsive rd29 gene of *Arabidopsis thaliana* and analysis of its promoter in transgenic plants. *Mol Gen Genet* **236**, 331–340.

Yoshida, R., Hobo, T., Ichimura, K., Mizoguchi, T., Takahashi, F., Aronso, J., Ecker, J. R. and Shinozaki, K. (2002). ABA-activated SnRK2 protein kinase is

required for dehydration stress signaling in *Arabidopsis*. *Plant Cell Physiol* **43**, 1473–1483.

Young, J. C., Moarefi, I. and Hartl, F. U. (2001). Hsp90: a specialized but essential protein-folding tool. *J Cell Biol* **154**, 267–273.

Zeevaart, J. and Creelman, R. (1988). Metabolism and physiology of abscisic acid. *Annu Rev Plant Physiol Plant Mol Biol* **39**, 439–473.

Zehr, B. D., Savin, T. J. and Hall, R. E. (1989). A one-step, low background coomassie staining procedure for polyacrylamide gels. *Anal Biochem* **182**, 157–159.